

Characterization of Ribonucleoside Diphosphate Reductase from
Thermoplasma acidophila

by

Jie Julie Wu
B.S., Chemistry, Stanford University
(1995)

Submitted to the Department of Chemistry
in Partial Fulfillment of the Requirements for the Degree of

Master of Science in Biological Chemistry

at the
Massachusetts Institute of Technology

September 1997

©1997 Massachusetts Institute of Technology
All Rights Reserved

Signature of Author _____

Department of Chemistry

July 3, 1997

Certified by__

JoAnne Stubbe

Thesis Advisor

Accepted by _____

Dietmar Seyferth

Chairman, Department Committee on Graduate Students

MASSACHUSETTS
INSTITUTE OF TECHNOLOGY
SEP 17 1997

LIBRARIES

*To my parents, Kui-hua Wu & Yi-yuan Ji,
for their love and inspiration*

Characterization of Ribonucleoside Diphosphate Reductase from
Thermoplasma acidophila

by
Jie Julie Wu

Submitted to the Department of Chemistry on July 3, 1997
in Partial Fulfillment of the Requirements for the Degree of
Master of Science

ABSTRACT

Ribonucleotide reductases (RNRs) catalyze the rate limiting step in DNA biosynthesis, the conversion of ribonucleotides to 2'-deoxyribonucleotides. Four classes of RNRs are currently known. Although each class differs in cofactor requirement, the allosteric regulation pattern and catalytic mechanism are conserved for all classes of RNRs. The ribonucleotide reductase from the archaeobacterium *Thermoplasma acidophila* (*T. acidophila* RDPR) was first purified and its gene was cloned into *E. coli* and sequenced in Benner's laboratory. Similar to the reductase from *Lactobacillus leichmannii*, it requires adenosylcobalamin for enzyme activity. The sequence of *T. acidophila* RDPR also provides a sequence link for all classes of RNRs. In this work, the purification method of *T. acidophila* RDPR was improved and additional activity assay procedures were developed. Several kinetic parameters of *T. acidophila* RDPR were determined. Initial studies on the regulation pattern of *T. acidophila* RDPR reveals that K_m values for substrates are substantially lower than other RNRs and that at low concentrations of effectors, regulatory patterns are similar. However, the regulation requires additional characterization. Stop flow UV-Visible studies showed that cob(II)alamin is formed in a kinetically competent fashion during catalysis. Rapid freeze quench EPR spectroscopy showed that cob(II)alamin exchanged coupled to a second radical species is formed as an intermediate. Inactivation studies showed that *T. acidophila* RDPR is inactivated by mechanism based inhibitors that have been extensively characterized with other RNRs. All the results suggest that *T. acidophila* RDPR is using a similar catalytic mechanism as the *Lactobacillus* enzyme.

Thesis Supervisor:

Professor JoAnne Stubbe

Title:

Novartis Professor of Chemistry and Biology

ACKNOWLEDGMENTS

First of all, I would like to thank my thesis advisor Professor JoAnne Stubbe for her support during my graduate school period and her guidance and patience during the preparation of this manuscript. I will always remember her genuine enthusiasm and dedication to science.

Next, I owe many thanks to all the past and present members in the Stubbe lab for providing such a friendly and supportive work environment. I am especially grateful to Stuart Licht, Dr. Wilfred von der Donk, and Dr. Christopher Lawrence for teaching me many techniques and helping me with the experiments. Their encouragement and input on my project were invaluable. I would like to thank Jennie, Wei, and Alex for those late night Chinatown runs; Kirsten for her jelly beans; Doug for his crazy bench music; and Pam for her birthday brownies. I would also like to thank the rest of the group, Silvia, Rick, Ute, Annette, and Joe, for many fond memories.

I also owe many gratitude to my friends outside the lab, Jianhua, Qing, Yansong, Chao, Xiaojun, for their encouragement and for many of the great moments we shared together. I wish them well with their careers.

Finally, I would like to thank my parents for making me who I am and for introducing me to chemistry. Their unconditional love will always be a constant in my life.

TABLE OF CONTENTS

	PAGE
Abstract.....	3
Acknowledgments	4
Table of Contents.....	5
Figures	10
Schemes	13
Tables	14
Abbreviations.....	15
CHAPTER 1	
Expression, Assay, and Purification of Recombinant <i>T. acidophila</i> RDPR.....	17
Introduction.....	18
Classes of Ribonucleotide Reductases	18
Ribonucleotide Reductase from <i>Thermoplasma acidophila</i>	19
Materials and Methods	20
Materials	20
Extraction and Restriction Mapping of Plasmid RNR/pET23b(+)	22
Quantitation and Gel Electrophoresis of Protein	22
Transformation of RNR/pET23b(+) into BL21(DE3) and JM109	22
Small Scale Induction to Analyze for Maximal Expression of <i>T. acidophila</i> RDPR	23
Tritium Exchange Assay on Crude Cell Lysate	23
Activity Assays for <i>T. acidophila</i> RDPR	24
[5, 8- ³ H]-ADP Assay	24

[8, 5'- ³ H] -GDP Assay	25
[5- ³ H]-CDP Assay	26
[2- ¹⁴ C]-CDP Assay	26
HPLC Analysis of [2- ¹⁴ C]-CDP Assay Products	27
HPLC Analysis of [2- ¹⁴ C]-CDP	27
Large Scale Growth of <i>T. acidophila</i> RDPR Overproducing Strain	
RNR/pET23b(+)/BL21(DE3)	28
Purification of <i>T. acidophila</i> RDPR.....	28
Protein Analysis During Purification	30
Determination of Extinction Coefficient	31
Results and Discussion	31
Extraction and Restriction Mapping of Plasmid RNR/pET23b(+)	31
Small Scale Induction Check on <i>T. acidophila</i> RDPR Expression.....	32
Tritium Exchange Assay on Crude Cell Lysate	33
Activity Assays for <i>T. acidophila</i> RDPR	34
Large Scale Growth of <i>T. acidophila</i> RDPR Overproducing Strain	
RNR/pET23b(+)/BL21(DE3)	36
Purification of <i>T. acidophila</i> RDPR.....	36
Determination of Extinction Coefficient	37
References.....	38
Schemes	39
Tables	42
Figures	44
 CHAPTER 2	
Allosteric Regulation and Kinetic Studies of <i>T. acidophila</i> RDPR	62

Introduction	63
Allosteric Regulation of Ribonucleotide Reductases	63
RDPR From Aerobically Grown <i>Escherichia coli</i> (Class Ia)	63
RTPR From Anaerobically Grown <i>Escherichia coli</i> (class III).....	64
Nrd-EF RDPR From <i>Salmonella typhimurium</i> (Class Ib).....	65
RTPR From <i>Lactobacillus leichmannii</i> (Class II)	66
Summary	67
Materials and Methods	68
Materials	68
Data Analysis.....	68
<i>T. acidophila</i> RDPR Used in Regulation and Kinetic Studies.....	69
(d)NTPs Used in Regulation Studies.....	70
AdoCbl K_m Determination with CDP as Substrate	70
DTT K_m Determination with CDP as Substrate	71
Allosteric Effects of (d)NTPs on ADP Reduction	71
Substrate ADP K_m Determination	72
Allosteric Effects of (d)NTPs on GDP Reduction	72
Substrate GDP K_m Determination	72
Allosteric Effects of (d)NTPs on CDP Reduction	73
Allosteric Effects of dNDPs on ADP Reduction	73
Results and Discussion	74
AdoCbl K_m Determination with CDP as Substrate	74
DTT K_m Determination with CDP as Substrate	74
<i>T. acidophila</i> RDPR Used in Regulation and Kinetic Studies.....	75

Allosteric Effects of (d)NTPs on ADP Reduction	75
Substrate ADP K_m Determination	77
Allosteric Effects of (d)NTPs on GDP Reduction	78
Substrate GDP K_m Determination	79
Allosteric Effects of (d)NTPs on CDP Reduction	80
Allosteric Effects of dNDPs on ADP Reduction	81
Summary	82
References.....	84
Schemes	86
Tables	92
Figures	104

CHAPTER 3

Mechanistic Characterization of *T. acidophila* RDPR

Introduction	132
Role of AdoCbl in Class II RNRs	132
Inactivation of RNRs with Mechanism-based Inhibitors	133
Materials and Methods	135
Materials	135
Stop-flow Experiment of <i>T. acidophila</i> RDPR.....	136
Rapid Freeze Quench EPR Experiment of <i>T. acidophila</i> RDPR	137
Time-dependent Inactivation of <i>T. acidophila</i> RDPR	139
Results and Discussion	140

Stop-flow Experiment of <i>T. acidophila</i> RDPR.....	140
Rapid Freeze Quench EPR Experiment of <i>T. acidophila</i> RDPR	144
RFQ-EPR Experiment with [5'- ¹ H]-AdoCbl.....	144
RFQ-EPR Experiment with [5'- ² H]-AdoCbl.....	145
The Mystery Peak Observed.....	147
Time-dependent Inactivation of <i>T. acidophila</i> RDPR	148
Experimental Concerns for the Time-dependent Inactivation Studies	148
Background Deactivation Observed for <i>T. acidophila</i> RDPR.....	151
dF ₂ CDP is a Potent Inhibitor of <i>T. acidophila</i> RDPR.....	151
N ₃ UDP and 2'VUDP as Inhibitors for <i>T. acidophila</i> RDPR	152
Summary	154
References.....	155
Schemes	157
Figures	159
 APPENDIX	
Appendix I: DNA and protein sequence of <i>T. acidophila</i> RDPR.....	175
Appendix II: Restriction map of <i>T. acidophila</i> RDPR DNA sequence	178
Appendix III: <i>T. acidophila</i> RDPR N-terminal sequencing report.....	179

FIGURES

- Figure 1.1** Plasmid map of RNR/pET23b(+).
- Figure 1.2** Plasmid map of pLysS.
- Figure 1.3** Restriction digest pattern with HindIII.
- Figure 1.4** Restriction digest pattern with BamHI, and NotI+NdeI.
- Figure 1.5** Sample growth curve of RNR/pET23b(+)/BL21(DE3).
- Figure 1.6** Sample induction gel of RNR/pET23b(+)/BL21(DE3).
- Figure 1.7** Sample TLC plate of deoxynucleosides and nucleosides separation.
- Figure 1.8** Sample [5, 8-³H]-ADP assay.
- Figure 1.9** Sample [8, 5'-³H] -GDP assay.
- Figure 1.10** Sample [5-³H]-CDP assay.
- Figure 1.11** Sample [2-¹⁴C]-CDP assay.
- Figure 1.12** HPLC analysis of [2-¹⁴C]-CDP assay product.
- Figure 1.13** HPLC analysis of [2-¹⁴C]-CDP.
- Figure 1.14** Q-Sepharose column elution profile: A260, A280 readings vs. fraction number.
- Figure 1.15** Q-Sepharose column elution profile: A280 reading and specific activity (cpm/AU) vs. fraction number.
- Figure 1.16** Sample SDS-PAGE gel of dATP affinity column fractions.
- Figure 1.17** Sample SDS-PAGE gel for *T. acidophila* RDPR purification.
- Figure 1.18** Sample UV spectrum for *T. acidophila* RDPR.
- Figure 2.1a** AdoCbl K_m determination.
- Figure 2.1b** AdoCbl K_m determination by Benner.
- Figure 2.2** DTT K_m determination.
- Figure 2.3a** UV spectrum of *T. acidophila* RDPR, batch IIa.
- Figure 2.3b** UV spectrum of *T. acidophila* RDPR, batch IIb.
- Figure 2.4a** Allosteric effect of (d)NTPs on ADP (10 μ M) reduction, Run 1.

- Figure 2.4b** Allosteric effect of (d)NTPs on ADP (10 μ M) reduction, Run 2.
- Figure 2.5a** Allosteric effect of (d)NTPs on ADP (1 mM) reduction, Run 1.
- Figure 2.5b** Allosteric effect of (d)NTPs on ADP (1 mM) reduction, Run 2.
- Figure 2.5c** Allosteric effect of (d)NTPs on ADP (1 mM) reduction, Run 3.
- Figure 2.6a** ADP K_m determination: no effector vs. 1 mM dGTP.
- Figure 2.6b** ADP K_m determination: no effector case.
- Figure 2.6c** ADP K_m determination by Benner's laboratory.
- Figure 2.7a** Allosteric effect of (d)NTPs on GDP (10 μ M) reduction, Run 1.
- Figure 2.7b** Allosteric effect of (d)NTPs on GDP (10 μ M) reduction, Run 2.
- Figure 2.8** Allosteric effect of (d)NTPs on GDP (1 mM) reduction, Run 1.
- Figure 2.9** Allosteric effect of (d)NTPs on GDP (10 μ M) reduction, with TR/TRR/NADPH.
- Figure 2.10a** GDP K_m determination (5-40 μ M): no effector vs. 1 mM dTTP.
- Figure 2.10b** GDP K_m determination (100-600 μ M): no effector vs. 1 mM dATP.
- Figure 2.11** Allosteric effect of (d)NTPs on CDP (10 μ M) reduction.
- Figure 2.12** Allosteric effect of (d)NTPs on CDP (1 mM) reduction.
- Figure 2.13** Allosteric effect of (d)NTPs on CDP (1 mM) reduction, with TR/TRR/NADPH.
- Figure 2.14** Allosteric effect of (d)NDPs on ADP (10 μ M) reduction.
- Figure 2.15** Allosteric effect of (d)NDPs on ADP (200 μ M) reduction.
- Figure 3.1a** Cob(II)alamin formation (0 - 1.2 s): absorbance change at 525nm.
- Figure 3.1b** Cob(II)alamin formation: absorbance change at 525nm.
- Figure 3.2a** Cob(II)alamin formation (0 - 1.2 s): absorbance change at 477nm.
- Figure 3.2b** Cob(II)alamin formation: absorbance change at 477nm.
- Figure 3.3** RFQ-EPR spectra of *T. acidophila* RDPR at 10 ms (9 scans) and 38 ms (6 scans) with [5'- 1 H]-AdoCbl.

- Figure 3.4** RFQ-EPR spectra of *T. acidophila* RDPR at 10 ms (9 scans) with that of *L. leichmannii* RTPR at 175 ms (10 scans) with [5'-¹H]-AdoCbl.
- Figure 3.5** RFQ-EPR spectra of *T. acidophila* RDPR at 10 ms (9 scans) and 38 ms (7 scans) with [5'-²H]-AdoCbl.
- Figure 3.6a** RFQ-EPR spectra of *T. acidophila* RDPR at 10 ms with [5'-¹H]-AdoCbl (9 scans) and [5'-²H]-AdoCbl (9 scans).
- Figure 3.6b** RFQ-EPR spectra of *T. acidophila* RDPR at 38 ms with [5'-¹H]-AdoCbl (6 scans) and [5'-²H]-AdoCbl (7 scans).
- Figure 3.7** The mystery peak observed due to incomplete mixing at 10 ms (13 scans).
- Figure 3.8** The mystery peak observed (13 scans) with normal peak at 10 ms with [5'-²H]-AdoCbl (9 scans).
- Figure 3.9** Enzyme stability in the presence of dGTP, with or without AdoCbl at 55°C.
- Figure 3.10** Enzyme stability at 0°C and 55°C in the absence of AdoCbl and dGTP.
- Figure 3.11** Time-dependent inactivation of *T. acidophila* RDPR by 2'-deoxy-2',2'-difluorocytidine 5'-diphosphate (dF₂CDP).
- Figure 3.12** Time-dependent inactivation of *T. acidophila* RDPR by 2'-azido-2'-deoxyuridine 5'-diphosphate (N₃UDP).
- Figure 3.13** Time-dependent inactivation of *T. acidophila* RDPR by 2'-deoxy-2'-methyleneuridine 5'-diphosphate (2'VUDP).

SCHEMES

- Scheme 1.1** Ribonucleotide reductase catalyzes a key step in DNA biosynthesis.
- Scheme 1.2** RNRs use a wide range of cofactors.
- Scheme 1.3** Proposed mechanism for nucleotide reduction RNRs.
- Scheme 2.1** Substrate specificity of ribonucleotide reductase is subject to allosteric control.
- Scheme 2.2** Schematic representation of RDPR from *E. coli* (Class Ia).
- Scheme 2.3** Schematic representation of RTPR from anaerobically grown *E. coli* (Class III).
- Scheme 2.4** Schematic representation of NrdEF RDPR from *S. typhimurium* (Class Ib).
- Scheme 2.5** Schematic representation of RTPR from *L. leichmannii*.(Class II).
- Scheme 2.6** Models for the allosteric regulation of all three classes of RNRs.
- Scheme 3.1** Possible roles of AdoCbl in thiyl radical generation in class II RNRs.
- Scheme 3.2** Mechanism of inhibition of *L. leichmannii*RTPR by a nucleotide analog.

TABLES

Table 1.1	Expected digest pattern of plasmid RNR/pET23b(+) and pLysS.
Table 1.2	Tritium exchange assay results.
Table 1.3	R _f values of deoxynucleosides and nucleosides.
Table 1.4	Sample purification table for <i>T. acidophila</i> RDPR.
Table 2.1a	Allosteric regulation of <i>E. coli</i> RDPR (Class Ia).
Table 2.1b	Allosteric regulation of <i>E. coli</i> RDPR (Class Ia).
Table 2.2	Allosteric regulation of anaerobic <i>E. coli</i> RTPR (Class III).
Table 2.3	Allosteric regulation of <i>NrdEF</i> RDPR from <i>S. typhimurium</i> (Class Ib).
Table 2.4	Allosteric regulation of <i>L. leichmannii</i> RTPR (Class II).
Table 2.5a	Summarized data for allesteric regulation of ADP reduction by specific activity (U/mg).
Table 2.5b	Summarized data for allesteric regulation of ADP reduction by percentage of activity.
Table 2.6a	Apparent K _m values for effectors of the anaerobic <i>E. coli</i> RTPR.
Table 2.6b	K _m values for substrates of the anaerobic <i>E. coli</i> RTPR.
Table 2.7a	Summarized data for allesteric regulation of GDP reduction by specific activity (U/mg).
Table 2.7b	Summarized data for allesteric regulation of GDP reduction by percentage of activity.
Table 2.8a	Summarized data for allesteric regulation of CDP reduction by specific activity (U/mg).
Table 2.8b	Summarized data for allesteric regulation of CDP reduction by percentage of activity.
Table 2.9a	Summarized data for allosteric effects of dNDPs on ADP reduction by specific activity (U/mg).
Table 2.9b	Summarized data for allosteric effects of dNDPs on ADP reduction by percentage of activity.
Table 3.1	Summarized rate data for stop flow experiment.

ABBREVIATIONS

A	adenosine
AdoCbl	5'-deoxyadenosylcobalamin
ADP	adenosine-5'-diphosphate
ATP	adenosine-5'-triphosphate
AU	Absorbance unit
BSA	bovine serum albumin
C	deoxycytidine
cat.	catlog number
CDP	cytidine-5'-diphosphate
Ci	curie
CIP	calf intestine alkaline phosphatase
dA	2'-deoxyadenosine
dADP	2'-deoxyadenosine-5'-diphosphate
dATP	2'-deoxyadenosine-5'-triphosphate
dC	2'-deoxycytidine
dCTP	2'-deoxycytidine-5'-triphosphate
dF ₂ CDP	2'-deoxy-2',2'-difluorocytidine 5'-diphosphate
dG	2'-deoxyguanosine
dGDP	2'-deoxyguanosine-5'-diphosphate
dGTP	2'-deoxyguanosine-5'-triphosphate
dTDP	2'-deoxythymidine-5'-diphosphate
DTT	dithiothreitol
dTTP	2'-deoxythymidine-5'-triphosphate
<i>E. coli</i>	<i>Escherichia coli</i>
EDTA	ethylenediaminetetraacetic acid
EPR	electron paramagnetic resonance

G	guanosine
GDP	guanosine-5'-diphosphate
HEPES	N-(2-hydroxyethyl)piperazine-1-ethanesulphonic acid
HPLC	high pressure liquid chromatography
IPTG	isopropyl β -D-thiogalactoside
kb	kilo base pairs
kDa	kilo daltons
<i>L. Leichmannii</i>	<i>Lactobacillus leichmannii</i>
LB	Luria-Bertani broth
MW	molecular weight
N ₃ UDP	2'-azido-2'-deoxyuridine 5'-diphosphate
NADPH	b-Nicotinamide adenine dinucleotide phosphate, reduced form
PAGE	polyacrylamide gel electrophoresis
PMSF	phenylmethanesulfonyl fluoride
PMSF	phenylmethylsulphonylfluoride
RDPR	ribonucleoside diphosphate reductase from <i>E. coli</i>
RFQ	rapid freeze quench
RNR	ribonucleotide reductase
RTPR	ribonucleoside triphosphate reductase from <i>L. leichmannii</i>
S. A.	specific activity
SDS	sodium dodecylsulfate
<i>T. acidophila</i>	<i>Thermoplasma acidophila</i>
TLC	thin layer chromatography
TR	thioredoxin
Tris	tris(hydroxymethyl)aminomethane
TRR	thioredoxin reductase
2'VUDP	2'-deoxy-2'-methylneuridine-5'-diphosphate

Chapter 1

Expression, Assay, and Purification of Recombinant *T. acidophila* RDPR

Introduction

Ribonucleotide reductases (RNRs) play a central role in DNA biosynthesis, catalyzing the conversion of nucleotides to 2'-deoxynucleotides (Scheme 1.1).¹⁻³ Based on their substrate preferences, ribonucleoside diphosphates or ribonucleoside triphosphates, they are named as RDPR or RTPR respectively. The classification of ribonucleotide reductases are introduced and background information about previous studies of *T. acidophila* RDPR is also presented.

Classes of Ribonucleotide Reductases

At present there are four classes of ribonucleotide reductases, three of which have been and continue to be under intense investigation.⁴ All the RNRs are believed to follow a radical based catalytic mechanism.⁵

There are four basic classes of RNRs based on their cofactor requirements to generate the thiyl radical essential for catalysis (Scheme 1.2). Class I enzymes, represented by RNRs from *E. coli* (RDPR), contain an unusual diferric cluster-tyrosyl radical cofactor. Class II enzymes, represented by RNR from *Lactobacillus leichmannii* (RTPR), require 5'-deoxyadenosylcobalamin (AdoCbl) as a cofactor. Class III enzymes, represented by RNR from anaerobically grown *E. coli* (anaerobic RTPR), contain an iron-sulfur cluster and bind S-adenosylmethionine (AdoMet) to generate a glycy radical. Class IV enzymes, not very well characterized, represented by RNR from *Brevibacterium ammoniagenes*, require a dinuclear manganese center and tyrosyl radical for catalysis.^{6,7}

The most recent proposal by Stubbe and coworkers for a generic nucleotide reduction mechanism is shown in Scheme 1.3.⁵ The key steps involve a cofactor-mediated formation of a transient thiyl radical which initiates the nucleotide reduction process by abstracting the 3'-hydrogen atom.⁸ After loss of H₂O, the two cysteines on the α -face of the nucleotide deliver the required reducing equivalents, generating a 3'-

ketodeoxynucleotide and a disulfide radical anion. This intermediate is subsequently reduced to give deoxynucleotides and a disulfide, regenerating the thiyl radical.

Ribonucleotide Reductase from *Thermoplasma acidophila*

The ribonucleotide reductase from the archaeobacterium *Thermoplasma acidophila* was first purified and its gene was cloned and sequenced in Benner's laboratory.^{9,10} It was then expressed in *E. coli* and shown to be a ribonucleoside diphosphate reductase (*T. acidophila* RDPR) and to require 5'-deoxyadenosylcobalamin (AdoCbl) as a cofactor for catalysis. The complete gene sequence of *T. acidophila* RDPR is shown in Appendix I. Benner's interest in evolution was the driving source for cloning and sequencing of this reductase and he has carried out extensive sequence comparison with other RNR. These studies revealed that the N-terminal segment (residues 1-150) of *T. acidophila* RDPR is homologous to the glycyl radical dependent anaerobic RNR (Class III) from *E. coli*; a second segment (residues 250-680) homologous to the catalytic domain of the iron-dependent aerobic RNR (Class I) R1 subunit from *E. coli*, yeast, and mammals and includes the redox active cysteines (Cys-250 and Cys-445) and the putative thiyl radical (Cys-434). Sequence searches also have established homology between the catalytic domain of AdoCbl-dependent RNR (class II) from *L. leichmannii* with another AdoCbl-dependent RNR from *Mycobacterium tuberculosis* which aligns well with the *T. acidophila* RNR sequence (residues 250-680). Therefore, while no similarity exists to adequately establish homology between the AdoCbl-dependent *L. leichmannii* RNR sequence and the iron-dependent aerobic *E. coli* RNR sequence, the statistically significant connections of the *L. leichmannii* RNR sequence via the *M. tuberculosis* RNR sequence to the *T. acidophila* RNR sequence then to aerobic *E. coli* RNR sequence permits a bridge to be made between the catalytic domain of the AdoCbl-dependent *L. leichmannii* RNR and the catalytic domain of the iron-dependent *E. coli* RNR.¹⁰

It is proposed by Reichard⁴ that all three classes of RNRs evolved from a common ancestor - i.e., divergent evolution based on the facts that the allosteric regulation patterns and the basic catalytic mechanisms of all the RNRs are conserved although the three classes of RNRs possess different substrate specificity and use different cofactors for radical generation. The discovery of the *T. acidophila* RNR sequence, together with the recently discovery of another AdoCbl-dependent RNR from archaeon *Pyrococcus furiosus*¹¹, which bears sequence homology to class I and class II RNRs, further provides convincing sequence evidences between the different classes of RNRs and strongly supports Reichard's proposal that all thress classes of RNRs evolved from a common ancestor.^{10,11} From both an evolutionary point of view, the study of the allosteric regulation pattern and mechanism of *T. acidophila* RDPR becomes especially interesting.

Building on previous work carried out in Benner's laboratory, *T. acidophila* RDPR has been expressed and purified in the Stubbe laboratory. Various activity assays have been developed for further allosteric regulation and mechanistic studies.

Materials and Methods

Materials

The clone pET23b/#8/0081293 in *E. coli* strain BL21(DE3)pLysS for the overexpression of the *Thermoplasma acidophila* RDPR was obtained from Steven Benner's laboratory at the University of Florida.^{9,10} The JM109 and BL21(DE3) competent cells were obtained from Novagen.

E. coli thioredoxin (TR) and thioredoxin reductase (TRR) were isolated from overproducing strains SK3918 (S.A. = 500 AU DTNB reduced·mg⁻¹·min⁻¹)¹² and K91/pMR14 (S.A. = 50 AU DTNB reduced·mg⁻¹·min⁻¹).¹³ Restriction endonucleases (NotI, NdeI, HindIII, and BamHI) were from New England Biolabs. Calf intestine

alkaline phosphatase (CIP) and DNase were from Boehringer Mannheim. QIAGEN-tip 100 Kit for plasmid extraction was from QIAGEN.

Cytidine 5'-diphosphate (CDP), adenosine 5'-diphosphate (ADP), guanosine 5'-diphosphate (GDP), 2'-deoxycytidine (dC), cytidine (C), 2'-deoxyadenosine (dA), adenosine (A), 2'-deoxyguanosine (dG), guanosine (G), 2'-deoxyguanosine-5'-triphosphate (dGTP), 5'-deoxyadenosylcobalamin (AdoCbl), nicotinamide adenine dinucleotide phosphate, reduced form (NADPH), streptomycin sulfate, phenylmethanesulfonyl fluoride (PMSF), adenosine 5'-triphosphate (ATP), potassium tetraborate, high range protein molecular weight standards (cat. M-3788, SDS-6H), bovine serum albumin (BSA), ampicillin, chloramphenicol, Q-Sepharose Fast Flow (cat. Q-1126) chromatography resin, and Sephadex G-25 Medium Fractionation Range (cat. G-25-150) chromatography resin were from Sigma. [5,8-³H]-ADP (28.5 Ci/mmol), [8, 5'-³H]-GDP (39.5 Ci/mmol), and [2-¹⁴C]-CDP (59.1 mCi/mmol) were from NEN. [5-³H]-CDP (22 Ci/mmol) was from Amersham Life Sciences. Powdered Trypton, Yeast Extract, and Agar were from Difco. Tris and IPTG were from Boehringer Mannheim. HEPES was from USB. EDTA, MgCl₂, MgSO₄, dithiothreitol (DTT), ammonium sulfate (AS), and hydroxyurea were from Mallinckrodt. Sep-pak C₁₈ cartridge, Centricons (Centriprep-30), and membranes (YM30) for Amicon ultrafiltration devices were provided by Millipore. AG 1-X2 Resin (50-100 mesh, chloride form) and β-mercaptoethanol were from Bio-Rad. BakerFlex II-F silica gel TLC plates (20 x 20 cm) were provided by VWR Scientific. [5'-³H] AdoCbl (8.1 × 10⁶ cpm/μmol) was kindly provided by Stuart Licht. dATP-Sepharose affinity resin was synthesized by extensive modifications of the procedure of Berglund & Eckstein¹⁴, as described by Knorre et al.¹⁵

UV-visible absorption spectra were recorded on a Hewlett-Packard 8452A diode-array spectrophotometer. All scintillation counting was performed on a Beckman LS 6500 multi-purpose scintillation counter using 9 mL Poly-Fluro scintillation fluid from PACKARD per 1 mL of aqueous solution. High Pressure Liquid Chromatography

(HPLC) was carried out using a Beckman 110 Solvent Delivery Module, 421A Controller, and a 163 Variable Wavelength Detector, in combination with an Alltech Econosil C₁₈ column.

Extraction and Restriction Mapping of Plasmid RNR/pET23b(+)

The initial glycerol stock of the clone pET23b/#8/0081293 in BL21(DE3)pLysS was streaked onto a fresh LB agar plate containing 100 µg/mL ampicillin and 30 µg/mL chloramphenicol, and incubated at 37°C overnight. A single colony was picked to inoculate a 10 mL LB culture containing 100 µg/mL ampicillin and 30 µg/mL chloramphenicol. After 12 h growth at 37°C, the cells were spun down in a 50 mL centrifuge tube at 6,000g for 15 min. The plasmid RNR/pET23b(+) was extracted using the QIAGEN-tip 100 Kit following the manufacturer's protocol.

Approximately 1 µg of extracted plasmid DNA was digested with restriction endonucleases HindIII, BamHI, and NotI+NdeI respectively in the manufacture-recommended NEB (New England Biolabs) buffers.

Quantitation and Gel Electrophoresis of Protein

The method of Lowry was used to determine the protein concentration.¹⁶ BSA was used as the protein standard. The SDS-PAGE method was used to analyze proteins based on their sizes.¹⁷ For the analysis of *T. acidophila* RDPR (calculated MW = 96.9 kDa), 7.5% polyacrylamide gels were used. Two high range MW markers from Sigma were used. The first one (cat. SDS-6H) contained bands of 29, 45, 66, 97.4, 116, and 205 kDa; the second one (cat. M-3788) contained bands of 36, 45, 55, 66, 84, 97, 116, and 205 kDa respectively.

Transformation of RNR/pET23b(+) into BL21(DE3) and JM109

The plasmid RNR/pET23b(+) was transformed into BL21(DE3) and JM109 strains respectively following Novagen's transformation protocol. LB agar plates containing 100 µg/mL ampicillin were used for colony selection.

Small Scale Induction to Analyze for Maximal Expression of *T. acidophila* RDPR

The experiment was done on both the original clone pET23b/#8/0081293 in BL21(DE3)pLysS and the new transformants in BL21(DE3). A single colony was used to inoculate a 10 mL LB culture containing the appropriate antibiotics (100 µg/mL ampicillin and 34 µg/mL chloramphenicol for the BL21(DE3)pLysS host strain; 100 µg/mL ampicillin for the BL21(DE3) host strain) and grown at 37°C. After the cell culture A_{600} reached between 0.6-1.0, IPTG was added to 0.6-1 mM final concentration. At each time point (0, 1, 2, 3, and 4 h), 1 mL cell culture was taken and spun down in a 1.5-mL Eppendorf tube in a microcentrifuge for 1 min after recording A_{600} . The supernatant was discarded and the Eppendorf tube was briefly spun for another 5 secs. Any remaining LB medium was removed with a pipet tip. The cell pellet was then resuspended in 2X SDS-PAGE gel loading buffer, typically 30-50 µL, to a final A_{600} of 30. The Eppendorf tube was then placed in a 100°C sand bath for 3 min and spun in a microcentrifuge for 1 min to pellet the cell debris. A 10-µL aliquot of the supernatant (~20 µg total protein) was loaded onto a 7.5% SDS-PAGE gel.

Tritium Exchange Assay on Crude Cell Lysate

RNR/pET23b(+)/BL21(DE3) cells (2.66 g) and RNR/pET23b(+)/JM109 cells (3.88 g), both obtained from a 500-mL culture started with a single colony, induced with 1 mM IPTG at $A_{600} = 0.5$, were resuspended in 12 mL of 0.1 M Tris-HCl, pH 8.0 at 4°C respectively. The cell suspension was passed through a small French Press cell at 16,000 psi. The lysate was centrifuged at 6,000 g for 15 min to remove the cell debris.

The tritium exchange assay procedure was a simplification of the standard procedure previously described.¹⁸ All procedures were carried out in the dark under dim red lights. An assay mixture of 50 μ L contained: 50 μ M ADP, 1 mM dGTP, 10 mM MgSO_4 , 10 mM DTT, 100 mM Tris-HCl pH 8.0, 90 μ M [$5\text{-}^3\text{H}$] AdoCbl (S.A.= 8.1×10^6 cpm/ μ mol), and lysate (0-17 μ L, 0-1000 μ g protein). The mixture except lysate was pre-incubated at 55°C for 5 min. Lysate (or buffer, in the control case) was added to start the exchange reaction. The reaction was stopped after 30 min by loading the mixture onto a Sep-pak C₁₈ cartridge which had been previously washed with 10 mL of MeOH followed by 10 mL of H₂O. The cartridge was washed with 3 mL of H₂O, and a 1-mL aliquot was removed for scintillation counting.

Activity Assays for *T. acidophila* RDPR

All the activity assays for *T. acidophila* RDPR were performed at 55°C in the dark under dim red lights.

[5, 8 -³H]-ADP Assay

This assay procedure was a modification of the previously described ADP assay procedure.¹⁰ The concentrated [5, 8-³H]-ADP stock (Lot number: 3238-149, 28.5 Ci/mmol, 99.5% as of 5/20/96) was lyophilized to remove ethanol and diluted with unlabelled ADP to desired specific activity. A typical final assay mixture contained in a volume of 260 μ L: 10 μ M ADP (S.A. = $\sim 2 \times 10^5$ cpm/nmol), 1 mM dGTP, 1 mM MgCl_2 , 10 mM DTT, 100 μ M AdoCbl, 25 mM HEPES pH 7.5, and 0.1-0.2 μ M (0.5-1 μ g/50 μ L) *T. acidophila* RDPR. The mixture including everything except AdoCbl was pre-incubated at 55°C for 2 min. At time zero a 50- μ L (usually <50 μ L, if corrected for AdoCbl volume) aliquot was removed, placed in a boiling water bath for 2 min, and then placed on ice. AdoCbl was added in the dark to start the reaction. A 50- μ L aliquot was removed at each desired time point. The aliquot was heated in a boiling water bath for 2 min to

stop the reaction, and then placed on ice. After all the time points were taken, 5 μ l of 1 M Tris solution (pH~11) and 5 U of calf intestine alkaline phosphatase were added to each aliquot. The solution was then incubated at 37°C for 1 h.

Deoxyadenosine (dA) was separated from adenosine (A) by chromatography on a (6.7 x 10 cm) silica gel plate (1/6 of the original (20 x 20 cm) plate) eluting with potassium tetraborate saturated methanol.¹⁰ Five time points (from a 260- μ L total assay volume) were spread evenly over the 6.7 cm length. Prior to chromatography, 10 nmol (1 μ L of 10 mM solution) of carrier dA and A were spotted onto the TLC plate respectively followed by 5 μ L of the ~ 60 μ L sample onto the same spot where carriers were spotted. The plate was dried with a heat gun, and then eluted with potassium tetraborate saturated methanol for ~ 40 min. The plate was visualized using UV light and the region of the plate containing the desired compound (dA) was cut out and soaked in 1 mL of water in a 20-mL scintillation vial for 10 min before the addition of 9 mL of Poly-Fluro scintillation fluid. The sample was well mixed by shaking and counted for 5 min. As a control, 5 μ l of the sample before TLC chromatography was also spotted onto TLC plate and analyzed for total radioactivity (dA + A) subsequent to elution with H₂O under same conditions. Product formed was calculated from the percentage of radioactivity of dA over the total radioactivity of dA and A.

[8, 5'-³H] -GDP Assay

The assay procedure was similar to the [5, 8-³H]-ADP assay described above. The concentrated stock of [8, 5'-³H] -GDP (Lot number: 3232-250, 39.5 Ci/mmol, 98.8% as of 10/28/96) was diluted with unlabelled GDP to the desired specific activity. Carrier dG and G (10 nmol, 1 μ L of 10 mM solution) were spotted onto the TLC plate respectively before the chromatography step. A typical final assay mixture contained in a volume of 260 μ L: 10 μ M GDP (S.A. = ~ 2 x 10⁵ cpm/nmol), 1 mM MgCl₂, 10 mM DTT, 100 μ M AdoCbl, 25 mM HEPES pH 7.5, and 0.1-0.2 μ M (0.5-1 μ g/50 μ L) *T. acidophila* RDPR.

[5-³H]-CDP Assay

The assay procedure was similar to the [5, 8-³H]-ADP and [8, 5'-³H]-GDP assay procedures described above. The concentrated stock of [5-³H]-CDP (Batch 41, 22 Ci/mmol, 95.9% as of 3/12/96) was diluted with unlabelled CDP to the desired specific activity. Carrier dC and C (10 nmol, 1 μ L of 10 mM solution) were spotted onto the TLC plate respectively before the chromatography step. A typical final assay mixture contained in a volume of 260 μ L: 10 μ M CDP (S.A. = $\sim 2 \times 10^5$ cpm/nmol), 1 mM MgCl₂, 10 mM DTT, 100 μ M AdoCbl, 25 mM HEPES pH 7.5, and 0.1-0.2 μ M (0.5-1 μ g/50 μ L) *T. acidophila* RDPR.

[2-¹⁴C]-CDP Assay

This assay procedure was a modification of the previously described [2-¹⁴C]-CTP assay procedure for RTPR.¹⁸ The concentrated stock of [2-¹⁴C]-CDP (Lot number: 3232-100, 59.1 mCi/mmol, 97.9% as of 1/29/96) was diluted with unlabelled CDP to the desired specific activity. A typical assay mixture contained in a final volume of 510 μ L: 1 mM CDP ($\sim 2 \times 10^3$ cpm/nmol), 1 mM dGTP, 1 mM MgCl₂, 30 mM DTT, 25 mM HEPES pH 7.5, 100 μ M AdoCbl, and 10 μ M (100 μ g/ 100 μ L) *T. acidophila* RDPR. The entire mixture, except AdoCbl, was pre-incubated at 55°C for 2 min. At time zero, a 100- μ L aliquot (usually <100 μ L, if corrected for AdoCbl volume) was removed and quenched with 50 μ L of 2% pre-chilled perchloric acid. AdoCbl was then added in the dark to start the reaction. A 100- μ L aliquot was removed at each time point, quenched with 50 μ L 2% pre-chilled perchloric acid by vortexing, and then placed on ice. After all the time points were taken, 12 μ L of 1 M KOH was added to each sample to neutralize the solution. Alkaline phosphatase buffer (50 mM Tris pH 8.5, 1 mM EDTA) (50 μ L) was added followed by addition of 5 U calf intestine alkaline phosphatase. The samples were then incubated at 37°C for 1 h.

Deoxycytidine (dC) and cytidine (C) were separated by (0.75 x 7 cm) AG1-X2 columns (borate form, 50-100 mesh) prepared by the method of Steeper and Stuart.¹⁹ Each column was pre-washed with 20 mL of water. After carrier dC and C (120 nmol) were added to each aliquot, the sample was loaded onto the column and then eluted with 13 mL of water. A 1-mL aliquot was subjected to scintillation counting.

HPLC Analysis of [2-¹⁴C]-CDP Assay Products

The remaining 12-mL aliquot of the 13-mL eluate from the [2-¹⁴C]-CDP assay described above was lyophilized and redissolved in 1 mL of H₂O. The 1-mL aliquot was subjected to reverse phase HPLC analysis using an Econosil C₁₈ column with H₂O as the eluate. At a flow rate of 1 mL/min, the column was washed with MeOH for 15 min and the eluate was switched to H₂O over a period of 15 min. The column was equilibrated in H₂O for an additional 15 min. After sample injection, the column was washed with H₂O at a flow rate of 1 mL/min, and 1-mL fractions were collected and analyzed by scintillation counting. Cytosine, cytidine (C), and deoxycytidine (dC) eluted isocratically in H₂O at ~ 5, 8.5, and 13 min respectively.

HPLC Analysis of [2-¹⁴C]-CDP

[2-¹⁴C]-CDP was converted to cytidine (C) by alkaline phosphatase and then analyzed by reverse phase HPLC to determine the radiochemical purity of the original [2-¹⁴C]-CDP. The reaction mixture contained in 50 µL: 0.27 µM [2-¹⁴C]-CDP (Lot number: 3232-100, S.A. = 2182 cpm/nmol), 5 U alkaline phosphatase, 5 mM Tris pH 8.5, 0.1 mM EDTA. The mixture was incubated at 37°C for 1 h, and 10 µL was diluted to 1 mL followed by the reverse phase HPLC analysis similar to the [2-¹⁴C]-CDP assay product analysis described above. The flow rate was reduced to 0.8 mL/min, and 0.8-mL fractions were collected and analyzed by scintillation counting. Cytosine, cytidine

(C), and deoxycytidine (dC) eluted isocratically in H₂O at ~ 6, 10.6, and 16 min respectively (corresponding to ~ 5, 8.5, and 13 min at 1 mL/min flow rate).

Large Scale Growth of *T. acidophila* RDPR Overproducing Strain

RNR/pET23b(+)/BL21(DE3)

This protocol was for a 15-L growth (10 x 1.5 L in 4 L flasks) using two floor shakers. Two freshly transformed colonies of the *T. acidophila* RDPR overexpressing strain RNR/pET23b(+)/BL21(DE3) were used to inoculate 2 x 100 mL LB media in 500 mL flasks. Ampicillin was freshly added to liquid LB medium to 100 µg/ mL at all stages. After ~ 10 h overnight growth at 30-32°C, 5 mL from one of the two 100 mL cultures ($A_{600} = \sim 0.77, 0.89$ respectively) was used to start each 1.5 L media in a 4 L flask at 37°C. When A_{600} reached ~ 0.6-0.8 after ~ 5 h growth (doubling time ~ 30 min), IPTG was added to 0.8 mM. A 1-mL sample was removed every h and A_{600} was recorded. Cells were harvested 4 h after induction by centrifugation at 8,000 g for 20 min, rapidly frozen in liquid nitrogen, and then stored at -80°C. Typically, ~23 g cells were obtained from the 15 L growth. A 7.5% SDS-PAGE gel was run to check the induction of *T. acidophila* RDPR.

Purification of *T. acidophila* RDPR

The purification procedure was modified from the original procedure developed by Tauer and Benner.¹⁰ All purification steps were carried out at 4°C. Aliquots of 100-500 µL were saved, from each stage of the purification for subsequent protein concentration determination and activity assays. Tris buffer was used throughout the entire purification process: 50 mM Tris, 1 mM EDTA, pH 8.0 (at 4°C) with freshly added 1 mM β-mercaptoethanol (70 µL/L). All columns were pre-equilibrated in this buffer and approximately 9-10 L was required for the entire purification.

Cells (23 g) were thawed and resuspended in ~ 90 mL Tris buffer, and lysed by passing through a French Press at 16,000 psi. Cell debris was removed by centrifugation at 10,000 g for 20 min. PMSF (dissolved in minimum amount of ethanol, ~ 1 mL) was added to 1 mM (0.17 mg/mL) final concentration to the supernatant. With stirring, streptomycin sulfate solution (5% (w/v) in Tris buffer) was added slowly to a final concentration of 1% (w/v) over a period of 15 min. The solution was stirred for an additional 15 min. Precipitated DNA was then removed by centrifugation at 10,000 g for 20 min. Ammonium sulfate solid was then added to the supernatant (~110 mL) slowly with stirring to 60% saturation (390 g/L) over a period of 20 min and the solution was left stirring for an additional 30-40 min. The protein precipitate was recovered by centrifugation at 10,000 g for 20 min. The protein pellet was then dissolved in ~ 22 mL of Tris buffer and loaded onto a (4.5 x 30) cm Sephadex G25 column (~ 500 mL bed volume) equilibrated in Tris buffer to remove excess ammonium sulfate and other small molecules. The protein containing fractions were pooled (~ 170 mL) and the conductivity was checked to ensure clean desalting.

The desalted protein solution was loaded onto a (6 x 16) cm Q-Sepharose Fast Flow column (~ 500 mL bed volume) equilibrated in Tris buffer and washed with Tris buffer until A_{280} reading was less than 0.1 to remove non-binding proteins. *T. acidophila* RDPR was then eluted with a linear (500 mL x 500 mL) 0 - 0.5 M NaCl gradient in Tris buffer containing 1 mM (0.17 mg/mL) PMSF. Activity assays (described in next section) as well as SDS-PAGE gels were run on every 2-3 fractions (400 drops, ~ 15 mL per fraction) and the *T. acidophila* RDPR containing fractions were pooled (~ 350 mL, eluting at ~ 0.3 M NaCl). The solution was then concentrated by the 400-mL Amicon using YM30 membrane to ~ 25 mL and then diluted back to 250 mL to decrease its ionic strength. The diluted protein solution was loaded onto a (3 x 20 cm) dATP-Sepharose affinity column at a rate of less than 1 mL/min. The affinity column was then washed with Tris buffer until A_{280} was less than 0.1. A 7.5% SDS-PAGE gel was run on the flow-through

to check affinity binding. *T. acidophila* RDPR was then eluted with 100 mL of 10 mM ATP in Tris buffer (pH carefully adjusted back to 7.6) and then washed with Tris buffer. The ATP containing fractions (~ 150 mL) were then combined and concentrated by the 400-mL Amicon with YM30 membrane. The solution was concentrated and diluted several times until A_{260} of the flow through was less than 0.05, ensuring the removal of excess ATP. The final protein solution was further concentrated via Centriprep-30 (clear base, MW cut-off 30,000 kDa) and exchanged into the storage buffer: 50 mM Tris pH 8.0, 1 mM EDTA, 1 mM DTT, 15% glycerol. The solution was rapidly frozen in liquid nitrogen and stored in aliquots at -80°C .

The G-25 column was cleaned by washing with 3 volumes of H_2O . The Q-Sepharose Fast Flow column was cleaned by washing with 3 volumes of 1 M NaCl. The dATP-Sepharose affinity column was cleaned immediately after use with 4 volumes of 0.1% SDS in H_2O at room temperature followed by an additional 4 volumes of H_2O .

Protein Analysis During Purification

A modified [5, 8- ^3H]-ADP assay was used during *T. acidophila* RDPR purification to monitor the activity for its convenience and time efficiency relative to the standard [5, 8- ^3H]-ADP assay described above. Typically, a cocktail for 40 assays (1.6-mL total volume) was prepared for each purification. All reagents including AdoCbl, but without *T. acidophila* RDPR were pre-mixed and stored frozen at -20°C wrapped in foil. The concentration of the reagents was 1.25x the desired final concentration: 10 μM ADP (S.A. = $\sim 2 \times 10^5$ cpm/nmol), 1 mM dGTP, 1 mM MgCl_2 , 10 mM DTT, 100 μM AdoCbl, 25 mM HEPES pH 7.5, 15 mM hydroxyurea. Hydroxyurea was added to prevent the interference from *E. coli* RNR activity. For a 50- μL total reaction mixture, 40 μL was from the assay cocktail and 10 μL was from either the protein solution or Tris buffer. A single fixed time point of 10-15 min at 55°C was used subsequent to the addition of protein solution to start the reaction. Removal of the phosphates with calf intestine

alkaline phosphatase was shortened to 30 min. No background counting control was performed, and the sample was only counted for 3 min. The assay can be completed in ~ 3 h.

Complimentarily, 7.5% SDS-PAGE gels were used to follow the course of purification. If the gels were prepared before starting a column, the entire procedure can be completed within 1.5 to 2 h.

Determination of Extinction Coefficient

Purified *T. acidophila* RDPR was treated with DNase in a volume of 1.1 mL: 25 mM HEPES (pH 7.5), 0.12 mM *T. acidophila* RDPR (12 µg/µL), 20 U DNase, 1 mM MgCl₂. The mixture was incubated at room temperature for 15 min. The protein solution was then loaded onto a (1.5 × 4.5) cm Sephadex G-25 column pre-equilibrated in Tris buffer (50 mM Tris, pH 8.0 at 4°C, 1 mM DTT) and washed with the same buffer. Fractions of 1 mL were collected and UV spectrum was taken. Protein concentration was determined on the same fraction using BSA as the protein standard. Extinction coefficient of *T. acidophila* RDPR was calculated according to Beer-Lambert Law.

Results and Discussion

Extraction and Restriction Mapping of Plasmid RNR/pET23b(+)

The restriction map of *T. acidophila* RDPR is attached in Appendix II. Since the plasmid RNR/pET23b(+) was extracted from BL21(DE3)pLysS cells, plasmid pLysS was extracted at the same time. The restriction maps of plasmid RNR/pET23b(+) (6.2 kb), and pLysS (4.9 kb) are shown in Figure 1.1 and Figure 1.2.

From the plasmid map, it can be seen that for RNR/pET23b(+), all four enzymes (NotI, NdeI, HindIII, and BamHI) are single cutters; for pLysS, BamHI cuts twice at location 1.87 kb and 2.51 kb, HindIII cuts once at location 1.5 kb, and neither NotI nor

NdeI cuts. The expected band sizes from the digests performed are listed in Table 1.1. The experimental results with HindIII, BamHI, and NotI+NdeI digests are shown in Figure 1.3 and Figure 1.4.

In Figure 1.3, the HindIII digest gave the expected 6.2 kb band for RNR/pET23b(+) and 4.9 kb band for pLysS. In Figure 1.4, BamHI digestion gave the expected 6.2 kb band for RNR/pET23b(+) and 0.64 kb, 4.26 kb bands for pLysS. The 0.64 kb band was rather faint on the agarose gel. The double digestion with NotI and NdeI gave bands of 2.65 kb and 3.55 kb for RNR/pET23b(+) and uncut circular pLysS which migrated differently from linear DNA. Colony 4 gave extra bands in the NotI+NdeI double digest which could have arisen from supercoiled circular pLysS DNA. Overall, the restriction mapping pattern confirmed the presence of both plasmids.

Small Scale Induction Check on *T. acidophila* RDPR Expression

No obvious induction was observed with the original clone pET23b/#8/0081293 in BL21(DE3)pLysS obtained from Benner. Modest induction was observed with the new transformants. A typical growth curve of RNR/pET23b(+)/BL21(DE3) is shown in Figure 1.5. The cell growth slowed down upon the addition of IPTG which usually correlates well with good induction. Induction was observed at starting A_{600} of 0.6-1.0, IPTG 0.6-1 mM. To save time and material, the final induction condition was chosen to be at A_{600} of 0.6-0.8 with 0.8 mM IPTG. Since maximum overexpression of *T. acidophila* RDPR is at a level estimated to be ~5% of total cellular protein, it is important not to overload the SDS-PAGE gel in order to observe clear induction on the gel. It should be noted that despite the theoretical MW of *T. acidophila* RDPR of 96.9 kDa, the enzyme migrates at 85 kDa based on the high range MW marker from Sigma as shown in Figure 1.6.

The discrepancy in MW by SDS-PAGE gel relative to its calculated MW based on gene sequence, caused us to submit the purified protein to MIT Biopolymer Lab for

automated Edman sequencing. The results, attached in Appendix III, are identical to that predicted by the gene sequence: MIKEV. Although C-terminal clipping remains a possibility, the fact the recombinant *T. acidophila* RDPR retains the native specific activity makes it less likely. It was also observed that RNR from archaeon *Pyrococcus furiosus* had a deduced protein MW of 200 kDa where as the native protein had a MW of 90 kDa as reported by Fontecave's Laboratory in France.¹¹ This discrepancy was caused by the presence of two inteins within the 200 kDa protein which presumably were spliced out to generate the 90 kDa mature enzyme. The presence of inteins in *T. acidophila* RDPR could also be a possibility for the MW discrepancy as there is "an apparently significant predisposition for inteins to insert within genes encoding DNA and nucleotide modifying enzymes of Archae.¹¹"

Tritium Exchange Assay on Crude Cell Lysate

This specific tritium exchange assay carried out was rather simplified as the purpose of the experiment was to check the expression of *T. acidophila* RDPR in BL21(DE3) cells. Only one time point was taken. The standard procedure¹⁸ should be followed for more quantitative analysis. Although it was previously shown that 3 mL of H₂O was sufficient to remove all the ³H₂O from the assay mixture,¹⁸ this control reaction should have been repeated.

The experimental results are listed in Table 1.2. When no lysate was added, there was a basal tritium exchange rate over the course of 30 min at 55°C. The host strain JM109 does not contain DE3 gene that produces T7 polymerase upon IPTG induction, thus no *T. acidophila* RDPR was expressed in JM109 cells. The result showed a slightly higher cpm value above background controls, with no enzyme dependence. This also showed that in normal *E. coli* cells, there was no significant tritium exchange activity which is specific for AdoCbl-dependent RNRs. Clear enzyme dependence was observed for BL21(DE3) host cells with the radioactivity released being significantly

above the background level indicating the expression of *T. acidophila* RDPR. These results clearly showed the overexpression of *T. acidophila* RDPR in BL21(DE3) upon IPTG induction.

Activity Assays for *T. acidophila* RDPR

Due to the low specific activity of *T. acidophila* RDPR (< 100 nmol/mg/min) compared with other RNRs, the coupled spectrophotometric assay with TR/TRR/NADPH reducing system is not sensitive enough for the detection of enzymatic activity. Therefore, radioactive assays are used for *T. acidophila* RDPR.

For the assays using ³H-labelled nucleotides, a sample TLC plate showing the separation of dA from A, dC from C, and dG from G is shown in Figure 1.7 with their R_f values listed in Table 1.3. It is shown that C and G do not dissolve very well in the eluent, thus leaving a long faint trail on the plate. However, the fact that the deoxynucleosides have greater R_f values relative to the nucleosides makes the product analysis possible. Clear time dependence was observed for the TLC based assays. Sample assay time curves are shown in Figure 1.8, Figure 1.9, and Figure 1.10 for the [5, 8-³H]-ADP, [8, 5'-³H]-GDP, and [5-³H]-CDP assays respectively.

To obtain good separation, particularly for dA and A, it was important to keep the spot small, dry the plate well, and preferably run the solvent front for greater than 8 cm. The background counts that co-migrate with the deoxynucleosides in time zero points for the TLC based assays relative to total radioactivity are close to the radiochemical impurity of the starting materials.

A sample assay time curve for the [2-¹⁴C]-CDP assay is shown in Figure 1.11. The time zero time point typically gave a high background of 300-400 cpm (corresponding to ~ 2% of total counts). It was noticed that the new lot purchased (Lot number: 3232-100) had a radiochemical purity of 97.9% as of 1/29/96 while the previous lot (Lot number: 2901-101) had a radiochemical purity of 99.5% as of 5/11/92. The same high

background was observed with different lots of borate columns. The HPLC analysis of the [2-¹⁴C]-CDP assay products, as shown in Figure 1.12, shows impurities eluting off at 3-5 mL. There is no peak at ~ 8.5 mL where C elutes as expected. At assay time point zero, there is no peak at ~ 13 mL where dC elutes; after 1 min, small amount of product dC is formed. The HPLC analysis on the [2-¹⁴C]-CDP substrate, as shown in Figure 1.13, shows impurities eluting at 3-5 mL before the major peak of C. The HPLC analysis results suggest that the high background is not caused by the borate column separation step. It likely arises from the impurity present in the initial substrate, possibly cytosine which elutes at ~ 5 mL and some other derivatives that can pass through the borate column. Although the background counts are high compared with previous experience in the Stubbe lab, it is still tolerable for current experimental purposes. For single turnover experiments, further purification of the substrate is required.

Attempts to use borate columns to separate dC from C in the [5-³H]-CDP assay as in the [2-¹⁴C]-CDP assay gave very high background counts (~ 10% of the total radioactivity loaded). This could be explained by the tritium washout by H₂O in the 5 position. Therefore, the TLC separation method is recommended for the [5-³H]-CDP assay.

Overall, when a comparison is made between the [2-¹⁴C]-CDP assay and the [³H]-nucleotide assays, the TLC based assays using [5, 8-³H]-ADP, [8, 5'-³H]-GDP, and [5-³H]-CDP are cost-efficient (~ \$300/250 μCi vs. ~ \$400/10 μCi) and have a higher sensitivity as the substrates have a higher specific activity. Therefore, the [³H]-nucleotide assays have been used during the enzyme purification process as only 0.5-1 μg protein are required per 50 μL assay aliquot, as well as in the allosteric regulation studies when low substrate concentrations (< 10 μM) are studied (Chapter 2). However, the borate column based [2-¹⁴C]-CDP assay is faster and better established than the TLC based assays.

Large Scale Growth of *T. acidophila* RDPR Overproducing Strain RNR/pET23b(+)/BL21(DE3)

As plasmid RNR/pET23b(+) carries ampicillin resistance, plasmid stability could be a potential problem.²⁰ Plasmid stability was checked once on a small 10 mL culture starting from a single colony following the standard protocol,²⁰ and no plasmid loss was observed. However, when liquid culture transfer was involved as when a small overnight culture was used to start a larger culture, the dilution factor becomes very important. Dilution of 1:40 was carried out once and the induction was very poor likely the result of plasmid loss. It was also noted that the A_{600} reading did not slow down upon addition of IPTG in that specific growth. It is thus recommended to use at least 1:200 dilution, especially when the overnight culture has reached stationary phase of $A_{600} \sim 1.3$. If the small culture is started from a single colony early in the morning and used before A_{600} reaches 1.0, the dilution factor can be lowered to 1:40. Overall, it is a good idea to minimize the final A_{600} of the small culture (by lowering growth temperature and reducing growth time) and to maximize the dilution factor at reasonable time expense.

Purification of *T. acidophila* RDPR

The purification procedure involves removal of nucleic acid and protein by standard batch fractionation procedures, followed by anion exchange chromatography on Q-Sepharose column. The results of the latter are shown in Figure 1.14 and Figure 1.15. The relative specific activity (cpm/ A_{280}) corresponded very well to the relative intensity of the *T. acidophila* RDPR band on SDS-PAGE gels. *T. acidophila* RDPR elutes at ~ 0.3 M NaCl as a quite sharp peak with light yellow color, followed by a broad intense yellow fraction. Based on the color, it can roughly be estimated in which fractions *T. acidophila* RDPR elutes. A shallower gradient of (500 mL x 500 mL) 0-0.5 M NaCl is now used and gives better separation.

The second column involves the use of dATP affinity column. As ATP co-elutes with *T. acidophila* RDPR, it is impossible to monitor the protein concentration with UV spectroscopy at A_{280} . One can either pool all the ATP fractions or run a quick SDS-PAGE gel (only half length of the gel needed to be run as there will only be one major band on the gel) to check the protein location and pool the appropriate fractions. An efficient way is to start concentrating the first 2-3 fractions (30-50 mL) that contain *T. acidophila* RDPR, while running the SDS-PAGE gel to check the latter fractions. A typical SDS-PAGE gel of dATP affinity column fractions is shown in Figure 1.16.

The activity assay on the dATP affinity column fractions did not correspond well with the protein density on the SDS-PAGE gel. The counts were low and at the same level for all the fractions. It could be that high ATP concentration (~ 10 mM) interfered with the assay. In the sample purification described, 100 mg of protein was obtained with specific activity of 40.5 nmol/min/mg based on the [2- 14 C] CDP assay. A sample purification table is shown in Table 1.4. A SDS-PAGE gel for the entire purification process is shown in Figure 1.17.

Determination of Extinction Coefficient

The UV spectrum of *T. acidophila* RDPR is shown in Figure 1.18. The final protein UV spectrum is found to have a max λ_{276} with a molar extinction coefficient of 56,000 $\text{cm}^{-1}\text{M}^{-1}$. However, it should be noted that it is assumed that *T. acidophila* RDPR has a similar tyrosine content as BSA which is the basis for the Lowry assay.

Sample Calculation:

$$A = \epsilon cl$$

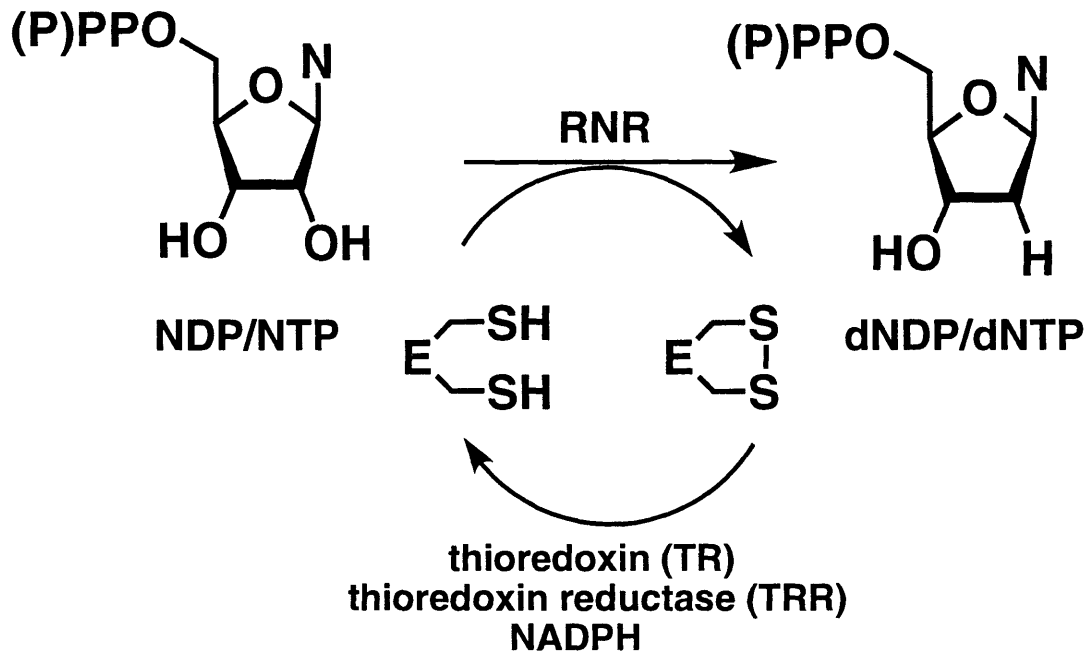
$$A_{276} = 0.52, l = 1 \text{ cm}$$

$$c = [\text{RDPR}] = 0.9275 \mu\text{g}/\mu\text{L} = 0.9275 \text{ g/L} / 10,000 \text{ g/mol} = 9.275 \mu\text{M}$$

$$\epsilon = 0.52 / 9.275 \mu\text{M} / 1 \text{ cm} = 56,000 \text{ cm}^{-1}\text{M}^{-1}.$$

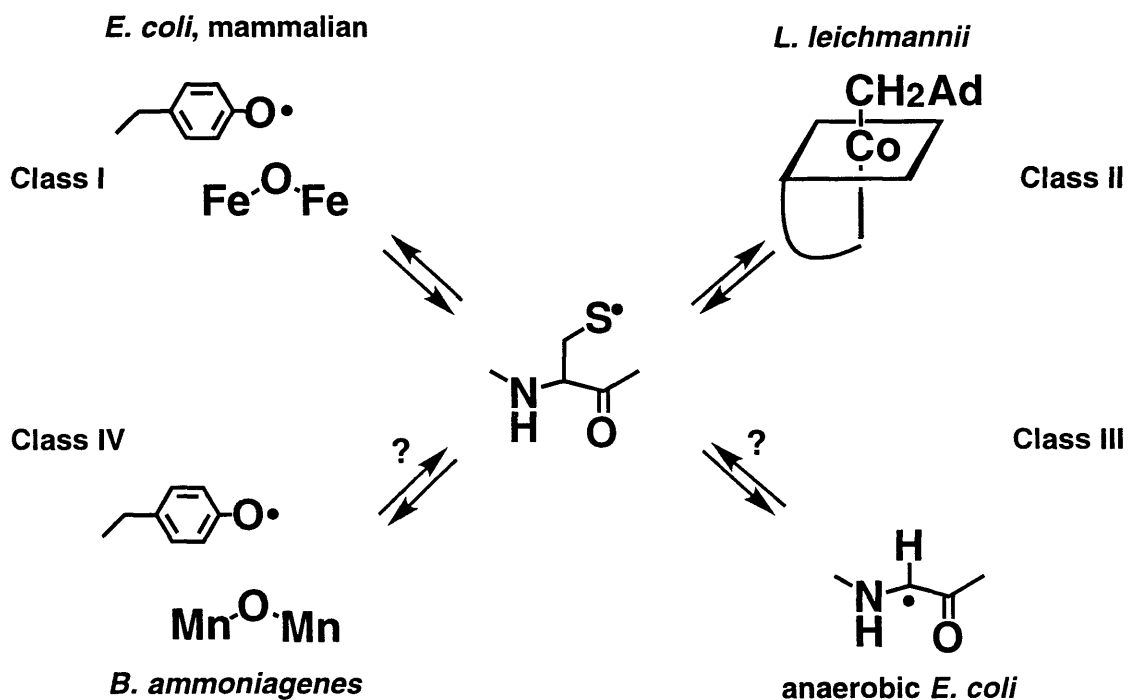
References

- (1) Thelander, L.; Reichard, P. *Ann. Rev. Biochem.* **1979**, *48*, 133-158.
- (2) Lammers, M.; Follmann, H. Ed., *The Ribonucleotide Reductases-A Unique Group of Metalloenzymes Essential for Cell Proliferation*; Springer-Verlag: Heidelberg, 1983.
- (3) Stubbe, J. *Adv. Enzymol. Relat. Areas Mol. Biol.* **1990**, *63*, 349-417.
- (4) Reichard, P. *Science* **1993**, *260*, 1773-1777.
- (5) Stubbe, J.; van der Donk, W. A. *Chem. Biol.* **1995**, *2*, 793-801.
- (6) Willing, A.; Follman, H.; Auling, G. *Eur. J. Biochem.* **1988**, *178*, 603-611.
- (7) Auling, G.; Follmann, H. in *Metal Ions in Biological Systems*; Sigel, H. Sigel, A. Ed.; Marcel Dekker, Inc., New York, 1994; Vol. 30, pp
- (8) Ashley, G. W.; Harris, G.; Stubbe, J. *J. Biol. Chem.* **1986**, *261*, 3958-3964.
- (9) Tauer, A., *Ph.D. Thesis, Eidgenossische Technische Hochschule*, **1994**.
- (10) Tauer, A.; Benner, S. A. *Proc. Natl. Acad. Sci.* **1997**, *94*, 53-58.
- (11) Riera, J.; Robb, F. T.; Weiss, R.; Fontecave, M. *Proc. atl. Acad. Sci.* **1997**,
- (12) Lunn, C. A.; Kathju, S.; Wallace, B. J.; Kushner, S.; Pigiet, V. *J. Biol. Chem.* **1984**, *259*, 10469-10474.
- (13) Russell, M.; Model, P. *J. Bacteriol.* **1985**, *163*, 238-242.
- (14) Berglund, O.; Eckstein, F. *Methods Enzymol.* **1974**, *34B*, 253-261.
- (15) Knorre, D. G.; Kurbatov, V. A.; Samukov, V. V. *FEBS Lett.* **1976**, *70*, 105-108.
- (16) Lowry, O. H., Rosebrough, N.J., Farr, A.L., & Randall, R.J. *J. Biol. Chem* **1951**, *193*, 265-275.
- (17) Laemmli, U. K. *Nature (London)* **1970**, *227*, 681-685.
- (18) Booker, S., *Ph.D. Thesis, MIT*, **1994**.
- (19) Steeper, J. R.; Steuart, C. D. *Anal. Biochem.* **1970**, *34*, 123-130.
- (20) Studier, F. W. ; R., A. H.; Dunn, J. J.; & Dubendorff, J. W. in *Methods in Enzymology*; Ed.; 1990; Vol. 185, pp 60-89.

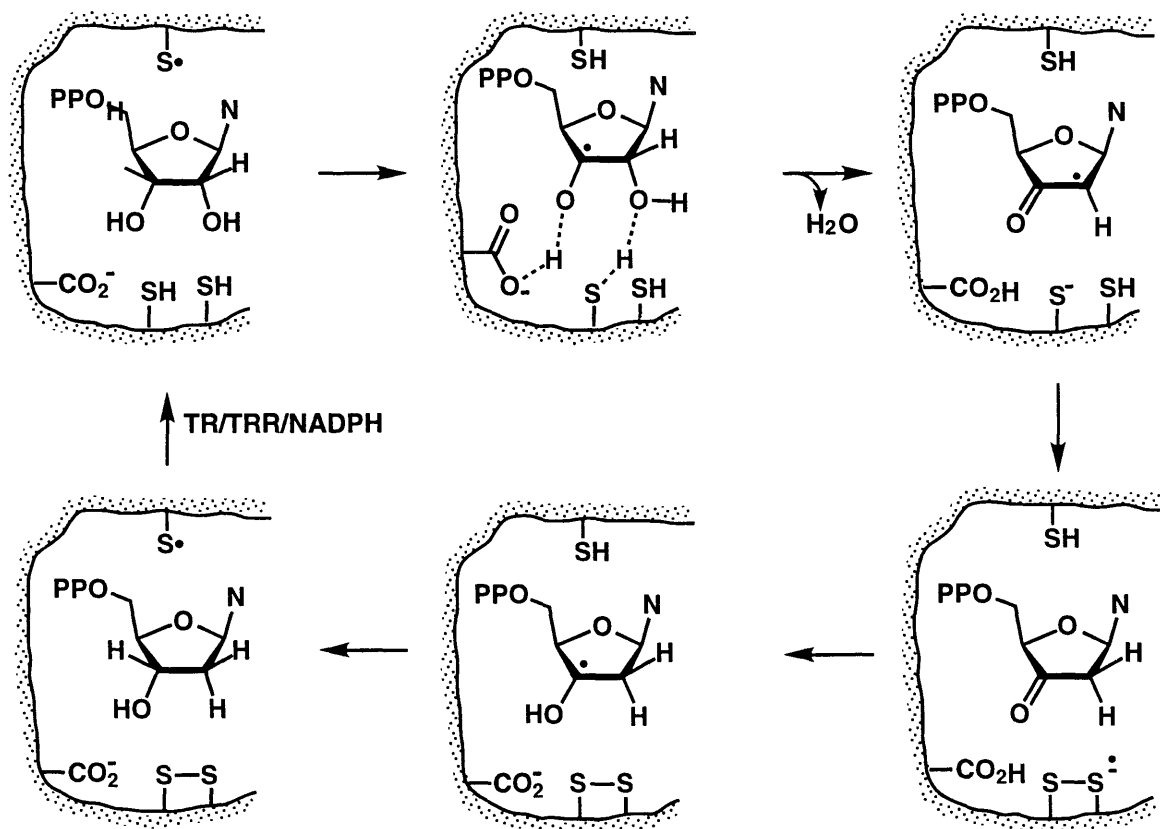


Scheme 1.1 Ribonucleotide reductase catalyzes a key step in DNA biosynthesis.

Courtesy of Dr. W. A. van der Donk.



Scheme 1.2 RNRs use a wide range of cofactors. The cofactors used by the four major classes of RNRs are shown. Although chemically diverse, it seems likely that each of these cofactors can be used to help form a thiyl radical (center), which is essential for catalysis in at least two, and probably all four, classes of RNRs. *Courtesy of Dr. W. A. van der Donk.*



Scheme 1.3 Proposed mechanism for nucleotide reduction by RNRs. A transient thiyl radical initiates the nucleotide reduction process by abstracting the 3'-hydrogen atom from the nucleoside diphosphate. H_2O is lost, and the two cysteines on the α -face of the nucleotide then deliver the required reducing equivalents, generating a 3'-ketodeoxynucleotide and a disulfide radical anion. This intermediate is subsequently reduced to give dNDP and a disulfide and to regenerate the thiyl radical. N, base.

Courtesy of Dr. W. A. van der Donk.

Table 1.1 Expected digest pattern of plasmid RNR/pET23b(+) and pLysS

Enzyme	RNR /pET23b(+)		pLysS	
	# of Site	Band Size (kb)	# of Site	Band Size (kb)
HindIII	1	6.2	1	4.9
BamHI	1	6.2	2	0.64, 4.26
NotI+NdeI	1+1	2.65, 3.55	0+0	circular

Table 1.2 Tritium exchange assay results

Host Strain	Lysate (μ L)	Protein (μ g)	Time (min)	$^3\text{H}_2\text{O}$ CPM
-	0	0	0	430
-	0	0	30	1227
JM109	3	168	30	1424
JM109	17	952	30	1436
BL21(DE3)	6	120	30	2865
BL21(DE3)	17	340	30	7398

Table 1.3 R_f values of deoxynucleosides and nucleosides*

	dA/A	dC/C	dG/G
dN	0.71	0.66	0.75
N	0.51	0.45	0.43

*The R_f values may vary slightly with different salt concentration in the assay mixture.

Table 1.4 Sample purification table for *T. acidophila* RDPR

Sample	Protein (mg)	S.A. * (U/mg)	Tot. U	Pur. Factor	Yield (%)
Lysate	1071	0.93	999.5	1.0	
DNA	2311	0.86	1977.0	0.9	100%
Q-sepharose	926	2.16	2000.0	2.3	100%
dATP	100	19.80	1980.0	21.4	100%

*Assay condition was as of the ADP assay used for purification described in the experimental section.

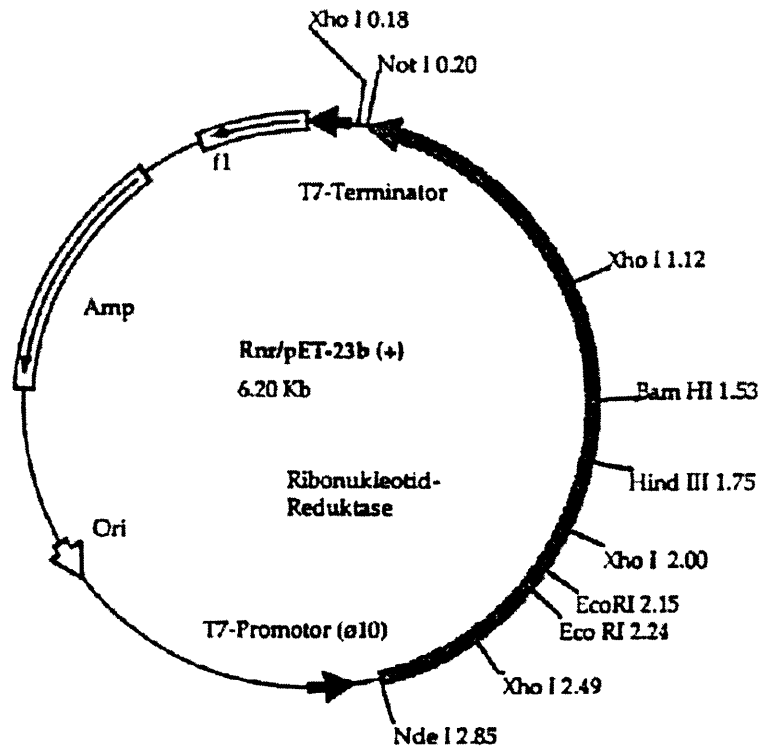


Figure 1.1 Plasmid map of RNR/pET23b(+). Selected sites are highlighted. *Adapted from Tauer, Thesis, p.87.*

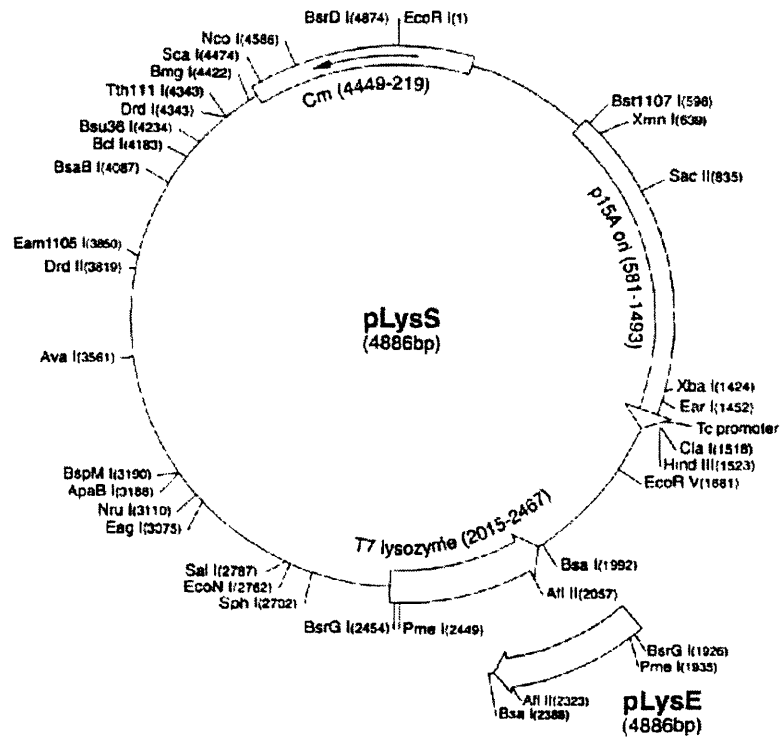


Figure 1.2 Plasmid map of pLysS. Selected sites are highlighted. *Adapted from Novagen's catalog, 1995, p. 96.*

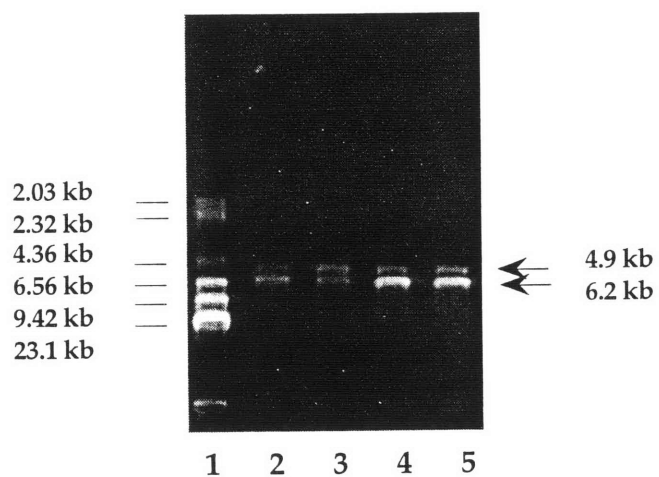


Figure 1.3 Restriction digest pattern with HindIII. Lane 1 contains the molecular size markers (HindIII digest of λ DNA). Lane 2-5: colony 1-4. *Source: Book I, p.47.*

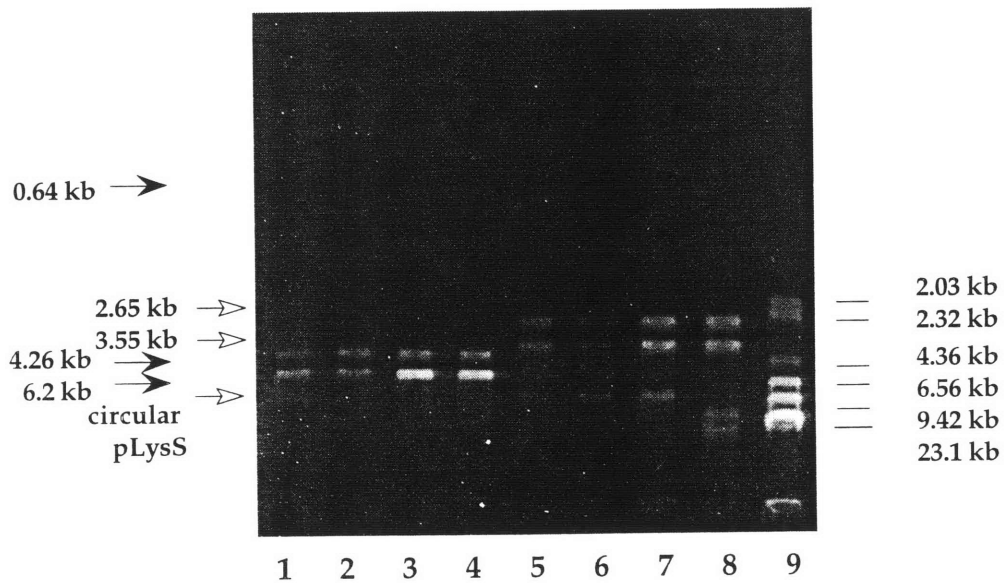


Figure 1.4 Restriction digest pattern with BamHI, and NotI+NdeI. Lane 1-4: colony 1-4 with BamHI; Lane 5-8: colony 1-4 with NotI+NdeI. *Source: Book I, p.47.*

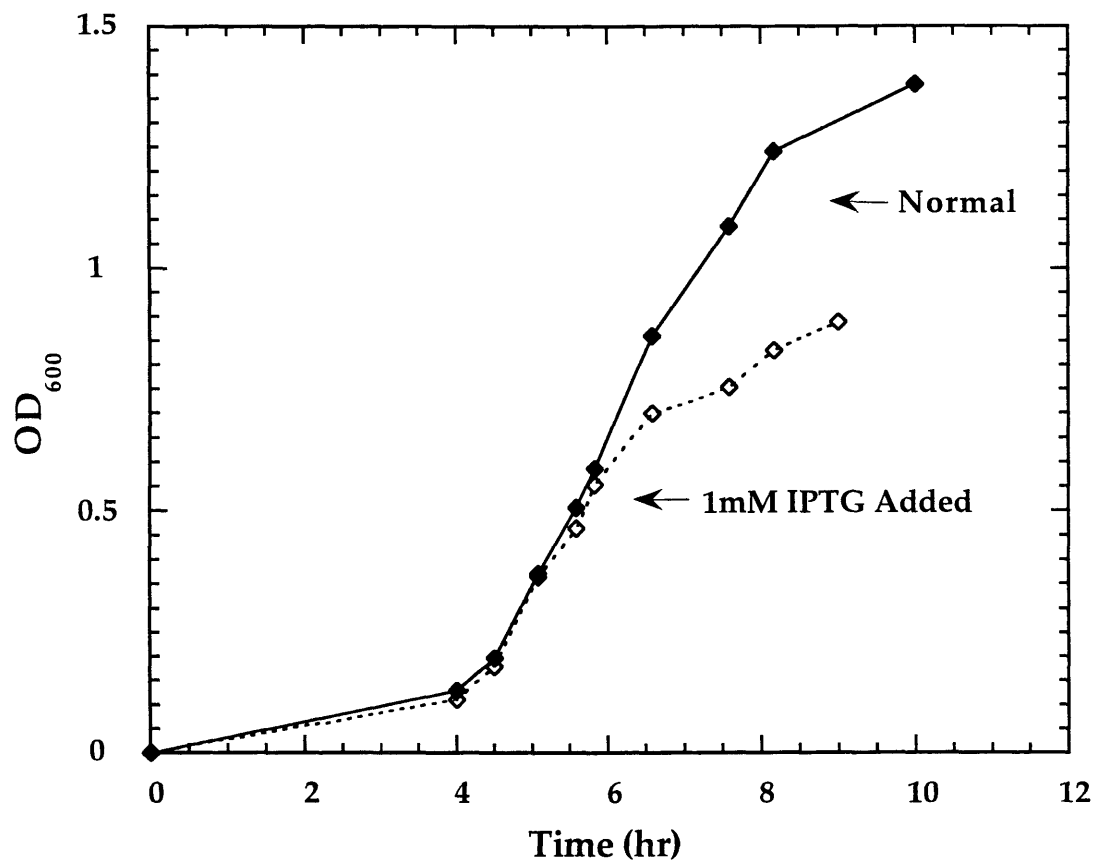


Figure 1.5 Sample growth curve of RNR/pET23b(+)/BL21(DE3). Started from a single colony, 100 µg/mL ampicillin, 10 mL culture size.

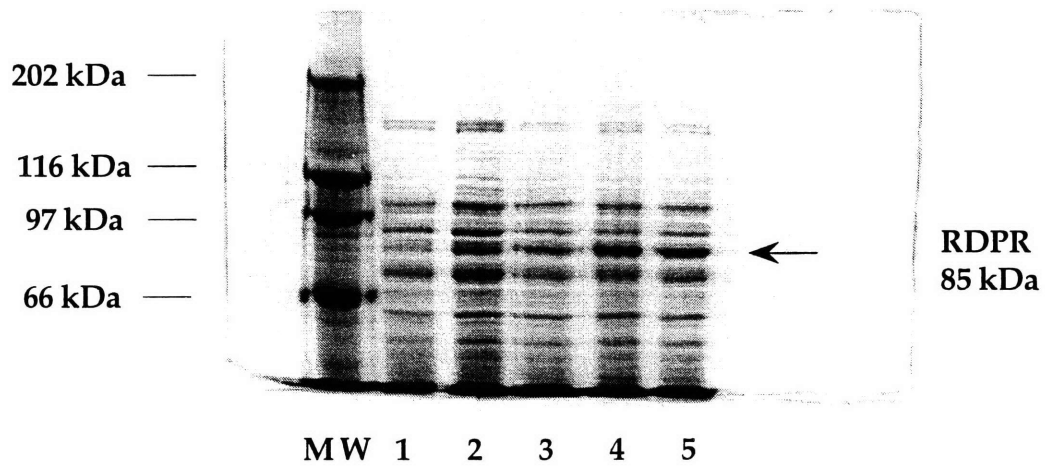


Figure 1.6 Sample induction gel of RNR/pET23b(+)/BL21(DE3). Lane 1: BL21(DE3) without plasmid. Lane 2-5, t = 0, 1, 3, 4 h. Induced at $A_{600} = 0.6$, IPTG = 0.8 mM.

Source: Book I, p.64.

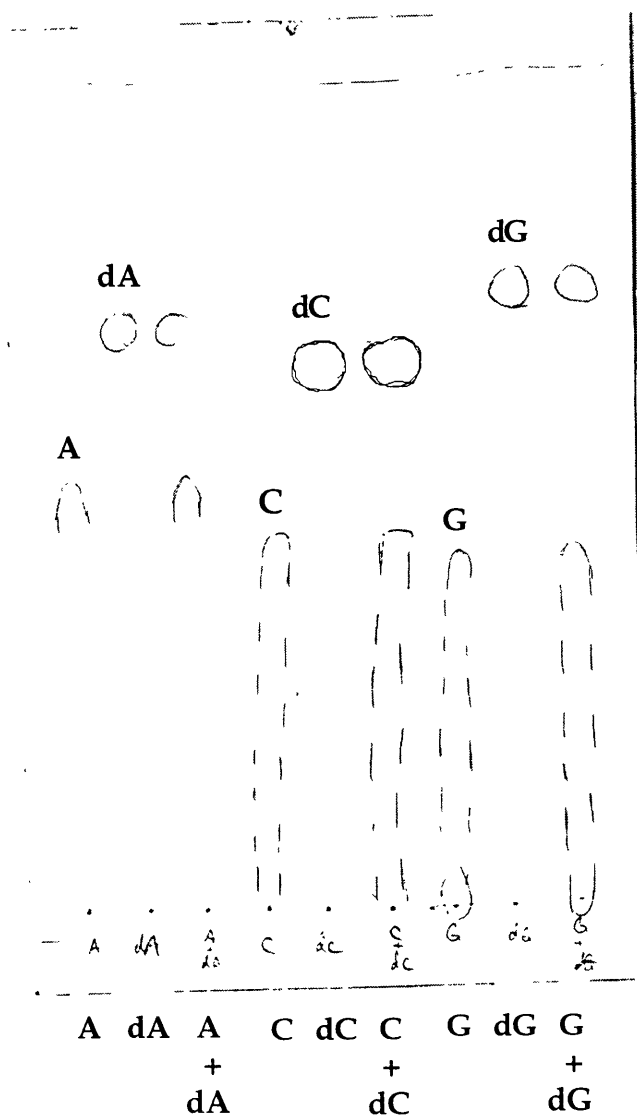


Figure 1.7 Sample TLC plate of deoxynucleosides and nucleosides separation. Eluted with potassium borate saturated methanol. Drawing is based on UV intensity.

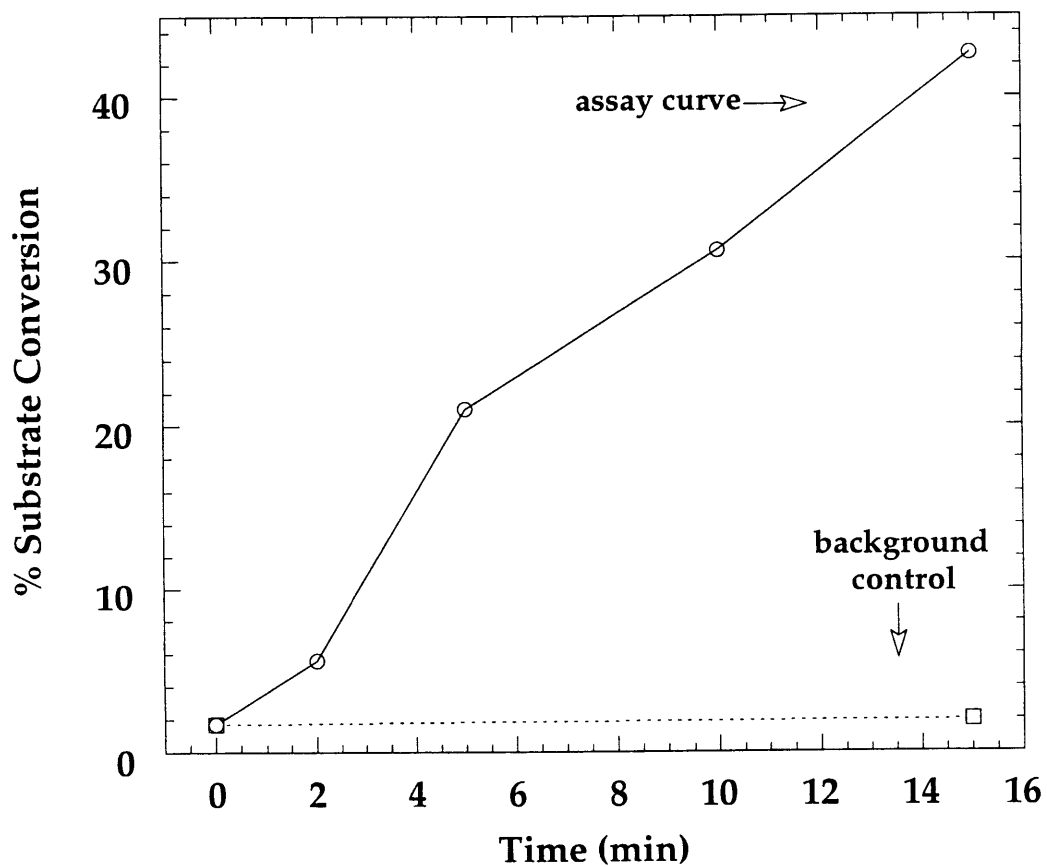


Figure 1.8 Sample [5, 8-³H]-ADP assay. Assay conditions: 10 μ M ADP (S.A. = 1.55×10^5 cpm/nmol), 1 mM $MgCl_2$, 10 mM DTT, 100 μ M AdoCbl, 1 mM dGTP, 100 mM Tris pH 8.0, 0.2 μ M *T. acidophila* RDPR. Source: Book II, p. 85.

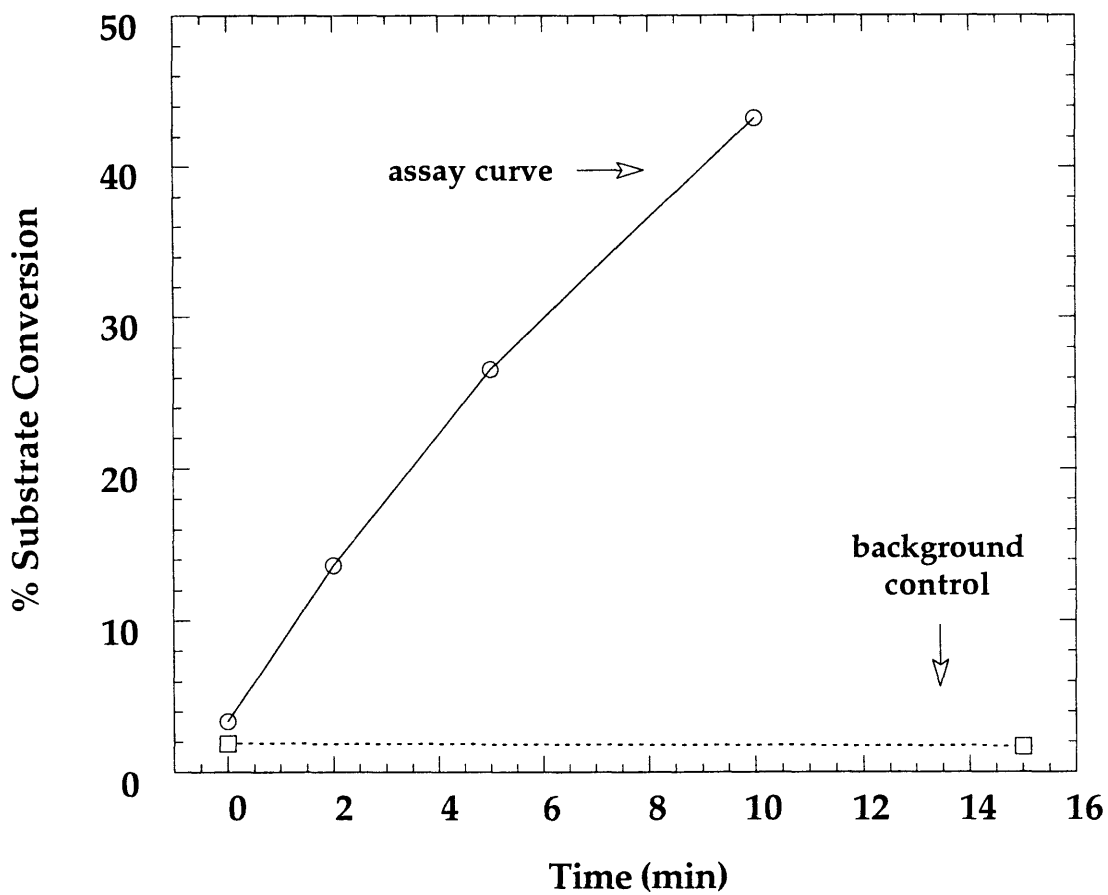


Figure 1.9 Sample [8, 5'-³H]-GDP assay. Assay conditions: 10 μ M GDP (S.A. = 2.2×10^5 cpm/nmol), 1 mM $MgCl_2$, 10 mM DTT, 100 μ M AdoCbl, 100 mM Tris pH 8.0, 0.053 μ M *T. acidophila* RDPR. Source: Book II, p.124.

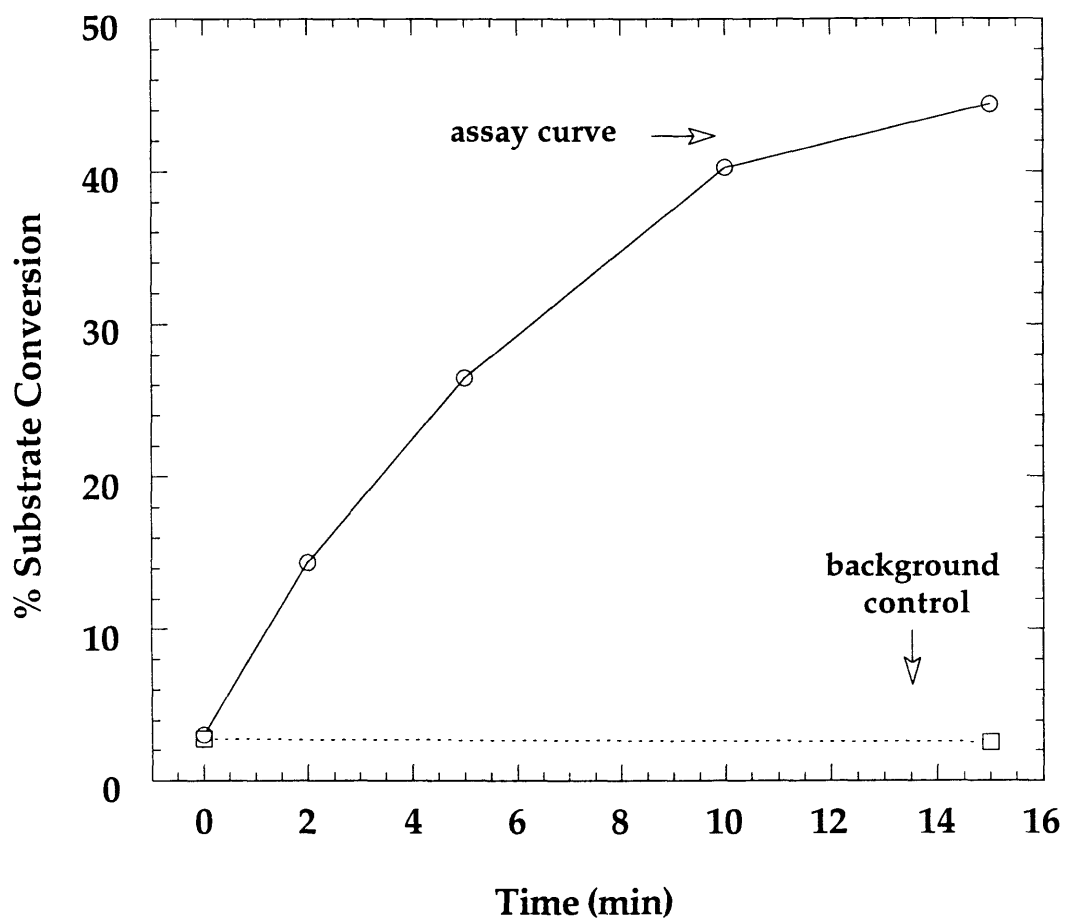


Figure 1.10 Sample [5-³H]-CDP assay. Assay conditions: 10 μ M CDP (S.A. = 2.5×10^5 cpm/nmol), 1 mM MgCl₂, 10 mM DTT, 100 μ M AdoCbl, 25 mM HEPES (pH 7.5), 0.1 μ M *T. acidophila* RDPR. Source: Book II, p.136.

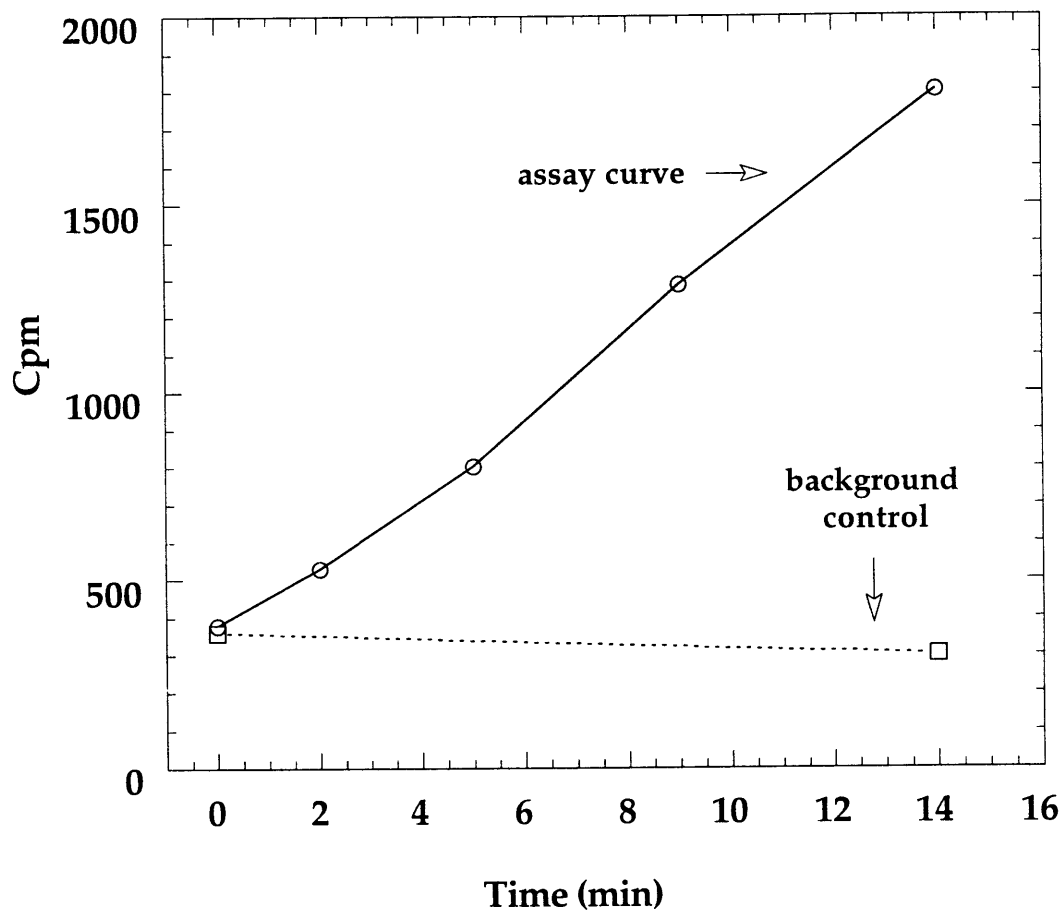


Figure 1.11 Sample [2-¹⁴C]-CDP assay. Assay conditions: 1 mM CDP (S.A. = 2.2×10^3 cpm/nmol), 1 mM MgCl₂, 30 mM DTT, 100 μM AdoCbl, 25 mM HEPES pH 7.5, 10 μM *T. acidophila* RDPR. Source: Book II, p.78

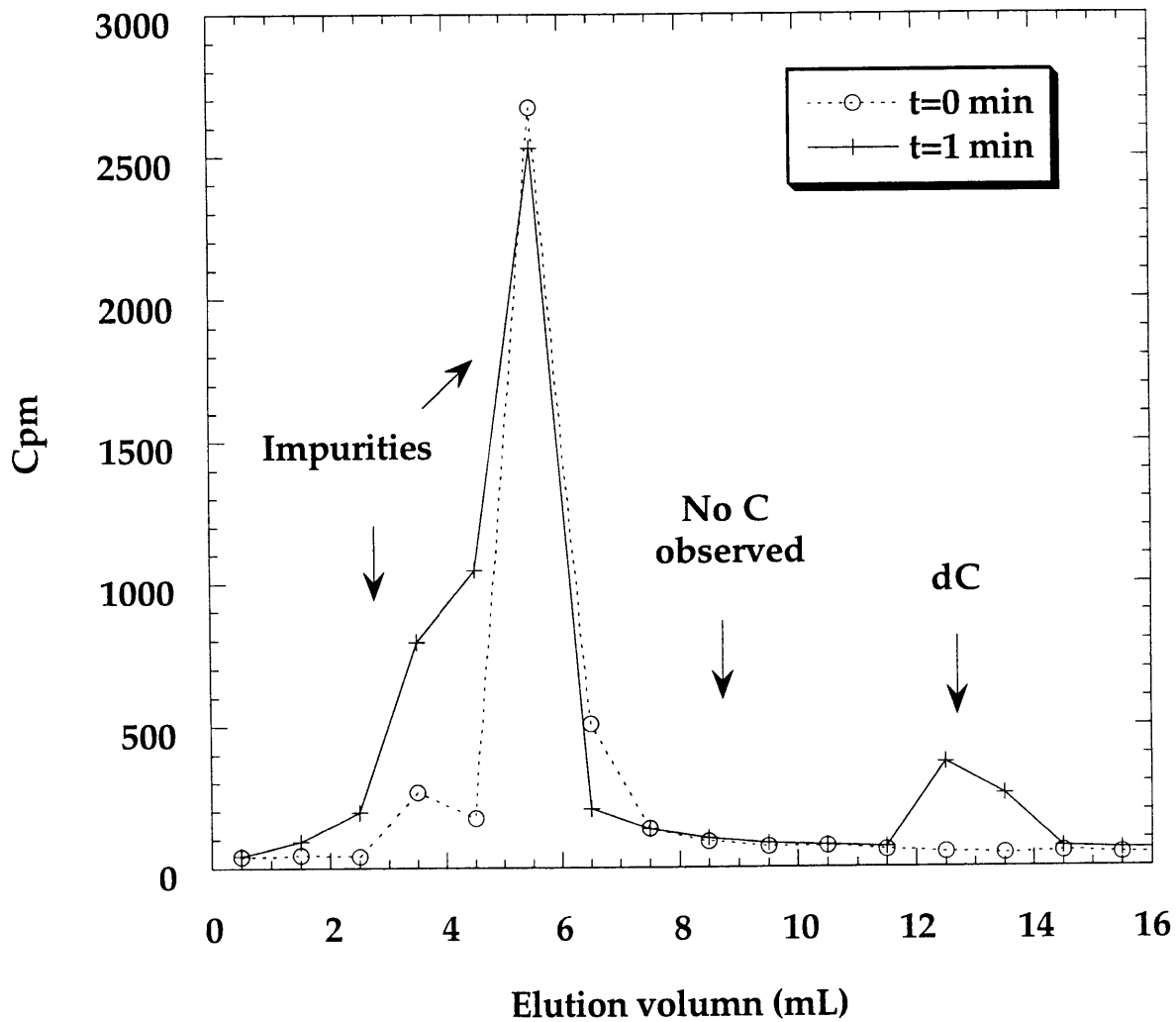


Figure 1.12 HPLC analysis of [2-¹⁴C]-CDP assay product. Eluted with H₂O. Flow rate: 1 mL/min. Fraction size: 1 mL. Source: Book II, p.44.

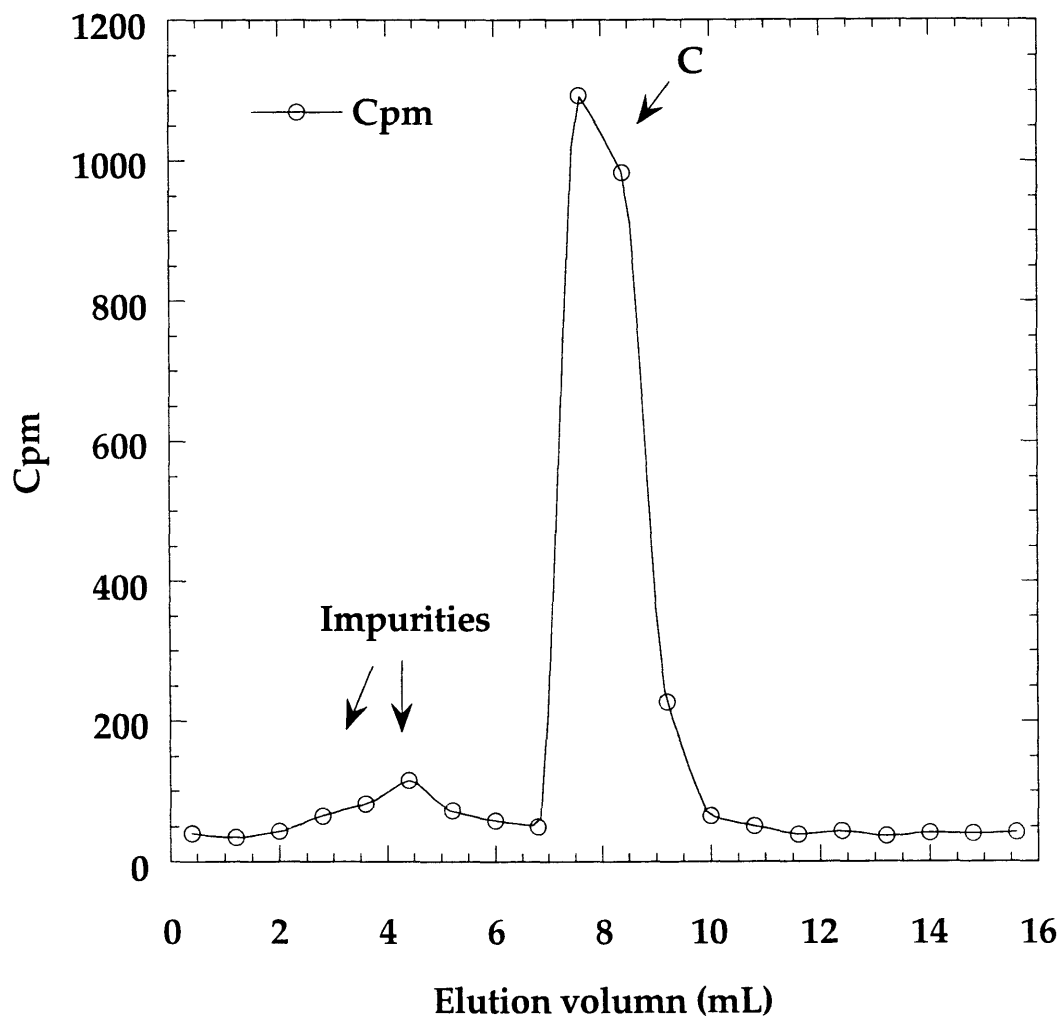


Figure 1.13 HPLC analysis of [2-¹⁴C]-CDP. Eluted with H₂O. Flow rate: 0.8 mL/min. Fraction size: 0.8 mL. *Source: Book II, p.60.*

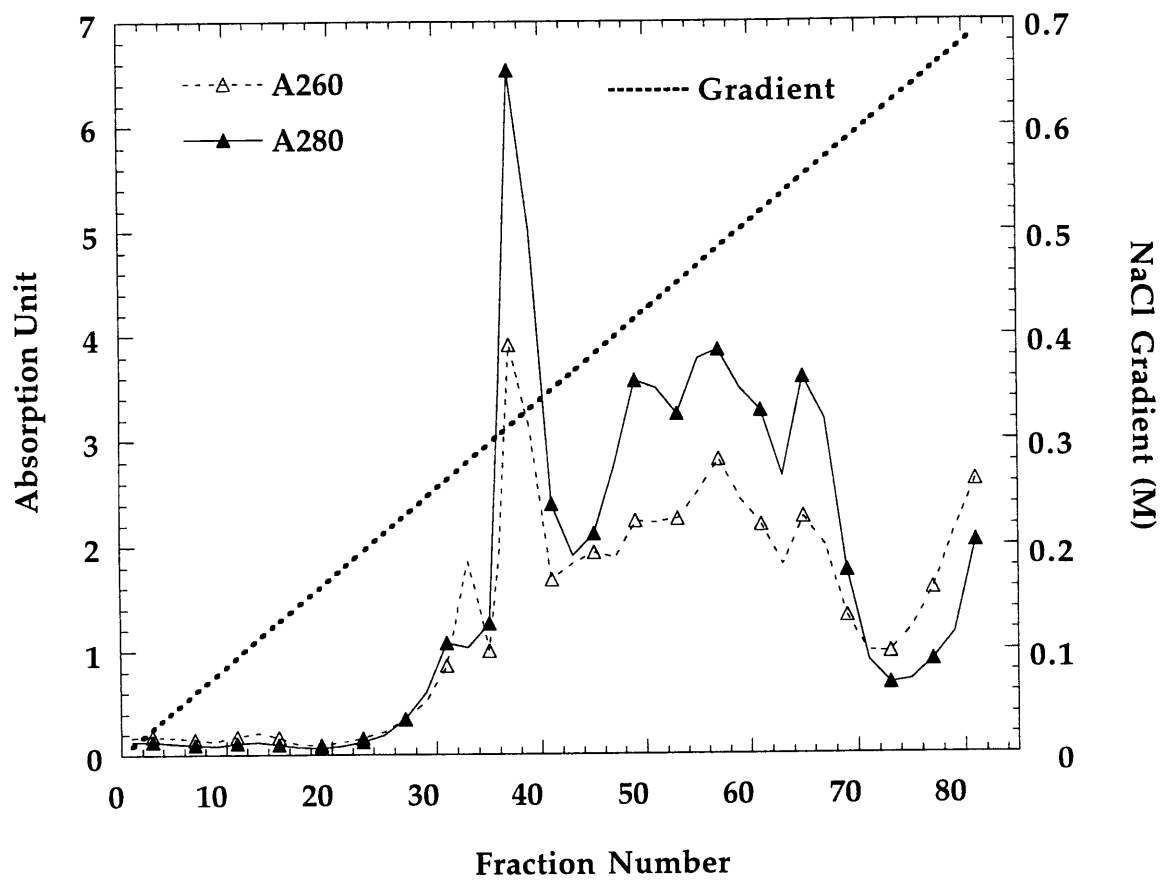


Figure 1.14 Q-Sepharose column elution profile: A260, A280 readings vs. fraction number. Linear (500 mL x 500 mL) 0 - 1 M NaCl gradient.

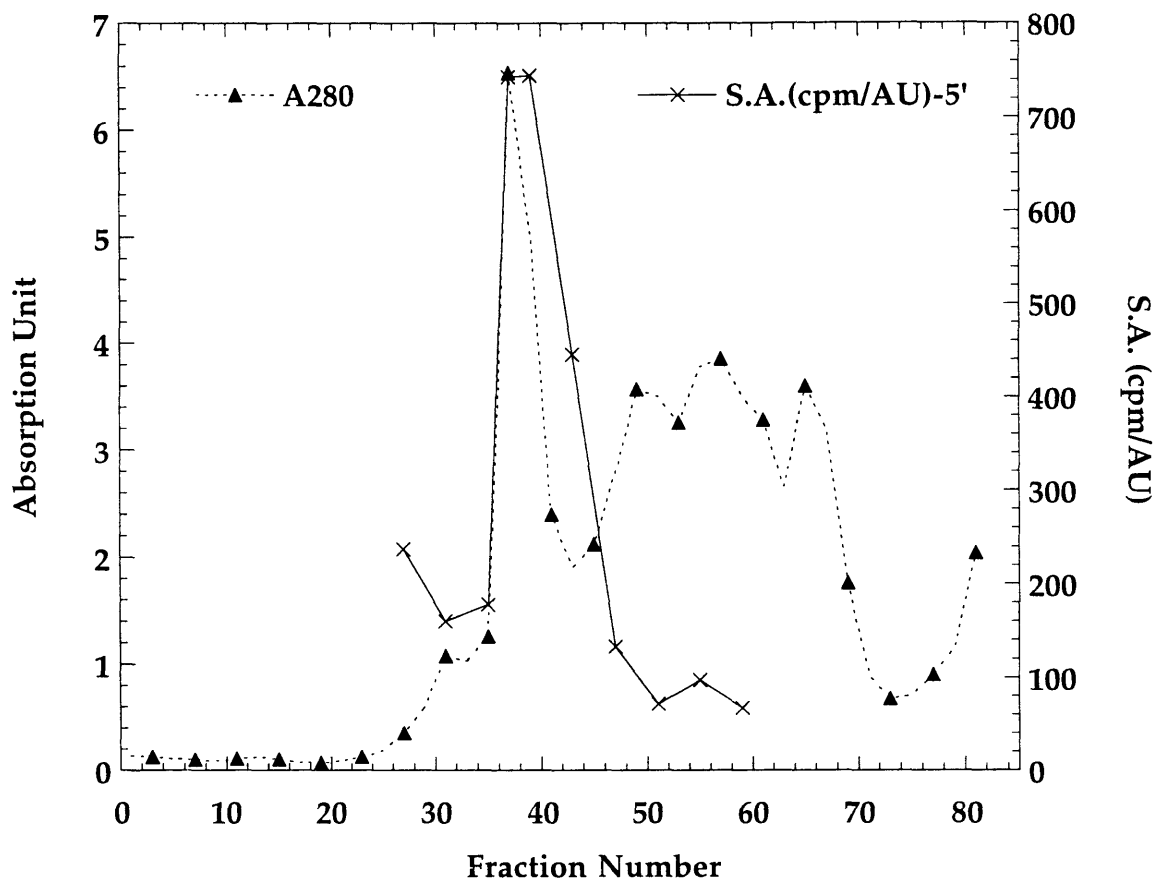


Figure 1.15 Q-Sepharose column elution profile: A280 reading and specific activity (cpm/ AU) vs. fraction number.

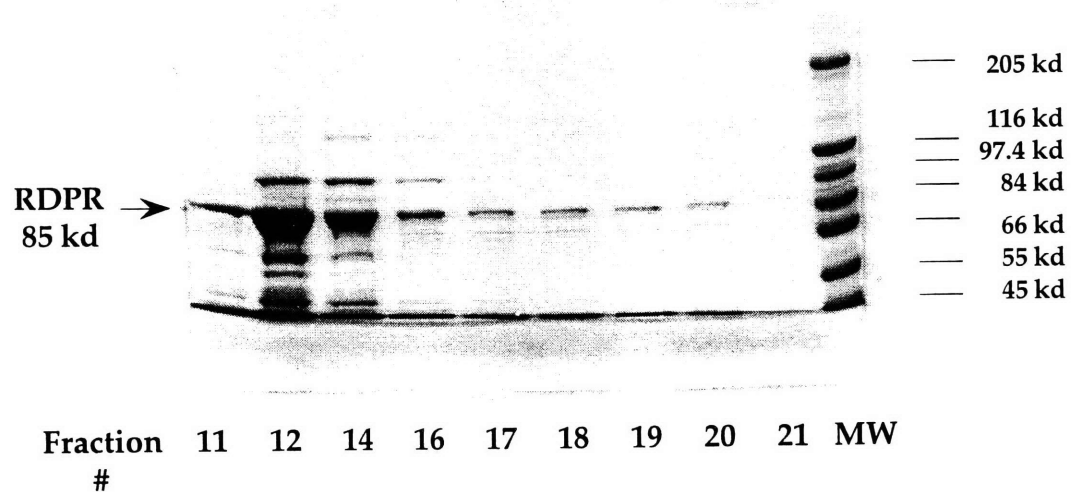


Figure 1.16 Sample SDS-PAGE gel of dATP affinity column fractions. Column size: 3 x 30 cm; Fraction size: 400 drops, ~ 25 mL.

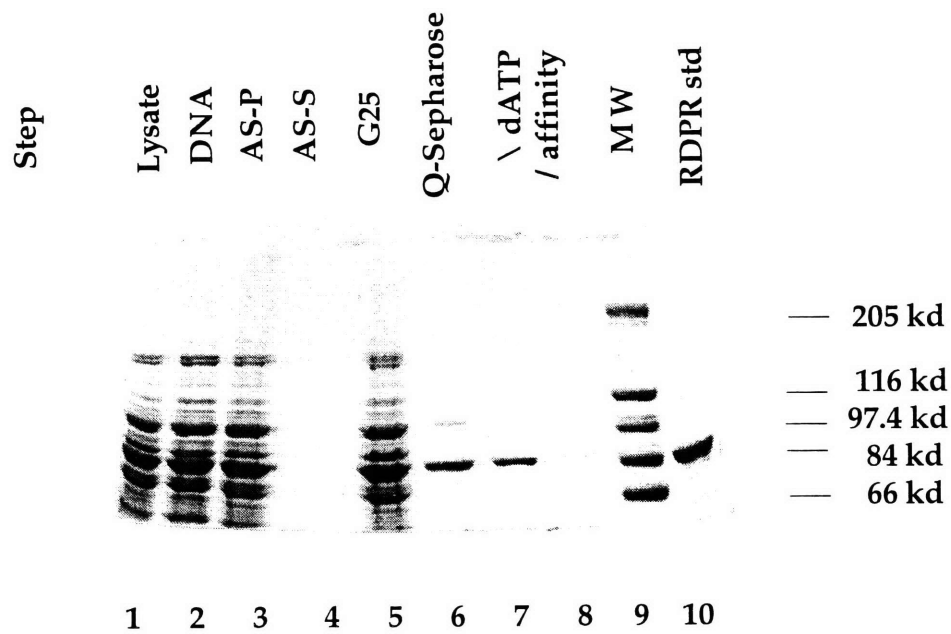


Figure 1.17 Sample SDS-PAGE gel for *T. acidophila* RDPR purification. AS-S: ammonium sulfate supernatant; AS-P: ammonium sulfate pellet. Lane 1-7, 9,10 contained ~ 20 µg protein. Lane 8: same as Lane 7, ~ 2 µg protein loaded. *Source: Book III, p.150.*

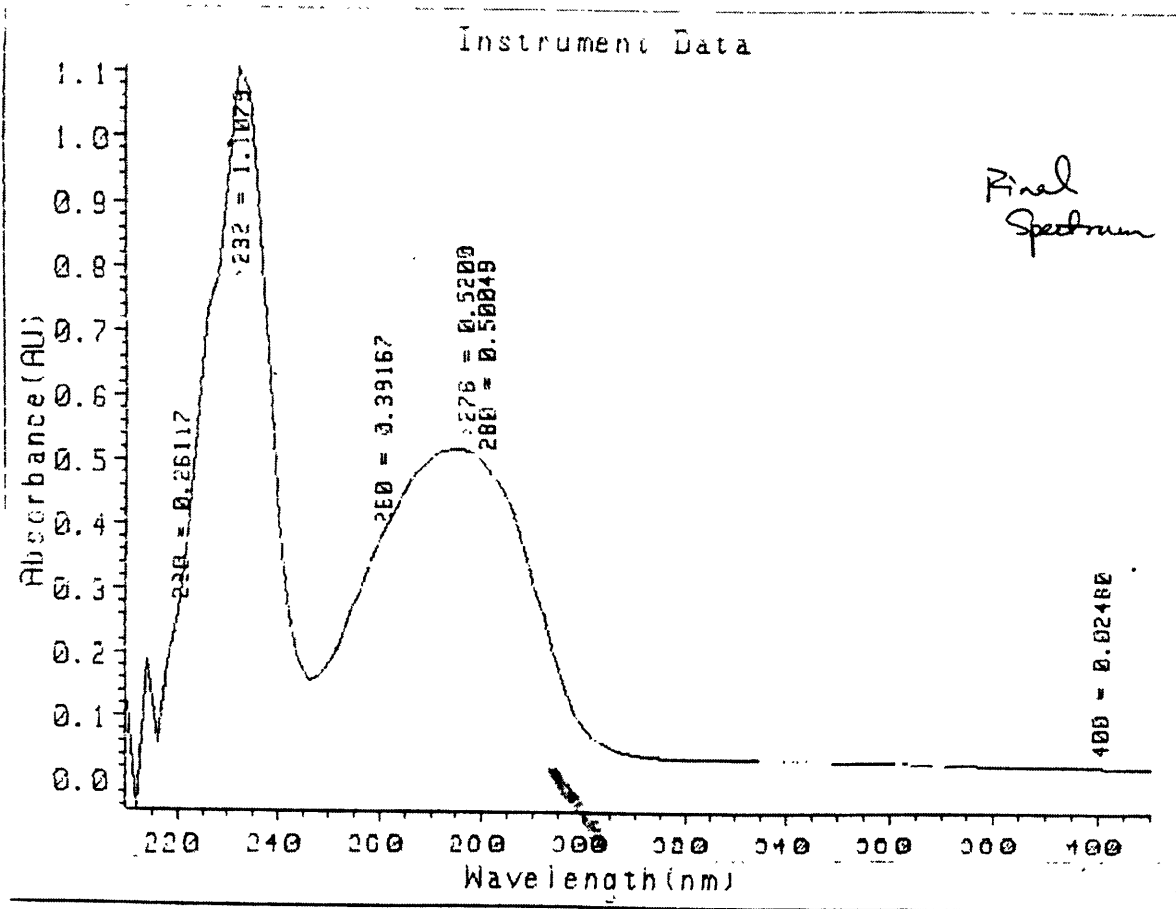


Figure 1.18 Sample UV spectrum for *T. acidophila* RDPR. Source: Book III, p.63.

Chapter 2

Allosteric Regulation and Kinetic Studies of *T. acidophila* RDPR

Introduction

Allosteric Regulation of Ribonucleotide Reductases

Ribonucleotide reductase catalyzes the reduction of the four ribonucleotides* to their corresponding deoxyribonucleotides, generating the precursors for DNA biosynthesis. The reductases are under strict allosteric control by dNTPs, the DNA building blocks, and ATP, the universal cellular energy source, to maintain the appropriate ratios of deoxynucleotide (dNTP) pools for DNA biosynthesis (Scheme 2.1).^{1,2} Brief descriptions of the allosteric regulatory patterns observed for each class of RNRs are presented below.

RDPR From Aerobically Grown *Escherichia coli* (Class Ia)**^{1,2,4}

RDPR from *Escherichia coli* is composed of two homodimeric subunits: R1 and R2 (Scheme 2.2). R1 contains the catalytic site with its redox active thiols, and R2, with its unusual diferric cluster-tyrosyl radical cofactor, generates the thiyl radical (Cys-439) required for catalysis via long range electron transfer.

Equilibrium dialysis experiments demonstrate that R1 contains two binding sites for allosteric effectors (ATP and dNTP) that govern both specificity and activity.⁵ One site binds only dATP and ATP and regulates the overall activity of the enzyme (originally called l-site because of its relatively low affinity for dATP with $K_d = 0.1-0.5 \mu\text{M}$) with ATP acting as a positive and dATP as a negative effector. The other site binds ATP, dATP, dTTP, and dGTP (originally called h-site because of its high affinity for dATP

* NDP or NTP (N = A, C, G, U). dTMP is synthesized from dUMP by thymidylate synthase thus provides the fourth DNA building block.

** Reichard et al. have suggested a subdivision of class I RNRs, with the *NrdAB* gene coded enzymes forming class Ia, and the *NrdEF* gene coded enzymes forming class Ib.³

with $K_d = 0.03 \mu\text{M}$) and regulates the enzyme's substrate specificity. Cys-292, which crystallographically at the dimer interface of R1, has been recently located to this site.⁶ This confirms previous photoaffinity and site directed mutagenesis studies.

Binding of effectors to the activity site and the specificity site results in conformational changes in the active site of the enzyme that leads to preferential binding of a particular substrate. As shown in Table 2.1a-b, with ATP at the activity site and ATP or dATP (low concentration, $< 1 \mu\text{M}$) at the specificity site, the enzyme reduces CDP and UDP. With ATP at the activity site and dTTP at the specificity site, the enzyme reduces GDP (and ADP). With ATP at the activity site and dGTP at the specificity site, the enzyme reduces ADP (and GDP). All combinations with dATP at the activity site are inactive.

Therefore the overall activity of RDPR is determined by the *in vivo* ratio between ATP and dATP, while the substrate specificity is determined by the balance of the deoxynucleotide pools. A single enzyme is therefore able to provide balanced building blocks for DNA biosynthesis.

RTPR From Anaerobically Grown *Escherichia coli* (class III)⁷

RTPR from anaerobically grown *Escherichia coli* is also composed of two homodimer subunits R1 and R2. R1 contains the glycyl free radical (Gly-681), while R2 contains a single iron-sulfur center and binds S-adenosylmethionine (SAM) required for glycyl free radical formation. Equilibrium dialysis experiments have shown that R1 contains two distinct effector binding sites (Scheme 2.3). One binds dGTP, dTTP, and dATP and regulates the reduction of purine substrates (ATP, GTP). The second binds dATP and ATP and regulates pyrimidine substrates (CTP, UTP). As shown in Table 2.2, RNR has a low basal nucleotide reduction rate. At both sites, dATP binding turns off the enzyme, whereas binding of the other nucleotides activates the enzyme up to 10-fold: ATP stimulates CTP and UTP reduction, dGTP stimulates ATP reduction, and dTTP

stimulates GTP reduction. dGTP and dTTP inhibit the reduction of the incorrect substrate; dATP inhibits reduction of all four. The physiological net effect is proposed to be the same as the class Ia enzymes.

***Nrd-EF* RDPR From *Salmonella typhimurium* (Class Ib)⁸**

The *Nrd-EF* gene of enterobacteriaceae *Salmonella typhimurium* has been cloned and expressed in *E. coli* to produce another ribonucleotide reductase (class Ib). In both *E. coli* and *S. typhimurium*, only the *Nrd-AB* gene coded class Ia enzymes are actively expressed. The *E. coli* and *S. typhimurium* chromosome thus have maintained the information for a potentially active additional class I ribonucleotide reductase, whose role *in vivo* is not yet known. However, NrdEF enzymes are used for the production of deoxyribonucleotides by other bacteria.³

Similar to the *Nrd-AB* class Ia enzyme, the *Nrd-EF* enzyme is also composed of two homodimeric subunits, R1E and R2F (compared to R1 and R2 in class Ia enzyme) (Scheme 2.5). R1E contains the catalytic site with its redox active thiols, and R2F contains a μ -oxo bridged dinuclear iron center and a tyrosyl radical. Together they catalyze ribonucleotide reduction, using dithiothreitol or reduced glutaredoxin, but not thioredoxin, as an electron donor.⁹

The allosteric regulation studies (Table 2.3) of this *Nrd-EF* enzyme have shown that dGTP stimulates ADP reduction, dTTP stimulates GDP reduction, and dATP (or ATP) stimulates CDP or UDP reduction. This pattern is similar to that of the normally expressed *Nrd-AB* class Ia enzyme with one major exception: dATP stimulates reduction of CDP (and UDP) under conditions when dATP strongly inhibits all activity of the class Ia *NrdAB* enzyme.

The R1E proteins from all class Ib reductases known so far lack the 50-60 N-terminal amino acids of the R1 proteins of class Ia. Binding experiments show that one R1E polypeptide of class Ib can only bind one dATP and that this binding occurs at the

substrate specificity site. Therefore, class Ib lacks the activity site of class Ia. This explains the differences in the allosteric effect of dATP between class Ia and Ib enzymes. In both cases, low concentrations of dATP stimulate the reduction of pyrimidine ribonucleotides. However, increasing the concentration of dATP above 1 μM inhibits the class Ia enzyme due to the presence of a second binding site for dATP, the activity site. The lack of such a site makes dATP stimulating at $> 1 \mu\text{M}$ for pyrimidine ribonucleotides reduction by class Ib enzymes.

RTPR From *Lactobacillus leichmannii* (Class II)^{1,2,10}

RTPR from *Lactobacillus leichmannii* is a monomer and uses 5'-deoxy-adenosylcobalamin (AdoCbl) as a cofactor. *L. leichmannii* RTPR reduces ribonucleoside triphosphates, and the products of the reaction thus act also as allosteric effectors. This leads to a complication in studying allosteric control. Equilibrium dialysis experiments have defined one common binding site for dNTPs with K_d values from 9 to 80 μM . This site is indicated as a regulatory site, but also binds substrate NTPs with a 100 to 1000-fold lower affinity. (Scheme 2.5)

Binding of dNTPs to the regulatory site greatly improves the enzyme's affinity for AdoCbl. Although the allosteric control of the substrate specificity is not as clear cut as for the *E. coli* RDPR and the effects are less pronounced, it can be ordered into the following scheme (Table 2.4): the presence of dATP stimulates CTP reduction, dCTP stimulates UTP reduction, dGTP stimulates ATP reduction. The effector dTTP was initially shown to stimulate GTP reduction, but later it was shown to be a positive effector only for ITP reduction. For GTP reduction, no effector is needed. DeoxyNTPs show little product inhibition, supporting the existence of a separate substrate binding site. No strong negative effector is known for *L. leichmannii* RTPR.

In general, the positive allosteric effectors show a qualitative similarity to those observed in other systems, with the exception of GTP reduction and dCTP as an

effector, which shows no allosteric activity on class Ia, Ib and III enzymes. Most enzymes that are allosterically regulated are multimeric.¹⁰ Thus *L. leichmannii* RTPR which is monomeric, is unique from the other reductases, and its mechanism represents an intriguing challenge to unravel.

Summary

In summary (Scheme 2.6), all three classes of enzymes have one property in common: a single protein reduces the four common ribonucleoside di- or triphosphates. Substrate specificity is determined by dNTPs and ATP acting as allosteric effectors. Thus, the presence of ATP makes the enzymes reduce CDP and UDP, dGTP favors ADP reduction, and dTTP favors GDP reduction. These effects are similar for all three classes (with perhaps some exceptions from class II enzyme, that are difficult to know, due to experimental difficulties). This is not the case for dATP. With enzymes belonging to class Ia, excepting the virus-coded reductase and class III, dATP is a general inhibitor. Enzymes belonging to class Ib and II are not inhibited by dATP. Instead, dATP stimulates the reduction of CDP (and UDP).⁸ At low concentrations it also stimulates class Ia CDP reduction.

The conserved allosteric regulatory pattern together with the conserved radical based mechanism of RNRs¹¹ has led Richard to propose that all RNRs have evolved from a common ancestor with class III RNRs as the progenitor.² The recently discovered *T. acidophila* RNR and *P. furiosus* RNR further provides sequence links among all the three classes of RNRs. The allosteric regulatory pattern of *T. acidophila* RNR is thus investigated as part of the characterization studies of this enzyme as well as further investigation of the notion of divergent evolution of RNRs.

Materials and Methods

Materials

T. acidophila RDPR was purified as described in Chapter 1. *E. coli* thioredoxin (TR) and thioredoxin reductase (TRR) were isolated from overproducing strains SK3918 (S.A. = 500 AU DTNB reduced·mg⁻¹·min⁻¹)¹² and K91/pMR14 (S.A. = 50 AU DTNB reduced·mg⁻¹·min⁻¹).¹³ Calf intestine alkaline phosphatase (CIP) and DNase were from Boehringer Mannheim.

Cytidine 5'-diphosphate (CDP), adenosine 5'-diphosphate (ADP), guanosine 5'-diphosphate (GDP), 2'-deoxyadenosine-5'-diphosphate (dADP), 2'-deoxyguanosine-5'-diphosphate (dGDP), 2'-deoxythymidine-5'-diphosphate (dTDP), 2'-deoxycytidine (dC), cytidine (C), 2'-deoxyadenosine (dA), adenosine (A), 2'-deoxyguanosine (dG), guanosine (G), adenosine 5'-triphosphate (ATP), 5'-deoxyadenosylcobalamin (AdoCbl), nicotinamide adenine dinucleotide phosphate, reduced form (NADPH), and Sephadex G-25 Medium Fractionation Range (cat. G-25-150) chromatography resin were from Sigma. 2'-Deoxyguanosine-5'-triphosphate (dGTP), 2'-deoxythymidine-5'-triphosphate (dTTP), 2'-deoxyadenosine-5'-triphosphate (dATP), and 2'-deoxycytidine-5'-triphosphate (dCTP) were from either Sigma or Boehringer Mannheim. [5,8-³H]-ADP (28.5 Ci/mmol), [8, 5'-³H]-GDP (39.5 Ci/mmol), and [2-¹⁴C]-CDP (59.1 mCi/mmol) were from NEN. [5-³H]-CDP (22 Ci/mmol) was from Amersham Life Sciences. Tris was from Boehringer Mannheim. HEPES was from USB. EDTA, MgCl₂, MgSO₄, and dithiothreitol (DTT) were from Mallinckrodt. Centricons (Centricon-30) were provided by Millipore.

Data Analysis

All the curve fits were carried out with KaleidaGraph 3.0.5 by Abelbeck Software. The slope of each assay time curve was obtained by a least square linear fit of, typically

5 time points per curve. In the case where product inhibition occurred, only the linear portion of the curve was used to obtain the slope.

The K_m values were obtained by fitting to the data to equation 2.1 and in the case of substrate inhibition, it was fit to equation 2.2 from Cleland (1979).

$$V = \frac{V_{\max}[S]}{K_m + [S]} \quad \text{Equation 2.1}$$

$$V = \frac{V_{\max}[S]}{K_m + [S] + [S]^2 / K_i} \quad \text{Equation 2.2}$$

***T. acidophila* RDPR Used in Regulation and Kinetic Studies**

There were three batches of *T. acidophila* RDPR used in the allosteric regulation and kinetic studies. Specific activity values vary depending on the substrate and effector concentrations used in the assay. The specific activity values reported for the 3 enzyme batches below were based on the standard [2-¹⁴C]-CDP assay described in Chapter 1 under the following standard conditions: 1 mM CDP (~ 2 × 10³ cpm/nmol), 1 mM dGTP, 1 mM MgCl₂, 30 mM DTT, 25 mM HEPES pH 7.5, 100 μM AdoCbl, and 10 μM (100 μg/ 100 μL) *T. acidophila* RDPR. The [2-¹⁴C]-CDP assay method was first used for *T. acidophila* RDPR as it is the standard assay method for *E. coli* RDPR and *L. leichmannii* RTPR in the Stubbe laboratory. However, TLC based assays method using tritium labeled substrate were mainly used later.

In this chapter, 1 U of enzyme activity is defined as 1 nmol substrate converted per min (1 U = 1 nmol/min). Based on the standard [2-¹⁴C]-CDP activity assay, Batch I obtained from the first large scale purification had a very low specific activity of 7 U/mg. Batch IIa obtained from a later purification had a much higher specific activity of 40 U/mg. Batch IIb enzyme was obtained by further purifying Batch IIa enzyme as described below and had a specific activity value of 42 U/mg (Batch I = 7 U/mg; Batch IIa = 40 U/mg; Batch IIb = 42 U/mg).

Batch IIb was obtained by the following procedure. *T. acidophila* RDPR from Batch IIa was treated with DNase in a volume of 1.1 mL: 25 mM HEPES (pH 7.5), 0.12 mM (12 $\mu\text{g}/\mu\text{L}$) *T. acidophila* RDPR, 20 U DNase, and 1 mM MgCl_2 . The mixture was incubated at room temperature for 15 min. The protein solution was then loaded onto a (1.5 x 4.5) cm Sephadex G-25 column pre-equilibrated in Tris buffer (50 mM Tris, pH 8.0 at 4°C, 1 mM DTT) and washed with the same buffer. The protein containing fractions were pooled and concentrated using Centricon-30 (clear O-ring, MW cut-off 30,000 kDa). Glycerol was added to the final concentrated protein solution to 15% and the protein solution was rapidly frozen in liquid nitrogen and stored in aliquots at -80°C.

(d)NTPs Used in Regulation Studies

For the dNTPs (dATP, dTTP, dCTP, and dGTP) and ATP from Sigma, all reagents were dissolved in 25 mM HEPES, pH 7.5 as ~10-20 mM stock solutions, with their concentrations determined by UV spectroscopy, and stored in small aliquots at -20°C. The pH of each solution was carefully checked and adjusted as needed to ~ 7.5. The dNTPs (dATP, dTTP, dCTP, and dGTP) from Boehringer Mannheim were provided as 100 mM stock solutions and were used directly.

AdoCbl K_m Determination with CDP as Substrate

The K_m of AdoCbl was determined using [2- ^{14}C]-CDP as the substrate. An assay mixture contained in a final volume of 100 μL : 2 mM CDP (S.A. = 1.8×10^3 cpm/nmol), 25 mM HEPES pH 7.5, 1 mM MgCl_2 , 30 mM DTT, 1 mM dGTP, 3.34 μM (33.4 $\mu\text{g}/100$ μL) *T. acidophila* RDPR (Batch IIa), and 0-250 μM AdoCbl. The mixture including everything except AdoCbl was pre-incubated at 55°C for 2 min. Various amount (0-250 μM) of AdoCbl was added to start each reaction at 55°C. After 30 min, the tubes were placed in a boiling water bath for 2 min to stop the reaction, and then placed on ice. After all the reactions were stopped, 10 μl of 1 M Tris solution (pH~11) and 5 U of calf

intestine alkaline phosphatase were added to each aliquot. The solution was then incubated at 37°C for 1 h. The product was then analyzed using the borate column method described in the [2-¹⁴C]-CDP activity assay in Chapter 1.

DTT K_m Determination with CDP as Substrate

The K_m of DTT was determined using [5-³H]-CDP as the substrate. An assay mixture contained in a final volume of 210 μ L: 1 mM CDP (S.A. = 1.4×10^3 cpm/nmol), 25 mM HEPES pH 7.5, 1 mM MgCl₂, 1 mM dGTP, 100 μ M AdoCbl, 6 μ M (60 μ g/100 μ L) *T. acidophila* RDPR (Batch IIa), and 0-50 mM DTT. The mixture including everything except AdoCbl was pre-incubated at 55°C for 2 min. At time zero a 100- μ L (usually <100 μ L, if corrected for AdoCbl volume) aliquot was removed, mixed with 50 μ L of 2% pre-chilled perchloric acid, and then placed on ice. AdoCbl was added in the dark to start the reaction at 55°C. After 10 min, a 100- μ L aliquot was removed and quenched with 50 μ L of 2% pre-chilled perchloric acid by vortexing, and then placed on ice. After all the reactions were stopped, 12 μ L of 1 M KOH was added to each aliquot to neutralize the solution. Alkaline phosphatase buffer (50 mM Tris pH 8.5, 1 mM EDTA) (50 μ L) was added followed by addition of 5 U calf intestine alkaline phosphatase. The sample was then incubated at 37°C for 1 h. The product was then analyzed using the borate column method described in the [2-¹⁴C]-CDP activity assay in Chapter 1.

Allosteric Effects of (d)NTPs on ADP Reduction

The allosteric effects of dNTPs and ATP on ADP reduction by *T. acidophila* RDPR were investigated. All the assays were carried out at 55°C using the standard [5, 8-³H]-ADP assay procedure described in Chapter 1. The regulation studies were carried out using DTT as the reductant, at low substrate (10 μ M ADP, S.A. = 1.5×10^5 cpm/nmol, 2 Runs) and high (1 mM ADP, S.A. = $\sim 2.5 \times 10^3$ cpm/nmol, 3 Runs) substrate

concentrations with 0.5 - 1 mM effectors. See Figure legends for detailed assay conditions.

Substrate ADP K_m Determination

The K_m value for ADP was determined in the absence and presence of 1 mM dGTP by varying the substrate concentration from 5-40 μ M. The assays were carried out using the standard [5, 8-³H]-ADP assay procedure described in Chapter 1. An assay mixture contained in a final volume of 260 μ L: 25 mM HEPES pH 7.5, 1 mM MgCl₂, 100 μ M AdoCbl, 30 mM DTT, 0.08 μ M (0.4 μ g/50 μ L) *T. acidophila* RDPR (Batch IIa), with or without 1 mM dGTP, and 5-40 μ M ADP (S.A. = 1.5×10^5 cpm/nmol).

Allosteric Effects of (d)NTPs on GDP Reduction

The allosteric effects of dNTPs and ATP on GDP reduction by *T. acidophila* RDPR were investigated. All the assays were carried out using the standard [8, 5'-³H]-GDP assay procedure described in Chapter 1. The regulation studies were carried out using either DTT or TR/TRR/NADPH as the reductant. With DTT, the studies were carried out at low substrate (10 μ M GDP, S.A. = 2.2×10^5 cpm/nmol, 2 Runs) and high substrate (1 mM GDP, S.A. = 2.3×10^3 cpm/nmol) concentrations. With TR/TRR/NADPH, the studies were carried out only at low substrate (10 μ M GDP, S.A. = 2.2×10^5 cpm/nmol) concentration. See Figure legend for detailed assay conditions.

Substrate GDP K_m Determination

T. acidophila RDPR activities at both high and low substrate concentrations of GDP were investigated. The assays were carried out using the standard [8, 5'-³H]-GDP assay procedure described in Chapter 1.

At low substrate concentrations (5-40 μ M), the assays were carried out in the absence and presence of 1 mM dTTP. An assay mixture contained in a final volume of 260 μ L:

25 mM HEPES pH 7.5, 1 mM MgCl₂, 100 μM AdoCbl, 30 mM DTT, 0.04 μM (0.2 μg/50 μL) *T. acidophila* RDPR (Batch IIa), with or without 1 mM dTTP, and 5-40 μM GDP (S.A. = 1.2×10^5 cpm/nmol).

At high substrate concentrations (100-600 μM), the assays were carried out in the absence and presence of 1 mM dATP. An assay mixture contained in a final volume of 260 μL: 25 mM HEPES pH 7.5, 1 mM MgCl₂, 100 μM AdoCbl, 30 mM DTT, 0.16 μM (0.8 μg/50 μL) *T. acidophila* RDPR, with or without 1 mM dATP, and 100-600 μM GDP (S.A. = 4.2×10^4 cpm/nmol).

Allosteric Effects of (d)NTPs on CDP Reduction

The allosteric effects of dNTPs and ATP on CDP reduction by *T. acidophila* RDPR were investigated. All the assays were carried out using the standard [2-¹⁴C]-CDP or [5-³H]-CDP assay procedure described in Chapter 1. The regulation studies were carried out using either DTT or TR/TRR/NADPH as the reductant. With DTT, the studies were carried out at low substrate (10 μM [5-³H]-CDP, S.A. = 4.5×10^5 cpm/nmol) and high substrate (1 mM [2-¹⁴C]-CDP, S.A. = 2.2×10^3 cpm/nmol) concentrations. With TR/TRR/NADPH, the studies were carried out only at high substrate (1 mM [2-¹⁴C]-CDP, S.A. = 2.2×10^3 cpm/nmol) concentration. See Figure legends for detailed assay conditions.

Allosteric Effects of dNDPs on ADP Reduction

dNDPs (dADP, dGDP, dTTP) were also investigated as potential allosteric effectors for *T. acidophila* RDPR. All the assays were carried out using the standard [5, 8-³H]-ADP assay procedure described in Chapter 1. The regulation studies were carried out using DTT as the reductant, at two different substrate concentrations (10 μM ADP, S.A. = 1.5×10^5 cpm/nmol; 200 μM ADP, S.A. = 3.9×10^4 cpm/nmol). See Figure legends for detailed assay conditions.

Results and Discussion

AdoCbl K_m Determination with CDP as Substrate:

The K_m for AdoCbl was determined with 2 mM CDP as substrate and 1 mM dGTP as effector. The results are shown in Figure 2.1a. Analysis of the data using Equation 2.1, the Michaelis-Menten equation

$$V = \frac{V_{\max} [S]}{K_m + [S]}$$

gives $K_{m(\text{AdoCbl})} = 2.4 \mu\text{M}$ and $V_{\max} = 31.5 \text{ U/mg}$. A similar experiment was previously carried out in Steven Benner's laboratory using ADP as the substrate (Figure 2.1b).¹⁴ The K_m value for AdoCbl under Benner's conditions appears to be $\sim 20 \mu\text{M}$ and V_{\max} is reached at $\sim 100 \mu\text{M}$ AdoCbl for ADP reduction. (However, the amount of enzyme used was not given, and the V_{\max} was not reported.) In both cases, the enzyme activity decreases at high AdoCbl concentration ($> 200 \mu\text{M}$). Therefore, $100 \mu\text{M}$ AdoCbl concentration has been used in the standard assay conditions. For *P. furiosus* RDPR, the K_m value for AdoCbl is reported to be $1 \mu\text{M}$ for CDP reduction,¹⁵ and for *L. leichmannii* RTPR, K_m value for AdoCbl is reported to be $1.3 \mu\text{M}$,¹⁶ on the same order as the $2.4 \mu\text{M}$ value obtained for *T. acidophila* RDPR.

DTT K_m Determination with CDP as Substrate

The K_m value for reductant DTT with 1 mM CDP and 1 mM dGTP as effector was determined. The experimental are shown in Figure 2.2. Analysis of the data, as described above, gives a $K_m(\text{DTT}) = 11.5 \text{ mM}$, $V_{\max} = 27.3 \text{ U/mg}$. The K_m value for DTT is reported to be 22 mM for *P. furiosus* RDPR.¹⁵ In the standard *T. acidophila* RDPR assays, a maximum of 30 mM DTT was used, while 40 mM DTT is used for *P. furiosus*

RDPR. Higher DTT concentration is believed to have destructive interactions with cofactor AdoCbl and is avoided.

***T. acidophila* RDPR Used in Regulation and Kinetic Studies**

The UV spectrum of *T. acidophila* RDPR Batch IIa and Batch IIb are shown in Figure 2.3a and Figure 2.3b respectively. The additional purification step for Batch IIb enzyme from Batch IIa only slightly shifted λ_{max} from 272 nm to 278 nm. And the specific activity value stayed about the same (40 U/mg vs. 42 U/mg).

Allosteric Effects of (d)NTPs on ADP Reduction

As described in introduction, dGTP is the positive effector for ADP (or ATP) reduction for all classes of RNRs. The allosteric effects of (d)NTPs on ADP reduction was first carried out at 10 μM ADP with DTT as reductant as a similar experiment was reported in Benner's laboratory.¹⁴ As the allosteric regulation studies with the anaerobic *E. coli* RTPR and Nrd-EF *S. typhimurium* RDPR were both carried out at millimolar substrate and effector concentrations (Table 2.2, Table 2.3),^{7,8} millimolar concentration of effectors were used in all the allosteric regulation studies carried out in this work. The *L. leichmannii* RTPR has a K_m value for ATP of 1.1 mM.¹⁶ Therefore, at 10 μM ADP, the *T. acidophila* RDPR may not be saturated with the substrate, the allosteric effect of (d)NTPs was thus also studied at 1 mM ADP. That is why K_m is determined.

The rate of formation of product at 10 μM ADP from 2 runs with DTT as reductant are shown in Figure 2.4a-b, and the ones obtained at 1 mM ADP from 3 runs with DTT as reductant are shown in Figure 2.5a-c. The calculated specific activity data and percentage-of-activity data together with Benner's data for ADP reduction are summarized in Table 2.5a-b.

Figure 2.4a (10 μ M ADP) was obtained first with enzyme Batch I and the results are very similar to those reported by Benner (Table 2.5a-b) where dGTP acts as a positive effector. Figure 2.5a (1 mM ADP) was obtained next with enzyme Batch IIa which had a much higher specific activity than Batch I, and the allosteric effects are quite different. The reduction is the fastest when no effector is present. The experiment was repeated with enzyme Batch IIa (Figure 2.5b) and the same effects as these observed in Figure 2.5a were observed. The different allosteric effects observed at different substrate concentrations led to the suspicion of possible nucleotide contaminants in the enzyme batches used. However, repetition of the experiments at both substrate concentrations with enzyme Batch IIb gave similar allosteric regulatory patterns as previous batches (Figure 2.4b and Figure 2.5c). Batch IIb had a similar specific activity value (42 U/mg vs. 40 U/mg) as Batch IIa, and the UV spectra of the two batches looked very similar (Figure 2.3a-b, λ_{max} at 272 nm and 278 nm respectively). Although λ_{max} is not exactly at 280 nm, the concentrated protein stock should only contain less than a few percent nucleotides. Upon another >50 fold dilution into the assay mixture, any nucleotide contaminants from the enzyme lot should be negligible.

There were also some other minor differences in the assay conditions between Figure 2.4a, and Figure 2.4b (10 μ M ADP), but they all seemed not to affect the overall regulatory pattern. The buffer used was 100 mM Tris pH 8.0 and 25 mM HEPES pH 7.5 respectively. The effector concentration in Figure 2.1a and Figure 2.1b were 0.5 mM and 1 mM respectively. The effector concentration is thought not be responsible for the observed differences as the enzyme is thought to be saturated with the effectors at millimolar concentration. dNTPs from two different sources were used and showed no difference.

The specific activities listed in Table 2.5a are not very consistent among parallel runs. The difference between data from Figure 2.4a and Figure 2.4b can mainly be contributed to the enzyme lot difference as Batch I had a much lower specific activity

than Batch IIb (7 U/mg vs. 42 U/mg based on the [2-¹⁴C]-CDP assay). In Figure 2.4a, most assay curves other than the dGTP curve lie close to the background level, the ADP reduction rates obtained from these curves thus may not be very accurate. The differences between data Figure 2.5a, b, and c are mainly from experimental errors. As the enzyme stock was very concentrated, a small change in enzyme volume can cause a big difference when calculating specific activity. In later runs, the enzyme stock was diluted first such that a reasonable volume (> 10 μL) were used. However, the overall regulatory patterns at each substrate concentration level are reproducible when the percentage of activity data are compared.

In summary, at 10 μM ADP, effector dGTP stimulates ADP reduction for 7-fold over the no effector case (Figure 2.4b) while at 1 mM ADP, the reduction is fastest when no effector is present. This pattern is as expected in the 10 μM ADP case, but not in the 1 mM ADP case.

Substrate ADP K_m Determination

Due to the unexpected allosteric regulatory pattern observed at 1 mM ADP, the K_m value of substrate ADP for *T. acidophila* RDPR was studied in the absence and presence of 1 mM dGTP, the positive effector for ADP reduction at 10 μM ADP.

The results are shown in Figure 2.6a-e. *T. acidophila* RDPR has a low basal rate for ADP reduction in the absence of any nucleotide effectors that is increased from 13 U/mg to 95 U/mg in the presence of 1 mM dGTP at [ADP] = 5 μM.

In the no effector case, analysis of the data, as described above, gives K_m (ADP, no effector) = 29.2 μM, V_{max} = 85.4 U/mg. However, for the 1 mM dGTP case, significant substrate inhibition is observed at [ADP] > 30 μM. Analysis of the data using equation

2.2

$$V = \frac{V_{max} [S]}{K_m + [S] + [S]^2 / K_i}$$

gives unreasonable values for kinetic parameters (Figure 2.6c). The models used are perhaps not appropriate for this specific case. And more data points need be obtained for further analysis.

The experimental results from the ADP K_m studies are in good agreement with the results from allosteric regulation studies. Substrate inhibition in the presence of 1 mM dGTP causes the rate to decrease at $[ADP] > 30 \mu\text{M}$, such that at 1 mM ADP, the rate of ADP reduction is only ~ 50% of that in the no effector case (Table 2.5b). The stimulating effect of dGTP for ADP reduction is only present at low ADP concentrations.

Previously, shown in Figure 2.6f, a K_m value of $64 \mu\text{M}$ is reported by Benner's laboratory in the presence of 1 mM dGTP.^{14,17} The two assay conditions are not exactly the same, a much higher overall ionic strength is present in Benner's conditions with 10 mM MgSO_4 and 100 mM Tris-HCl pH 8.0. Additional experiments need to be carried out to investigate the discrepancy between the two values reported.

Nevertheless, the ADP K_m value is rather low compared to two other reductases. *L. leichmannii* RTPR has a K_m value for ATP of 1.1 mM.¹⁶ The K_m values of several substrates for anaerobic *E. coli* RTPR, are listed in Table 2.6, all in the millimolar concentration range. However, for *P. furiosus* RDPR, a K_m value for CDP of $70 \mu\text{M}$ was reported. It would be interesting to compare the allosteric regulation of *T. acidophila* RDPR with that of *P. furiosus* RDPR as both reductases function at high temperature (55°C , 80°C respectively).

Allosteric Effects of (d)NTPs on GDP Reduction

As described in introduction section, dTTP is the positive effector for GDP (or GTP) reduction in most classes of RNRs except for *L. leichmannii* RTPR where no effector is required for GTP reduction. Similar to the regulation studies carried out for ADP, the allosteric effects of (d)NTPs on GDP reduction was carried out at $10 \mu\text{M}$ GDP and 1 mM GDP. In the latter case, it was anticipated that the enzyme should be saturated.

The rate of product formation obtained at 10 μ M GDP with DTT as reductant from 2 runs are shown in Figure 2.7a-b, the ones obtained at 1 mM GDP with DTT as reductant are shown in Figure 2.8, and the ones obtained at 10 μ M GDP with TR/TRR/NADPH as reductant are shown in Figure 2.9. The calculated specific activity data and percentage-of-activity data for GDP reduction are summarized in Table 2.7a-b.

From Figure 2.7a-b, at 10 μ M GDP, GDP reduction is fastest in the absence of any effectors, and is strongly inhibited by 1 mM dGDP. Again, differences in buffer used, effector source, enzyme source showed no significant difference in the overall regulatory pattern. From Figure 2.8, at 1 mM GDP, although GDP reduction still has a strong basal rate (20 U/mg), it is stimulated by dATP and ATP for 3-4 fold (60.7, 84.5 U/mg). The TR/TRR/NADPH reductant system at 10 μ M GDP (Figure 2.9) showed a similar regulatory pattern as the DTT reductant system. GDP reduction is fastest in the absence of any effectors or in the presence of 1 mM dTTP, and is strongly inhibited by 1 mM dGTP. The data in Figure 2.9 are quite scattered and the specific activity values are much smaller than the DTT reductant system. However, the TR/TRR/NADPH experiment was only carried out once for *T. acidophila* RDPR. The concentrations of TR, TRR, and NADPH were chosen empirically based on the conditions for *L. leichmannii* RTPR, which may not be the optimal nucleotide reduction conditions for *T. acidophila* RDPR.

In summary, although dTTP is the expected positive effector for GDP reduction for most classes of RNRs, it is not the case for *T. acidophila* RDPR. Again, the pattern at two substrate concentrations are different. At 10 μ M GDP, no effector is required. At 1 mM GDP, dTTP is inhibitory while dATP and ATP stimulates the reaction for 3-4 fold. However, the low substrate concentration case (10 μ M GDP) is similar to that of *L. leichmannii* RTPR which does not require any effector for GTP reduction.

Substrate GDP K_m Determination

Due to different allosteric regulatory patterns observed for GDP reduction at different substrate concentrations, its K_m was studied. As a K_m value of 0.24 mM for GTP was previously reported for *L. leichmannii* RTPR,¹⁰ the studies were carried out using a 5-40 μ M range in the absence and presence of 1 mM dTTP, the expected effector for most classes of RNRs; and at 100-600 μ M concentration range in the absence and presence of 1 mM dATP, the observed positive effector at 1 mM GDP. The experimental results are shown in Figure 2.10a and Figure 2.10b. Consistent with the allosteric regulation studies, GDP reduction is fastest in the absence of any effectors at low substrate concentration range (10-30 μ M), and dATP stimulates GDP reduction at the high concentration end (100-600 μ M). However, unlike the ADP case, the *T. acidophila* RDPR activity was independent of the concentration of substrate (5-40 μ M, 100-600 μ M). A possible explanation for this observation is that the K_m value for GDP is extremely low and the K_m determination was not carried out in the right concentration range. It is possible that dTTP will show a stimulating effect at submicromolar GDP concentration. The decrease in activity at 5 μ M GDP seems to support this hypothesis. However, more data points between 0-10 μ M GDP need to be obtained in order to reach any conclusion. [8, 5'-³H]-GDP used in Figure 2.10a had a specific activity of 1.2×10^5 cpm/nmol, which is still quite below the initial [8, 5'-³H]-GDP stock (S.A. = 39.5 Ci/mmol). In theory, if the initial stock solution is carefully diluted, one should be able to measure enzyme activity in the range of 0-10 μ M GDP. However, the determination of both the GDP concentration and its specific activity would require multiple dilutions, which may reduce their accuracy.

Allosteric Effects of (d)NTPs on CDP Reduction

As described in introduction, ATP (or dATP) stimulates CDP reduction for all classes of RNRs. The allosteric regulation on CDP reduction was first investigated at 1 mM CDP as initially only the [2-¹⁴C]-CDP assay was available. Due to the relatively

low specific activity and high cost of the ^{14}C labeled substrate comparing to other ^3H labeled substrates, it was impractical to look at micromolar CDP concentrations for K_m measurements with $[2\text{-}^{14}\text{C}]\text{-CDP}$. The $[5\text{-}^3\text{H}]\text{-CDP}$ assay was only recently developed, and the allosteric regulatory pattern at $10\ \mu\text{M}$ CDP was thus investigated. The K_m value for CDP still needs to be determined.

The assay time curves obtained at $10\ \mu\text{M}$ CDP with DTT as reductant are shown in Figure 2.11, the ones obtained at $1\ \text{mM}$ CDP with DTT as reductant are shown in Figure 2.12, and the ones obtained at $1\ \text{mM}$ CDP with TR/TRR/NADPH as reductant are shown in Figure 2.13. The calculated specific activity data and percentage-of-activity data for CDP reduction are summarized in Table 2.8a-b.

With DTT as reductant, at $10\ \mu\text{M}$ CDP, CDP reduction is fastest in the presence of $1\ \text{mM}$ dTTP (100%), two times of the basal reduction rate (56%) in the absence of any effectors, while dATP (41%) and ATP (47%) slightly inhibit the reaction. At $1\ \text{mM}$ CDP, CDP reduction is fastest in the presence of $1\ \text{mM}$ dGTP with a high basal rate (67%) while dATP (15%) and ATP (41%) inhibit the reaction. The allosteric regulatory pattern using TR/TRR/NADPH reducing system at $1\ \text{mM}$ CDP, is similar to the DTT case. CDP reduction is fastest in the presence of $1\ \text{mM}$ dGTP, but the basal rate is much lower (30%).

The allosteric regulation studies on CDP reduction is not as complete as the ADP and GDP studies described above. Based on present data, dATP and ATP do not shown any stimulation effects under conditions investigated. On the contrary, dATP appears to be an inhibitor.

Allosteric Effects of dNDPs on ADP Reduction

As the allosteric regulation of *T. acidophila* RDPR is not as well defined as other RNRs, it was suspected deoxynucleotide diphosphates could act as potential allosteric effectors. The role of dNDPs as potential allosteric effectors was studied for ADP

reduction of which the K_m value is known. dCDP was not used as it was not commercially available at the time of the experiment. The studies were carried out at 10 μM and 200 μM ADP. The assay time curves obtained are shown in Figure 2.14 and Figure 2.15 and the calculated specific activity and percentage-of-activity data are summarized in Table 2.9a and Table 2.9b respectively.

At 10 μM ADP, all the dNDPs investigated inhibited the reaction. At 200 μM ADP, the inhibitory effects were less. As dNDPs are products of *T. acidophila* RDPR, both substrates and products can be competing for the same active site. At higher substrate concentration, ADP was able to compete with the dNDPs, thus the inhibitory effects were less. Although dCDP was not investigated, overall dNDPs do not appear to have any allosteric effects on *T. acidophila* RDPR.

Summary

Despite all the regulation studies carried out on three substrates, the allosteric regulatory pattern remains elusive for *T. acidophila* RDPR. However, based on the information obtained, some insights can be gained for *T. acidophila* RDPR for future experimental designs. From the K_m studies, unlike other RNRs with K_m values in the millimolar concentration range, *T. acidophila* RDPR seems to have substrate K_m values on the order of micromolar concentrations (29.2 μM for ADP in the absence of effector, the K_m value for GDP is probably even lower). This could be related to the fact that *T. acidophila* is a thermophile as the other hyperthermophilic *P. furiosus* RDPR also has K_m value in the same concentration range (70 μM for CDP). It could well be that the regulation studies carried out were not probing the right substrate concentration range. The *in vivo* concentrations of the substrate NDPs are not yet known for *T. acidophila*. The low specific activity, and substrate inhibition observed for *T. acidophila* suggest that the *in vitro* assay conditions may not simulate the *in vivo* conditions very well. It should be noted that, unlike the *E. coli* RDPR, neither DTT nor TR/TRR/NADPH reductant

system used in the *in vitro* assay is natural for *T. acidophila* RDPR. This is also likely the cause of the low specific activity of *T. acidophila* RDPR as mechanistic studies revealed that cob(II)alamin formation occurs in a kinetically competent fashion (Chapter 3). The low specific activity of *T. acidophila* RDPR also requires radioactive assays that are less flexible and very time consuming comparing to the spectrophotometric assays for *E. coli* RDPR and *L. leichmannii* RTPR. As there are many variables in the assay conditions, it is hard to test all the conditions given the inflexibility and time constraints of the radioactive assays.

Given the low substrate K_m values of *T. acidophila* RDPR, the regulation data at 1 mM substrate concentrations may not be very meaningful. The "expected" regulatory pattern is observed at 10 μ M ADP where dGTP acts as a positive effector, and the 10 μ M GDP case where no effector is required for its reduction is not unprecedented as it is also the case for *L. leichmannii* RTPR. The K_m value for CDP is yet to be determined, nevertheless, there is always complications when dATP and ATP are the expected effectors. Based on models for other RNRs presented in the introduction, multiple dATP binding sites could be present. Considering the fact that *T. acidophila* RDPR can be purified by dATP-affinity chromatography (so can anaerobic *E. coli* RTPR,¹⁸ aerobic *E. coli* R1, NrDEF RDPR from *S. typhimurium*,⁹ and *P. furiosus* RDPR,¹⁵ but not RTPR from *L. leichmannii*), there definitely exists an dATP binding site in *T. acidophila* RDPR. For the other AdoCbl-dependent *P. furiosus* RDPR, dATP acts as a strong inhibitor¹⁵ which is unlike *L. leichmannii* RTPR (class II), but similar to the *E. coli* RDPR (class Ia) and anaerobic *E. coli* RTPR (class III). For *T. acidophila* RDPR, dATP acts as positive effectors only at 1 mM GDP, whereas is inhibitory in other cases, but the inhibitory effect is not particularly strong. Binding experiments are probably the best tool to identify the allosteric sites involving dATP and other effectors.

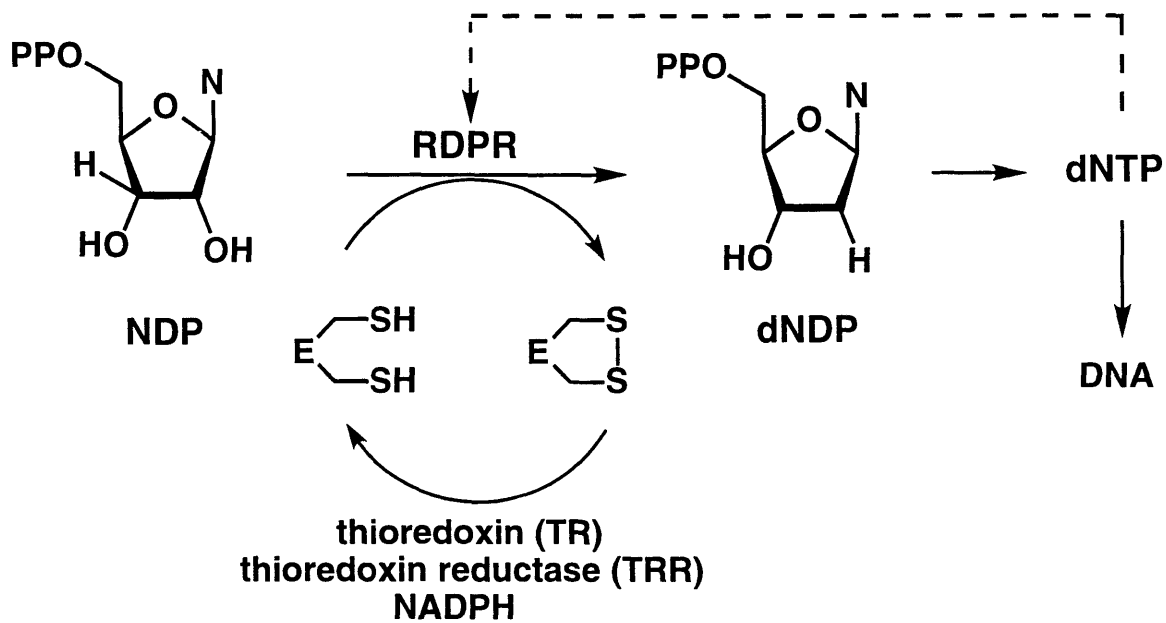
Although more experiments need be carried out to further define the allosteric regulatory pattern for *T. acidophila* RDPR, it is still evident that *T. acidophila* RDPR is

subject to allosteric control as its activity can be greatly affected by the presence of deoxynucleotides. Different assay conditions, especially substrate, and effector concentrations need be systematically tested in order to best simulate the *in vivo* conditions of *T. acidophila*, and obtain more meaningful data.

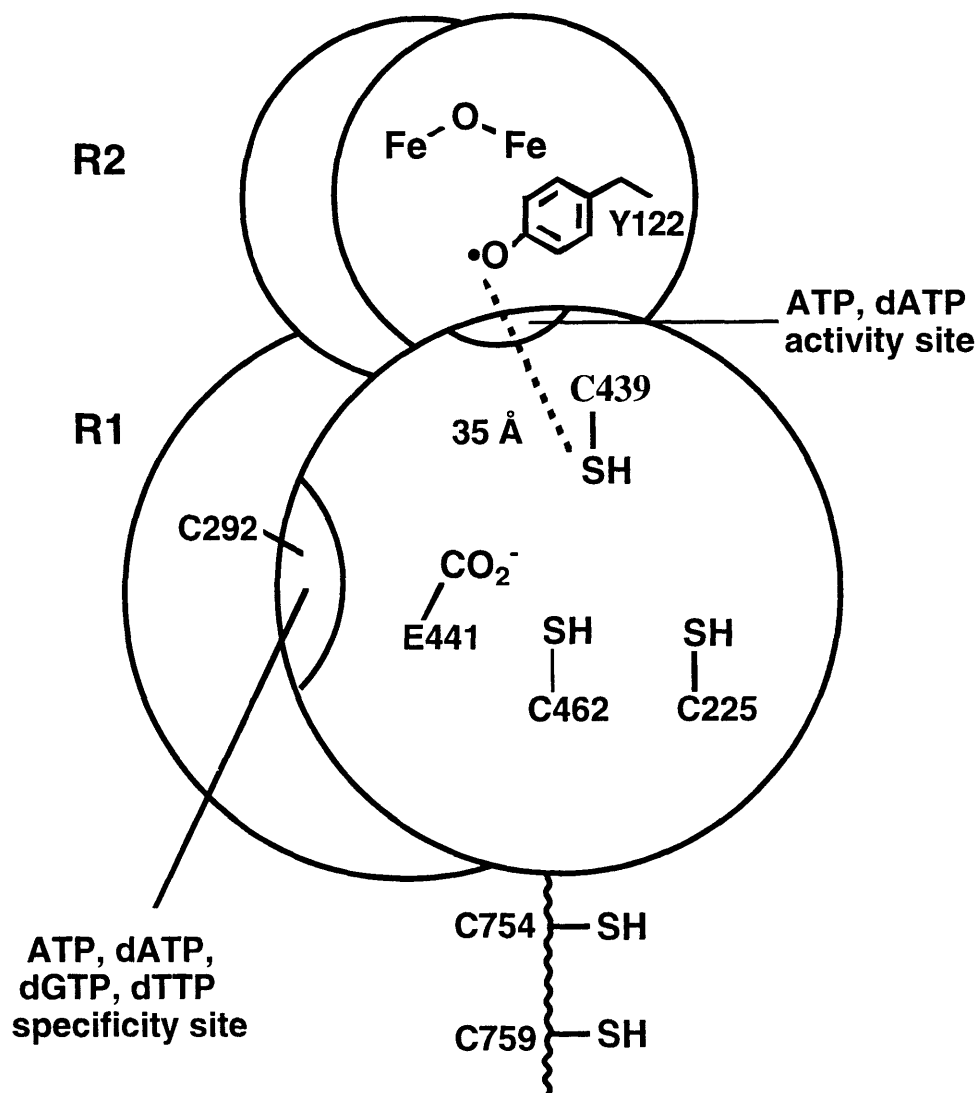
References:

- (1) Eriksson, S.; Sjöberg, B. M. in *Allosteric Enzymes*; Hervé, G. Ed.; CRC, Boca Raton, 1989; Vol. pp 189-215.
- (2) Reichard, P. *Science* **1993**, *260*, 1773-1777.
- (3) Jordan, A.; Pontis, E.; Aslund, F.; Hellman, U.; Gibert, I.; Reichard, P. *J. Biol. Chem.* **1996**, *271*, 8779-8785.
- (4) Brown, N. C.; Reichard, P. *J. Mol. Biol.* **1969**, *46*, 39-55.
- (5) von Döbeln, U.; Reichard, P. *J. Biol. Chem.* **1976**, *251*, 3616.
- (6) Ormö, M.; Sjöberg, B. M. *Eur. J. Biochem.* **1996**, *241*, 363-367.
- (7) Eliasson, R.; Pontis, E.; Sun, X.; Reichard, P. *J. Biol. Chem.* **1994**, *269*, 26052-26057.
- (8) Eliasson, R.; Pontis, E.; Jordan, A.; Reichard, P. *The Journal of Biological Chemistry* **1996**, *271*, 26582-26587.
- (9) Jordan, A.; Pontis, E.; Atta, M.; Krook, M.; Gibert, I.; Barbe, J.; Reichard, P. *Proc. Natl. Acad. Sci.* **1994**, *91*, 12892-12896.
- (10) Thelander, L.; Reichard, P. *Ann. Rev. Biochem.* **1979**, *48*, 133-158.
- (11) Stubbe, J.; van der Donk, W. A. *Chem. Biol.* **1995**, *2*, 793-801.
- (12) Lunn, C. A.; Kathju, S.; Wallace, B. J.; Kushner, S.; Pigiet, V. *J. Biol. Chem.* **1984**, *259*, 10469-10474.
- (13) Russell, M.; Model, P. *J. Bacteriol.* **1985**, *163*, 238-242.
- (14) Tauer, A., *Ph.D. Thesis, Eidgenössische Technische Hochschule*, **1994**.
- (15) Riera, J.; Robb, F. T.; Weiss, R.; Fontecave, M. *Proc. atl. Acad. Sci.* **1997**,

- (16) Booker, S.; Stubbe, J. *Proc. Natl. Acad. Sci. USA* **1993**, *90*, 8352-8356.
- (17) Tauer, A.; Benner, S. A. *Proc. Natl. Acad. Sci.* **1997**, *94*, 53-58.
- (18) Eliasson, R.; Fontecave, M.; Jörnvall, H.; Krook, M.; Pontis, E.; Reichard, P. *Proc. Natl. Acad. Sci. USA* **1990**, *87*,

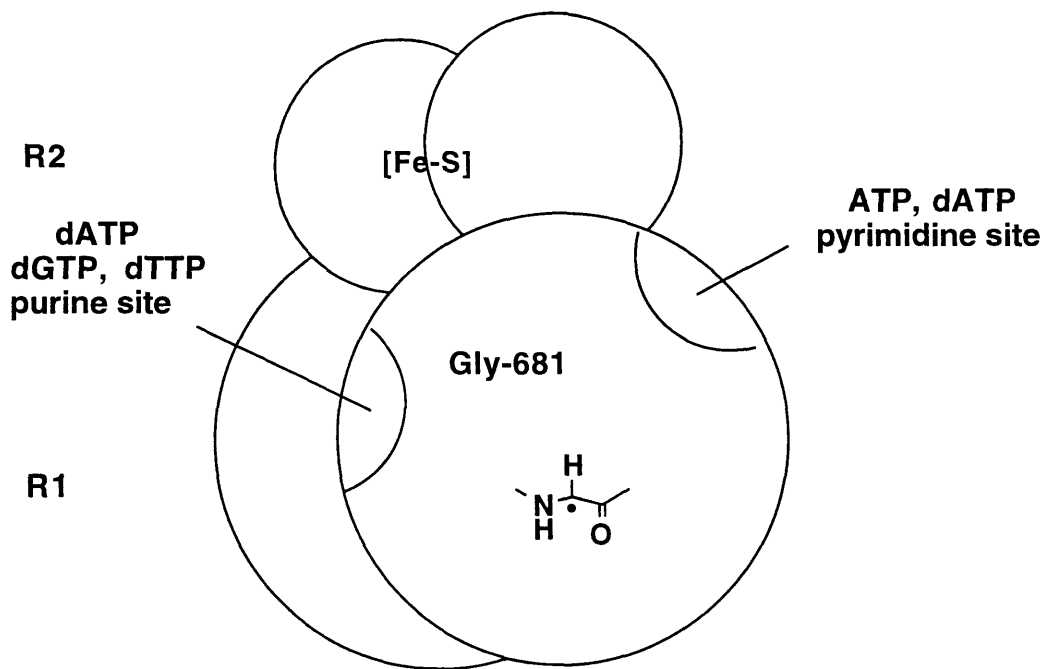


Scheme 2.1 Substrate specificity of ribonucleotide reductase is subject to allosteric control. One enzyme reduces all four common substrates. The substrate specificity is determined by the *in vivo* balance of the deoxynucleotide pool. One enzyme is therefore able to provide balanced building blocks for DNA biosynthesis. The example shown is that for *E. coli* RDPR. *Courtesy of Dr. W. A. van der Donk.*

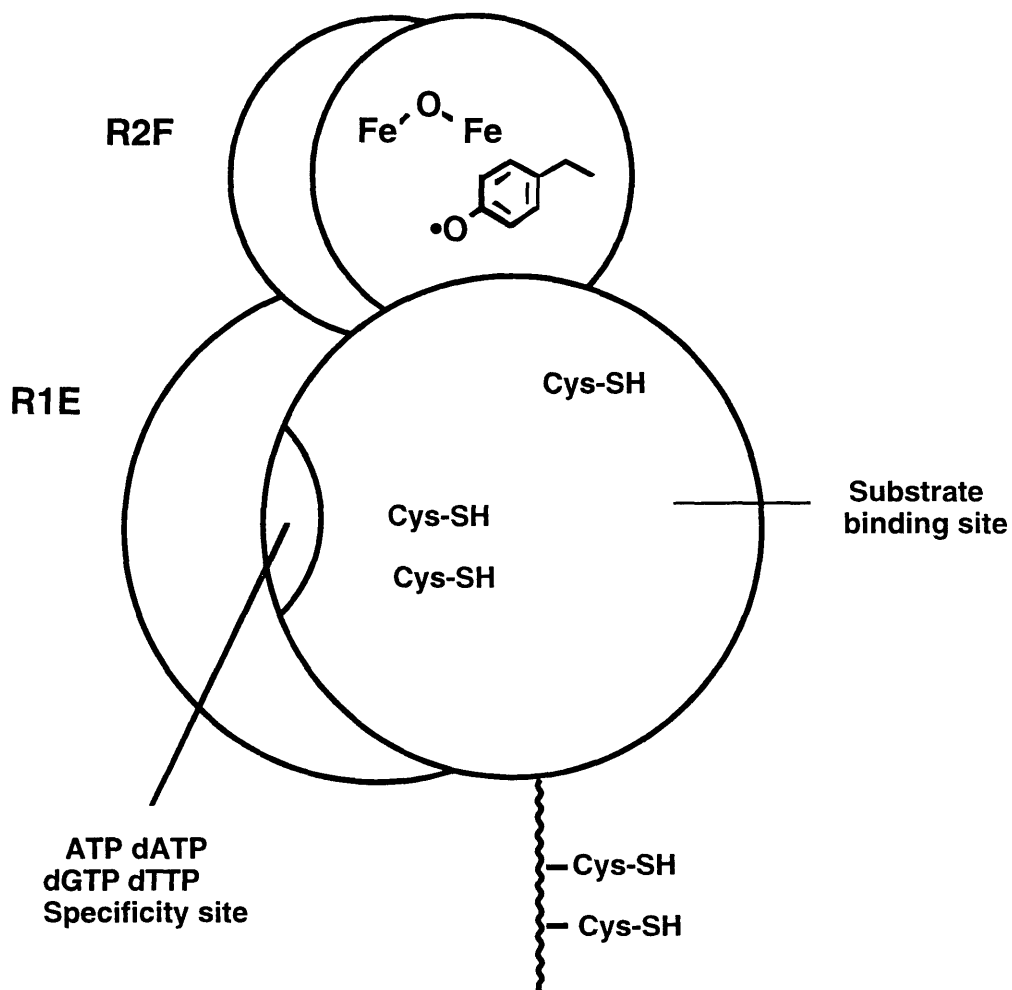


Scheme 2.2 Schematic representation of RDPR from *E. coli* (Class Ia). R1 subunit contains the catalytic site with its redox active thiols and two kinds of allosteric sites, one regulating the overall reactivity of the enzyme by binding ATP and dATP, the other regulating its substrate specificity by binding allosteric effectors (ATP, dATP, dGTP, dTTP). Protein R2, with its unusual diferric cluster-tyrosyl radical cofactor, generates the thiyl radical (Cys-439) required for catalysis via long range electron transfer.

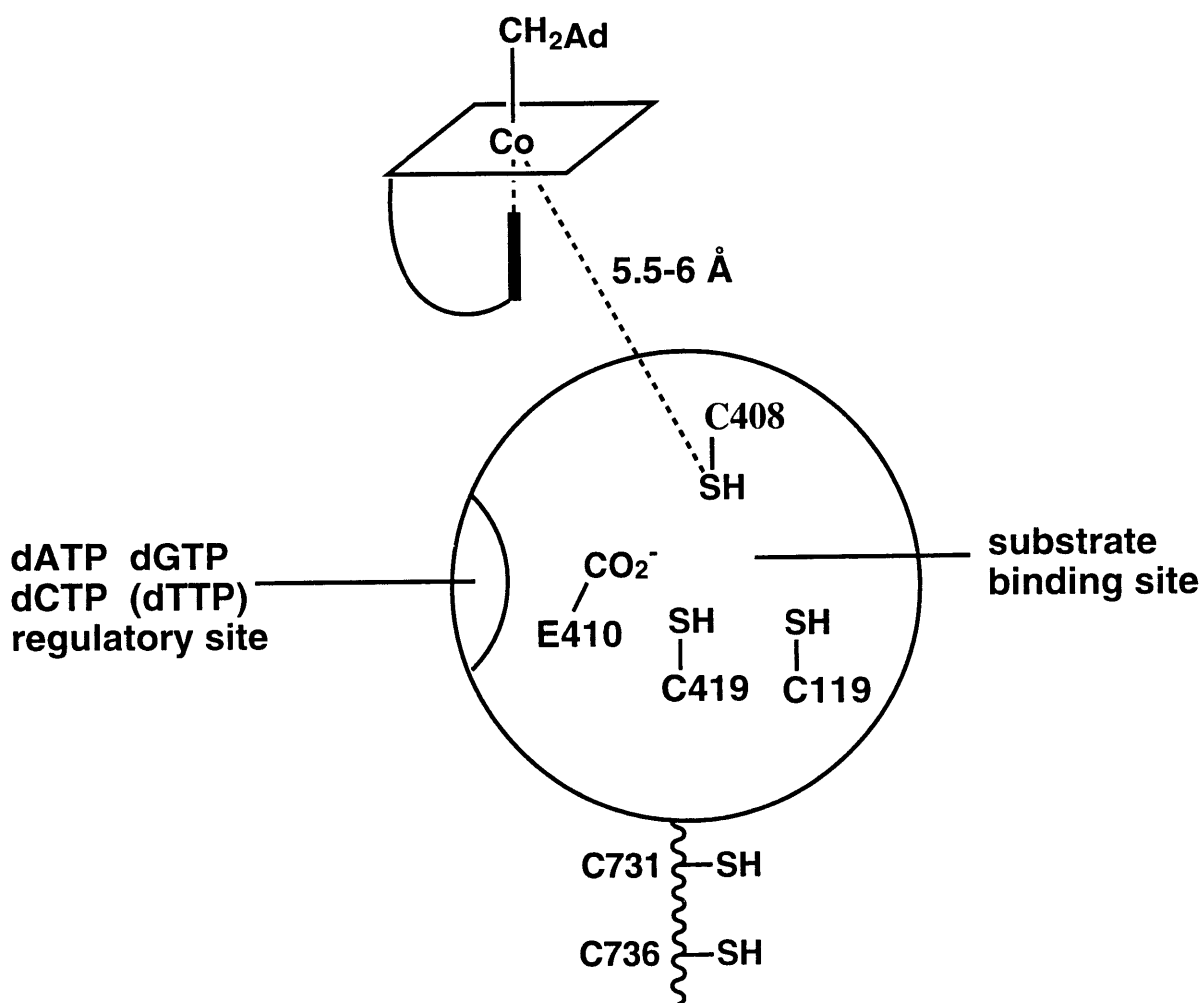
Courtesy of Dr. W. A. van der Donk.



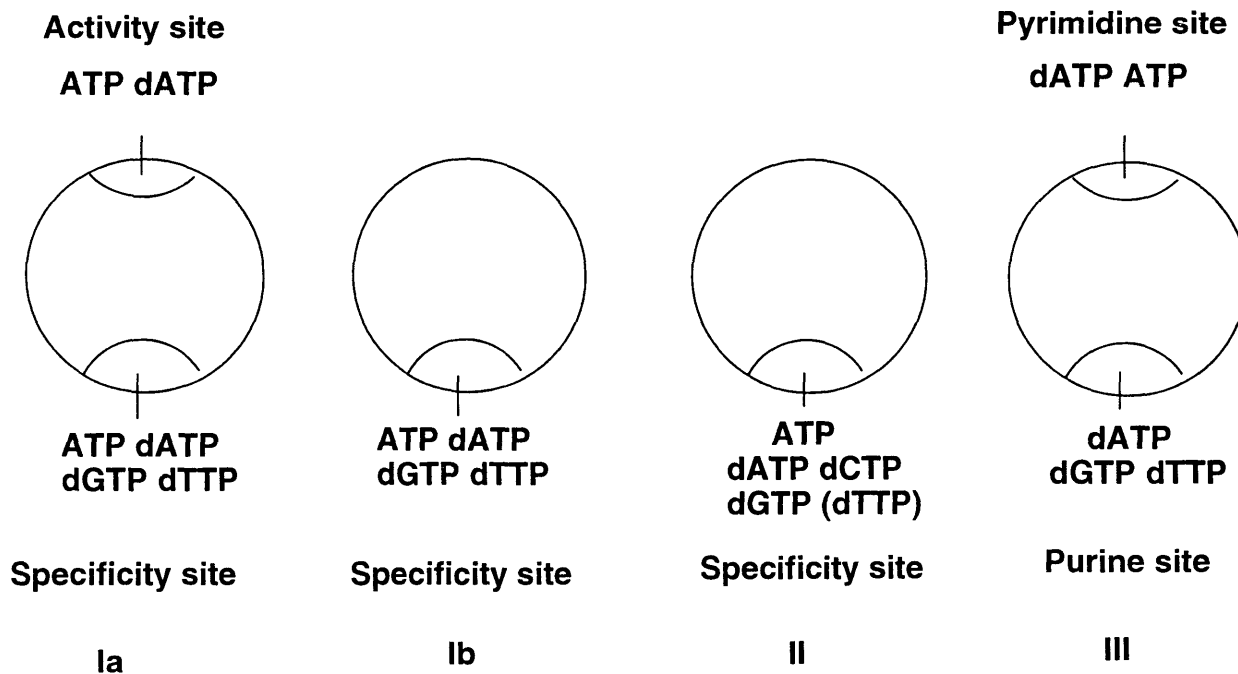
Scheme 2.3 Schematic representation of RTPR from anaerobically grown *E. coli* (Class III). *E. coli* anaerobic RTPR is composed of two homodimer subunit R1 and R2. R1 contains the glycyl free radical (Gly-681), while R2 contains a single iron-sulfur center and binds S-adenosylmethionine required for glycyl radical formation. It contains two distinct effector binding sites. One binds dGTP, dTTP, and dATP and regulates the reduction of ATP and GTP (purine site). The second binds dATP and ATP and regulates the reduction of CTP and UTP (pyrimidine site).



Scheme 2.4 Schematic representation of NrDEF RDPR from *S. typhimurium* (Class Ib). R1E subunit contains the catalytic site with its redox active thiols and one specificity site binding allosteric effectors (ATP, dATP, dGTP, dTTP). Protein R2F, contains a μ -oxo bridged dinuclear iron center and a tyrosyl radical.



Scheme 2.5 Schematic representation of RTPR from *L. leichmannii*. (Class II). The enzyme is a monomer and requires 5'-deoxyadenosylcobalamin (AdoCbl) as a cofactor. It contains a regulatory site which binds allosteric effector deoxyribonucleotides and a separate substrate binding site. The binding of dNTPs at the regulatory site increases the affinity for AdoCbl and also controls the substrate specificity at the substrate binding site. *Courtesy of Dr. W. A. van der Donk.*



Scheme 2.6 Models for the allosteric regulation of all three classes of RNRs.⁸ Only one subunit monomer containing the allosteric sites is shown in Ia, Ib, and III. For Ia, Ib, and II, binding of effectors at the specificity site controls substrate specificity. For III, binding of effector at the purine site regulates purine reduction while binding of effector at the pyrimidine site regulates pyrimidine reduction. In Ia and III, binding of dATP at the activity site of Ia or either site of III turns off the enzyme activity, therefore dATP acts as a general inhibitor. (For class Ia, at $[dATP] < 1 \mu M$, it stimulates CDP and UDP reduction. See text for details.) In Ib and II, only one specificity site is present and dATP is not generally inhibitory.

Table 2.1a Allosteric regulation of *E. coli* RDPR (Class Ia).¹⁰

Effector binding to		Reduction of			
activity site	specificity site	ADP	GDP	CDP	UDP
0	ATP	0	0	+	+
0	dTTP	+	+	+	+
0	dGTP	+	+	0	0
ATP	ATP or dATP	0	0	+	+
ATP	dTTP	(+)	+	-	-
ATP	dGTP	+	(+)	nd	nd
dATP	any effector	-	-	-	-

*0 = no effect; + = stimulation; - = inhibition; and nd = not determined.

Table 2.1b Allosteric regulation of *E. coli* RDPR (Class Ia).¹

Effector	Substrate			
	ADP	GDP	CDP	UDP
None	12	21	25	7
dATP**			130	120
dTTP	100	120	100*	110
dGTP	110	88		
ATP			110	120

Activities are given in percent. (*) denotes the substrate and effector combination used for correlation of the other activities measured with the respective enzyme. Only the action of the prime effectors is indicated. **At [dATP] < 1 μ M only.

Table 2.2 Allosteric regulation of anaerobic *E. coli* RTPR (Class III).⁷

Effector	Substrate			
	ATP	GTP	CTP	UTP
None	45	15	80	20
dATP	2	0	20	0
dTTP	5	195	25	5
dCTP	40	20	ND*	15
dGTP	240	5	15	0
ATP	ND*	35	290	245

*ND, Not done. Enzyme (2.7 μ g) was incubated with various labeled substrates (1-2 mM and effectors (0.5 mM) under standard conditions. The reaction was started by the addition of substrate mixture to the preincubation mixture, and anaerobic incubation was continued for 20 min at room temperature before the reactions were stopped with 0.5 mL of 1 M HClO₄. Activities are in milliunits. One milliunit of enzyme activity is 1 pmol of dCTP formed per min.¹²

Table 2.3 Allosteric regulation of *NrdEF* RDPR from *S. typhimurium* (Class Ib).⁸

Effector	Substrate			
	ADP	GDP	CDP	UDP
None	0	0	10	20
dATP	7	24	100	100
dTTP	3	100	72	50
dCTP	0	18	ND	ND
dGTP	100	39	30	45
ATP	ND	17	60	90

ND = Not done. The reduction of the four ribonucleoside diphosphate substrates (0.5 mM) was determined in separate experiments in the presence of the various indicated effector nucleoside triphosphates (50 mM* for deoxynucleotides, 2 mM for ATP). Incubations were at 37°C for 20 min with 1-1.5 µg of each protein. The activities obtained with the best effector are given as 100% and correspond to 0.18 unit for ADP, 0.17 for CDP, 0.14 for GDP, and 0.10 for UDP. One unit of enzyme activity is 1 nmol of product formed during 1 min.

* This number is what was originally in the paper, likely a mistake.

Table 2.4 Allosteric regulation of *L. leichmannii* RTPR (Class II).¹

Effector	Substrate			
	ATP	GTP	CTP	UTP
Added				
None	20	100*	36	14
dATP			100	
dCTP				37
dGTP	100			

Activities are given in percent. (*) denotes the substrate and effector combination used for correlation of the other activities measured with the respective enzyme. Only the action of the prime effectors is indicated.

Table 2.5a Summarized data for allosteric regulation of ADP reduction by specific activity (U/mg).

Effector	[ADP]=10 μ M			[ADP]=1mM		
	Benner's ¹	Figure 2.4a ²	Figure 2.4b ³	Figure 2.5a ⁴	Figure 2.5b ⁵	Figure 2.5c ⁶
		I	IIb	IIa	IIa	IIb
None	0	1.54	13.67	40.4	59.8	83.6
dATP	0	0.69	8.2	20.6	25.9	33.9
dATP (10 μ M)				37.8	52.8	61.2
dTTP	2.66	0.66	10.91	17.1	10.5	37.4
dCTP	0	0.67	25.19	21.5	22.2	32.1
dGTP	40.43	13.8	95.6	22.6	27.1	37.0
ATP	0	1.74	14.43	18.3	30.0	40.0

Table 2.5b Summarized data for allosteric regulation of ADP reduction by percentage of activity.

Effector	[ADP]=10 μ M			[ADP]=1mM		
	Benner's ¹	Figure 2.4a ²	Figure 2.4b ³	Figure 2.5a ⁴	Figure 2.5b ⁵	Figure 2.5c ⁶
		I	IIb	IIa	IIa	IIb
None	0	11.2	14.3	100	100	100
dATP	0	5.0	8.6	50.9	43.4	40.6
dATP (10 μ M)				93.6	88.3	73.3
dTTP	6.6	4.8	11.4	42.2	17.6	44.8
dCTP	0	4.9	26.4	53.3	37.1	38.4
dGTP	100	100	100	56.0	45.3	44.2
ATP	0	12.6	15.1	45.3	50.3	47.9

¹Assay conditions: 100 mM Tris-HCl, pH 8.0, 10 μ M ADP, 100 μ M AdoCbl, 10 mM DTT, 10 mM MgSO₄, 50°C, [Effector] = 10 μ M. *Source: Tauer, Thesis, p.31.*

²Assay conditions: 10 μ M ADP (S.A. = 1.5×10^5 cpm/nmol), 1 mM MgCl₂, 10 mM DTT, 100 μ M AdoCbl, 100 mM Tris pH 8.0, 0.2 μ M (1 μ g/50 μ L) *T. acidophila* RDPR (Batch I), and effector of choice (No effector, 0.5 mM dATP, 0.5 mM dTTP, 0.5 mM dCTP, 0.5 mM dGTP, or 0.5 mM ATP; dNTPs were from Sigma). *Source: Book II, p. 85.*

³Assay conditions: 10 μ M ADP (S.A. = 1.5×10^5 cpm/nmol), 1 mM MgCl₂, 10 mM DTT, 100 μ M AdoCbl, 25 mM Hepes pH 7.5, 0.1 μ M (0.5 μ g/50 μ L) *T. acidophila* RDPR (Batch IIb), and effector of choice (No effector, 1 mM dATP, 1 mM dTTP, 1 mM dCTP, 1 mM dGTP, or 1 mM ATP; dNTPs were from Boehringer Mannheim). *Source: Book III, p. 78.*

⁴Assay conditions: 1 mM ADP (S.A. = 5.2×10^3 cpm/nmol), 1 mM MgCl₂, 30 mM DTT, 100 μ M AdoCbl, 25 mM Hepes pH 7.5, 4 μ M (20 μ g/50 μ L) *T. acidophila* RDPR (Batch IIa), and effector of choice (No effector, 1 mM dATP, 10 μ M dATP, 1 mM dTTP, 1 mM dCTP, 1 mM dGTP, or 1 mM ATP; dNTPs were from Sigma). *Source: Book III, p. 44.*

⁵Assay conditions: 1 mM ADP (S.A. = 2.1×10^3 cpm/nmol), 1 mM MgCl₂, 30 mM DTT, 100 μ M AdoCbl, 25 mM Hepes pH 7.5, 4.33 μ M (21.7 μ g/50 μ L) *T. acidophila* RDPR (Batch IIa), and effector of choice (No effector, 1 mM dATP, 10 μ M dATP, 1 mM dTTP, 1 mM dCTP, 1 mM dGTP, or 1 mM ATP; dNTPs were from Sigma). *Source: Book III, p. 52.*

⁶Assay conditions: 1 mM ADP (S.A. = 2.1×10^3 cpm/nmol), 1 mM MgCl₂, 30 mM DTT, 100 μ M AdoCbl, 25 mM Hepes pH 7.5, 4 μ M (20 μ g/50 μ L) *T. acidophila* RDPR (Batch IIb), and effector of choice (No effector, 1 mM dATP, 10 μ M dATP, 1 mM dTTP, 1 mM dCTP, 1 mM dGTP, or 1 mM ATP; dNTPs were from Sigma). *Source: Book III, p. 67.*

Table 2.6 K_m values for substrates of the anaerobic *E. coli* RTPR.⁷ The values were calculated from linear Lineweaver-Burk plots obtained from the results of experiments in which substrate concentration was varied at a fixed concentration of the appropriate stimulating modulator whose concentration is recorded in the table.

Substrate	K_m (mM)	Effector (mM)
ATP	4	dGTP(0.2)
CTP*	0.5	ATP (0.4)
GTP	0.4	dTTP (0.8)
UTP	1	ATP (0.4)

* K_m for CTP is 4 mM in the absence of ATP; 0.45 mM in the presence of 0.1 mM ATP.

Table 2.7a Summarized data for allosteric regulation of GDP reduction by specific activity (U/mg).

Effector	DTT			TR/TRR/NADPH
	[GDP] =10 μ M		[GDP]=1 mM	[GDP] = 10 μ M
	Figure 2.7a ⁷ IIa	Figure 2.7b ⁸ IIb	Figure 2.8 ⁹ IIb	Figure 2.9 ¹⁰ IIa
None	77	76.2	20.7	9.1
dATP	25.4	22.9	84.5	7.6
dTTP	30.7	53.9	9.3	9.4
dCTP	36.4	43.6	11	8.8
dGTP	3.1	4.6	4.9	1.7
ATP	54.2	40.8	60.7	7.7

Table 2.7b Summarized data for allosteric regulation of GDP reduction by percentage of activity.

Effector	DTT			TR/TRR/NADPH
	[GDP] =10 μ M		[GDP]=1 mM	[GDP] = 10 μ M
	Figure 2.7a ⁷ IIa	Figure 2.7b ⁸ IIb	Figure 2.8 ⁹ IIb	Figure 2.9 ¹⁰ IIa
None	100	100	24.6	97
dATP	33	30.1	100	81.5
dTTP	39.9	70.7	11	100
dCTP	47.3	57.2	13	93.8
dGTP	4.1	6	5.9	17.9
ATP	70.4	53.5	71.8	81.9

⁷Assay conditions: 10 μ M GDP (S.A. = 2.2×10^5 cpm/nmol), 1 mM MgCl₂, 10 mM DTT, 100 μ M AdoCbl, 100 mM Tris pH 8.0, 0.051 μ M (0.256 μ g/50 μ L) *T. acidophila* RDPR (Batch IIa), and effector of choice (No effector, 0.5 mM dATP, 0.5 mM dTTP, 0.5 mM dCTP, 0.5 mM dGTP, or 0.5 mM ATP; the dNTPs were from Sigma). *Source: Book II, p.124.*

⁸Assay conditions: 10 μ M GDP (S.A. = 2.2×10^5 cpm/nmol), 1 mM MgCl₂, 10 mM DTT, 100 μ M AdoCbl, 25 mM Hepes pH 7.5, 0.1 μ M (0.5 μ g/50 μ L) *T. acidophila* RDPR (Batch IIb), and effector of choice (No effector, 1 mM dATP, 1 mM dTTP, 1 mM dCTP, 1 mM dGTP, or 1 mM ATP; the dNTPs were from Boehringer Mannheim). *Source: Book III, p. 82.*

⁹Assay conditions: 1 mM GDP (S.A. = 2.3×10^3 cpm/nmol), 1 mM MgCl₂, 30 mM DTT, 100 μ M AdoCbl, 25 mM Hepes pH 7.5, 4 μ M (20 μ g/50 μ L) *T. acidophila* RDPR (Batch IIb), and effector of choice (No effector, 10 μ M dATP, 1 mM dATP, 1 mM dTTP, 1 mM dCTP, 1 mM dGTP, or 1 mM ATP; the dNTPs were from Boehringer Mannheim). *Source: Book III, p. 84.*

¹⁰Assay conditions: 10 μ M GDP (S.A. = 2.2×10^5 cpm/nmol), 1 mM MgCl₂, 40 μ M TR, 2 μ M TRR, 1 mM NADPH, 100 μ M AdoCbl, 100 mM Tris pH 8.0, 0.053 μ M (0.256 μ g/50 μ L) *T. acidophila* RDPR (Batch IIa), and effector of choice (No effector, 0.5 mM dATP, 0.5 mM dTTP, 0.5 mM dCTP, 0.5 mM dGTP, or 0.5 mM ATP; the dNTPs were from Sigma). *Source: Book II, p.125.*

Table 2.8a Summarized data for allesteric regulation of CDP reduction by specific activity (U/mg).

Effectors	DTT		TR/TRR/NADPH
	[CDP]=10 μ M	[CDP] = 1 mM	[CDP] = 1 mM
	Figure 11 ¹¹ IIb	Figure 12 ¹² I	Figure 13 ¹³ I
None	46.5	6.1	2.2
dATP**	33.9	1.4	1.5
dTTP	82.4	5.7	5.5
dCTP	63.6	nd*	nd*
dGTP	64.7	9.1	7.4
ATP	39.3	3.8	2.7

Table 2.8b Summarized data for allesteric regulation of CDP reduction by percentage of activity.

Effectors	DTT		TR/TRR/NADPH
	[CDP]=10 μ M	[CDP] = 1 mM	[CDP] = 1 mM
	Figure 11 ¹¹ IIb	Figure 12 ¹² I	Figure 13 ¹³ I
None	56.4	67.1	29.8
dATP**	41.1	15.3	20.2
dTTP	100	62.9	75.1
dCTP	77.2	nd*	nd*
dGTP	78.5	100	100
ATP	47.7	41.2	36.3

*nd = not done. ** In Figure 12 and Figure 13, dATP was at 0.1 mM while the other effectors were at 0.5 mM.

¹¹Assay conditions: 10 μ M [5-³H]-CDP (S.A. = 45×10^5 cpm/nmol), 1 mM MgCl₂, 10 mM DTT, 100 μ M AdoCbl, 25 mM Hepes pH 7.5, 0.1 μ M (0.5 μ g/50 μ L) *T. acidophila* RDPR (Batch Iib), and effector of choice (No effector, 1 mM dATP, 1 mM dTTP, 1 mM dCTP, 1 mM dGTP, or 1 mM ATP; the dNTPs were from Boehringer Mannheim). *Source: Book III, p.136.*

¹²Assay conditions: 1 mM [2-¹⁴C]-CDP (S.A. = 2.2×10^3 cpm/nmol), 1 mM MgCl₂, 25 mM Hepes pH 7.5, 30 mM DTT, 100 μ M AdoCbl, 10 μ M (100 μ g/100 μ L) *T. acidophila* RDPR (Batch I), and effector of choice (No effector, 0.1 mM dATP, 0.5 mM dTTP, 0.5 mM dCTP, 0.5 mM dGTP, or 0.5 mM ATP; the dNTPs were from Sigma). *Source: Book II, p.78.*

¹³Assay conditions: 1 mM [2-¹⁴C]-CDP (S. A. = 2.2×10^3 cpm/nmol), 1 mM MgCl₂, 25 mM Hepes pH 7.5, 4 mM NADPH, 200 μ M TR, 2 μ M TRR, 100 μ M AdoCbl, 10 μ M (100 μ g/100 μ L) *T. acidophila* RDPR (Batch I), and effector of choice (No effector, 0.1 mM dATP, 0.5 mM dTTP, 0.5 mM dCTP, 0.5 mM dGTP, or 0.5 mM ATP; the dNTPs were from Sigma). *Source: Book II, p.74.*

Table 2.9a Summarized data for allosteric effects of dNDPs on ADP reduction by specific activity (U/mg).

Effector	[ADP] = 10 μ M	[ADP] = 200 μ M
	Figure 14 ¹⁴	Figure 15 ¹⁵
	Iib	Iib
None	26.9	46.1
dADP	2	20.3
dTDP	0.8	9.5
dGDP	9.8	43

Table 2.9b Summarized data for allosteric effects of dNDPs on ADP reduction by percentage of activity.

Effector	[ADP] = 10 μ M	[ADP] = 200 μ M
	Figure 14 ¹⁴	Figure 15 ¹⁵
	Iib	Iib
None	100	100
dADP	7.3	44.1
dTDP	2.9	20.6
dGDP	36.4	93.3

¹⁴Assay conditions: 10 μ M (S.A. = 148,787 cpm/nmol), 0.224 μ M (1.12 μ g/50 μ L) *T. acidophila* RDPR (Batch Iib), 1 mM MgCl₂, 25 mM Hepes pH 7.5, 100 μ M AdoCbl, 30 mM DTT, and effector of choice (No effector, 0.5 mM dADP, 0.5 mM dTDP, or 0.5 mM dGDP). *Source: Book III, p.114.*

¹⁵Assay conditions: 200 μ M ADP (S.A. = 39,150 cpm/nmol), 0.64 μ M (3.2 μ g/50 μ L) *T. acidophila* RDPR (Batch Iib), 1 mM MgCl₂, 25 mM Hepes pH 7.5, 100 μ M AdoCbl, 30 mM DTT, and effector of choice (No effector, 0.5 mM dADP, 0.5 mM dTDP, or 0.5 mM dGDP). *Source: Book III, p.114.*

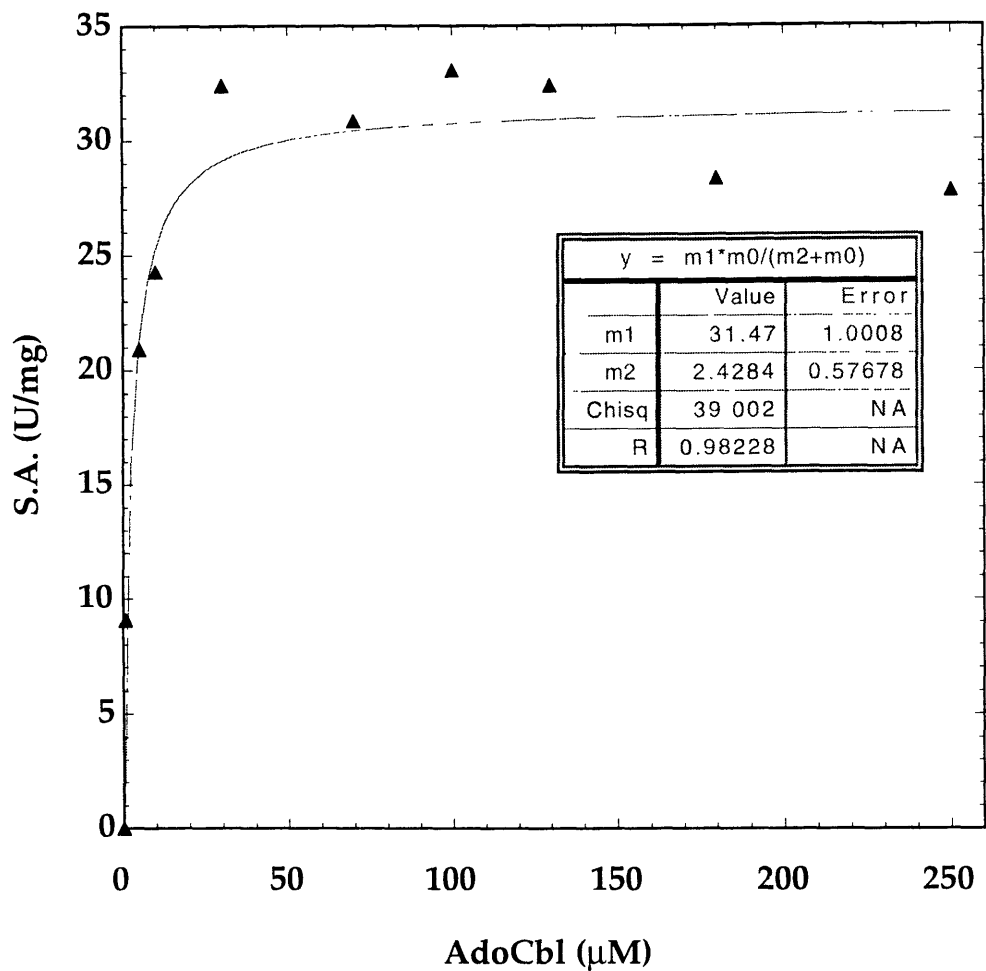
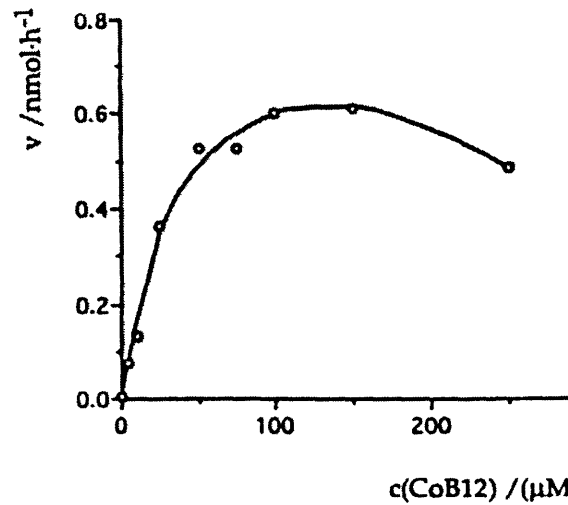


Figure 2.1a AdoCbl K_m determination. Assay conditions: 2 mM CDP (S.A. = 1.8×10^3 cpm/nmol), 25 mM Hepes pH 7.5, 1 mM $MgCl_2$, 30 mM DTT, 1 mM dGTP, 3.34 μM (33.4 $\mu g/100 \mu L$) *T. acidophila* RDPR (Batch IIa), and 0-250 μM AdoCbl. The data is fit to the standard Michaelis-Menten equation:

$$V = \frac{V_{max}[S]}{K_m + [S]}$$

where m_1 is V_{max} , m_2 is K_m . Source: Book II, p.114.

Abbildung 13: Coenzym B12-Abhängigkeit der Reduktion von ADP durch die Ribonukleotid-Reduktase aus *Thermoplasma acidophila*



Legende: Die Reaktion wurde in 100 mM Tris-HCl, pH 8.0, 10 μM ADP, 1 mM dGTP, 10 mM Dithiothreitol, 10 mM Magnesiumsulfat bei 50°C und variiertem Coenzym B12-Konzentration durchgeführt.

$c(\text{CoB12})$: Coenzym B12-Konzentration

Figure 2.1b AdoCbl K_m determination by Benner. K_m appears to be around $\sim 30 \mu\text{M}$. Source: Tauer, Thesis, p.34.

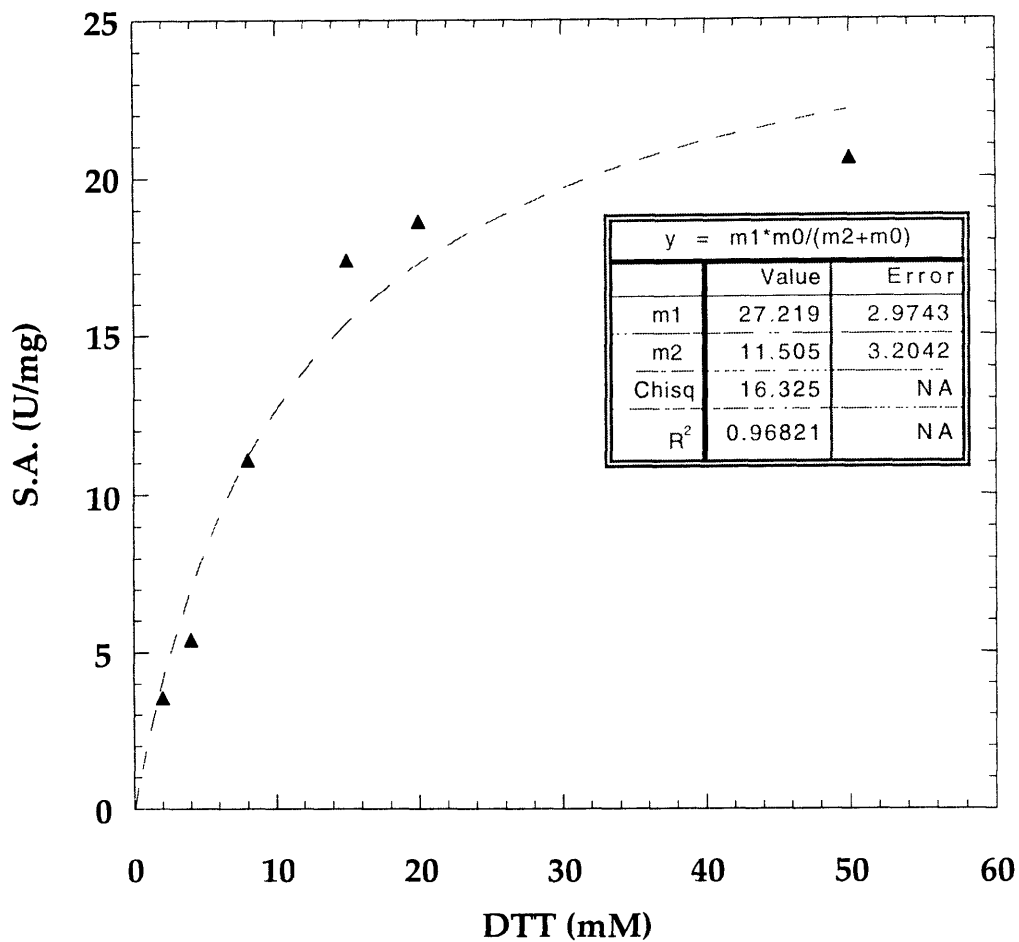


Figure 2.2 DTT K_m determination. Assay conditions: 1 mM CDP (S.A. = 1.4×10^3 cpm/nmol), 25 mM HEPES pH 7.5, 1 mM $MgCl_2$, 1 mM dGTP, 100 μ M AdoCbl, 6 μ M (60 μ g/100 μ L) *T. acidophila* RDPR (Batch IIa), and 0-50 mM DTT. The data is fit to the standard Michaelis-Menten equation: $V = \frac{V_{max}[S]}{K_m + [S]}$ where m1 is V_{max} , m2 is K_m . Source: Book III, p.35.

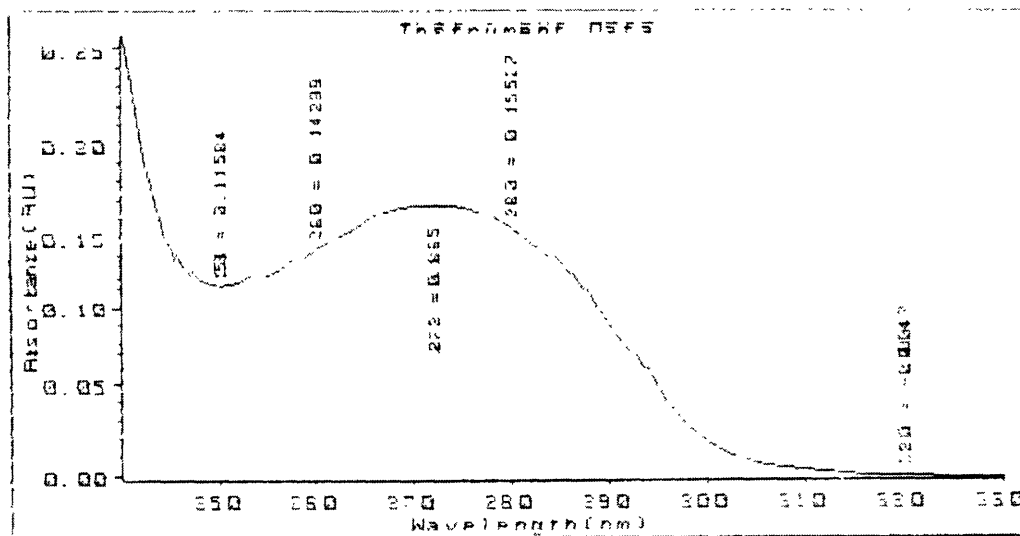


Figure 2.3a UV spectrum of *T. acidophila* RDPR, batch IIa. λ_{\max} is at 272 nm.

Source: Book III, p.58.

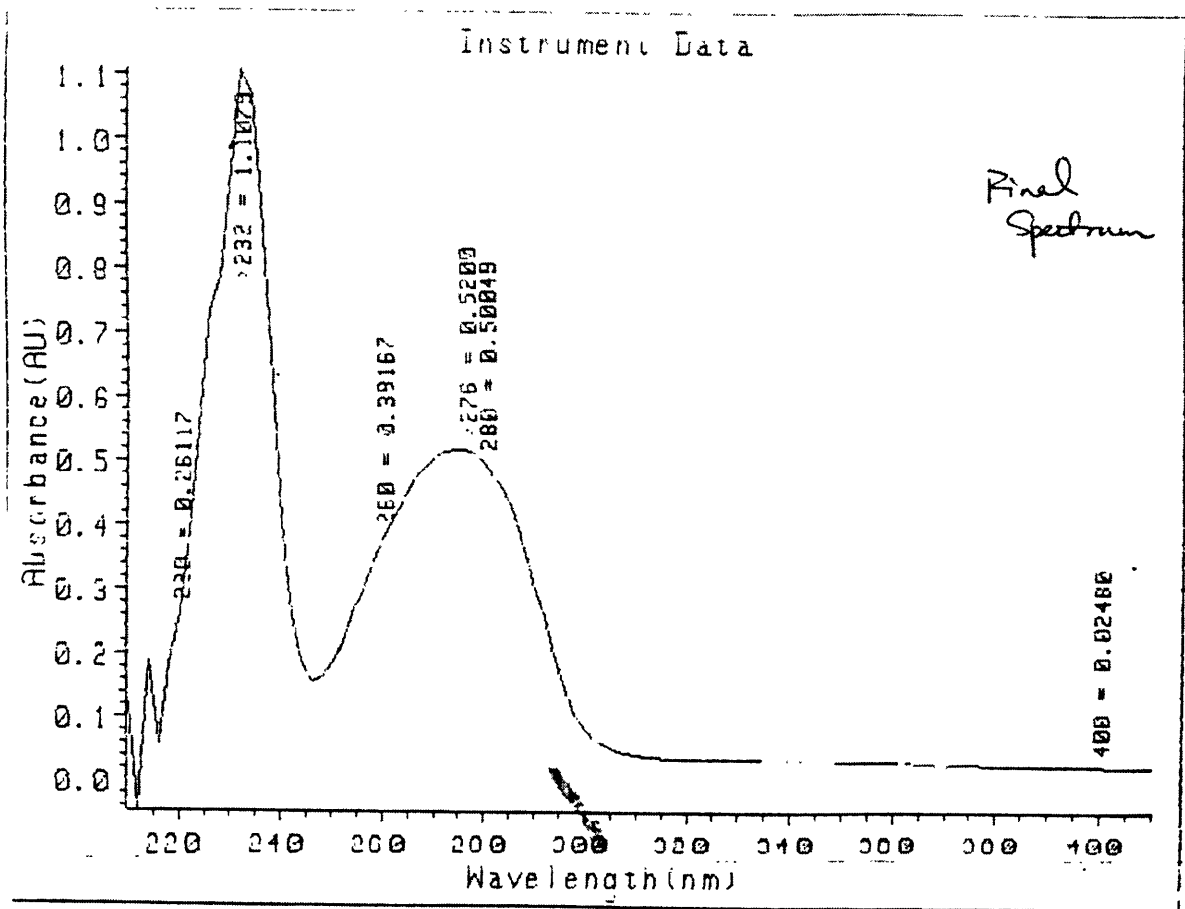


Figure 2.3b UV spectrum of *T. acidophila* RDPR, batch IIb. λ_{\max} is at 278 nm.

Source: Book III, p.63.

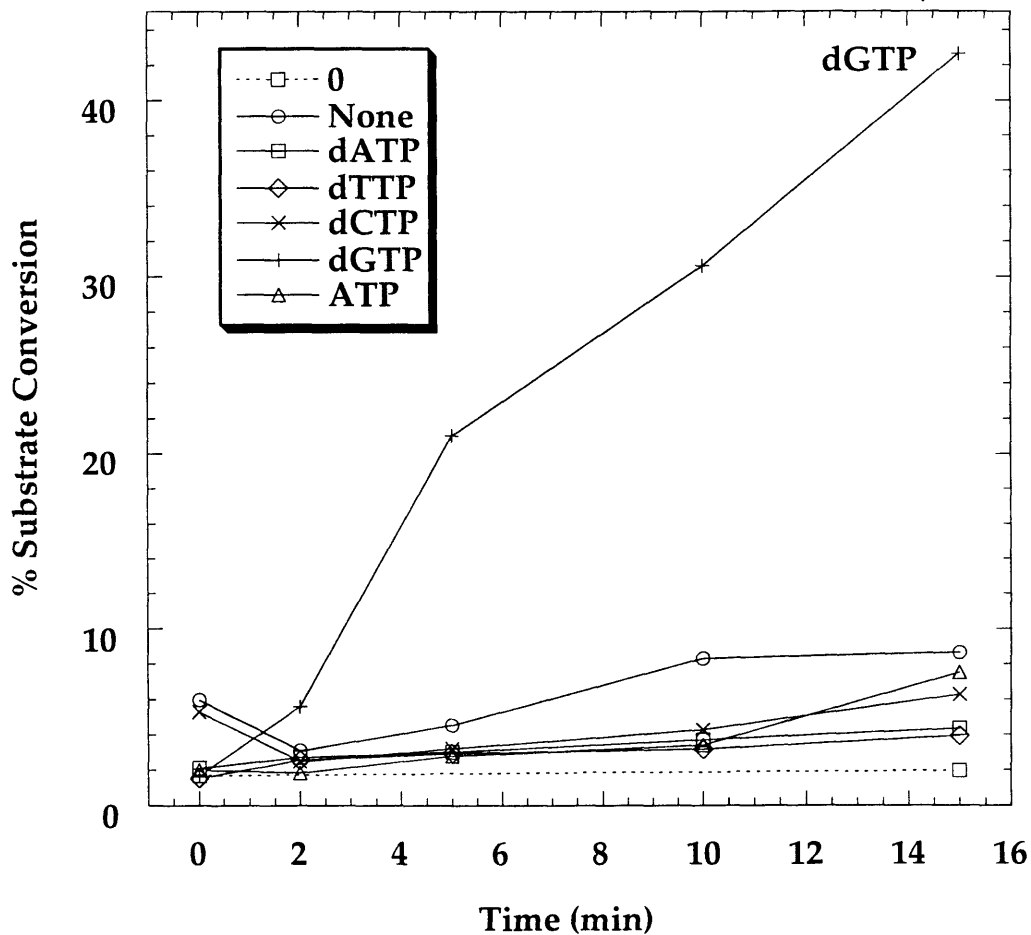


Figure 2.4a Allosteric effect of (d)NTPs on ADP (10 μ M) reduction, Run 1. An assay mixture contained in a final volume of 260 μ L: 10 μ M ADP (S.A. = 1.5×10^5 cpm/nmol), 1 mM $MgCl_2$, 10 mM DTT, 100 μ M AdoCbl, 100 mM Tris pH 8.0, 0.2 μ M (1 μ g/50 μ L) *T. acidophila* RDPR (Batch I), and effector of choice (No effector, 0.5 mM dATP, 0.5 mM dTTP, 0.5 mM dCTP, 0.5 mM dGTP, or 0.5 mM ATP; dNTPs were from Sigma). A background control mixture included everything except AdoCbl with 0.5 mM dGTP as the effector. 0: background control; None: no effector. Source: Book II, p. 85.

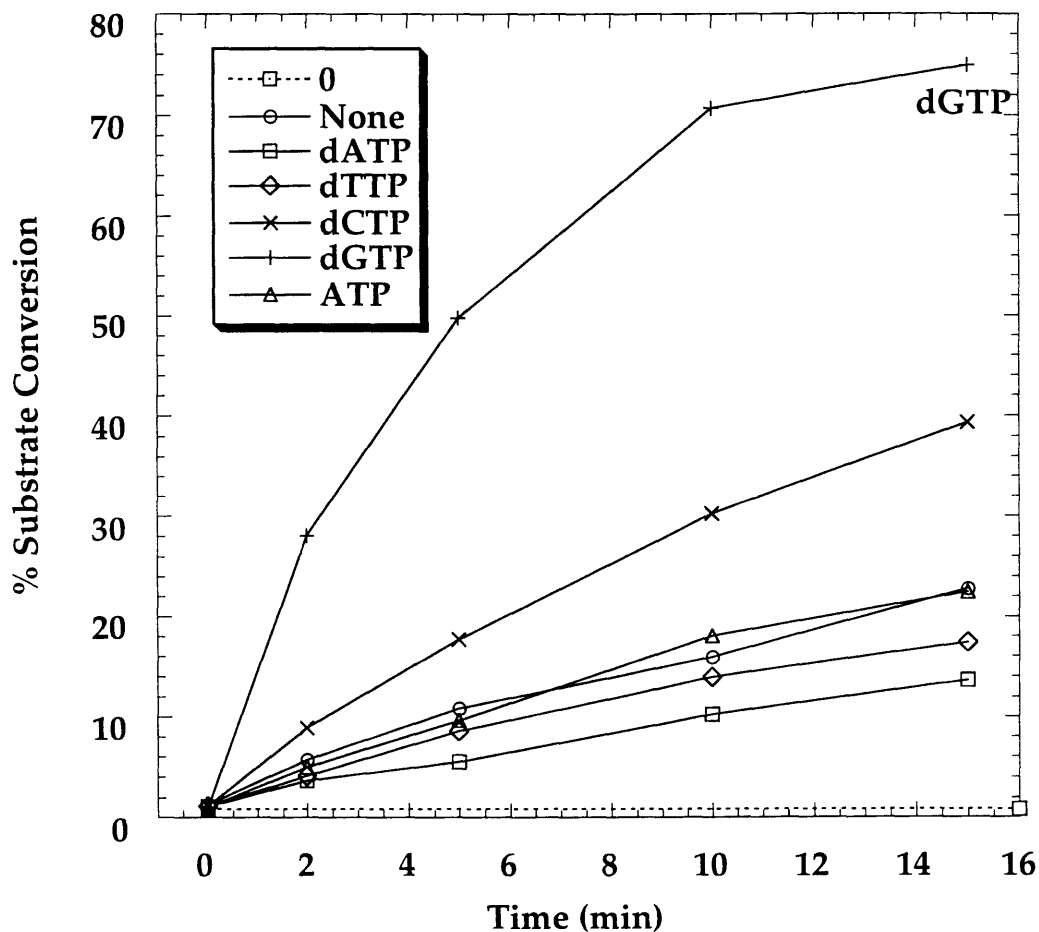


Figure 2.4b Allosteric effect of (d)NTPs on ADP (10 μ M) reduction, Run 2. An assay mixture contained in a final volume of 260 μ L: 10 μ M ADP (S.A. = 1.5×10^5 cpm/nmol), 1 mM $MgCl_2$, 10 mM DTT, 100 μ M AdoCbl, 25 mM HEPES pH 7.5, 0.1 μ M (0.5 μ g/50 μ L) *T. acidophila* RDPR (Batch IIb), and effector of choice (No effector, 1 mM dATP, 1 mM dTTP, 1 mM dCTP, 1 mM dGTP, or 1 mM ATP; dNTPs were from Boehringer Mannheim). A background control mixture included everything except AdoCbl with 1 mM dGTP as the effector. 0: background control; None: no effector. *Source: Book III, p. 78.*

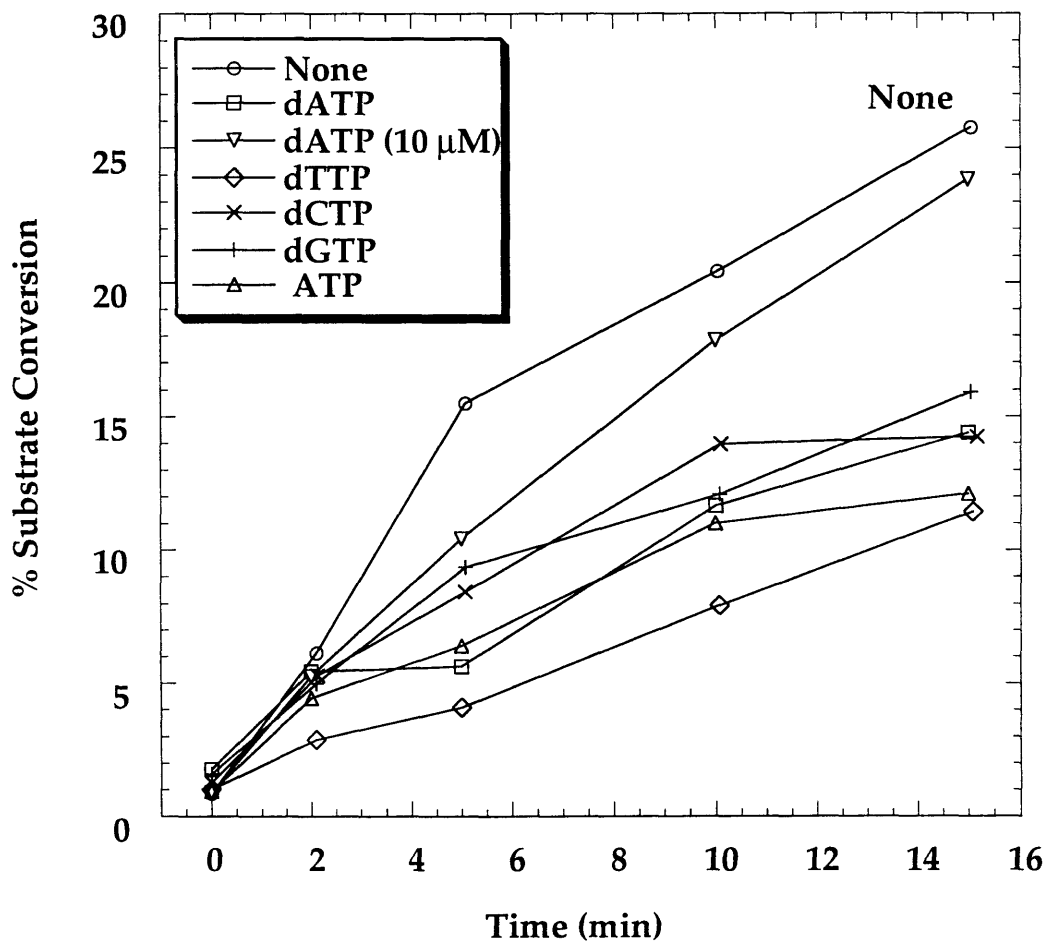


Figure 2.5a Allosteric effect of (d)NTPs on ADP (1 mM) reduction, Run 1. An assay mixture contained in a final volume of 260 μL : 1 mM ADP (S.A. = 5.2×10^3 cpm/nmol), 1 mM MgCl_2 , 30 mM DTT, 100 μM AdoCbl, 25 mM HEPES pH 7.5, 4 μM (20 $\mu\text{g}/50 \mu\text{L}$) *T. acidophila* RDPR (Batch IIa), and effector of choice (No effector, 1 mM dATP, 10 μM dATP, 1 mM dTTP, 1 mM dCTP, 1 mM dGTP, or 1 mM ATP; dNTPs were from Sigma). A background control mixture included everything except AdoCbl with 1 mM dGTP as the effector. 0: background control; None: no effector. *Source: Book III, p. 44.*

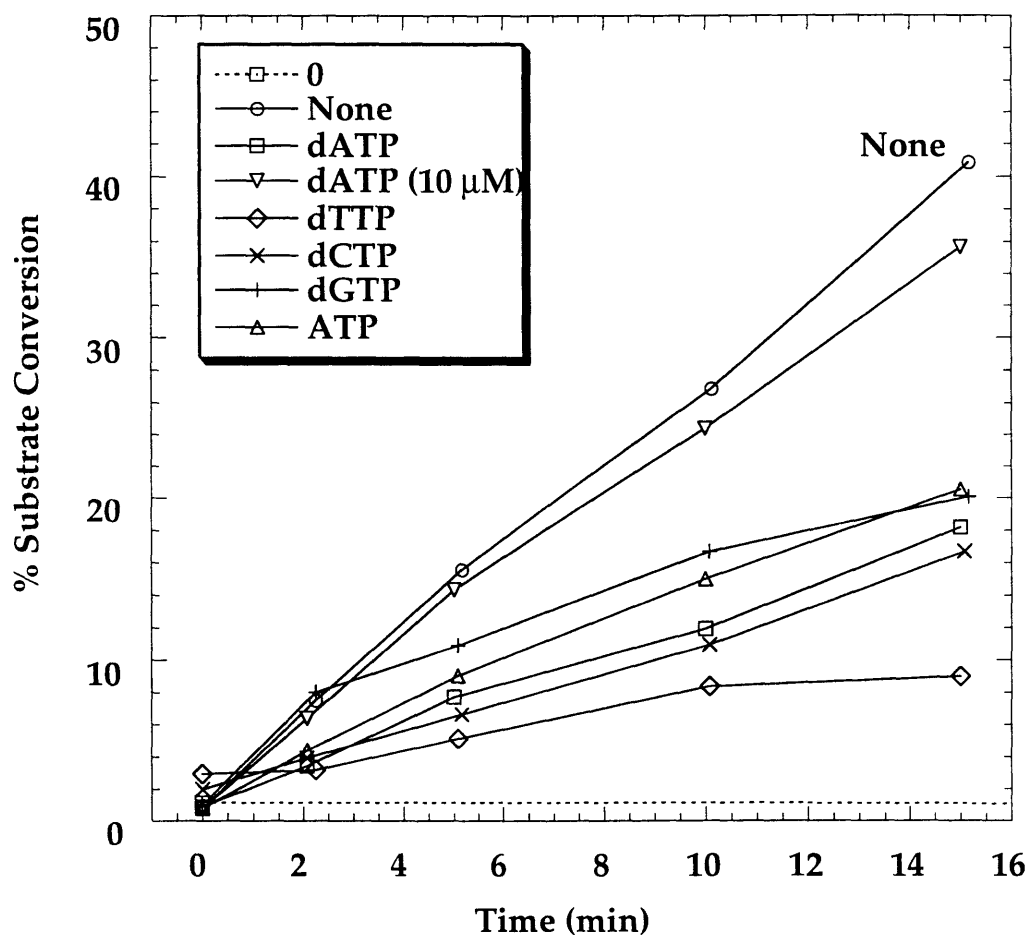


Figure 2.5b Allosteric effect of (d)NTPs on ADP (1 mM) reduction, Run 2. An assay mixture contained in a final volume of 260 μL : 1 mM ADP (S.A. = 2.1×10^3 cpm/nmol), 1 mM MgCl_2 , 30 mM DTT, 100 μM AdoCbl, 25 mM HEPES pH 7.5, 4.33 μM (21.7 $\mu\text{g}/50 \mu\text{L}$) *T. acidophila* RDPR (Batch IIa), and effector of choice (No effector, 1 mM dATP, 10 μM dATP, 1 mM dTTP, 1 mM dCTP, 1 mM dGTP, or 1 mM ATP; dNTPs were from Sigma). A background control mixture included everything except AdoCbl with 1 mM dGTP as the effector. 0: background control; None: no effector. Source: Book III, p. 52.

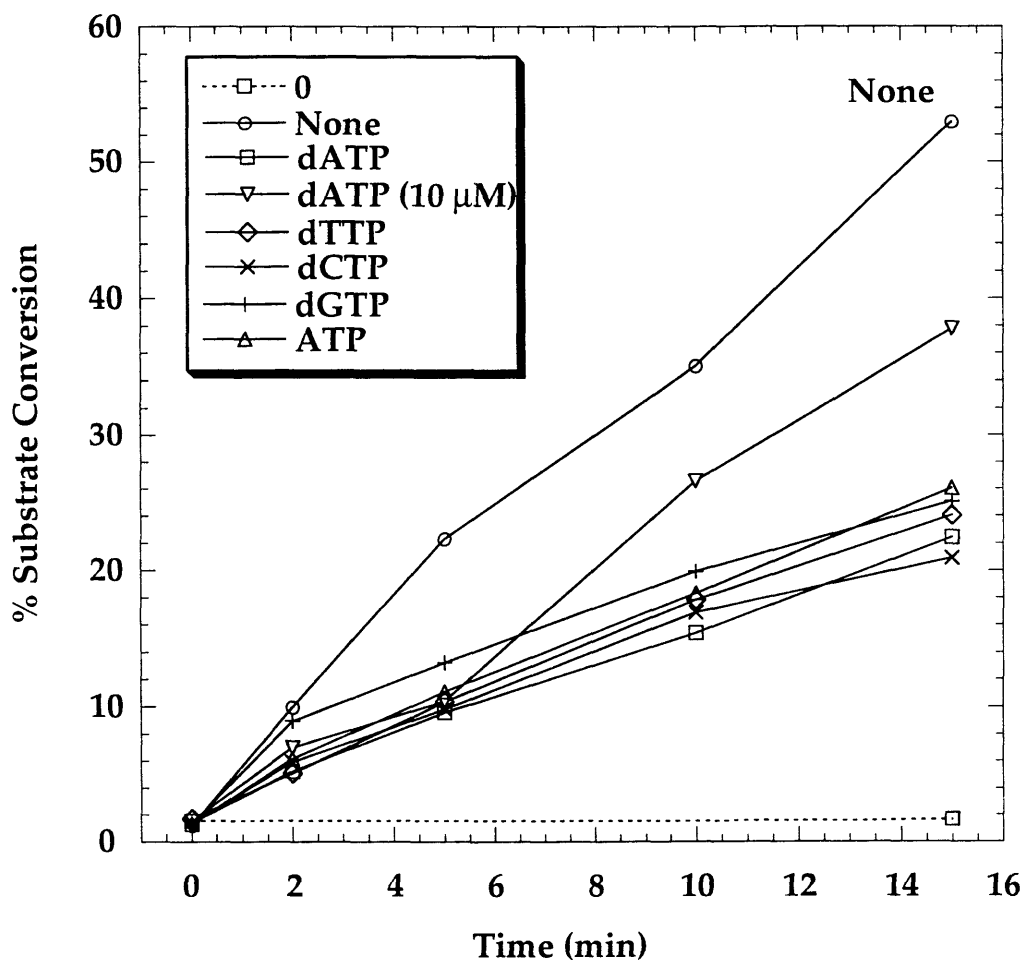


Figure 2.5c Allosteric effect of (d)NTPs on ADP (1 mM) reduction, Run 3. An assay mixture contained in a final volume of 260 μL : 1 mM ADP (S.A. = 2.1×10^3 cpm/nmol), 1 mM MgCl_2 , 30 mM DTT, 100 μM AdoCbl, 25 mM HEPES pH 7.5, 4 μM (20 $\mu\text{g}/50 \mu\text{L}$) *T. acidophila* RDPR (Batch IIb), and effector of choice (No effector, 1 mM dATP, 10 μM dATP, 1 mM dTTP, 1 mM dCTP, 1 mM dGTP, or 1 mM ATP; dNTPs were from Sigma). A background control mixture included everything except AdoCbl with 1 mM dGTP as the effector. 0: background control; None: no effector. *Source: Book III, p. 67.*

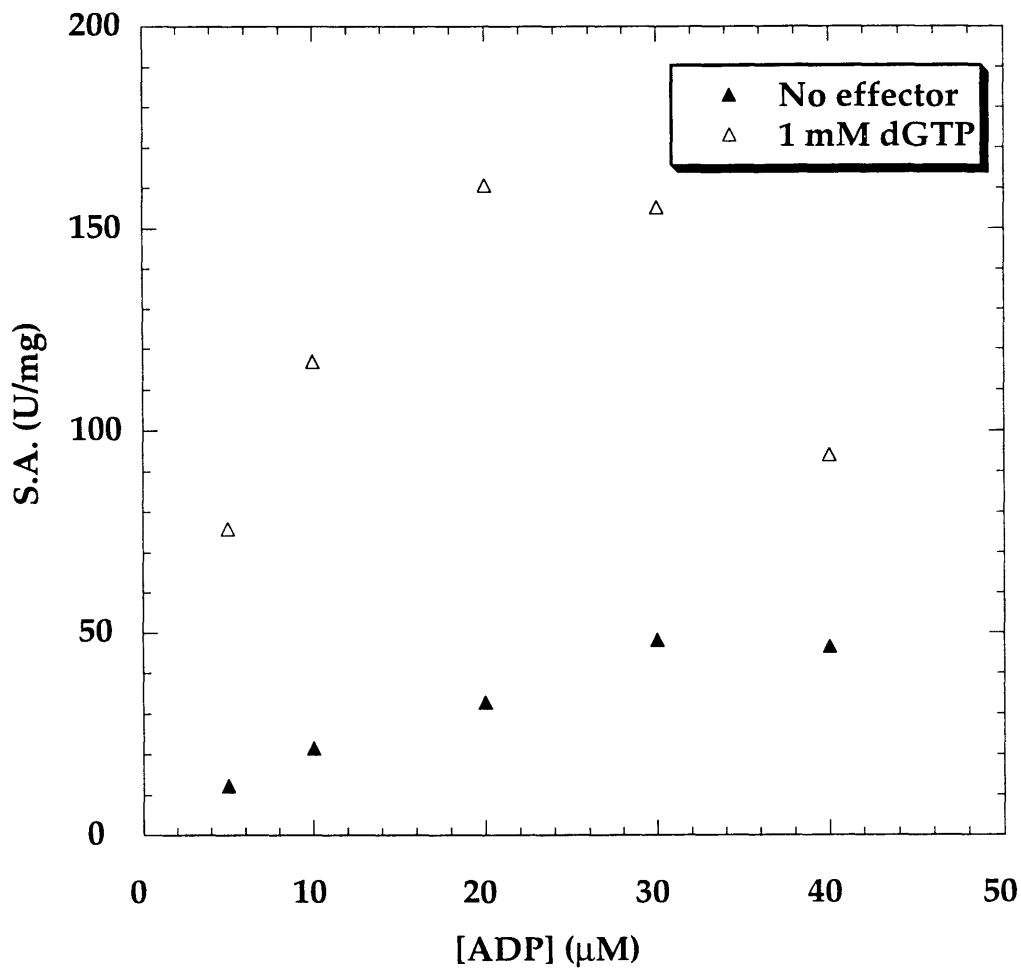


Figure 2.6a ADP K_m determination: no effector vs. 1 mM dGTP. An assay mixture contained in a final volume of 260 μL : 25 mM HEPES pH 7.5, 1 mM MgCl_2 , 100 μM AdoCbl, 30 mM DTT, 0.08 μM (0.4 $\mu\text{g}/50 \mu\text{L}$) *T. acidophila* RDPR (Batch IIb), with or without 1 mM dGTP, and 5-40 μM ADP (S.A. = 1.5×10^5 cpm/nmol). The reaction was carried out at 55°C. Source: Book III, p.117.

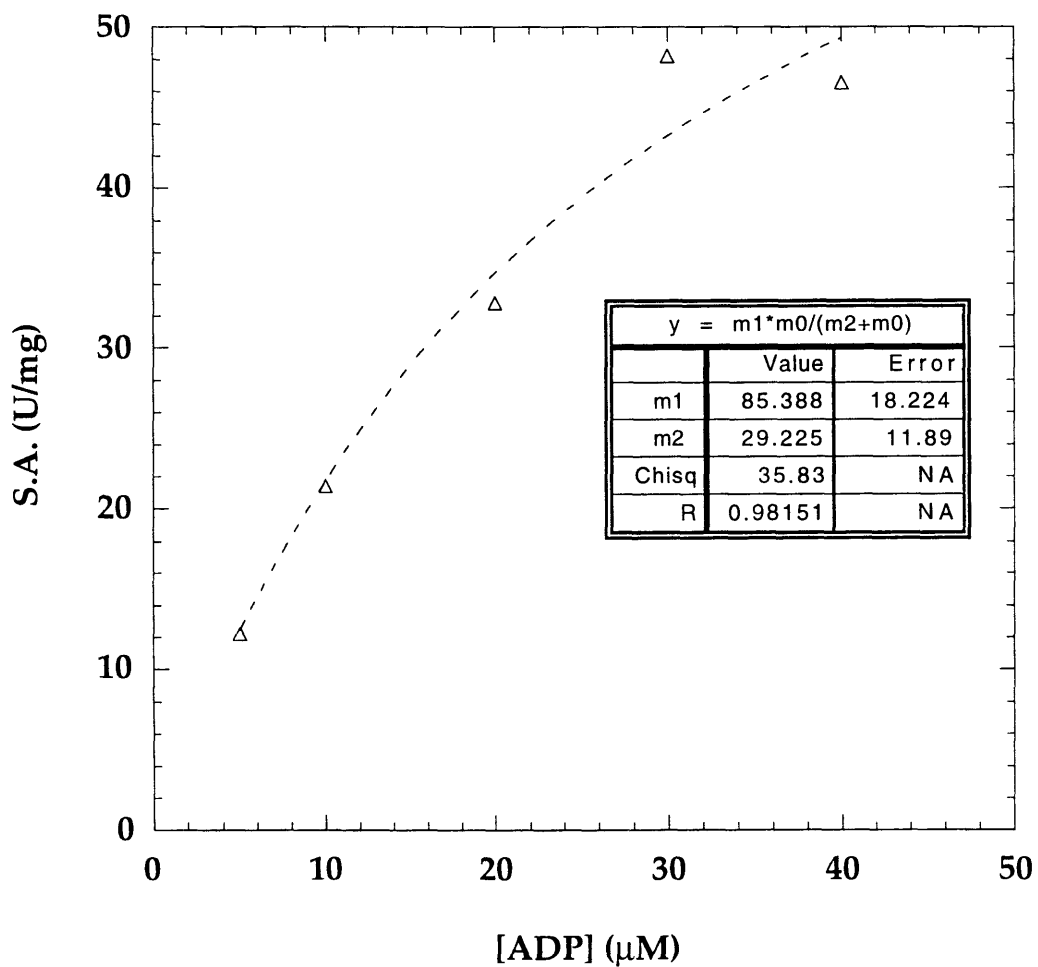


Figure 2.6b ADP K_m determination: no effector case. The data is fit to the standard Michaelis-Menten equation: $V = \frac{V_{\max}[S]}{K_m + [S]}$ where $m1$ is V_{\max} , $m2$ is K_m .

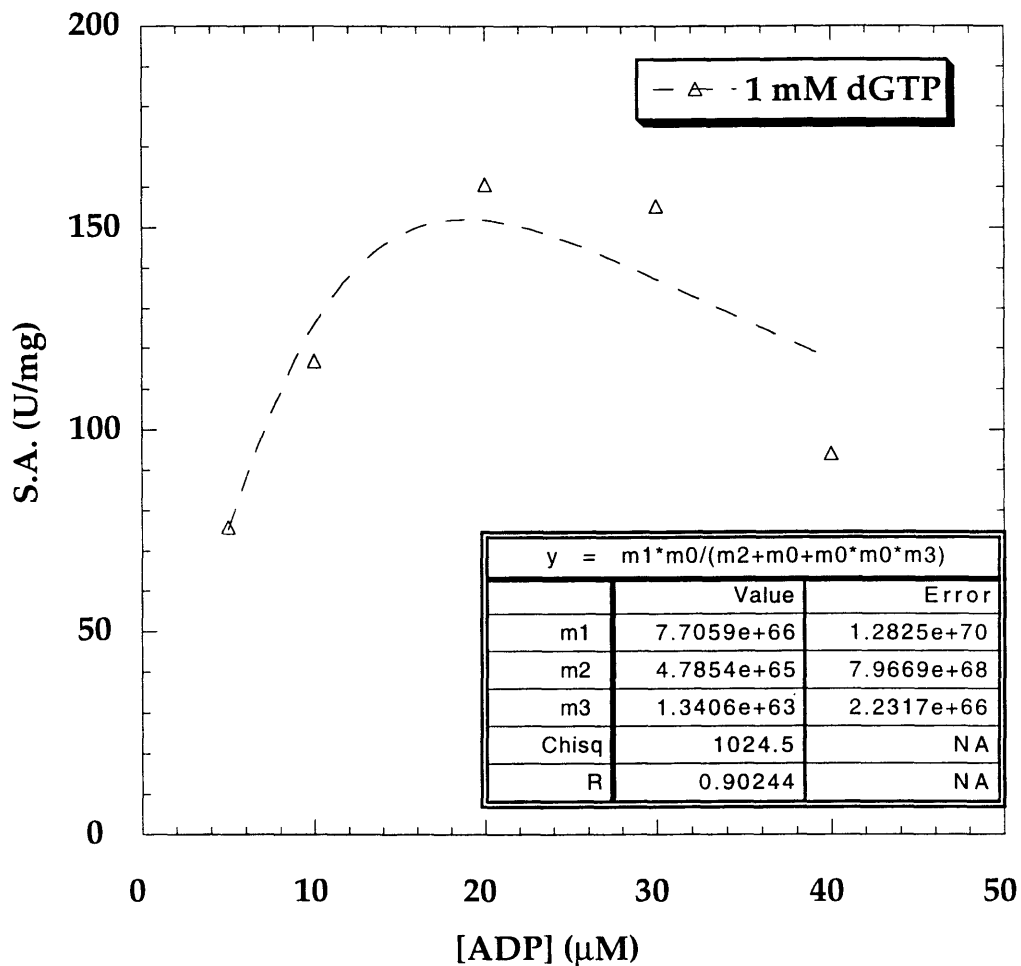


Figure 2.6c ADP K_m determination: 1 mM dGTP case. The data is fit to Equation 2.2 $V = \frac{V_{\max}[S]}{K_m + [S] + [S]^2 / K_i}$ where m1 is V_{\max} , m2 is K_m , and m3 is $1/K_i$. Initial values chosen: m1=150, m2=30, m3=0.03. The final values obtained are obviously out of range. Starting with different initial values did not help. It was unable to obtain reasonable values for all the kinetic parameters.

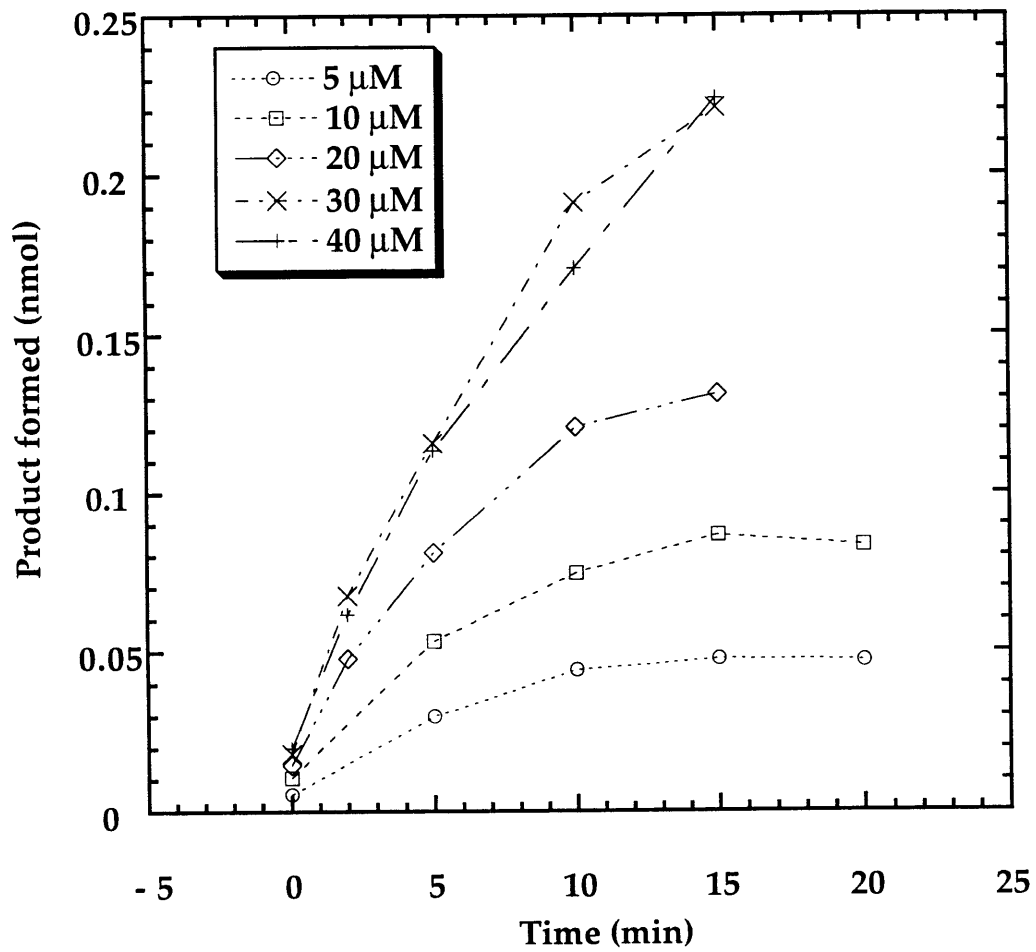


Figure 2.6d ADP K_m determination: no effector case. Shown are the original rate of product formation data used to obtain enzyme activity in Figure 2.6a.

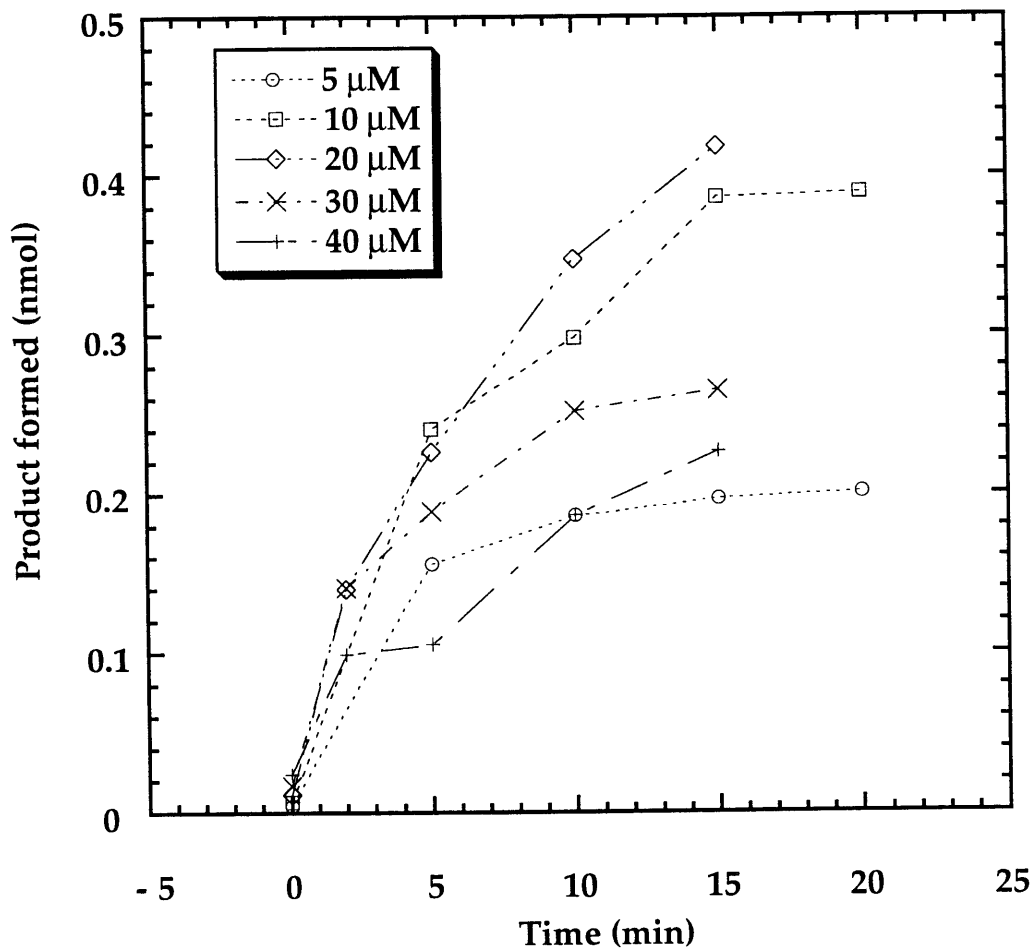
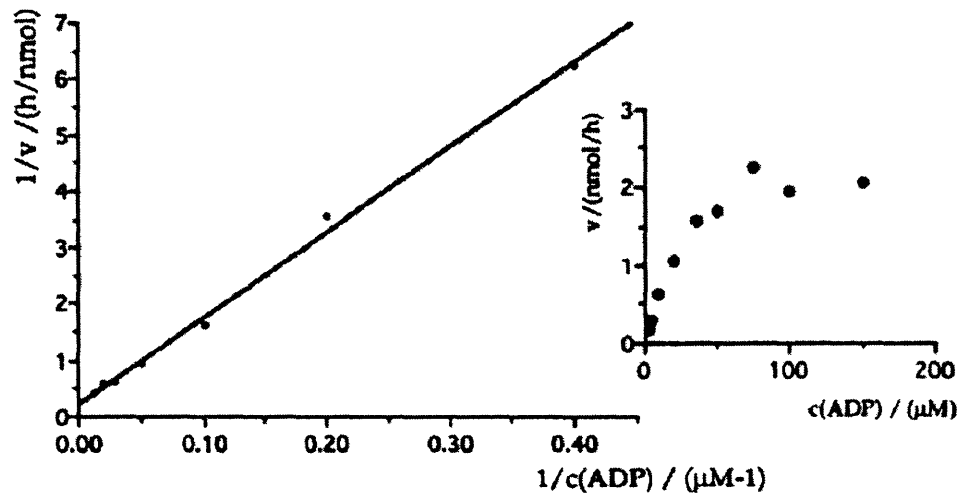


Figure 2.6e ADP K_m determination: 1 mM dGTP case. Shown are the original rate of product formation data used to obtain enzyme activity in Figure 2.6a.

Abbildung 10: Umsatz an ADP in Abhängigkeit der Substrat-Konzentration der Ribonukleotid-Reduktase aus *Thermoplasma acidophila*



Legende: Die Reaktion wurde in 100 mM Tris-HCl, pH 8.0, 100 μM Coenzym B12, 1 mM dGTP, 10 mM Dithiothreitol, 10 mM Magnesiumsulfat bei 50°C und variierenden ADP-Konzentrationen durchgeführt.

Figure 2.6f ADP K_m determination by Benner's laboratory. K_m is reported to be 64 μM . Assay conditions: 100 mM Tris-HCl, pH 8.0, 100 μM AdoCbl, 1 mM dGTP, 10 mM DTT, 10 mM MgSO_4 , 50°C. Source: Tauer, Thesis, p.30.

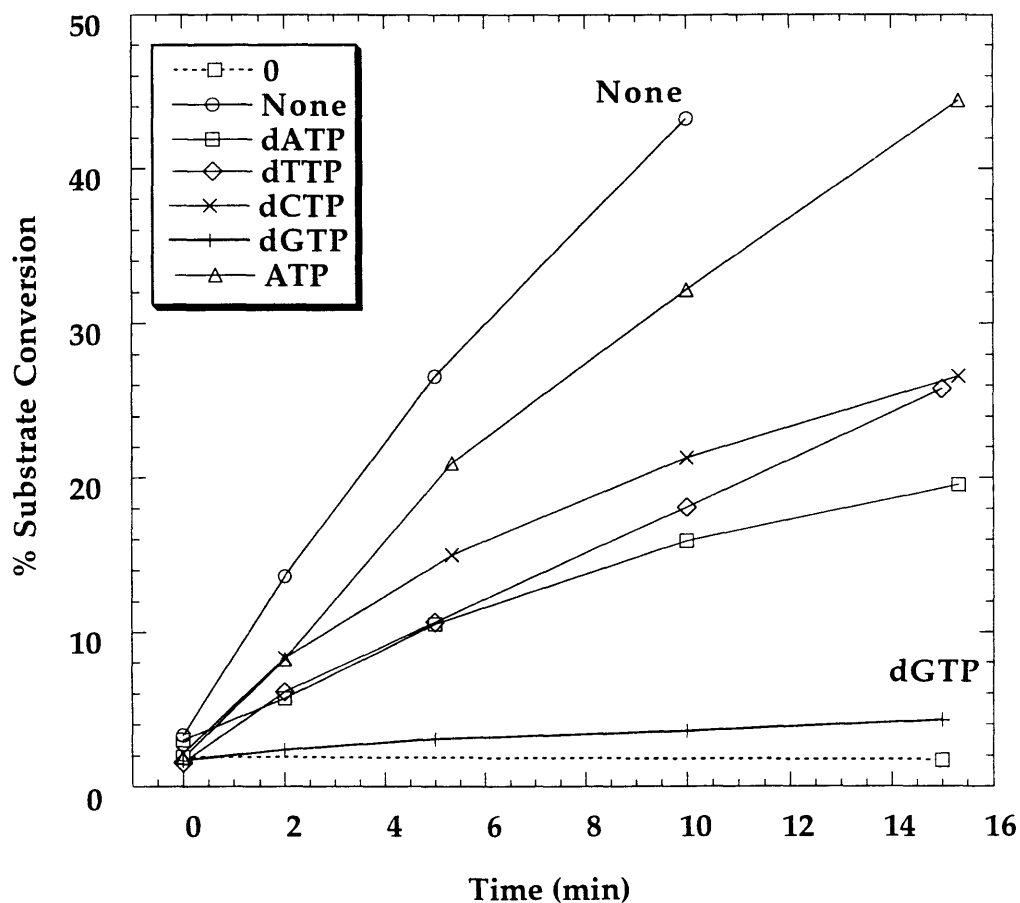


Figure 2.7a Allosteric effect of (d)NTPs on GDP (10 μ M) reduction, Run 1. Assay conditions: 10 μ M GDP (S.A. = 2.2×10^5 cpm/nmol), 1 mM $MgCl_2$, 10 mM DTT, 100 μ M AdoCbl, 100 mM Tris pH 8.0, 0.051 μ M (0.256 μ g/50 μ L) *T. acidophila* RDPR (Batch IIa), and effector of choice (No effector, 0.5 mM dATP, 0.5 mM dTTP, 0.5 mM dCTP, 0.5 mM dGTP, or 0.5 mM ATP; the dNTPs were from Sigma). A background control mixture included everything except AdoCbl with no effector. 0: background control; None: no effector. *Source: Book II, p.124.*

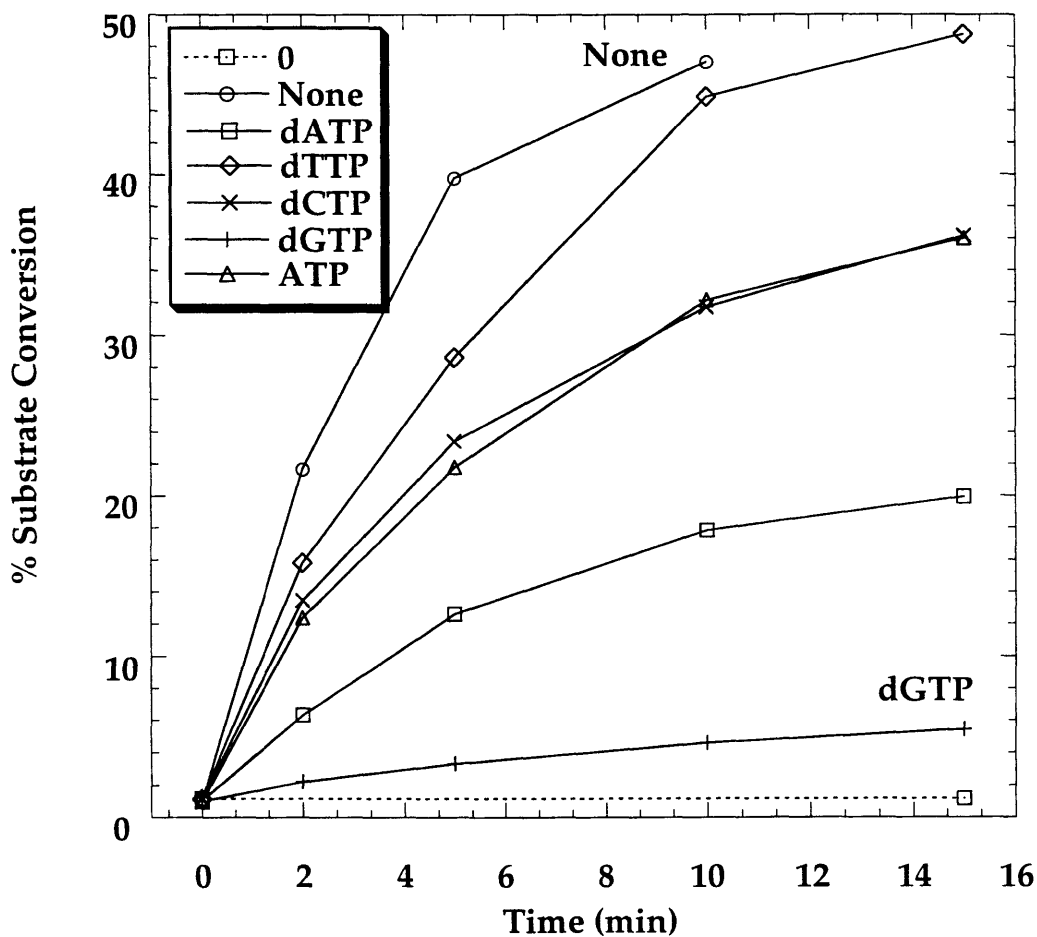


Figure 2.7b Allosteric effect of (d)NTPs on GDP (10 μ M) reduction, Run 2. Assay conditions: 10 μ M GDP (S.A. = 2.2×10^5 cpm/nmol), 1 mM $MgCl_2$, 10 mM DTT, 100 μ M AdoCbl, 25 mM HEPES pH 7.5, 0.1 μ M (0.5 μ g/50 μ L) *T. acidophila* RDPR (Batch IIb), and effector of choice (No effector, 1 mM dATP, 1 mM dTTP, 1 mM dCTP, 1 mM dGTP, or 1 mM ATP; the dNTPs were from Boehringer Mannheim). A background control mixture included everything except AdoCbl with no effector. 0: background control; None: no effector. *Source: Book III, p.82.*

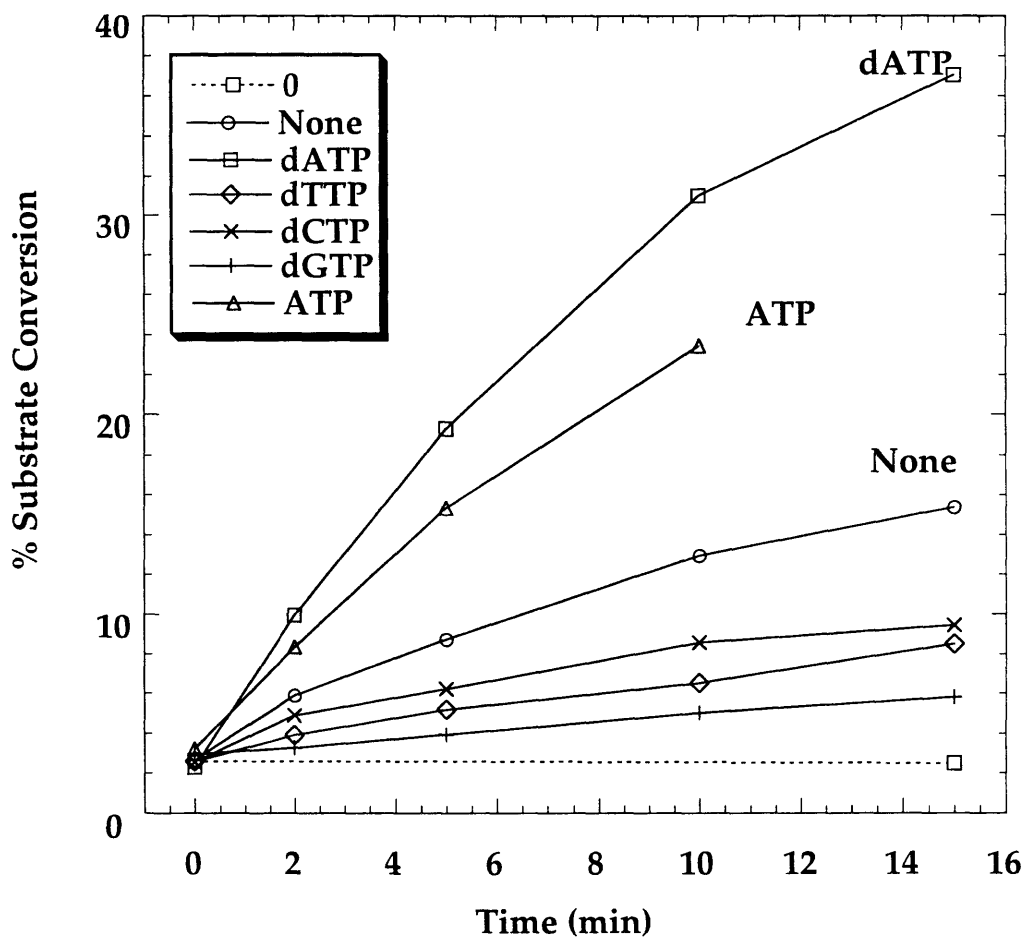


Figure 2.8 Allosteric effect of (d)NTPs on GDP (1 mM) reduction, Run 1. Assay conditions: 1 mM GDP (S.A. = 2.3×10^3 cpm/nmol), 1 mM $MgCl_2$, 30 mM DTT, 100 μ M AdoCbl, 25 mM HEPES pH 7.5, 4 μ M (20 μ g/50 μ L) *T. acidophila* RDPR (Batch IIb), and effector of choice (No effector, 10 μ M dATP, 1 mM dATP, 1 mM dTTP, 1 mM dCTP, 1 mM dGTP, or 1 mM ATP; the dNTPs were from Boehringer Mannheim). A background control mixture included everything except AdoCbl with no effector. 0: background control; None: no effector.

Source: Book III, p.84.

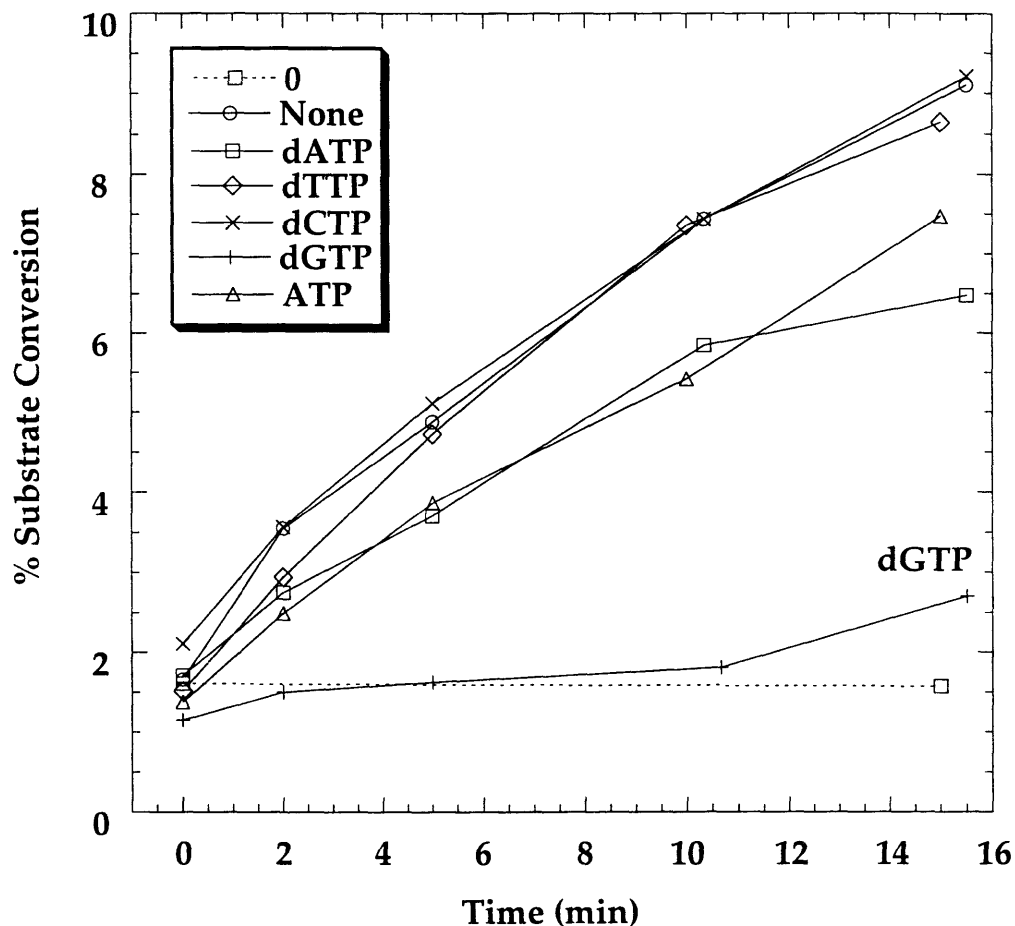


Figure 2.9 Allosteric effect of (d)NTPs on GDP (10 μ M) reduction, with TR/TRR/NADPH. Assay conditions: 10 μ M GDP (S.A. = 2.2×10^5 cpm/nmol), 1 mM $MgCl_2$, 40 μ M TR, 2 μ M TRR, 1 mM NADPH, 100 μ M AdoCbl, 100 mM Tris pH 8.0, 0.053 μ M (0.256 μ g/50 μ L) *T. acidophila* RDPR (Batch IIa), and effector of choice (No effector, 0.5 mM dATP, 0.5 mM dTTP, 0.5 mM dCTP, 0.5 mM dGTP, or 0.5 mM ATP; the dNTPs were from Sigma). A background control mixture included everything except AdoCbl with no effector. 0: background control; None: no effector. Source: Book II, p.125.

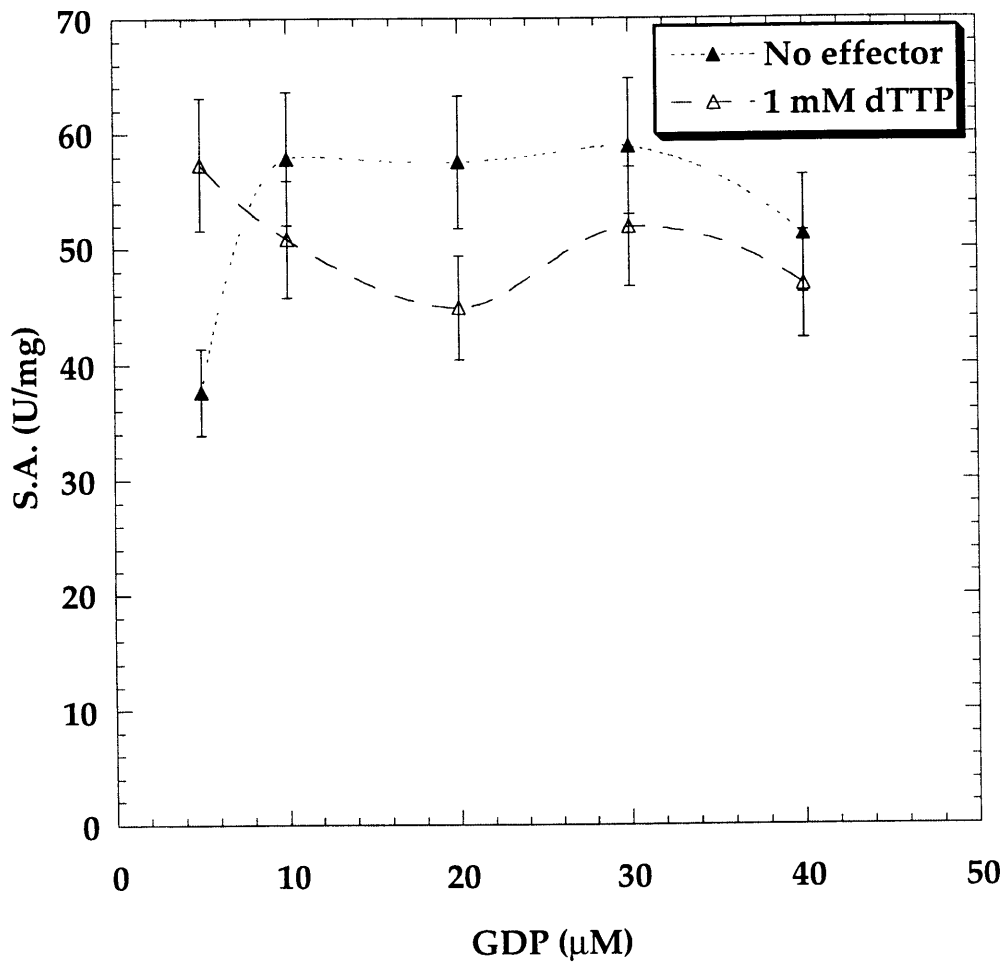


Figure 2.10a GDP K_m determination (5-40 μM): no effector vs. 1 mM dTTP. An assay mixture contained in a final volume of 260 μL : 25 mM HEPES pH 7.5, 1 mM MgCl_2 , 100 μM AdoCbl, 30 mM DTT, 0.04 μM (0.2 $\mu\text{g}/50 \mu\text{L}$) *T. acidophila* RDPR (Batch IIa), with or without 1 mM dTTP, and 5-40 μM GDP (S.A. = 1.2×10^5 cpm/nmol). *Source: Book III, p.122.*

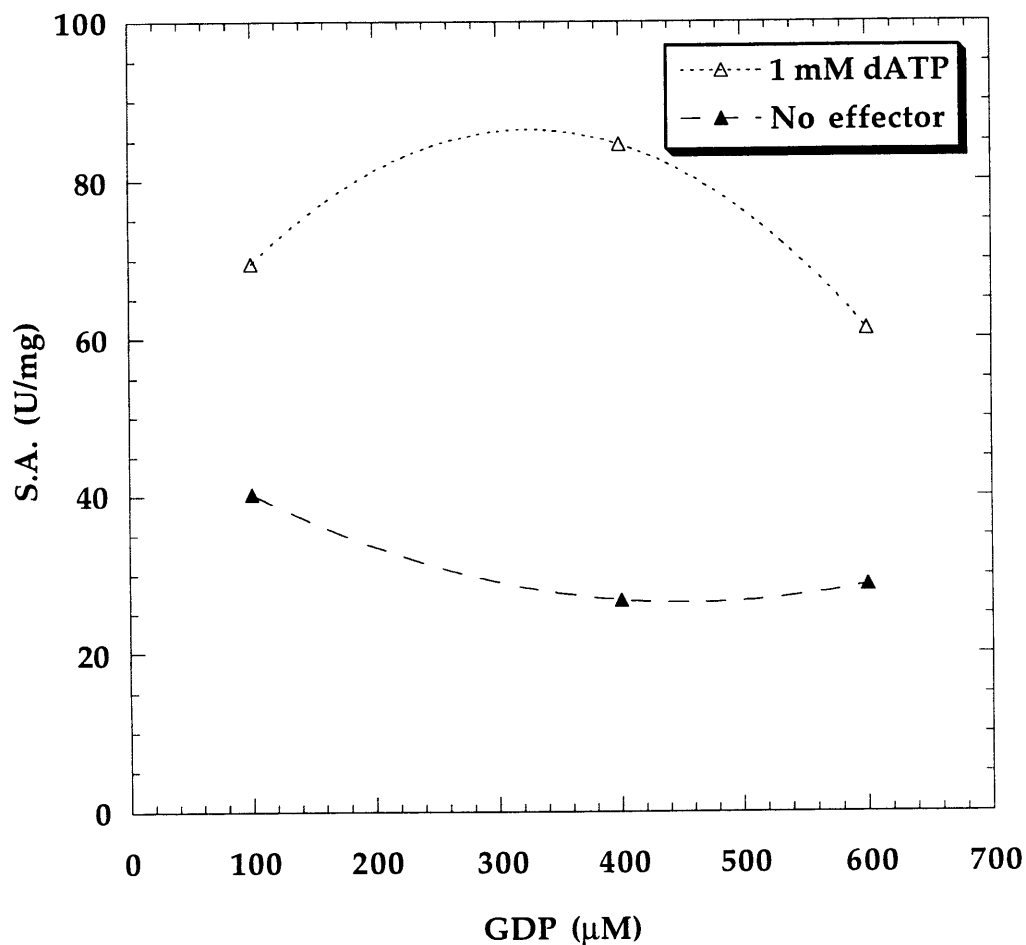


Figure 2.10b GDP K_m determination (100-600 μM): no effector vs. 1 mM dATP. An assay mixture contained in a final volume of 260 μL : 25 mM HEPES pH 7.5, 1 mM MgCl_2 , 100 μM AdoCbl, 30 mM DTT, 0.16 μM (0.8 $\mu\text{g}/50 \mu\text{L}$) *T. acidophila* RDPR (Batch IIb), with or without 1 mM dATP, and 100-600 μM GDP (S.A. = 4.2×10^4 cpm/nmol). Source: Book III, p.122.

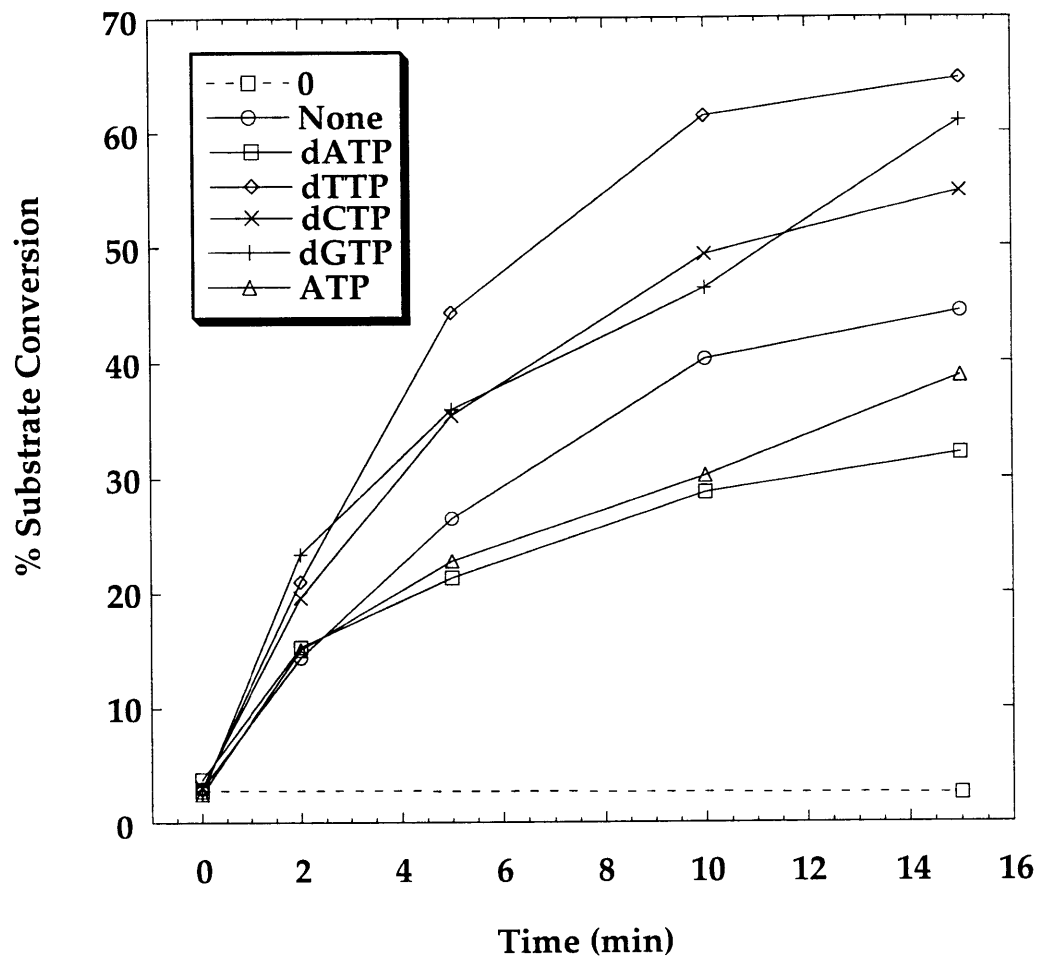


Figure 2.11 Allosteric effect of (d)NTPs on CDP (10 μ M) reduction. Assay conditions: 10 μ M [5- 3 H]-CDP (S.A. = 4.5×10^5 cpm/nmol), 1 mM $MgCl_2$, 10 mM DTT, 100 μ M AdoCbl, 25 mM Hepes pH 7.5, 0.1 μ M (0.5 μ g/50 μ L) *T. acidophila* RDPR, and effector of choice (No effector, 1 mM dATP, 1 mM dTTP, 1 mM dCTP, 1 mM dGTP, or 1 mM ATP; the dNTPs were from Boehringer Mannheim). A background control mixture included everything except AdoCbl with no effector. 0: background control; None: no effector. Source: Book III, p.136.

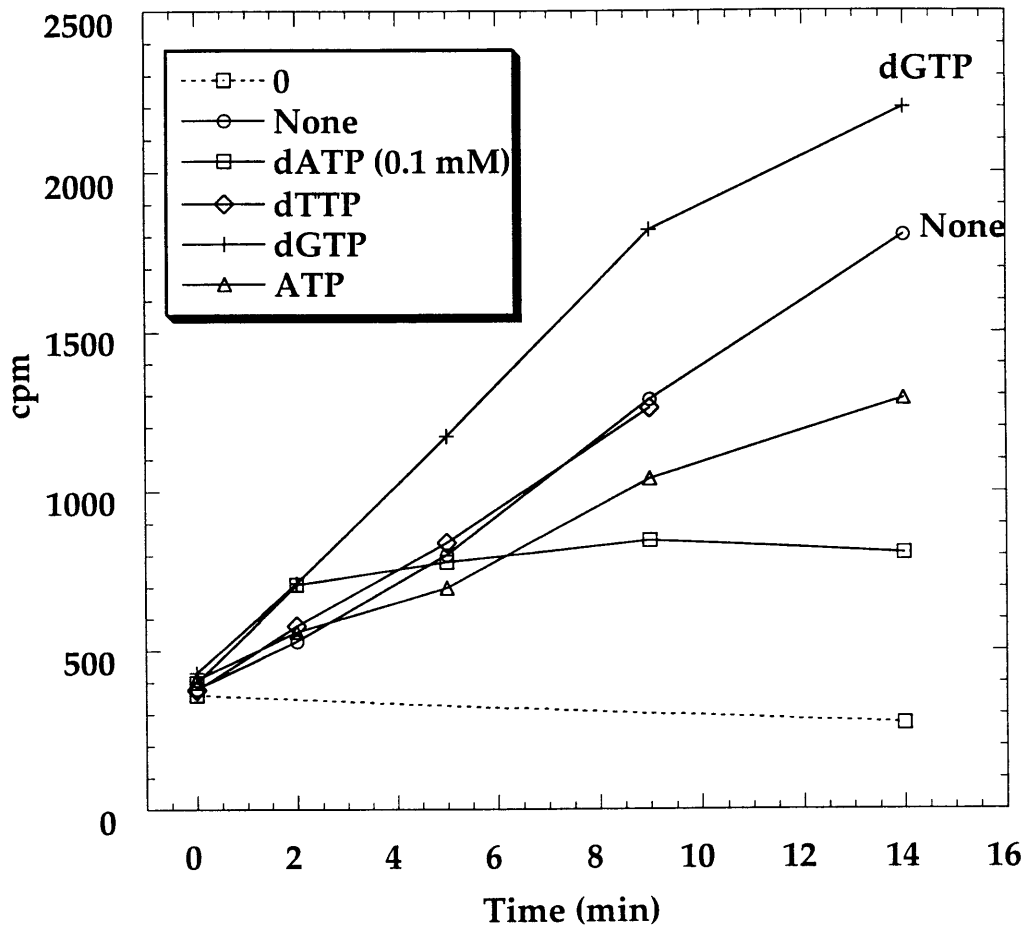


Figure 2.12 Allosteric effect of (d)NTPs on CDP (1 mM) reduction. Assay conditions: 1 mM [2-¹⁴C]-CDP (2.2×10^3 cpm/nmol), 1 mM MgCl₂, 25 mM Hepes pH 7.5, 30 mM DTT, 100 μM AdoCbl, 10 μM (100 μg/100 μL) *T. acidophila* RDPR, and effector of choice (No effector, 0.1 mM dATP, 0.5 mM dTTP, 0.5 mM dCTP, 0.5 mM dGTP, or 0.5 mM ATP; the dNTPs were from Sigma). A background control mixture included everything except AdoCbl with 0.1 mM dATP as the effector. 0: background control; None: no effector. *Source: Book II, p.76.*

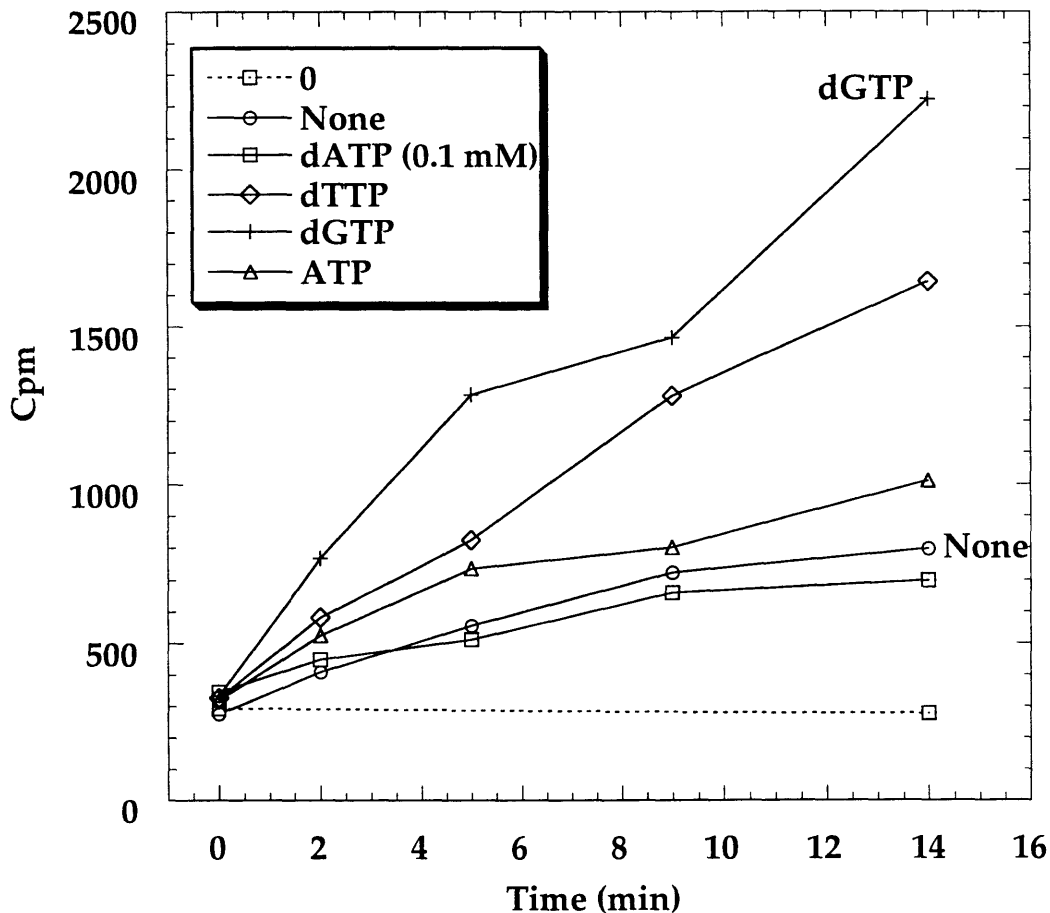


Figure 2.13 Allosteric effect of (d)NTPs on CDP (1 mM) reduction, with TR/TRR/NADPH. Assay conditions: 1 mM [2-¹⁴C]-CDP (S. A. = 2.2×10^3 cpm/nmol), 1 mM MgCl₂, 25 mM Hepes pH 7.5, 4 mM NADPH, 200 μM TR, 2 μM TRR, 100 μM AdoCbl, 10 μM (100 μg/100 μL) *T. acidophila* RDPR, and effector of choice (No effector, 0.1 mM dATP, 0.5 mM dTTP, 0.5 mM dCTP, 0.5 mM dGTP, or 0.5 mM ATP; the dNTPs were from Sigma). A background control mixture included everything except AdoCbl with 0.1 mM dATP as the effector. 0: background control; None: no effector. *Source: Book II, p.74.*

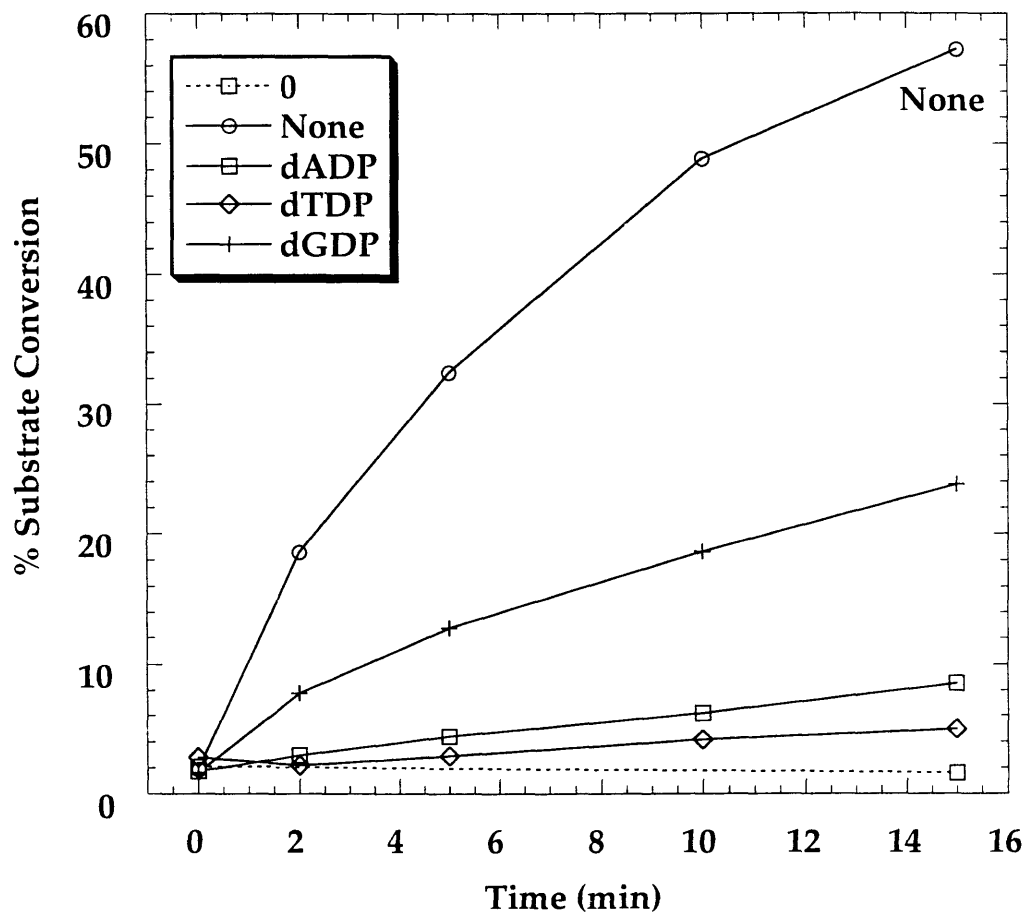


Figure 2.14 Allosteric effect of (d)NDPs on ADP (10 μM) reduction. Assay conditions: 10 μM (S.A. = 1.5×10^5 cpm/nmol), 0.224 μM (1.12 $\mu\text{g}/50 \mu\text{L}$) *T. acidophila* RDPR, 1 mM MgCl_2 , 25 mM HEPES pH 7.5, 100 μM AdoCbl, 30 mM DTT, and effector of choice (No effector, 0.5 mM dADP, 0.5 mM dTDP, or 0.5 mM dGDP). A background control mixture included everything except AdoCbl with no effector. 0: background control; None: no effector. *Source: Book III, p.114.*

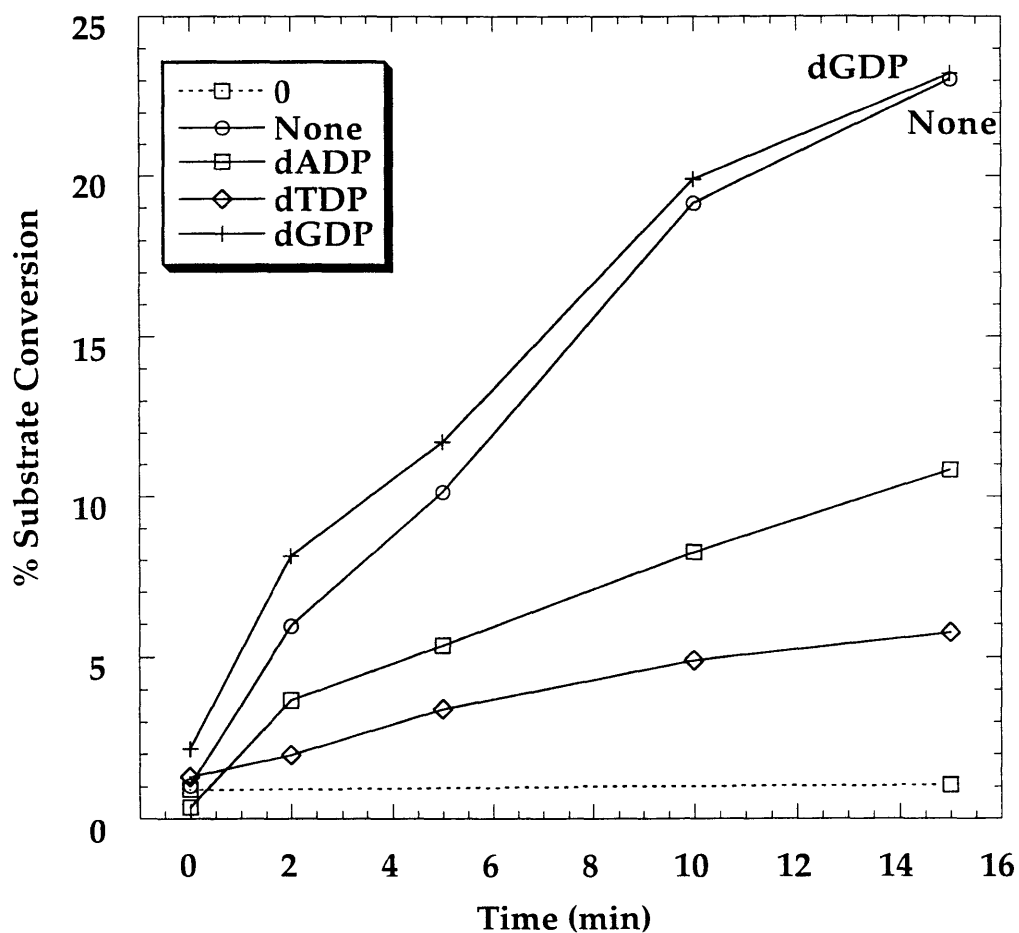


Figure 2.15 Allosteric effect of (d)NDPs on ADP (200 μM) reduction. Assay conditions: 200 μM ADP (S.A. = 3.9×10^4 cpm/nmol), 0.64 μM (3.2 $\mu\text{g}/50 \mu\text{L}$) *T. acidophila* RDPR, 1 mM MgCl_2 , 25 mM HEPES pH 7.5, 100 μM AdoCbl, 30 mM DTT, and effector of choice (No effector, 0.5 mM dADP, 0.5 mM dTDP, or 0.5 mM dGDP). A background control mixture included everything except AdoCbl with no effector. 0: background control; None: no effector. *Source: Book III, p.114.*

Chapter 3
Mechanistic Characterization of *T. acidophila* RDPR

Introduction

Function of AdoCbl in Class II RNRs

For class II RNRs, AdoCbl is required for enzymatic activity. The role of this cofactor has been extensively studied in RTPR from *Lactobacillus leichmannii*. The mechanism for thiyl radical formation is shown in Scheme 3.1. It is proposed that AdoCbl generates in a concerted fashion a Cys-408 radical concomitant with 5'-deoxyadenosine and cob(II)alamin.¹ The transiently formed thiyl radical is believed to be a common intermediate formed in all classes of RNRs despite the different cofactors required for its generation.²

As previously described in Chapter 1, Stubbe and coworkers have proposed that the thiyl radical then initiates catalysis by abstraction of the 3'-hydrogen of the nucleotide substrate. The 2'-hydroxyl is then eliminated as H₂O, and a 3'-keto-2'-deoxynucleotide radical is formed. The two cysteines on the α -face of the nucleotide deliver the required reducing equivalents, to generate a 3'-ketodeoxynucleotide and a disulfide radical anion intermediate. This intermediate is further reduced to generate the 3'-ketyl-deoxynucleotide radical and a disulfide linkage between the two cysteines. Re-abstraction of the hydrogen from Cys-408 by the 3'-ketyl radical completes the first turnover and regenerates the thiyl radical.²

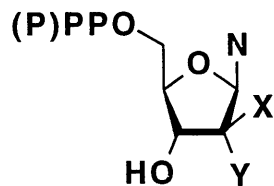
The first evidence for carbon-cobalt bond homolysis came from the observation that *L. leichmannii* RTPR catalyzes the exchange of the 5'-hydrogens of AdoCbl with solvent in the presence of a deoxynucleotide effector and reductant, but in the absence of substrate.^{3,4} Recent studies by Licht have shown that reductant is not required for this exchange. Furthermore, the kinetics of this exchange reaction suggest that hydrogen is exchanged with a rate constant of 95 s⁻¹, implying that it is mechanistically informative. The exchange reaction has been studied in detail by Blakley and coworkers by stop-flow UV-Vis spectroscopy⁵ and by rapid freeze

quench (RFQ) EPR spectroscopy.⁶ Cob(II)alamin formation occurs with a rate constant of $\sim 40 \text{ s}^{-1}$.⁵ If substrate is present this rate constant increases to $> 200 \text{ s}^{-1}$.¹ In comparison with turnover number of $\sim 2 \text{ s}^{-1}$ for dNTP production by *L. leichmannii* RTPR,⁷ carbon-cobalt bond cleavage is kinetically competent to be involved in nucleotide reduction.

As the EPR parameters of this intermediate are drastically different from those of cob(II)alamin and 5'-dA bound to RTPR when turnover is not taking place, Blakley and coworkers proposed that RTPR catalyzes the carbon-cobalt bond cleavage to form 5'-dA \cdot and cob(II)alamin.^{5,6} Licht et al. have repeated these EPR experiments in addition to rapid acid quench experiments.¹ However, replacement of [5'-¹H]-AdoCbl with [5'-²H]-AdoCbl or [5'-¹³C]-AdoCbl in the RFQ-EPR experiment gave no alteration of hyperfine interactions expected if 5'-dA \cdot was present. With β -(²H)cysteine RTPR, the EPR experiments revealed a sharpening of hyperfine interactions attributed to cobalt(II), suggesting an exchange coupled cob(II)alamin interacting with a thiyl radical. In the acid quench experiment, 5'-dA was trapped stoichiometrically with the amount of cob(II)alamin. These studies in conjunction with recent site directed mutagenesis studies and isotope effect studies suggest that the function of AdoCbl is to generate a thiyl radical in a concerted fashion with 5'-dA and cob(II)alamin.

Inactivation of RNRs with Mechanism-based Inhibitors

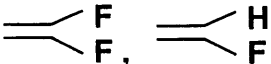
To probe the mechanism of nucleotide reduction, substrate analogs (mechanism based inhibitors) have proven to be exceedingly useful. In fact, 2'-substituted 2'-deoxynucleotides have been shown to be mechanism-based inhibitors for all three classes of RNRs: *E. coli* RDPR (class I),^{8-9,16} *L. leichmannii* RTPR,^{11,14,17-20} and *Corynebacterium nephridii* RDPR (class II),^{21,22} and anaerobic *E. coli* RTPR (class III).²³



X = H, Y = F, Cl, N₃, Br, I, SH

Y = H, X = Cl, F, Br

X, Y = F, F

X, Y = 

The general mechanism by which these inhibitors work is summarized in Scheme 3.2.² The initial step, as in the case of nucleotide reduction, is 3'-hydrogen atom abstraction by a thiyl radical. Deprotonation of the 3'-hydroxyl concomitant with removal of the leaving group, X, results in formation of a 2'-deoxy-3'-ketonucleotide radical which can then be reduced from either the top face (β -face) or the bottom face (α -face) of the inhibitor. Reduction from the bottom face results in the inability to regenerate the thiyl radical on Cys408, and hence the loss of AdoCbl. Reduction from the top face results in the regeneration of the thiyl radical, hence, the regeneration of AdoCbl. In both cases, a 3'-ketodeoxynucleotide is generated and dissociates into solution. It then chemically decomposes to generate PPPi, free nucleic-acid base and 2-methylene 3(2H) furanone. The furanone species inactivates RDPR by nonspecific alkylation of the reductase. Therefore, one nucleotide analog can inactivate RNRs via two different mechanisms: destruction of the cofactor or alkylation of the enzyme. Inactivation studies with 2'-azido-2'-deoxynucleotides,^{13,15} 2'-methylene-2'-deoxynucleotides, 2'-difluoro-2'-deoxynucleotides,²⁴ 2'-fluoromethylene-2'-deoxynucleotides,¹⁶ and mutant RDPR²⁵ have also provided additional insight to the mechanism of nucleotide reduction.²⁶ Recently, inactivation studies carried out with 2'-arasubstituted nucleotides for *L.*

leichmannii RTPR¹⁸ have shown an inactivation mechanism similar to the case with X in the ribo configuration.

The similarities between all ribonucleotide reductases when they interact with these substrate analogs have provided strong support for the postulation by the Stubbe laboratory -- despite the cofactor diversity, the catalytic mechanism for nucleotide reduction are very similar.

As sequence comparison of *T. acidophila* RDPR with other RNRs provides a convincing link between all the three different RNR classes, some preliminary mechanistic characterization of *T. acidophila* RDPR has been carried out using similar approaches to those previously developed for other RNRs. *L. leichmannii* RTPR serves as an excellent mechanistic model for the study of *T. acidophila* RDPR mechanism.

Materials and Methods

Materials

T. acidophila RDPR was purified as described in Chapter 1. *E. coli* thioredoxin (TR) and thioredoxin reductase (TRR) were isolated from overproducing strains SK3918 (S.A. = 500 AU DTNB reduced·mg⁻¹·min⁻¹)²⁷ and K91/pMR14 (S.A. = 50 AU DTNB reduced·mg⁻¹·min⁻¹).²⁸ Calf intestine alkaline phosphatase (CIP) and DNase were from Boehringer Mannheim.

Adenosine-5'-diphosphate (ADP), 5'-deoxyadenosylcobalamin (AdoCbl), and nicotinamide adenine dinucleotide phosphate, reduced form (NADPH) were from Sigma. 2'-Deoxyguanosine-5'-triphosphate (dGTP) was from Boehringer Mannheim. [5'-²H]-AdoCbl and CuSO₄ standard solution were kindly provided by Stuart Licht. [5, 8-³H]-ADP (28.5 Ci/mmol) was from NEN. [5-³H]-CDP (22

Ci/mmol) was from Amersham Life Sciences. 2'-Deoxy-2'-methylneuridine-5'-diphosphate (2'VUDP) and 2'-deoxy-2',2'-difluorocytidine 5'-diphosphate (dF₂CDP) were provided by Morris Robins at Brigham Young University. 2'-Azido-2'-deoxyuridine 5'-diphosphate (N₃UDP) was synthesized by Scott Salowe in the Stubbe laboratory. Tris was from Boehringer Mannheim. HEPES was from USB. MgCl₂, dithionite, and dithiothreitol (DTT) were from Mallinckrodt. Isopentane (reagent grade) was from Aldrich.

Suprasil quartz EPR sample tubes (O.D. 4 mm, I.D. 2.4 mm, 7 inches long) for RFQ were obtained from Wilmad Glass Company. RC6 LAUDA circulating water bath was from Brinkmann.

Stop-flow Experiment of *T. acidophila* RDPR

The experimental procedure was similar to what was previously described.¹ An Applied Photophysics DX.17MV spectrophotometer was used for the stop-flow spectroscopy. The loading and drive syringes were filled with 50 mM dithionite, septum-sealed, and left overnight. The sample lines were then flushed with 20 mL of 25 mM HEPES pH 7.5, which had been deoxygenated by bubbling argon through it for 3 h. The syringes and lines were maintained at 48.7°C via a RC6 LAUDA circulating water bath from set at 55°C. Argon was bubbled through the bath for 3 h preceding the acquisition of data and through the entire course of the experiment. All reactants were deoxygenated by stirring under an argon atmosphere for 20 min. Syringe B containing AdoCbl and the reaction chamber were covered with aluminum foil during the course of the experiment. Syringe A contained in a final volume of 1.5 mL: 0.5 mM ADP, 0.5 mM dGTP, 50 μM *T. acidophila* RDPR, 100 μM TR, 4 μM TRR, 4 mM NADPH, 25 mM HEPES (pH 7.5); Syringe B contained in a final volume of 4 mL: 0.5 mM ADP, 0.5 mM dGTP, 0.2 mM AdoCbl, 25 mM HEPES (pH 7.5). Upon equal volume mixing, the following final concentrations were

reached: 0.5 mM ADP, 0.5 mM dGTP, 100 μ M AdoCbl, 25 mM HEPES (pH 7.5), 25 μ M *T. acidophila* RDPR. The formation of cob(II)alamin was measured by monitoring change in A₅₂₅ and again at A₄₇₇ and 6 runs were carried out at each wavelength. Concentrations of AdoCbl and cob(II)alamin were calculated based on the following extinction coefficients: for AdoCbl, $\epsilon_{525} = 8,000 \text{ M}^{-1}\text{cm}^{-1}$, $\epsilon_{477} = 5,800 \text{ M}^{-1}\text{cm}^{-1}$; for cob(II)alamin, $\epsilon_{525} = 3,200 \text{ M}^{-1}\text{cm}^{-1}$, $\epsilon_{477} = 9,200 \text{ M}^{-1}\text{cm}^{-1}$; and $\Delta\epsilon_{525} = 4,800 \text{ M}^{-1}\text{cm}^{-1}$, $\Delta\epsilon_{477} = 3,400 \text{ M}^{-1}\text{cm}^{-1}$.

As the *T. acidophila* RDPR used was stored in the presence of 1 mM DTT. A background run where the enzyme storage buffer (~ 326 μ L used for 1.5 mL of total volume) (50 mM Tris, pH 8.0, 1 mM DTT, 15% glycerol) replaced the enzyme solution was carried out to check for the possible degradation of AdoCbl due to the presence of DTT (< 0.1 mM after final mixing) and high temperature.

Rapid Freeze Quench EPR Experiment of *T. acidophila* RDPR

The experimental procedure was designed based on previous studies of Licht, et al.¹ The RAM velocity was set to 2 cm/sec as required for 4:1 mixing and the RAM displacement was set to 7 mm to achieve ~ 300 μ L final total volume (including ~ 250 μ L sample volume, and dead volume in the loop and the mixer). All the EPR tubes were calibrated, and only the ones that had a volume within 5% to each other were used in the same set of experiment. The solutions were deoxygenated by stirring under an argon atmosphere for 20 min before being loaded into syringes anaerobically. The syringes and lines were maintained at 55°C via a RC6 LAUDA circulating water bath. The line from Syringe B containing AdoCbl was covered with aluminum foil during the course of the experiment. Syringe A (maximum volume 2 mL) contained in a final volume of 1.2 mL: 1 mM ADP, 1 mM dGTP, 84 μ M TR, 2.3 μ M TRR, 2.5 mM NADPH, 500 μ M *T. acidophila* RDPR, and 25 mM HEPES pH 7.5. Syringe B (maximum volume 0.5 mL) contained in a final volume

of 0.5 mL: 1 mM ADP, 1 mM dGTP, 2 mM [5'-¹H]-AdoCbl, and 25 mM HEPES pH 7.5. Upon 4:1 mixing of Syringe A to B respectively, the following final concentrations were reached: 1 mM ADP, 1 mM dGTP, 67.2 μM TR, 1.84 μM TRR, 2 mM NADPH, 400 μM *T. acidophila* RDPR, 400 μM AdoCbl, and 25 mM HEPES pH 7.5. The reaction was quenched in the dark under dim red light in isopentane (at -140°C) at 10 ms and 38 ms respectively (corresponding to hose number 6.4, the shortest, and hose number 32 respectively).

In a second experiment, [5'-²H]-AdoCbl replaced [5'-¹H]-AdoCbl in Syringe B. The *T. acidophila* RDPR concentration was 425 μM in Syringe A, and 340 μM in the final concentration, 15% less than the one used above. Accordingly, [5'-²H]-AdoCbl was reduced to 1.7 mM in Syringe B, and 340 μM in the final concentration. The experimental conditions were otherwise the same.

An Update Instrument System 1000 was used for the rapid freeze quench experiment. The EPR spectra were recorded on a Bruker ESP-300 instrument. The cooling system for the EPR instrument consisted of the quartz sample holder and temperature controller from a Bruker VT 1000 system connected to a transfer line delivering N₂ (at 25 L/min) through a copper heat exchanger maintained at 77K with liquid N₂. The sample temperature was maintained at 103 K.

An EPR spectrum of a CuSO₄ standard (1.03 mM CuSO₄, 2 mM NaClO₄, 0.01 M HCl, 20% (v/v) glycerol) in a same size EPR tube was recorded at the same temperature prior to recording any protein samples.

The instrument settings for the CuSO₄ sample were: Scan Range: 1100 G; Field Set: 2900 G; Time Constant: 328 ms; Modulation Amplitude: 5 G; Modulation Frequency: 100 kHz; Receiver Gain: 1 × 10⁵; Microwave Power: 100 μW; Microwave Frequency: 9.41 GHz; Sweep Time: 335 sec; Resolution of Field Axis: 2048.

The instrument settings for all the protein samples were: Scan Range: 1100 G; Field Set: 3250 G; Time Constant: 328 ms; Modulation Amplitude: 5 G; Modulation

Frequency: 100 kHz; Receiver Gain: 5×10^5 ; Microwave Power: 10 mW; Microwave Frequency: 9.41 GHz; Sweep Time: 335 sec; Resolution of Field Axis: 1024.

Time-dependent Inactivation of *T. acidophila* RDPR

The effects of several previously studied mechanism based inhibitors of RNRs (N_3 UDP, 2'VUDP, and dF₂CDP), were investigated with *T. acidophila* RDPR. The time-dependent inactivation study procedure was a modification of what was previously described.¹⁹ All the studies were carried out in the dark under dim red lights at 55°C. The reaction mixture contained in a final volume of 110 μ L: 60 μ M (90 μ g/ 15 μ L) *T. acidophila* RDPR, 25 mM HEPES (pH 7.5), 1 mM MgCl₂, 100 μ M AdoCbl, 1 mM NADPH, 150 μ M TR, 2 μ M TRR, and the inhibitor at selected concentrations: 60 μ M, 300 μ M, and 600 μ M for N_3 UDP; 60 μ M for 2'VUDP; 60 μ M and 120 μ M for dF₂CDP. The concentrated inhibitor stock was diluted with 25 mM HEPES (pH 7.5) such that a final volume of ~ 5 - 10 μ L of inhibitor was required for the inactivation mixture. In a background control reaction, the inhibitor was replaced with ddH₂O in the inactivation mixture.

The inactivation mixture including everything except AdoCbl and the inhibitor was pre-incubated at 55°C for 2 min. After the addition of AdoCbl, a 15- μ L aliquot was removed as a zero time point and processed the same way as the subsequent 15- μ L aliquots described below. Inactivation was quickly initiated by the addition of inhibitor. The inactivation mixture was rapidly mixed and incubated at 55°C.

At predetermined time points, 15 μ L of the inactivation mixture was removed and diluted 10 fold into 135 μ L of assay mixture. The assay mixture (135 μ L) including everything except AdoCbl was also pre-incubated at 55°C for ~ 2 min, AdoCbl was then added to the assay mixture followed by rapid mixing with the 15- μ L aliquot removed from the incubation mixture, to final concentrations in a volume of 150 μ L: 1 mM [5, 8-³H]-ADP (S.A. = 2.1×10^3 cpm/nmol), 100 μ M AdoCbl,

30 mM DTT, 1 mM MgCl₂, and 25 mM HEPES (pH 7.5). In a time zero control for the assay mixture, 15 μL of 25 mM HEPES (pH 7.5) buffer replaced the 15-μL inactivation mixture.

The 150-μL assay solution was then incubated at 55°C for an additional period, typically ~ 10 min, to allow normal substrate reduction to proceed before it was placed in a boiling water bath for 2 min to stop the reaction and then placed on ice. After all the time points were taken, 15 μL of 1 M Tris solution (pH~11) and 10 U of calf intestine alkaline phosphatase were added to each aliquot. The solution was then incubated at 37°C for 1 h. A small portion (5 μL out of ~ 170 μL) of the solution was then analyzed for product (dA) formation using the TLC method previously described in the [5, 8-³H]-ADP activity assay in Chapter 1.

In some of the earlier runs (for 2'VUDP, N₃UDP and background control studies), [5-³H]-CDP was used as the normal substrate in the assay mixture. The assay time was 10 min and the product formation (dC) was quantitated using the borate column method described in the [2-¹⁴C]-CDP activity assay in Chapter 1. The assay mixture contained in the final volume of 150 μL: 1 mM [5-³H]-CDP (S.A. = 8.9 x 10³ cpm/nmol), 100 μM AdoCbl, 1 mM dGTP, 1 mM MgCl₂, 30 mM DTT, 25 mM HEPES pH 7.5.

Results and Discussion:

Stop-flow Experiment of *T. acidophila* RDPR

Previous stop-flow studies of Tamao & Blakley⁵ and Licht et al.¹ have shown that *L. leichmannii* RTPR catalyzes exchange of 5'-hydrogens of AdoCbl with solvent and formation of cob(II)alamin and 5'-dA from AdoCbl. Under exchange conditions when only effector and reductant are present, the rate constant of cob(II)alamin formation is ~ 40 s⁻¹. Under turnover conditions when the substrate

is also present, the rate constant of cob(II)alamin formation is $> 200 \text{ s}^{-1}$. In comparison with the turnover number for *L. leichmannii* RTPR of $\sim 2 \text{ s}^{-1}$,⁷ carbon-cobalt bond homolysis is obviously kinetically competent for nucleotide reduction. The exchange reaction has been observed for *T. acidophila* RDPR.²⁹ Turnover number of this enzyme (0.27 s^{-1}) is substantially reduced from the *L. leichmannii* RTPR even though the assay is conducted at 55°C . A similar stop-flow experiment was carried out with *T. acidophila* RDPR under turnover conditions ($[\text{ADP}] = 0.5 \text{ mM}$) to examine the kinetic competency of carbon-cobalt bond homolysis catalyzed by *T. acidophila* RDPR.

During the stop-flow experiment, although ideally the reaction should be carried out at 55°C , the optimal temperature for nucleotide reduction by *T. acidophila* RDPR,³⁰ the final temperature of the metal reaction chamber could only reach 48.7°C . Raising the water bath temperature from 55°C to 62°C failed to increase the reaction chamber temperature. Apparently heat dissipation from the metal reaction chamber caused temperature to stabilize at 48.7°C . Additional heat insulation materials are needed to cover the reaction chamber in future experiments to achieve 55°C .

AdoCbl has a λ_{max} of 525 nm and cob(II)alamin has a λ_{max} of 477 nm in the UV-vis spectrum region where other reaction components have negligible absorbance. The wavelength of 525 nm and 477 nm are then chosen where the absorbance change of the AdoCbl/cob(II)alamin pair are the largest.⁵

The control reaction where the *T. acidophila* RDPR storage buffer replaced *T. acidophila* RDPR showed no absorbance change at 525 nm and 477 nm, indicating that the amount of DTT present in the enzyme storage buffer ($< 0.1 \text{ mM}$ after final mixing) was not causing any significant AdoCbl degradation over the 2 s period monitored by the stop flow experiment. *T. acidophila* RDPR stock solution was therefore used directly.

The averaged data obtained from 6 runs each at 525 nm and 477 nm in the stop-flow experiment are shown in Figure 3.1a-b and Figure 3.2a-b respectively. As this preliminary experiment was carried out when *T. acidophila* RDPR yield per purification was still relatively low (~ 60 mg), the final enzyme concentration was only 25 μM . At this protein concentration, even if a stoichiometric amount of 25 μM cob(II)alamin could be formed, a maximal absorbance change of 0.12 at 525 nm would be observed ($\Delta\epsilon_{525} = 4,800 \text{ M}^{-1}\text{cm}^{-1}$, $\Delta\epsilon_{477} = 3,400 \text{ M}^{-1}\text{cm}^{-1}$). In the experimental results obtained, the maximal absorbance change was only ~ 0.012 at 525 nm and ~ 0.009 at 477 nm, corresponding to ~ 0.1 equivalent of cob(II)alamin formed. Although the stop flow trace obtained is very similar to that previously observed by Tamao and Blakley⁵ for RTPR from *L. leichmannii*, the absorbance changes (~ 0.01) is near the instrument detection limit, accounting for only ~ 1.5% of the total background absorbance (~ 0.78) from AdoCbl. Therefore, higher concentrations of *T. acidophila* RDPR are required for future stop-flow experiments to obtain more reliable kinetic data for rigorous kinetic analysis.

Although the data can be fit to a minimal mechanism using sophisticated kinetic models and computer programs such as KINSIM, it would not be very informative at this stage as there would be many sets of rate constants that would fit the data. At this stage, it is more important to obtain the approximate time scale of carbon-cobalt bond homolysis, rather than the assignment of microscopic rate constants. The data were fit with simple double exponential using the APL software provided by Applied Photophysics:

$$y = A_0 \times \text{EXP}(-k_1 \times t) + B_0 \times \text{EXP}(-k_2 \times t) + C_0$$

where C_0 is the background absorbance, A_0 and B_0 are amplitudes, k_1 and k_2 are rate constants. The rate data are summarized in Table 3.1.

Table 3.1 Summarized rate data for stop flow experiment.

Trace	A_0	B_0	C_0	k_1	k_2	Variance
525 nm	0.1601	-7.9×10^{-3}	0.7821	-84.33	-11.46	4.605×10^{-7}
477 nm	-1.13×10^{-2}	9.45×10^{-3}	0.7716	-152.9	-5.282	8.02×10^{-7}

The fits give time constants and amplitudes for the two phases of the absorbance change. Each number is composed of a number of microscopic rate constants, and the time constants of the exponentials are related to the rates of approach to equilibrium for cob(II)alamin formation and AdoCbl reformation. Although they are not equivalent to the microscopic rate constants, using the data at 525 nm with the smaller normalized variance value, cob(II)alamin formation should be on the order of $\sim 80 \text{ s}^{-1}$, while AdoCbl reformation be on the order of 11 s^{-1} . A close examination of the two data fits reveals that at $\sim 38 \text{ ms}$ the absorbance at 525 nm decreases to a minimum, while at $\sim 24 \text{ ms}$ the absorbance at 477 nm increases to a maximum. (The 477 nm runs were performed right after the 525 nm runs. The reason why the maximal absorbance changes occur at two different time points at the two wavelengths is not immediately clear.)

Considering the maximal turnover number so far obtained for *T. acidophila* RDPR of 0.27 sec^{-1} (S.A. = $0.16 \mu\text{mol}\cdot\text{mg}^{-1}\cdot\text{min}^{-1}$, Figure 2.6a, $[\text{ADP}] = 20 \mu\text{M}$), the carbon-cobalt bond homolysis is obviously occurring in a kinetically competent fashion. However, it should be noted that the *in vivo* nucleotide reduction may and probably will be faster than that of the *in vitro* rate as unnatural reductant (DTT) is used in the *in vitro* assays.

This preliminary experiment only examined cob(II)alamin formation under turnover conditions with very small absorbance changes above background. Further experiments need be carried out with a higher enzyme concentration to

obtain more reliable apparent rate constants for cob(II)alamin formation. It would also be interesting to investigate the rate of cob(II)alamin formation under exchange conditions when the substrate is absent.

Rapid Freeze Quench EPR Experiment of *T. acidophila* RDPR

As described in the introduction, previous studies of Licht¹ have shown that rapid mixing of *L. leichmannii* RTPR, reductant, and substrate, with AdoCbl resulted in formation of a paramagnetic species which was revealed by detailed EPR analysis to be cob(II)alamin coupled to a thiyl radical. One of the key experiments carried out was rapidly mixing *L. leichmannii* RTPR with [5'-¹H]-AdoCbl and [5'-²H]-AdoCbl respectively. Based on the mechanism model described in Scheme 3.1, the cobalt(II) hyperfine interactions in the two cases should differ if 5'-dA[•] is present as an intermediate. This is shown not to be the case for *L. leichmannii* RTPR. In order to determine if *T. acidophila* RDPR behaves in the same fashion, similar RFQ-EPR experiments were carried out.

RFQ-EPR Experiment with [5'-¹H]-AdoCbl

Samples for analysis by EPR spectroscopy were obtained by rapidly mixing 400 μM *T. acidophila* RDPR with 400 μM [5'-¹H]-AdoCbl in the presence of 1 mM ADP, 1 mM dGTP, and reductant (TR/TRR/NADPH) with quenching into liquid isopentene (at -140°C) at 10 and 38 ms. The RFQ-EPR spectra obtained are shown in Figure 3.3.

The signals at the two time points look very similar except that the one at 38 ms time point has a quite hyperbolic background. A possible cause for this irregular background is water condensation in the quartz sample holder which could cause the diode current to shift during spectrum recording at liquid N₂ temperature. Integration of the signal observed in the 10 ms spectrum gave a spin quantitation of

~0.28 if a typically packing factor of 0.7 is used. The 38 ms time point spectrum appears to have a larger intensity per scan than the 10 ms time point spectrum. However, as the baseline is very curved, integration was not performed on this spectrum.

A comparison of the spectrum of *T. acidophila* RDPR with [5'-¹H]-AdoCbl at 10 ms with that of *L. leichmannii* RTPR with [5'-¹H]-AdoCbl at 175 ms also in the presence of substrate (1 mM ATP)¹ is shown in Figure 3.4. The overall line shapes are very similar. In the *T. acidophila* RDPR spectrum, however, the cob(II)alamin hyperfine features ($I = 7/2$) are not as evident as the ones observed in the *L. leichmannii* RTPR spectrum. The Zeeman splitting value is ~ 42 G for the *T. acidophila* RDPR spectrum compared to 50 G for the *L. leichmannii* RTPR spectrum. Although the two spectrum were recorded at the same EPR settings and have similar overall line shapes, the respective g values differ slightly. The g values of the cob(II)alamin spin and the sharp feature are 2.14 and 2.004 for *T. acidophila* RDPR, 2.12 and 1.99 for *L. leichmannii* RTPR respectively. However, based on EPR theory, the g values for the two paramagnetic species do not have to be the same as the microenvironment of the two species are not the same.

RFQ-EPR Experiment with [5'-²H]-AdoCbl

In order to determine if 5'-dA• contributed to the spectrum shown in Figure 3.3, a similar RFQ-EPR experiment was carried out with [5'-²H]-AdoCbl. Samples for analysis by EPR spectroscopy were obtained by rapidly mixing 340 μM *T. acidophila* RDPR with 340 μM [5'-²H]-AdoCbl (provided by Licht) in the presence of 1 mM ADP, 1 mM dGTP and reductant (TR/TRR/NADPH) with quenching into liquid isopentene (at -140°C) at 10 and 38 ms. The RFQ-EPR spectra obtained are shown in Figure 3.5 . The signals at the two time points look very similar despite the poor signal to noise ratio.

A comparison of the *T. acidophila* RDPR EPR spectra with [5'-¹H]-AdoCbl and [5'-²H]-AdoCbl at 10 ms and 38 ms are shown in Figure 3.6a and Figure 3.6b respectively. The signal to noise ratio of the spectra with [5'-²H]-AdoCbl is not as good as the one with [5'-¹H]-AdoCbl. The spectra with [5'-²H]-AdoCbl also have lower intensity per scan. Integration of the signal obtained with [5'-²H]-AdoCbl at 10 ms gives spin quantitation of ~ 0.07 using a typical packing factor of 0.7. Although 15% less of *T. acidophila* RDPR was used in the [5'-²H]-AdoCbl experiment (340 μM vs. 400 μM), the number of equivalents of spin per *T. acidophila* RDPR was not expected. At every time point, a secondary isotope effect in forward direction and a primary isotope effect in reverse direction should increase the amount of cob(II)alamin, ??? Another possible reason for this discrepancy is inconsistent packing factors between the two samples. However, qualitatively, the EPR spectra of *T. acidophila* RDPR with [5'-¹H]-AdoCbl and [5'-²H]-AdoCbl look very similar as expected. As the spectra with [5'-²H]-AdoCbl have very poor signal to noise ratio, this experiment needs be repeated, preferably using the same enzyme concentration (400 μM), for quantitative analysis. In addition, these experiments need to be examined under exchange conditions, where the carbon-cobalt bond presumably will not reform.

The preliminary RFQ-EPR studies carried out with *T. acidophila* RDPR suggested that *T. acidophila* RDPR uses the same catalytic mechanism as *L. leichmannii* RTPR. Cob(II)alamin is formed within ~ 10 ms, and 5'-dA· does not appear to be present as an intermediate. However, the experiment needs to be repeated in order to carry out quantitative analysis. Similar to the studies carried out for *L. leichmannii* RTPR, further RFQ-EPR experiments of *T. acidophila* RDPR with AdoCbl, for example, in the absence of substrate or reductant, with [β-²H]-cysteine *T. acidophila* RDPR would be useful to further characterize the nature of the paramagnetic species

observed. Site-directed mutagenesis experiments will also be useful to identify the putative thiyl radical (Cys-434).³⁰

From the previously described stop flow experiments, a maximum absorbance change at 525 nm was reached at ~ 38 ms, thus RFQ-EPR sample was quenched at 38 ms. As there could be an additional ~ 10 ms of dead time for sample freezing, a shorter time point of ~ 10 ms was also chosen for the RFQ-EPR experiment. However, it should be noted that the previously described stop flow experiments were carried out at different enzyme, substrate, and AdoCbl concentrations. Ideally, all the experimental conditions should be carried out under the same conditions to see if the kinetics of cob(II)alamin formation monitored by stop flow spectroscopy are the same as those monitored by RFQ-EPR. And again, the packing factor of the experimenter needs to be determined.

The Mystery Peak Observed

In the first attempt to obtain EPR data, mixing 400 μM *T. acidophila* RDPR with 400 μM [5'-²H]-AdoCbl, with reagent concentrations in both syringes identical to the [5'-¹H]-AdoCbl experiment, although a quenched sample at 10 ms was obtained, it was not pink indicating the instrument mixer was malfunctioning such that [5'-²H]-AdoCbl was not present at significant concentrations. As 4:1 mixing of protein to AdoCbl was used, the sample volume was not significantly differently from the well mixed samples as AdoCbl volume would only count for 20% of the final volume.

However, as shown in Figure 3.7, a weak radical signal was still observed for this sample. Integration of this signal gives ~ 0.03 equivalence using a typical packing factor of 0.7. An overlay of this signal with the sample quenched at 10 ms with good mixing (Figure 3.5) is shown in Figure 3.8. Coincidentally, the mystery peak has the same g value as the sharp feature present in the spectrum obtained with good mixing at $g = 2.004$. The nature of the sharp feature in the *L. leichmannii* RTPR EPR

spectrum (Figure 3.4), at a slightly different g value ($g = 1.990$), is not yet identified, but is thought to be unrelated to the spectrum of the intermediate.¹

An explanation of this mystery peak could simply be contamination present in the sample, or e' signals arising from free electrons in the EPR tube. Although the sample was not pink, it is still possible that a small amount of AdoCbl was mixed to generate some radical intermediate, given the broad weak signal present in the $g = 2.14$ region. The protein could also have contained some other unidentified EPR active metal species in which case a further metal analysis of *T. acidophila* RDPR is required. It is also known that in the case of flavoprotein mitochondrial amine oxidase, no metal is required for radical generation.³¹ An EPR spectrum of the tube, or the solution in Syringe A containing protein, substrate, effector, and reductants need to be taken in order to narrow the possibilities.

Time-dependent Inactivation of *T. acidophila* RDPR

Time-dependent inactivation studies with mechanism-based inhibitors have played a key role in elucidating the nucleotide reduction mechanism by RNRs. Three previously known mechanism-based inhibitors for other RNRs (N_3 UDP, 2'VUDP, and dF₂CDP) are studied with *T. acidophila* RDPR to further explore the catalytic mechanism of this archae enzyme.

Experimental Concerns for the Time-dependent Inactivation Studies

The procedure for the time-dependent inactivation studies of *T. acidophila* RDPR described in the experimental section is the final experimental design. Initially, AdoCbl instead of the inhibitor was used to start the inactivation reaction, as inactivation should not start in the absence of AdoCbl. With this initiation method, the time zero aliquot already contained inhibitor. Since AdoCbl was already present in the assay mixture, for potent inhibitors or inhibitors at high

concentrations that would inactivate *T. acidophila* RDPR in less than 1 min, this initiation method made it impossible to obtain an accurate value for nucleotide production at time zero. Therefore, the inhibitor was used to initiate the inactivation reaction in the final experimental design.

As previously mentioned, [5-³H]-CDP was used as the normal substrate in the assay mixture in earlier runs with inhibitor N₃UDP, 2'³VUDP and background control studies. However, high background levels of radioactivity were observed in the time zero control for the assay mixture due to tritium washout from the 5 position during the use of the borate columns. [5, 8-³H]-ADP was therefore used as the normal substrate in the assay mixture in later runs for dF₂CDP studies.

Ideally the enzyme should be passed through a Sephadex column to remove unbound inhibitor and other small molecules before being placed in the assay mixture. However, for practical concerns, the dilution method described was used instead. As *T. acidophila* RDPR has a specific activity of less than 0.16 μmol·mg⁻¹·min⁻¹, either large amounts of enzyme or substrate with high radioactive specific activity is required in order to obtain reliable kinetic data. A relatively small dilution factor of 1:10 was used to reduce the amount of enzyme and radioactivity consumed. However, larger dilution factor may be required for potent inhibitors.

As only a single time point was used for each assay mixture, for each specific set of assay conditions, it has been verified that the single assay time point lies in the linear range of the assay time curve. Although ADP K_m studies have shown that the maximal specific activity of *T. acidophila* RDPR is achieved at 20 - 30 μM ADP in the presence of 1 mM dGTP (Chapter 2, Figure 2.6a), higher concentration of normal substrate in the assay mixture provides protection against inactivation in the dilution method where inhibitor will also be present in the assay mixture. However, due to substrate inhibition observed for ADP reduction in the presence of dGTP, but not in the absence of any effectors, ~ 200 μM ADP in absence of any

effector ($K_m = 29.2 \mu\text{M}$) might be more appropriate than 1 mM ADP as less enzyme will be consumed and a larger dilution factor can be achieved, though at the expense of amount of radioactivity used.

Although most of the activity assays described in Chapter 1 and 2 used DTT as reductant, DTT has been found to protect RNRs against 2'-methylene-2'-deoxycytidine 5'-diphosphate (2'VCDP) inactivation.²⁴ Therefore, the TR/TRR/NADPH reducing system was used in the inactivation mixture, while DTT was still used in the assay mixture.

The cause of the low data quality with the N_3UDP and 2'VUDP studies reported below can mainly be contributed to inadequate experimental design. The inactivation studies with N_3UDP and 2'VUDP were carried out prior to those with dF₂CDP in which the experimental design had been optimized. As all the reactions were carried out in dark under dim red lights, low visibility can easily cause problems. All tubes should be labeled and arranged in order prior to the start of the experiment. Although everything has to be done quickly, it is important to make sure all the solution volumes removed from the inactivation mixture are consistent and accurate, and there are no additional drops attached to the outside of the pipet tips! It is always a good idea to prepare excess inactivation mixture (110 μL for 6 time points, 15 μL per time point) in case the solution runs short in the last time point due to inaccurate pipetting or accidental loss of sample volume. The pipetmans should be calibrated. When multiple inactivation reactions are carried out together as in the N_3UDP studies, one has to be very concentrated as there will be many time points to catch. I started the runs 20 s apart in my case. It is always a good idea to practice first and choose the number of parallel runs at one's own level of comfort. Two P-20 pipetmans were used for convenience, one was used for the addition inhibitor (5 - 10 μL) and removing aliquots from the inactivation mixture

(15 μ L), the other was used for the addition of AdoCbl to the inactivation mixture and the assay mixture.

Background Inactivation Observed for T. acidophila RDPR

From the initial inactivation studies performed, a high background inactivation rate was observed for the control reaction where no inhibitor was present. The initial inactivation mixture control contained: 60 μ M (90 μ g/ 15 μ L) *T. acidophila* RDPR, 25 mM HEPES pH 7.5, 1 mM MgCl₂, 100 μ M AdoCbl, 1 mM dGTP, 1 mM NADPH, 150 μ M TR, 2 μ M TRR, with neither inhibitor, nor normal substrate. dGTP was initially selected as a potential allosteric effector. As shown in Figure 3.9, the presence of AdoCbl apparently further destabilizes the enzyme over the course of 20 min. However, as shown in Figure 3.10, when both 100 μ M AdoCbl and 1 mM dGTP are excluded from the inactivation mixture control, the enzyme remains stable at both 0°C and 55°C over the course of 20 min, excluding the possibility that high temperature (55°C) is a factor in enzyme destabilization. The cause of the additive destabilization effects of AdoCbl and dGTP in the absence of normal substrate on *T. acidophila* RDPR is not very clear. However, for the case of AdoCbl, if AdoCbl goes through carbon cobalt bond homolysis to form 5'-dA and cob(II)alamin, the two species formed could inhibit the reaction non-covalently and competitively as has previously been observed with the *L. leichmannii* enzyme.

Due to the background inactivation problem observed, in the final experimental design, the inactivation mixture contained no effector, and AdoCbl was always added as late as possible to both the inactivation mixture and the assay mixture. The overall reaction time course was also reduced to 5 min to minimize the background inactivation rate.

dF₂CDP is a Potent Inhibitor of T. acidophila RDPR

dF₂CDP has been shown to be potent inhibitors for both class I and class II RNRs. dF₂CDP irreversibly and stoichiometrically inactivates *E. coli* RDPR rapidly and DTT does not protect against inactivation. With 16-fold excess of inhibitor dF₂CDP over RDPR ([RDPR] = 1.25 μM), all RDPR activity is lost with a $t_{1/2}$ = 30 s.²⁴ 2'-Deoxy-2',2'-difluorocytidine 5'-triphosphate (dF₂CTP) rapidly inactivates *L. leichmannii* RTPR with > 90% activity loss in 15 s ([RTPR] = 15 μM, [dF₂CTP] = 15 μM).²⁰

From the experimental data obtained in this work, shown in Figure 3.11, dF₂CDP is also shown to be a potent inhibitor for *T. acidophila* RDPR and inactivates the enzyme stoichiometrically in less than 1 min. Since dF₂CDP inactivates the enzyme so fast, it was impossible to investigate the effect of AdoCbl or allosteric effectors on the rate of inactivation. In order to further explore inactivation kinetics, a chemical quench method needs be used and the enzyme may have to be separated from the inhibitor before it is assayed for activity. Although the detailed inactivation kinetics are not yet known, the fact that *T. acidophila* RDPR is stoichiometrically inactivated by the previously known mechanism based inhibitor dF₂CDP for other RNRs strongly suggests that *T. acidophila* RDPR also employs a similar catalytic mechanism as other RNRs.

***N*₃UDP and 2'VUDP as Inhibitors for *T. acidophila* RDPR**

Previous Inactivation Studies with 2'-Azido-2'-deoxynucleotides

Inactivation studies with 2'-azido-2'-deoxynucleotides have been carried out for all three classes of RNRs. It is shown to be potent inhibitor of class I and class III RNRs, but not class II RNRs.

N₃UDP has been shown to be a potent inhibitor for *E. coli* RDPR. Incubation of 1 equivalent N₃UDP with *E. coli* RDPR (10 μM) results in stoichiometric inactivation of the enzyme and the loss of tyrosyl radical.¹³ 2'-Azido-2'-deoxyuridine 5'-triphosphate (N₃UTP) and 2'-azido-2'-deoxyadenosine- 5'-triphosphate (N₃ATP) are

not very potent inhibitors for *L. leichmannii* RTPR [Ashley et. al; in press]. They exhibit time-dependent inactivation at millimolar concentrations with multiphasic kinetics. Incubation of 25 μM *L. leichmannii* RTPR with 260 μM N_3UTP or 260 μM N_3ATP only leads to $\sim 50\%$ activity loss after 10 min. 2'-Azido-2'-deoxycytidine 5'-triphosphate (N_3CTP) is shown to be a potent inhibitor for anaerobic *E. coli* RTPR.²³ Incubation of 6 μg anaerobic *E. coli* RTPR in a volume of 50 μL with 0.16 mM N_3CTP in the presence of 1 mM ATP for 5 min leads to the loss of 97% of its activity.

Previous Inactivation Studies with 2'-Methylene-2'-deoxynucleotides

Inactivation studies with 2'-deoxy-2'-methylenenucleotides have been carried out for class I and class II RNRs. It is shown to a potent inhibitor for both classes of RNRs.

Inactivation studies for *E. coli* RDPR with 2'-deoxy-2'-methylenenucleotides were previously carried out by Baker et al..²⁴ 2'-Deoxy-2'-methyleneuridine (2'VUDP) shows increased inactivation of *E. coli* RDPR over the concentration range of 0 - 0.42 mM ($[\text{RDPR}] = 1.25 \mu\text{M}$) with a $K_i = 0.83 \text{ mM}$ and $k_{\text{inact}} = 0.015 \text{ s}^{-1}$. In contrast, the cytidine derivative 2'-deoxy-2'-methylencytidine (2'VCDP) inactivates *E. coli* RDPR much more rapidly with a half life of inactivation less than 1 min at 70 μM of 2'VCDP ($[\text{RDPR}] = 1.25 \mu\text{M}$), a much lower concentration of inhibitor. Inactivation of RDPR with both derivatives is shown to be irreversible. However, it is noted that DTT protects RDPR from inactivation by 2'VCDP. The differences in the concentration dependence on the inactivation between these two derivatives may be related to similar differences observed with their corresponding substrates $K_m = 220 \mu\text{M}$, $V_{\text{max}} = 0.87 \text{ U/mg}$ for UDP and $K_m = 50 \mu\text{M}$, $V_{\text{max}} = 1.2 \text{ U/mg}$ for CDP.

Inactivation studies for *L. leichmannii* RTPR with 2'-deoxy-2'-methylenenucleotides were previously carried out by Lawrence¹⁹ in the Stubbe

laboratory. 2'-Deoxy-2'-methylene-5'-triphosphate (2'VCTP) is shown to be a potent inhibitor that inactivates RTPR at 0.5 μM ($[2'VCTP] = 0.5 \mu\text{M}$, effector $[dATP] = 0.12 \text{ mM}$) with a $t_{1/2} = 34 \text{ s}$. Both cofactor AdoCbl and effector dATP are required for complete inactivation.

Experimental Results for T. acidophila RDPR

The experimental results obtained for *T. acidophila* RDPR are shown in Figure 3.12 and Figure 3.13 respectively. N_3UDP is not a potent inhibitor for *T. acidophila* RDPR. Significant inactivation is only observed at a millimolar concentration of inhibitor (10 equivalence, 600 μM N_3UDP). It may be a good idea to check the purity of both inhibitors by HPLC in case of possible degradation upon storage. The 2'VUDP study was only carried out at a low inhibitor concentration (1 equivalence, 60 μM 2'VUDP). The concentration dependence of this inhibitor on *T. acidophila* RDPR inactivation needs to be studied. Although the data points are scattered, it is still obvious that N_3UDP and 2'VUDP are much less potent inhibitors for *T. acidophila* RDPR compared with dF₂CDP.

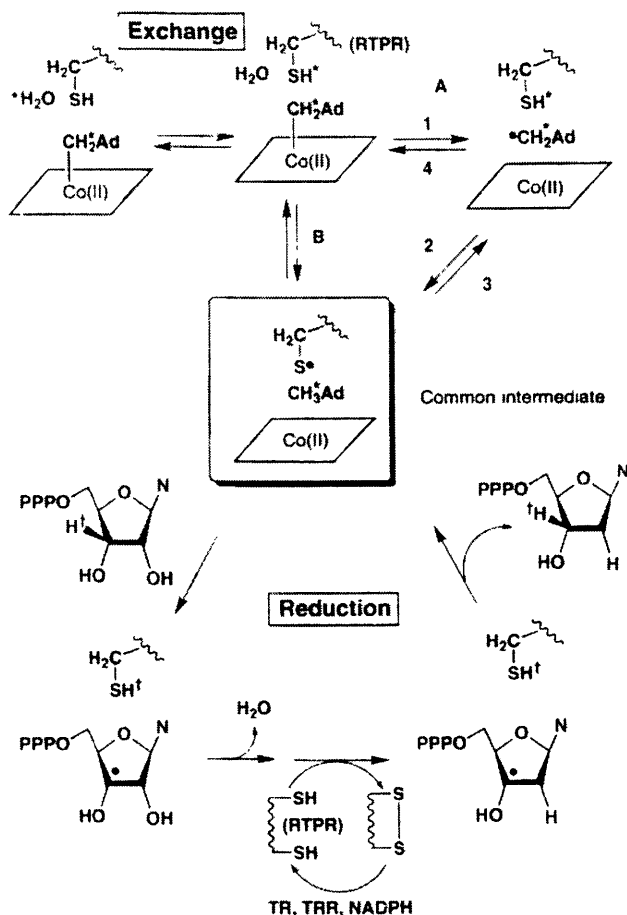
Summary

Overall, the preliminary results from all the mechanistic studies performed strongly suggest that *T. acidophila* RDPR, though from an archaeobacterium, has the conserved radical-based catalytic mechanism as other RNRs from eukaryotes and prokaryotes. The role of AdoCbl in *T. acidophila* RDPR is also likely to be the same as in the other AdoCbl-dependent RTPR from *L. leichmannii*. These studies provide another piece of evidence that all RNRs, although they may be evolutionary far apart, employ the conserved radical-based catalytic mechanism.

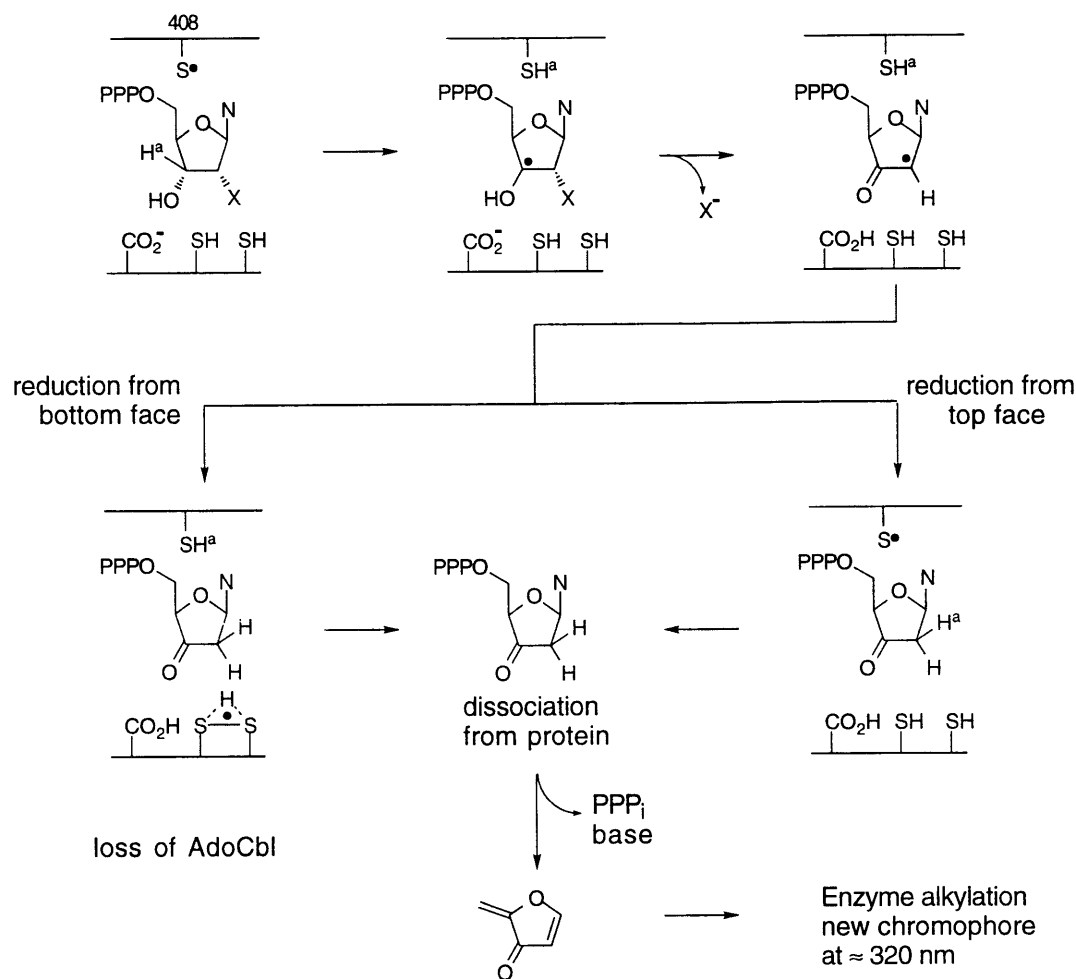
References:

- (1) Licht, S. L.; Gerfen, G. J.; Stubbe, J. *Science* **1996**, 271, 477-481.
- (2) Stubbe, J.; van der Donk, W. A. *Chem. Biol.* **1995**, 2, 793-801.
- (3) Hogenkamp, H. P. C. ; G., R. K.; Brownson, C.; Blakley, R. L.; Vitols, E. *The Journal of Biological Chemistry* **1968**, 243, 799-808.
- (4) Abeles, R. H.; Beck, W. S. *The Journal of Biological Chemistry* **1967**, 242, 3589-3593.
- (5) Tamao, Y.; Blakley, R. L. *Biochem.* **1973**, 12, 24-34.
- (6) Orme-Johnson, W. H.; Beinert, H.; Blakley, R. L. *J. Biol. Chem.* **1974**, 249, 2338-2343.
- (7) Booker, S.; Stubbe, J. *Proc. Natl. Acad. Sci. USA* **1993**, 90, 8352-8356.
- (8) Stubbe, J.; Kozarich, J. W. *J. Biol. Chem.* **1980**, 255, 5511-5513.
- (9) Sjöberg, B.-M.; Gräslund, A.; Eckstein, F. *J. Biol. Chem.* **1983**, 258, 8060-8067.
- (10) Ator, M.; Salowe, S. P.; Stubbe, J.; Emptage, M. H.; Robins, M. J. *J. Am. Chem. Soc.* **1984**, 106, 1886-1887.
- (11) Harris, G.; Ator, M.; Stubbe, J. *Biochemistry* **1984**, 23, 5214-5225.
- (12) Ator, M. A.; Stubbe, J. *Biochemistry* **1985**, 24, 7214-7221.
- (13) Salowe, S. P.; Ator, M.; Stubbe, J. *Biochemistry* **1987**, 26, 3408-3416.
- (14) Ashley, G. W.; Harris, G.; Stubbe, J. *Biochemistry* **1988**, 27, 4305-4310.
- (15) Salowe, S. P.; Bollinger Jr., J. M.; Ator, M.; Stubbe, J.; McCracken, J.; Peisach, J.; Samano, M. C.; Robins, M. J. *Biochemistry* **1993**, 32, 12749-12760.
- (16) van der Donk, W. A.; Yu, G.; Silva, D. J.; Stubbe, J.; McCarthy, J. R.; Jarvi, E. T.; Matthews, D. P.; Resvick, R. J.; Wagner, E. *Biochemistry* **1996**, 35, 8381-8391.
- (17) Harris, G.; Ashley, G. W.; Robins, M. J.; Tolman, R. L.; Stubbe, J. *Biochemistry* **1987**, 26, 1895-1902.

- (18) Ashley, G. W.; Lawrence, C. C.; Stubbe, J. *Tetrahedron in press*,
- (19) Lawrence, C. C., Progress Report: March - December 1994;
Massachusetts Institute of Technology, **1994**,
- (20) Silva, D. J. **1996**,
- (21) Ong, S. P. ; M., S. C.; Hogenkamp, H. P. C. *Biochemistry* **1993**, *32*, 11397-11404.
- (22) McFarlan, S. C.; Ong, S. P.; Hongenkamp, H. P. C. *Biochemistry* **1996**, *35*, 4485-4491.
- (23) Eliasson, R.; Pontis, E.; Eckstein, F.; Reichard, P. *J. Biol. Chem.* **1994**, *269*, 26116-26120.
- (24) Baker, C. H.; Banzon, J.; Bollinger Jr., J. M.; Stubbe, J.; Samano, V.; Robins, M. J.; Lippert, B.; Jarvi, E.; Resvick, R. *J. Med. Chem.* **1991**, *34*, 1879-1884.
- (25) Mao, S. S.; Johnston, M. I.; Bollinger, J. M.; Stubbe, J. *Proc. Natl. Acad. Sci. U.S.A.* **1989**, *86*, 1485-1489.
- (26) Stubbe, J. *Adv. Enzymol. Relat. Areas Mol. Biol.* **1990**, *63*, 349-417.
- (27) Lunn, C. A.; Kathju, S.; Wallace, B. J.; Kushner, S.; Pigiet, V. *J. Biol. Chem.* **1984**, *259*, 10469-10474.
- (28) Russell, M.; Model, P. *J. Bacteriol.* **1985**, *163*, 238-242.
- (29) Tauer, A., *Ph.D. Thesis, Eidgenossische Technische Hochschule*, **1994**.
- (30) Tauer, A.; Benner, S. A. *Proc. Natl. Acad. Sci.* **1997**, *94*, 53-58.
- (31) Stubbe, J. *Annu. Rev. Biochem.* **1989**, *58*, 257-285.



Scheme 3.1 Possible roles of AdoCbl in thiol radical generation in class II RNRs. Reaction pathway A (1-4) has been excluded based on work carried out by Licht et al. (1996). The carbon-cobalt bond is homolytically cleaved to form 5'-dA, cob(II)alamin and a thiyl radical -- the common protein radical employed by all classes of RNRs -- in a concerted fashion. The thiyl radical then initiates the nucleotide reduction process as previously described (Scheme 1.3). *Adapted from Licht et al., 1996.*



Scheme 3.2 Mechanism of inhibition of *L. leichmannii* RTPR by a nucleotide analog. After abstraction of the 3'-hydrogen atom by the thiyl radical, the leaving group, X⁻, is lost generating a 3'-keto-2'-deoxynucleotide radical. This species can be reduced from either the top face or the bottom face. If reduction occurs from the top face, the thiyl radical cannot be regenerated and the enzyme is inactivated. Reduction from the bottom face results in a 3'-ketodeoxynucleotide which dissociates from the active site and decomposes to yield the 2'-methylene-3(2H)-furanone, which non-specifically alkylates and inactivates the enzyme. *Courtesy of Dr. W. A. van der Donk.*

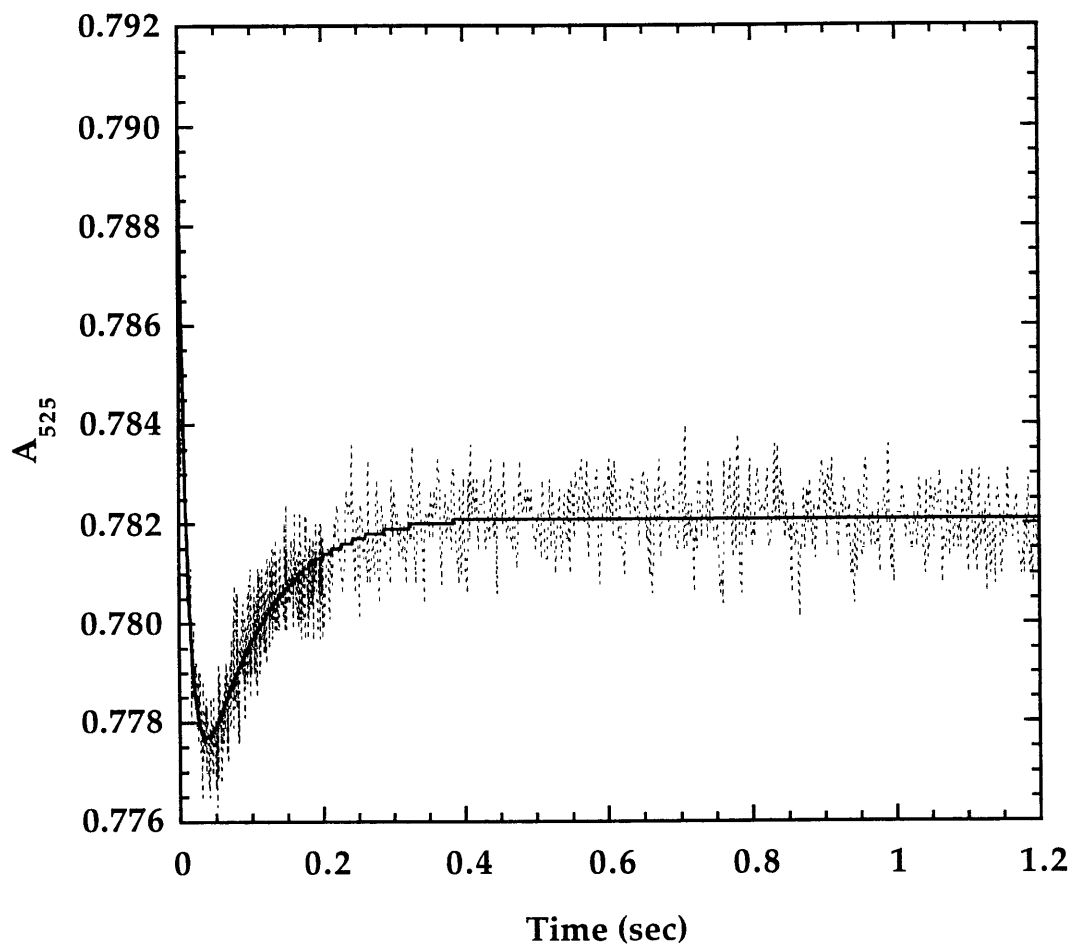


Figure 3.1a Cob(II)alamin formation (0 - 1.2 s): absorbance change at 525 nm. Final reactant concentrations after equal volume mixing were: 0.5 mM ADP, 0.5 mM dGTP, 100 μ M AdoCbl, 25 mM HEPES (pH 7.5), 25 μ M *T. acidophila* RDPR. Black dots are data from the average of 6 runs. Solid line is the double exponential curve fit. *Source: Book II, p.121.*

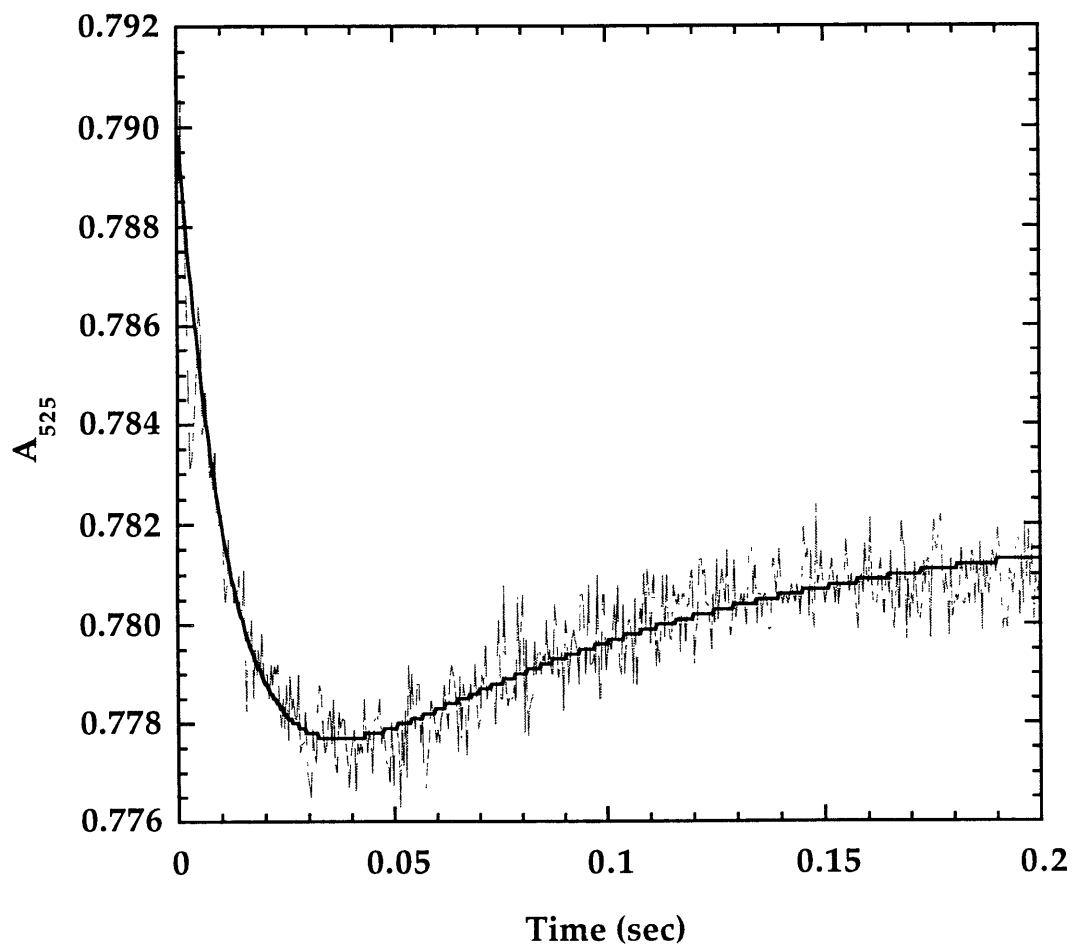


Figure 3.1b Cob(II)alamin formation: absorbance change at 525 nm. Same as Figure 3.1a, 0 - 200 ms region only. Absorbance minimum is reached at ~ 38 ms with a maximal absorbance change of 0.012.

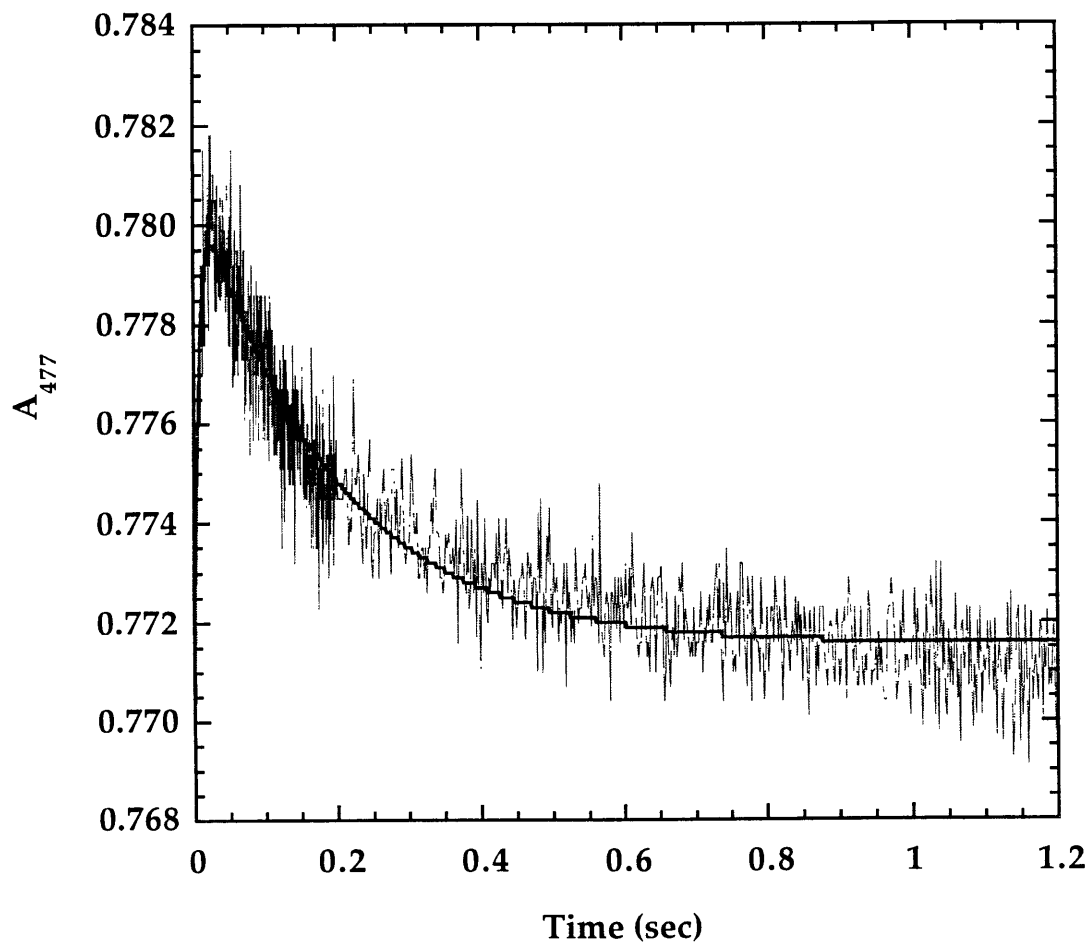


Figure 3.2a Cob(II)alamin formation (0 - 1.2 s): absorbance change at 477 nm. Final reactant concentrations after equal volume mixing were: 0.5 mM ADP, 0.5 mM dGTP, 100 μ M AdoCbl, 25 mM HEPES (pH 7.5), 25 μ M *T. acidophila* RDPR. Black dots are data from the average of 6 runs. Solid line is the double exponential fit.

Source: Book II, p.121.

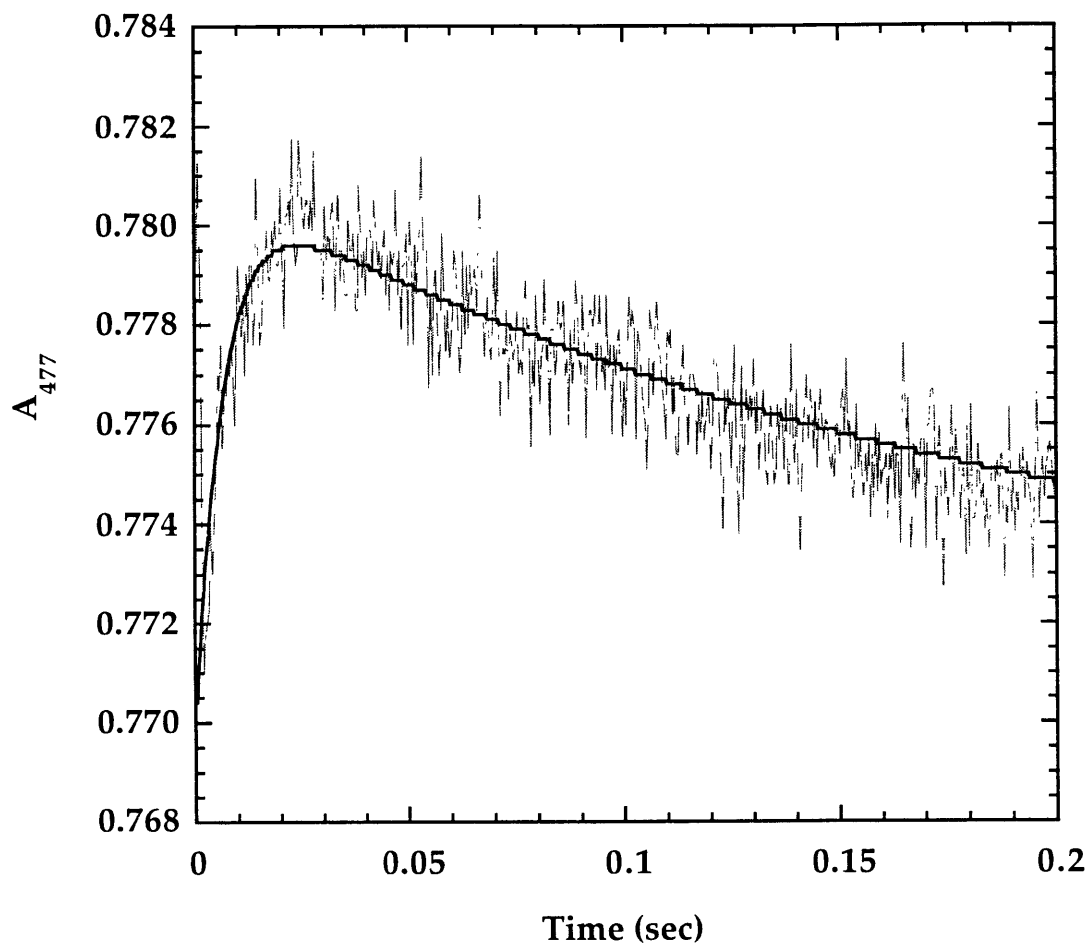


Figure 3.2b Cob(II)alamin formation: absorbance change at 477 nm. Same as Figure 3.2a, 0 - 200 ms region only. Absorbance maximum is reached at ~ 24 ms with a maximal absorbance change of 0.009.

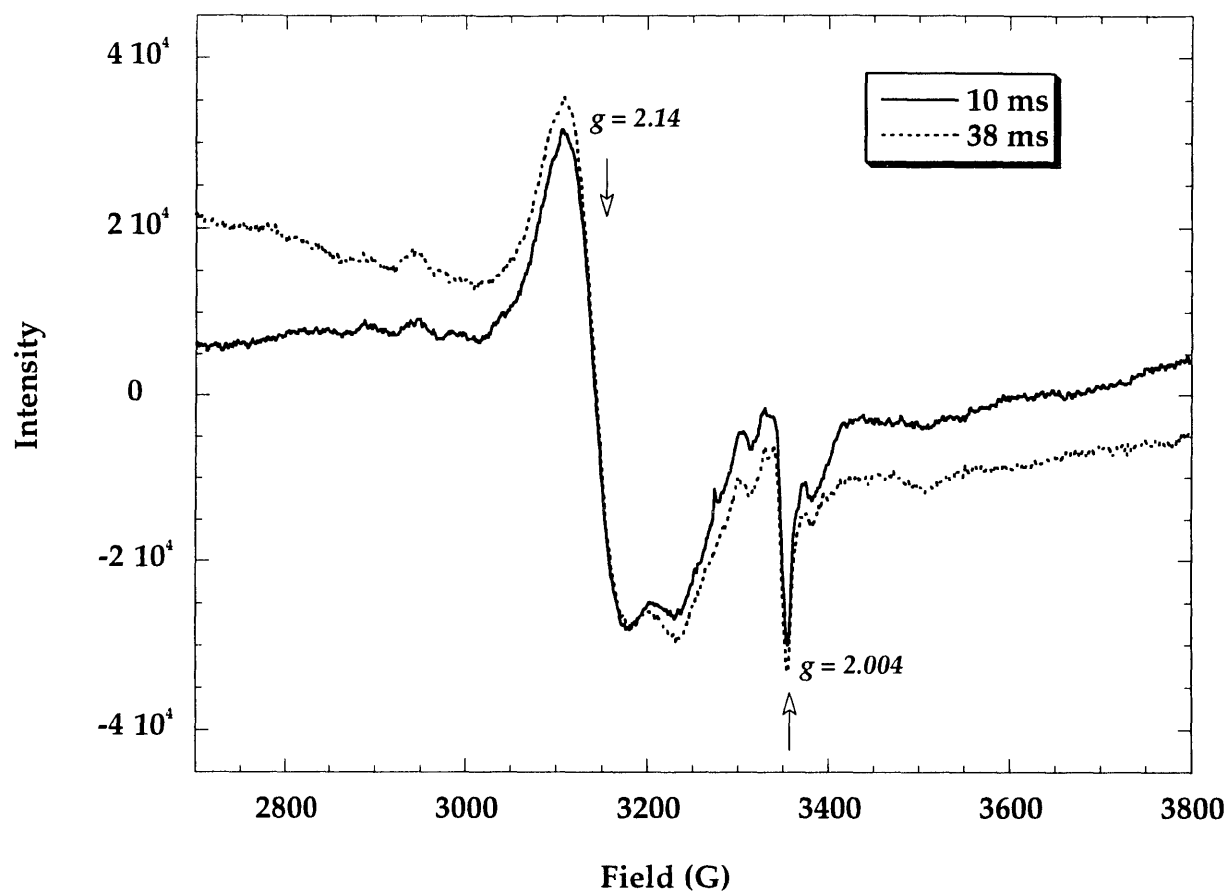


Figure 3.3 RFQ-EPR spectra of *T. acidophila* RDPR at 10 ms (9 scans) and 38 ms (6 scans) with $[5\text{-}^1\text{H}]\text{-AdoCbl}$. Scan Range: 1100 G; Field Set: 3250 G; Time Constant: 328 ms; Modulation Amplitude: 5 G; Modulation Frequency: 100 kHz; Receiver Gain: 5×10^5 ; Microwave Power: 10 mW; Microwave Frequency: 9.41 GHz; Sweep Time: 335 sec; Resolution of Field Axis: 1024.

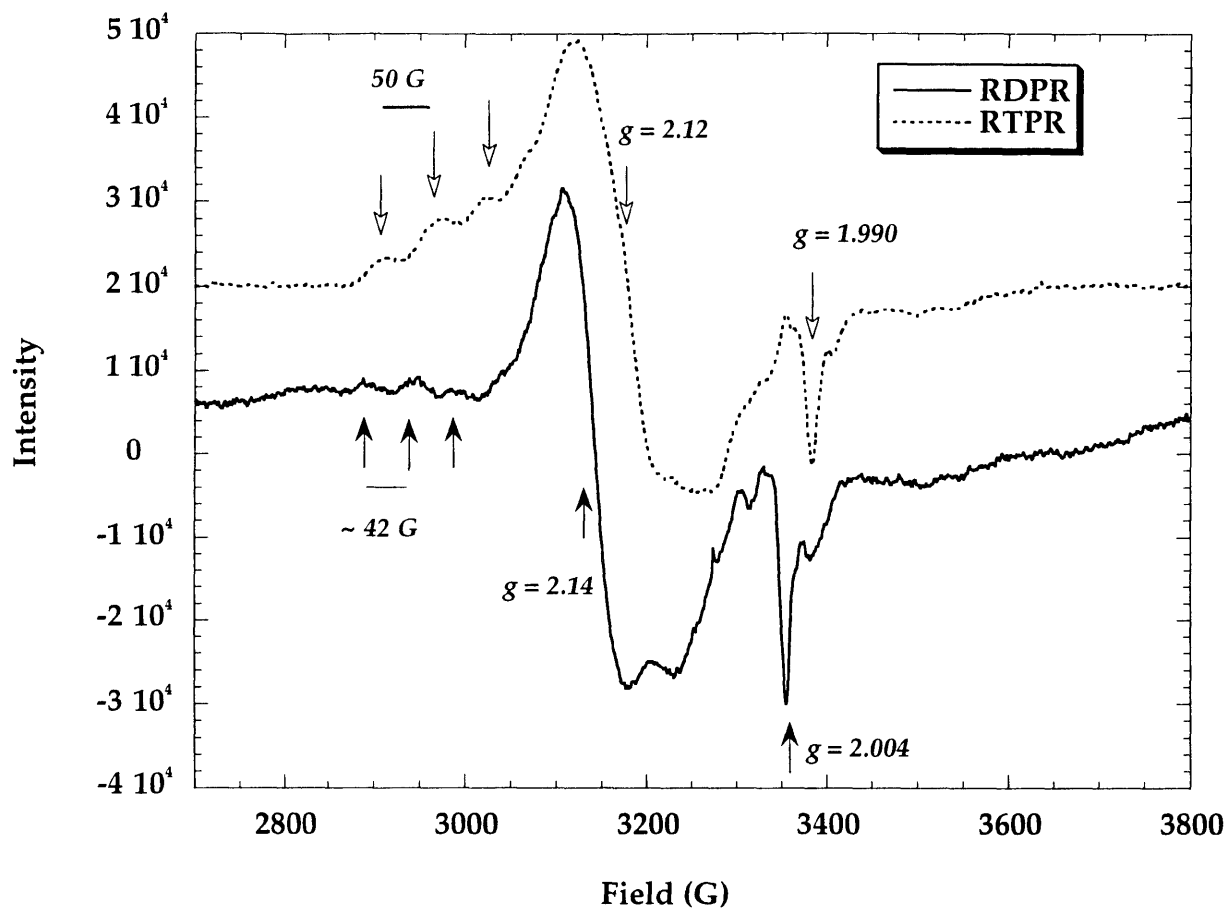


Figure 3.4 RFQ-EPR spectra of *T. acidophila* RDPR at 10 ms (9 scans) with that of *L. leichmannii* RTPR at 175 ms (10 scans) with $[5\text{-}^1\text{H}]\text{-AdoCbl}$. Scan Range: 1100 G; Field Set: 3250 G; Time Constant: 328 ms; Modulation Amplitude: 5 G; Modulation Frequency: 100 kHz; Receiver Gain: 5×10^5 ; Microwave Power: 10 mW; Microwave Frequency: 9.41 GHz; Sweep Time: 335 sec; Resolution of Field Axis: 1024. Source of RTPR spectrum: Licht, 1996.

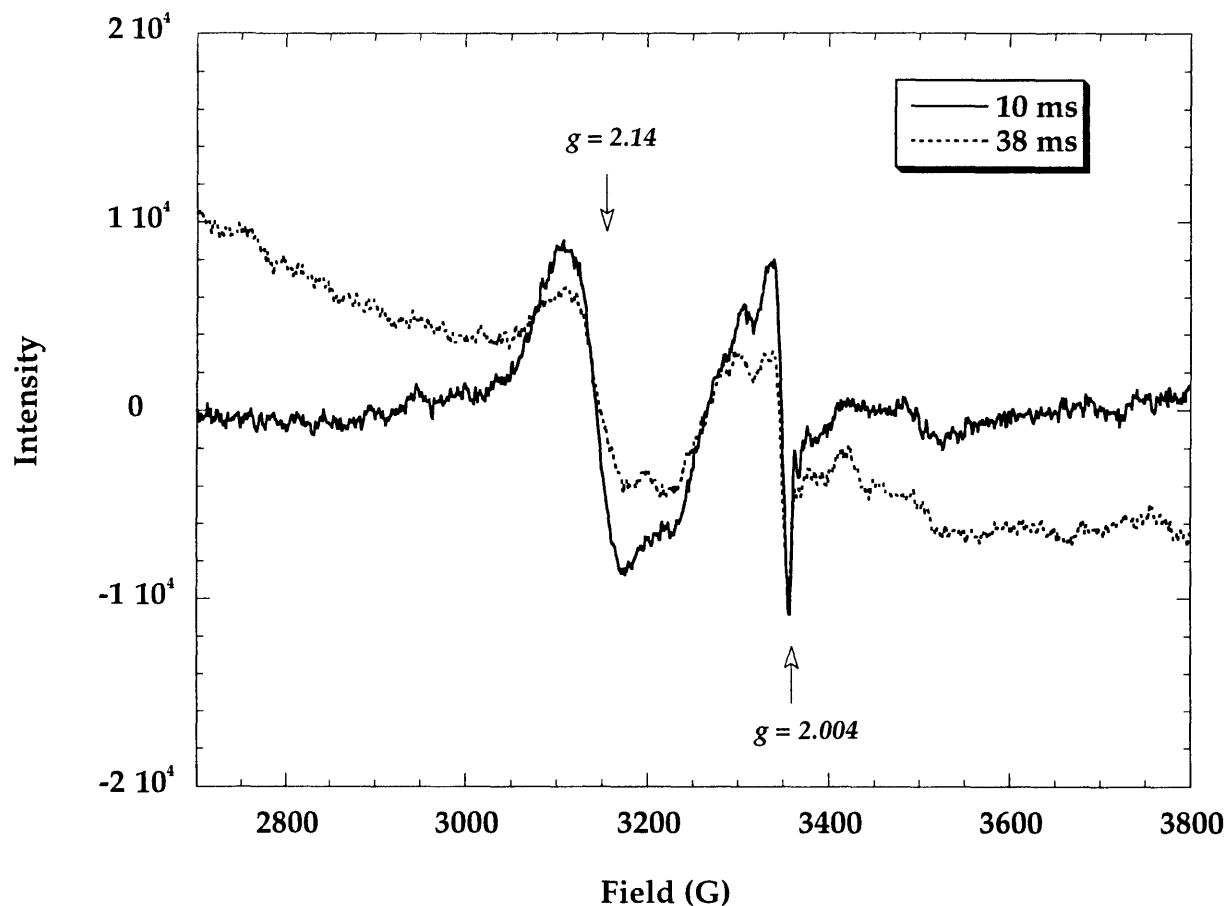


Figure 3.5 RFQ-EPR spectra of *T. acidophila* RDPR at 10 ms (9 scans) and 38 ms (7 scans) with [5'- ^2H]-AdoCbl. Scan Range: 1100 G; Field Set: 3250 G; Time Constant: 328 ms; Modulation Amplitude: 5 G; Modulation Frequency: 100 kHz; Receiver Gain: 5×10^5 ; Microwave Power: 10 mW; Microwave Frequency: 9.41 GHz; Sweep Time: 335 sec; Resolution of Field Axis: 1024.

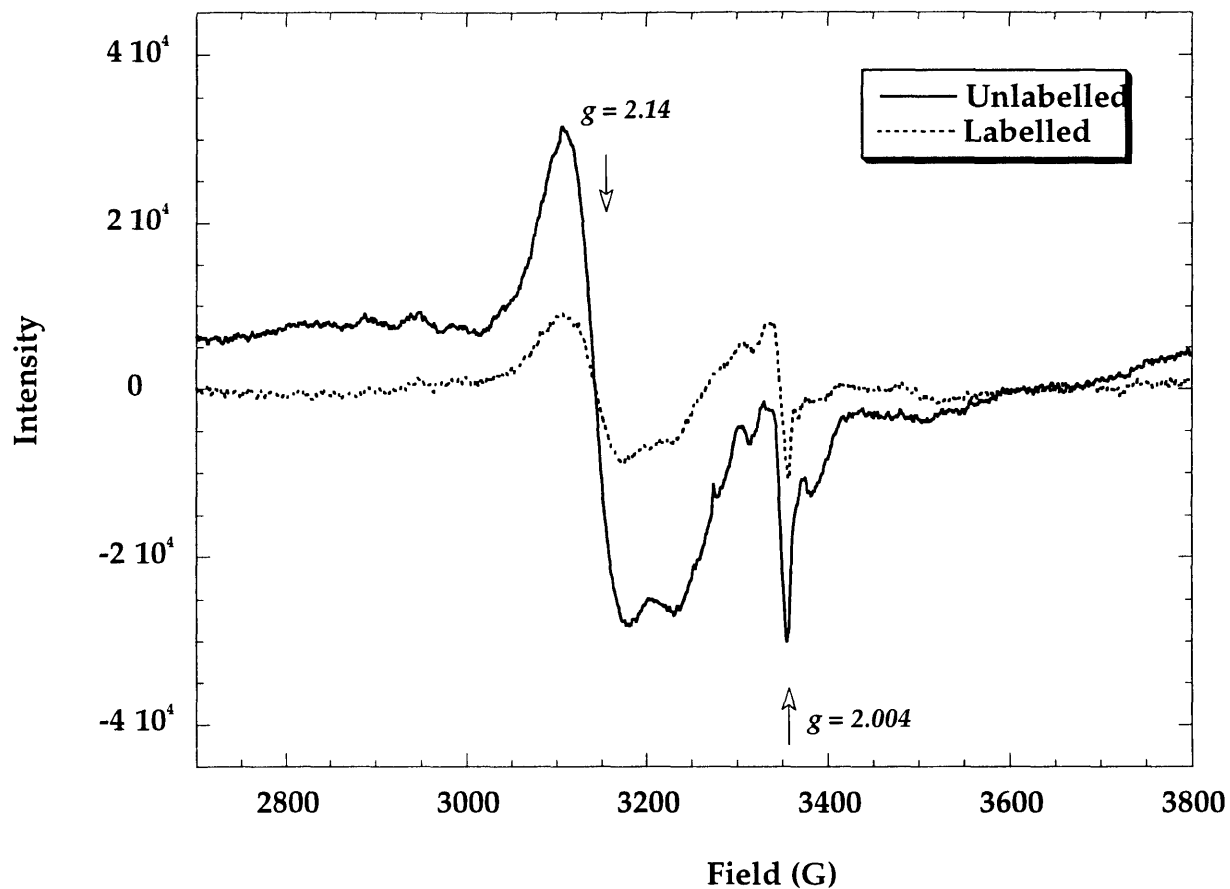


Figure 3.6a RFQ-EPR spectra of *T. acidophila* RDPR at 10 ms with [5'- ^1H]-AdoCbl (9 scans) and [5'- ^2H]-AdoCbl (9 scans). Scan Range: 1100 G; Field Set: 3250 G; Time Constant: 328 ms; Modulation Amplitude: 5 G; Modulation Frequency: 100 kHz; Receiver Gain: 5×10^5 ; Microwave Power: 10 mW; Microwave Frequency: 9.41 GHz; Sweep Time: 335 sec; Resolution of Field Axis: 1024.

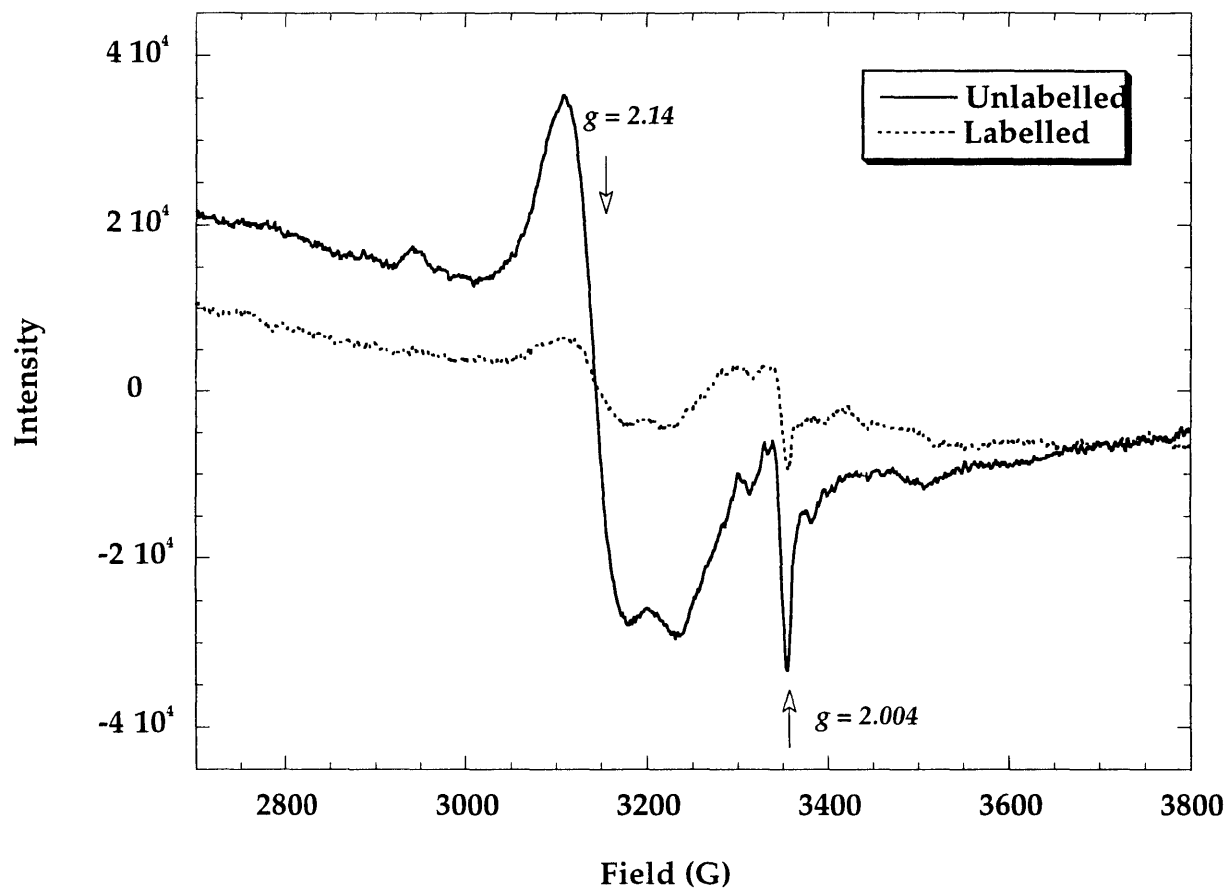


Figure 3.6b RFQ-EPR spectra of *T. acidophila* RDPR at 38 ms with $[5\text{-}^1\text{H}]\text{-AdoCbl}$ (6 scans) and $[5\text{-}^2\text{H}]\text{-AdoCbl}$ (7 scans). Scan Range: 1100 G; Field Set: 3250 G; Time Constant: 328 ms; Modulation Amplitude: 5 G; Modulation Frequency: 100 kHz; Receiver Gain: 5×10^5 ; Microwave Power: 10 mW; Microwave Frequency: 9.41 GHz; Sweep Time: 335 sec; Resolution of Field Axis: 1024.

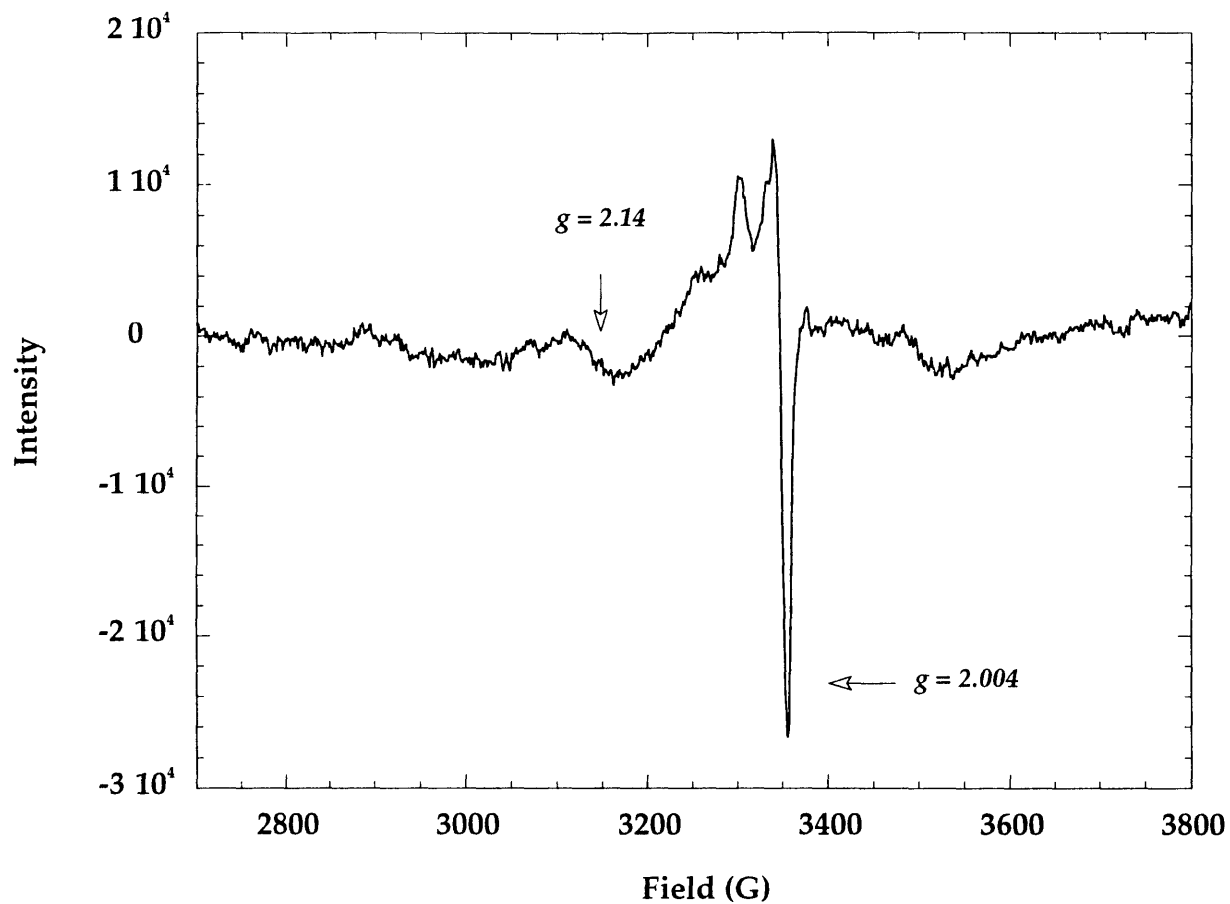


Figure 3.7 The mystery peak observed due to incomplete mixing at 10 ms (13 scans). Scan Range: 1100 G; Field Set: 3250 G; Time Constant: 328 ms; Modulation Amplitude: 5 G; Modulation Frequency: 100 kHz; Receiver Gain: 5×10^5 ; Microwave Power: 10 mW; Microwave Frequency: 9.41 GHz; Sweep Time: 335 sec; Resolution of Field Axis: 1024.

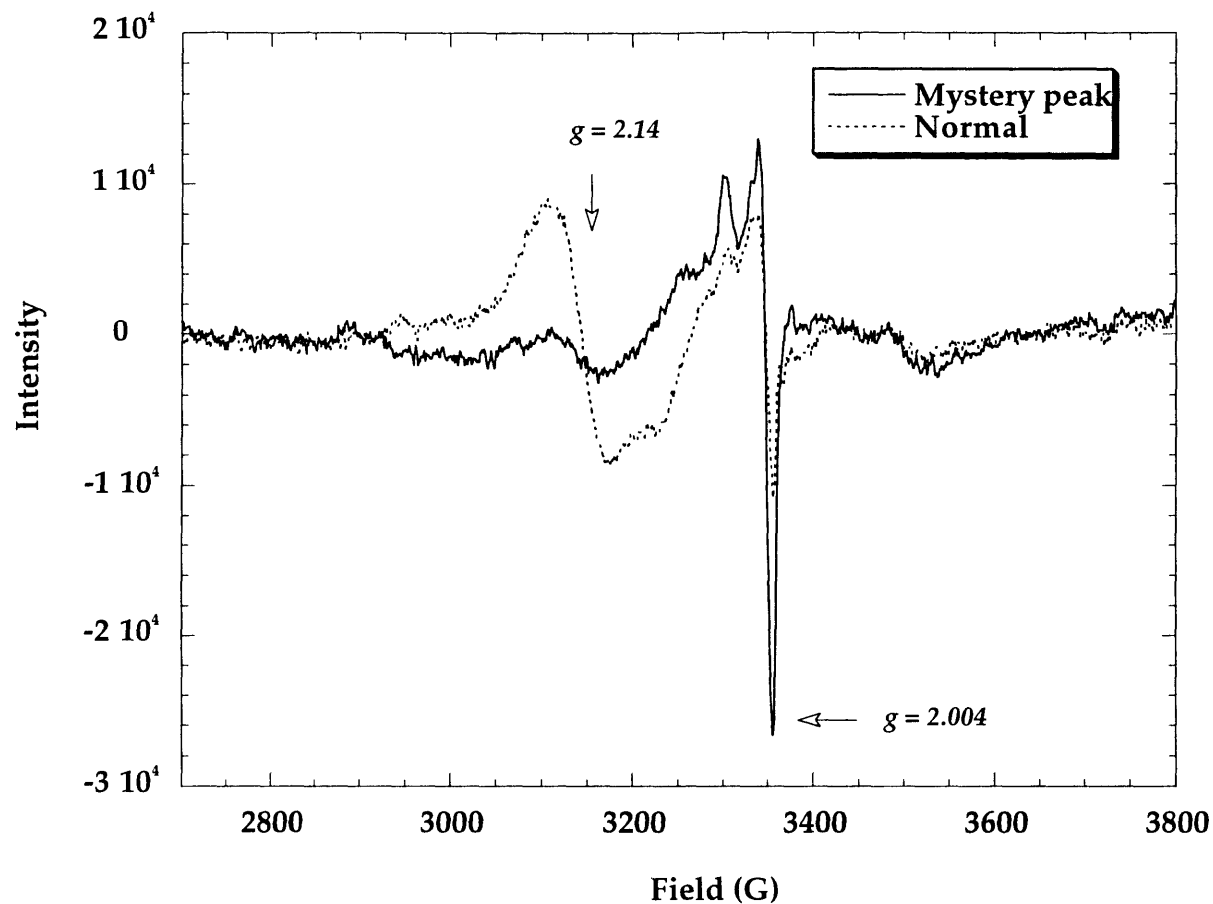


Figure 3.8 The mystery peak observed (13 scans) with normal peak at 10 ms with [5'- ^2H]-AdoCbl (9 scans). Scan Range: 1100 G; Field Set: 3250 G; Time Constant: 328 ms; Modulation Amplitude: 5 G; Modulation Frequency: 100 kHz; Receiver Gain: 5×10^5 ; Microwave Power: 10 mW; Microwave Frequency: 9.41 GHz; Sweep Time: 335 sec; Resolution of Field Axis: 1024.

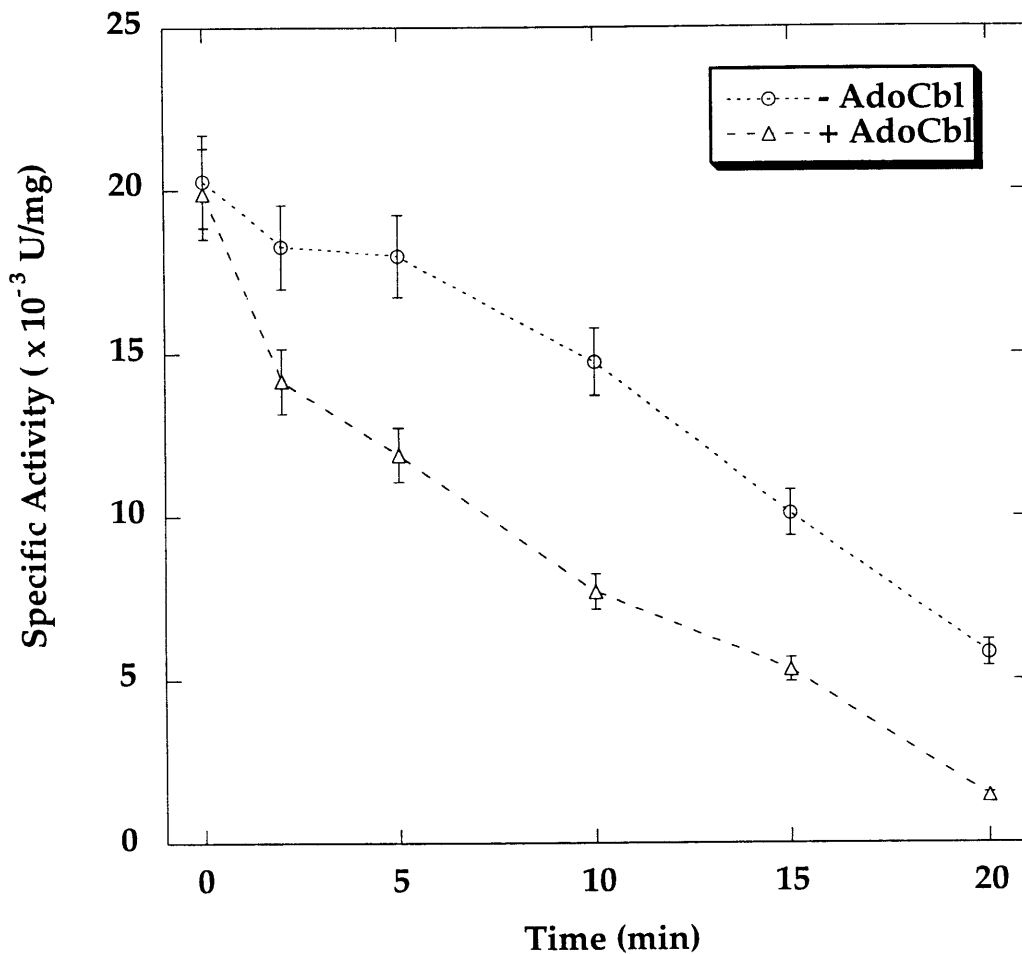


Figure 3.9 Enzyme stability in the presence of dGTP, with or without AdoCbl at 55°C. The reaction mixture contained: 60 μ M (90 μ g/ 15 μ L) *T. acidophila* RDPR, 25 mM HEPES (pH 7.5), 1 mM MgCl₂, 1 mM NADPH, 150 μ M TR, 2 μ M TRR, 1 mM dGTP, with or without 100 μ M AdoCbl. The assay mixture contained: 1 mM [5-³H]-CDP (S.A. = 8.9 $\times 10^3$ cpm/nmol), 100 μ M AdoCbl, 1 mM dGTP, 1 mM MgCl₂, 30 mM DTT, 25 mM HEPES pH 7.5. Assay time was 10 min. Source: Book III, p.20.

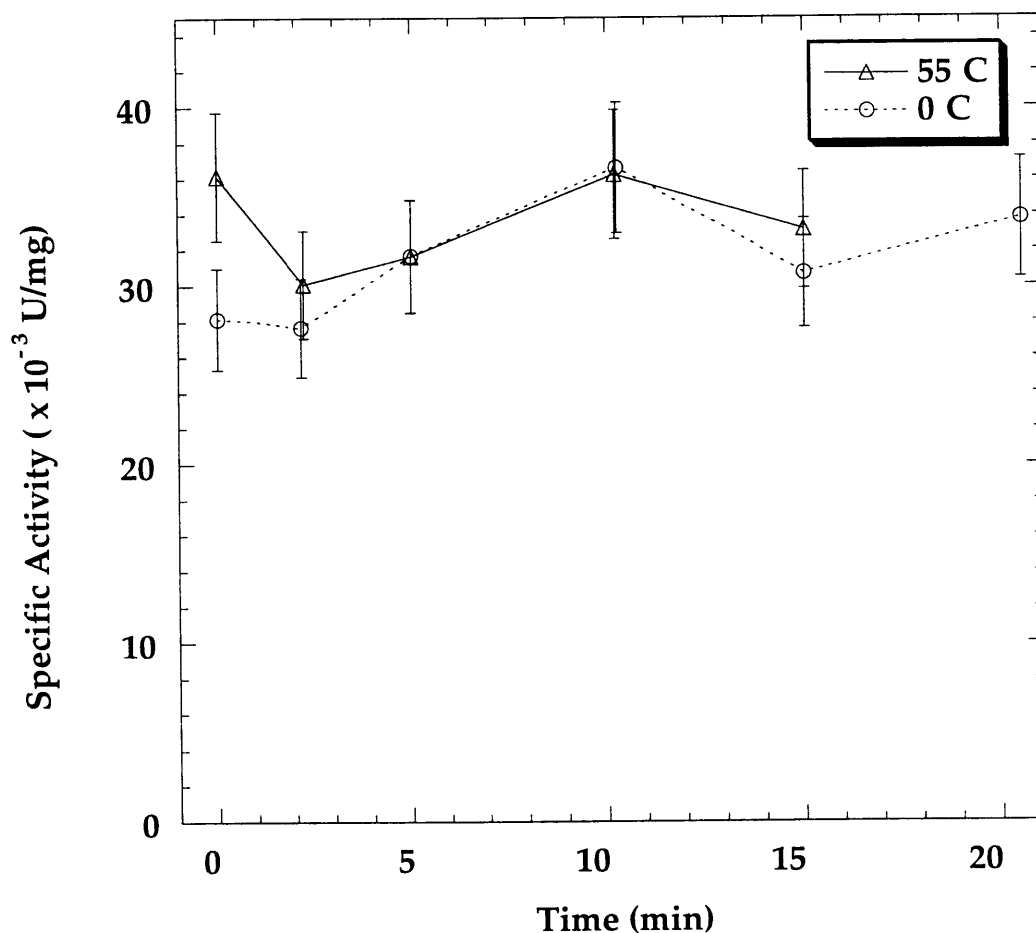


Figure 3.10 Enzyme stability at 0°C and 55°C in the absence of AdoCbl and dGTP. The reaction mixture contained: 60 μM (90 μg / 15 μL) *T. acidophila* RDPR, 25 mM HEPES (pH 7.5), 1 mM MgCl_2 , 1 mM NADPH, 150 μM TR, 2 μM TRR. The assay mixture contained: 1 mM $[5\text{-}^3\text{H}]\text{-CDP}$ (S.A. = 8.9×10^3 cpm/nmol), 100 μM AdoCbl, 1 mM dGTP, 1 mM MgCl_2 , 30 mM DTT, 25 mM HEPES pH 7.5. Assay was carried out for 8 min at 55°C . The reaction mixture was either incubated at 55°C or left on ice. Timing started 2 min after incubating one reaction mixture at 55°C. Source: Book III, p.30.

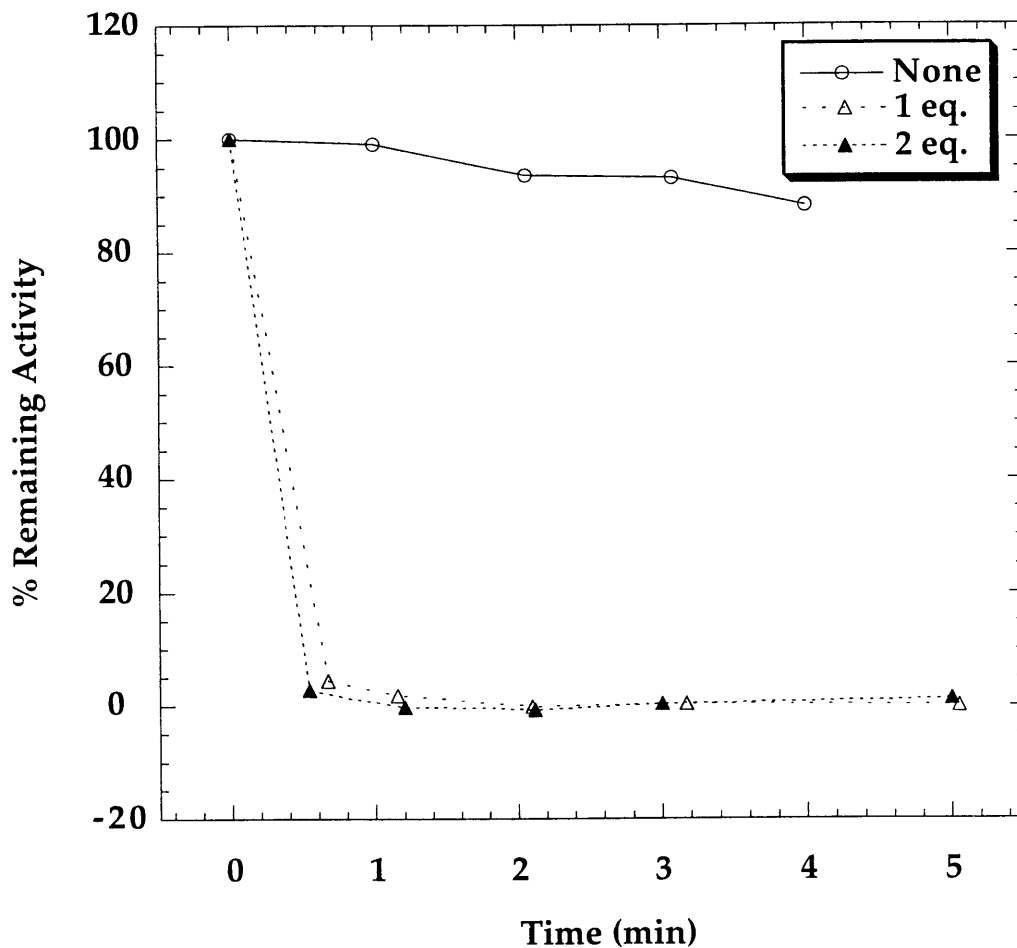


Figure 3.11 Time-dependent inactivation of *T. acidophila* RDPR by 2'-deoxy-2',2'-difluorocytidine 5'-diphosphate (dF₂CDP). The reaction mixture contained: 60 μM (90 μg/ 15 μL) *T. acidophila* RDPR, 25 mM HEPES (pH 7.5), 1 mM MgCl₂, 100 μM AdoCbl, 1 mM NADPH, 150 μM TR, 2 μM TRR, and 60 μM or 120 μM dF₂CDP. The assay mixture contained: 1 mM [5, 8-³H]-ADP (S.A. = 2.1 × 10³ cpm/nmol), 100 μM AdoCbl, 30 mM DTT, 1 mM MgCl₂, and 25 mM HEPES (pH 7.5). Assay time was 10 min. *Source: Book III, p.64.*

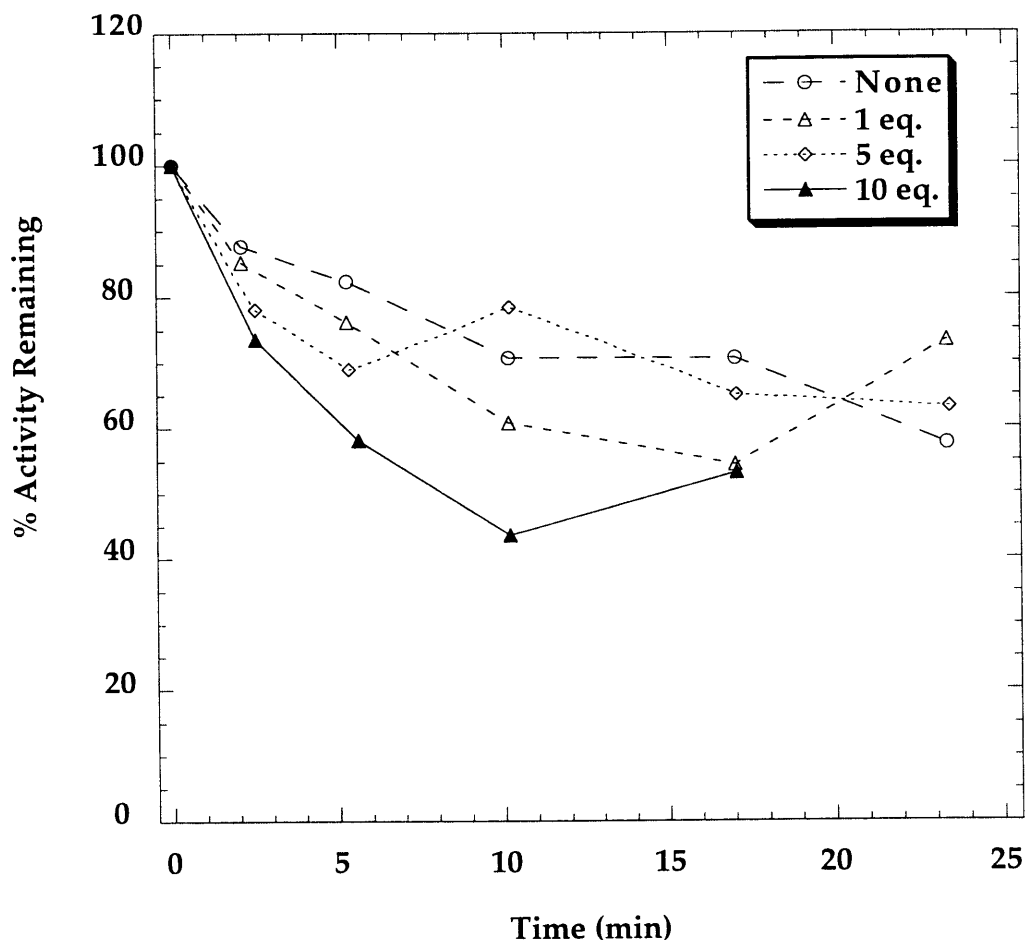


Figure 3.12 Time-dependent inactivation of *T. acidophila* RDPR by 2'-azido-2'-deoxyuridine 5'-diphosphate (N₃UDP). The reaction mixture contained: 60 μM (90 μg/ 15 μL) *T. acidophila* RDPR, 25 mM HEPES (pH 7.5), 1 mM MgCl₂, 100 μM AdoCbl, 1 mM NADPH, 150 μM TR, 2 μM TRR, and 60 μM, 300 μM, or 600 μM of N₃UDP. The assay mixture contained: 1 mM [5-³H]-CDP (S.A. = 8.9 × 10³ cpm/nmol), 100 μM AdoCbl, 1 mM dGTP, 1 mM MgCl₂, 30 mM DTT, 25 mM HEPES pH 7.5. Assay time was 10 min. Data points are scattered. See discussion for possible causes. *Source: Book III, p.32.*

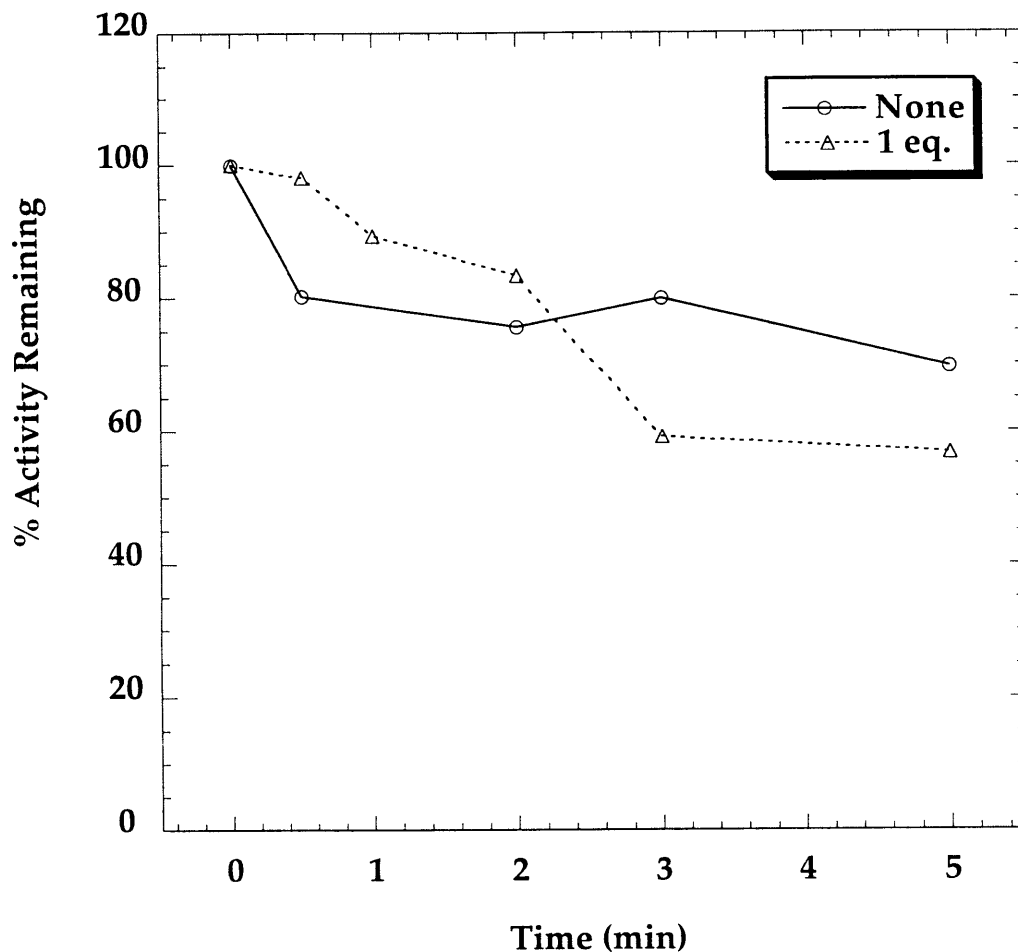


Figure 3.13 Time-dependent inactivation of *T. acidophila* RDPR by 2'-deoxy-2'-methyleneuridine-5'-diphosphate (2'VUDP). The reaction mixture contained: 60 μM (90 μg / 15 μL) *T. acidophila* RDPR, 25 mM HEPES (pH 7.5), 1 mM MgCl_2 , 100 μM AdoCbl, 1 mM NADPH, 150 μM TR, 2 μM TRR, and 60 μM 2'VUDP. The assay mixture contained: 1 mM $[5\text{-}^3\text{H}]\text{-CDP}$ (S.A. = 8.9×10^3 cpm/nmol), 100 μM AdoCbl, 1 mM dGTP, 1 mM MgCl_2 , 30 mM DTT, 25 mM HEPES pH 7.5. Assay time was 10 min. *Source: Book III, p.41.*

Appendix I *T. acidophila* RDPR protein and DNA sequence.

LOCUS TAU73619 3589 bp DNA BCT 05-NOV-1996
DEFINITION *Thermoplasma acidophilum* ribonucleotide reductase gene, complete

ACCESSION U73619
NID g1657992
SOURCE *Thermoplasma acidophilum*.
ORGANISM *Thermoplasma acidophilum*
Archaea; Euryarchaeota; Thermoplasmales; Thermoplasmaceae;
Thermoplasma.

REFERENCE1 (bases 1 to 3589)
AUTHORS Tauer,A. and Benner,S.A.
TITLE The B12-dependent ribonucleotide reductase from the archaebacterium *Thermoplasma acidophila*. An evolutionary solution to the ribonucleotide reductase conundrum
JOURNAL Proc. Natl. Acad. Sci. U.S.A. (1997) 94, 53-58
Submitted (07-OCT-1996) Chemistry, University of Florida, Buckman Dr., Gainesville, FL 32611, USA

Translation =

"MIKEVVKRDGTVVPFEKNKITMAIYKAMLSVKNGTMKD AEQLADKVVARLKDKERPSVEEIQDVVEDVLMTSKIDGK
TFTDVAKSYILYREKRRAIREEKELMGVKDDLKLT LNAV KVL EARYLLKDEDEGKIIETPRQMFRRVASHIGIVEALYDIK
YKKTGKVPENAEIIGKVSPTQEEVLRRAFGYMKEDGII EGT FEEFMDFIQTKGTSAGHYINRFEEVMSSLDFV P NSPTLMN
AGTKLGQLSACFVLPVGD SIEDIFETLKN TALIHKSGGGTGF SFSRLRPKDDIVGSTKGVASGPV S FMKIFDVTTDVIKQGG
KRRGANMGILNYPDIMEFILSKDSENKVL SNFNISVGTDDFFDKLDND D YVDLVNPRTKKIMKRIKAREIWD A IIDQ
AWKTADPGLIFLDEINRKNPVKNVGD IESTNPCGEQPLLPYESCNLGSINLSKYVVDGKKIDFDRLRETVWTATRFLDDVI
DANKFPVEQIKK VTRMTRKIGLGVMGFADMLIKLEIPYNSWEALEIGEKVMSFINDESHKASQALAEERAVFPAWYGSE
WEKEGIKMRNSTTTTIIAPTGTISIIAGCSSSIEPIFALAFVRHVLNGQELLEVNPLFEEKTRELGIYSEELMRQVAETGNLEN
VKINEEVKKIFVTAHEIDPQWHVLMQATFQRYCDSGVSKTINMRSDATREDIARAYRMAKDLHCKGITVYRDKSKTVQ
VLTAGTAETKKPEEKEVIELVTKMPDKYLKIDSTFD PACRRESAINEKILIIYICIFIKIIFAVGSCFRNAPMGISPFKGVQTA
SRVLCRLYAPVPYVSVLKVTFDLVERYLWPVLLAEVSQYYPHIIRGHP"

BASE COUNT 984 a 844 c 956 g 805 t

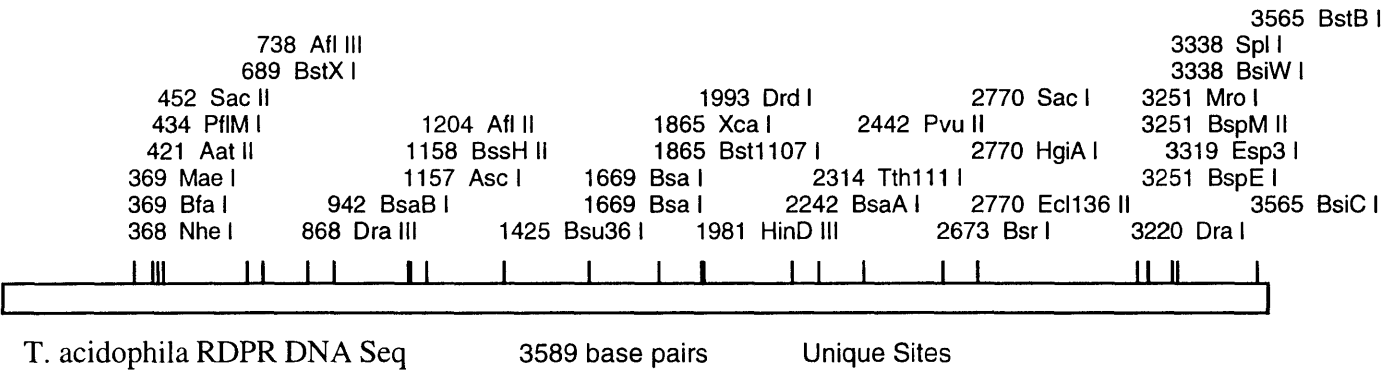
ORIGIN

1 TAATCTGCAC CATGTTCTTG TCCTTTAGGA AGAAAGCGAG GGATTTGACA AATGTCAGGC
61 CTCCGTCCTT TGC GCGGATA GCGCTGCGA TCTTCTCCC TATCTCCATG TTCGATGTGT
121 TAAGATTCAC GTTGTACGCT ATGAGGAAAT CCCTGGCCCC TATTATGGAA GCTCCCGCCT
181 TGCCAACCAC TGAAGGCCCG AAATCCGGCT TCCATTTTTC CTCTTTTATG GCCTCCTTGA
241 GCTGCTCATA CAGGAAGTTC TTGTTCTTA TGGCGGCAAG ATCGGACCTG TCAGCCTCTG
301 TGC GGCCTCA GCGTACAGAT ACACCGGTAT GCCCAGGTCC TCTCCAATC TCTTTCCAAG
361 ATCCCTGGCT AGCCTGACGC ATGTTTCCAT CTTTGTGTCC TGCAGCGGCA CGAAGGGTAT
421 GACGTCTGCA GCACCAAACC TTGGATGCTC TCCGCGGTGT GCATCCATGT CTATGATCTC

481 GGCCGCAGCC TTTATGCCGG CAAATGCAGC ATCTACGGCC TTTGAGCTGT CGCACACGAA
541 CGTTATGACG GATCTGTTGT GGTTCCGATC CATCTCCACG TCCAGGATCT TCACGGTGTC
601 AACCGAGGCT ATCGCATCCC TTATCCTGTT CACCCTGTCTG CGGTCCCTAC CCTCGCTGAA
661 GTTGGGTACG CATTCAACAA GAGACATGCC AGGATCATGG CATTGTTATG AATAAACAAT
721 GCTATGCGCT ATACTGTACA TGTGATCATA AATGTGATCA AACCTGTTAC AAAAGATTAA
781 ACTACATCCT ATCACATCAT ATTAACTGAT AAAATAACGT AAACGTAACA TAAAAAGTAT
841 TCAACACACA AAGGATAAAA CAAAACCCAC GGTGTGAAGA TGATCAAGGA AGTAGTTAAA
901 AGGGATGGAA CGGTAGTACC GTTTGAAAAG AACAAGATCA CGATGGCGAT CTACAAGGCC
961 ATGCTCTCTG TCAAGAACGG AACCATGAAG GATGCCGAGC AGCTTGCTGA CAAGGTTGTG
1021 GCAAGGCTGA AGGACAAGGA GAGGCCTTCC GTTGAGGAGA TACAGGATGT GGTTGAAGAC
1081 GTGCTGATGA CCTCGAAGAT AGACGGAAAG ACATTCACAG ACGTGGCCAA GTCATACATA
1141 CTGTACAGGG AAAAGAGGCG CGCCATAAGG GAAGAGAAGG AACTCATGGG CGTCAAGGAT
1201 GATCTTAAGC TCACACTTAA CGCGGTCAAG GTTCTCGAGG CCAGATACCT GCTCAAGGAT
1261 GAGGATGGAA AGATAATTGA AACACCAAGG CAGATGTTCA GGC GCGTTGC GTCGCACATA
1321 GGCATAGTGG AGGCCCTGTA CGATTACATC AAGTACAAGA AGACGGGCAA AGTGCCTGAA
1381 AATGCGGAGA TCATAGGAAA GGTATCACCG ACGCAGGAGG AGTCCCTCAG GAGGGCCTTC
1441 GGCTACATGA AGGAGGACGG CATAATCGAG GGAACCTTCG AGGAATTCAT GGAATTCATA
1501 CAGACCAAGG GAACCTCGGC CGGCCATTAC ATAAACAGGT TCGAGGAGGT CATGTCATCG
1561 CTGGACTTTG TTCCGAATTC ACCCACGCTG ATGAATGCCG GAACAAAGCT GGGGCAGCTC
1621 TCTGCCTGTT TTGTGCTGCC GGTTGGAGAC AGCATAGAGG ATATATTCGA GACCCTGAAG
1681 AACACCGCAC TTATACACAA GTCCGGCGGT GGGACCGGTT TCTCATTCTC GAGGCTCAGG
1741 CCAAAGGACG ACATCGTGGG ATCGACGAAG GGGGTGGCAT CAGGGCCGGT ATCGTTCATG
1801 AAGATATTCG ATGTTACCAC AGACGTGATA AAGCAGGGTG GCAAGAGGCG CGGAGCCAAC
1861 ATGGGTATAC TCAACTACAA CCATCCTGAC ATAATGGAGT TCATACTGAG CAAGGACTCT
1921 GAAAACAAGG TACTGAGCAA TTTCAACATC TCGGTCCGTG TCACGGACGA TTTCTTCGAC
1981 AAGCTTGACA ACGACGATTA CGTCGATCTC GTGAATCCGA GGACAAAGAA GATAATGAAG
2041 AGGATAAAGG CAAGAGAGAT ATGGGACGCC ATAATAGACC AGGCTTGAA GACCGCTGAT
2101 CCAGGCCTGA TATTCCTGGA CGAAATAAAC AGGAAGAACC CTGTGAAGAA CGTCGGGGAC
2161 ATAGAATCCA CGAACCCGTG CGGGGAACAG CCTCTTCTTC CGTATGAATC CTGCAACCTT
2221 GGATCCATAA ACCTGTCTAA GTACGTGGTG GACGGAAAGA AGATCGATTT TGACAGGCTC
2281 AGGGAGACTG TGTGGACTGC TACACGCTTC CTTGACGATG TCATAGATGC AAACAAGTTC
2341 CCGGTAGAAC AGATAAAGAA GGTACAGAGG ATGACCAGGA AGATAGGACT CGGTGTTATG
2401 GGCTTCGCTG ACATGCTCAT AAAGCTCGAG ATACCGTACA ACAGCTGGGA GGCCCTGGAG
2461 ATTGGGGAGA AGGTTATGAG CTCATCAAC GATGAGAGCC ACAAGGCATC GCAGGCTCTG
2521 GCCGAGGAAC GCGCGGTATT CCCGGCATGG TACGGATCGG AATGGGAGAA GGAGGGCATA
2581 AAGATGAGGA ACTCCACGAC CACCACCATA GCACCCACGG GAACCATATC GATAATAGCT
2641 GGCTGCTCAT CGTCCATAGA GCCCATATTT GCACTGGCAT TTGTCAGGCA CGTTCTGAAC
2701 GGCCAGGAGC TTCTTGAGGT CAACCCGCTG TTTGAGGAAA AGACGCGCGA GCTTGAATA
2761 TACTCCGAGG AGCTCATGAG GCAGGTTGCG GAGACAGGAA ACCTGGAGAA CGTGAAGATA
2821 AACGAGGAGG TCAAGAAGAT ATTCGTCACG GCCCATGAGA TAGATCCGCA GTGGCATGTG
2881 CTGATGCAGG CGACGTTCCA GAGGTACTGC GATTCGGGTG TATCGAAGAC CATCAACATG

2941 AGGAGCGACG CAACCCGCGA GGATATTGCC AGGGCTTACA GGATGGCCAA GGATCTGCAC
3001 TGCAAGGGCA TAACAGTCTA CAGGGACAAG AGCAAGACCG TCCAGGTGTT GACGGCAGGG
3061 ACGGCCGAGA CAAAGAAGCC GGAAGAGAAG GAGGTAATCG AGCTGGTCAC GAAGATGCCA
3121 GACAAGTACC TGAAGATCGA TTCAACATTC GATCCCGCCT GCCGACGGGA AAGTGCGATA
3181 AATGAAAAAA TCCTGATCAT TTATATCTGT ATTTTCATTT TTAAAATAAT CTCGCAGTA
3241 GGTTCTTGTT TCCGGAATGC CCCTATGGGA ATATCACCTT TCAAGGGTGT ACAAACCTGCT
3301 TCCCGTGTAC TGATCTGCCG TCTCTATGCT CCTGTACCGT ACGTTTCTGT TCTCAAGGTA
3361 ACTTTTGACC TCGTTGAGCG CTATCTCTGG CCTGTTGTTT TCCTGGCTGA GGTGAGTCAG
3421 TATTATCCGC ATATCATCCG TGGCCACCCT TGATATGGCT TCCGCAGACT GTTCATTGGA
3481 AAGATGCCCG TGATCGCTCA GTATTCTCCT CTTCAGTGCT TCAGGGTAGC TTCCGGTCCT
3541 GAGCATCTCA ACATCATGGT TGGATTGAA TCGGAGAATG TCTGAATTC

Appendix II Restriction map of *T. acidophila* RDPR DNA sequence.



Appendix III *T. acidophila* RDPR N-terminal sequencing report

238-1048, 1087 JRS: 3-9379

Protein Microsequence Report

I.D.: S6431
 Sample Name: A
 Date: 9/17/96
 Investigator: WU
 Laboratory: STUBBE
 Molec Weight: 969 KD
 Sample Matrix: 50 mM Tris, pH 8.0, 2mM Tris pH 8.0, 5% glycerol

cycle	assignment (PTH AA)	pMoles	other residues present (pmol) / notes
0			
1	MET	12.8	
2	ILE	12.7	
3	LYS	5.8	
4	GLU	5.1	
5	VAL	9.4	

Additional Notes:

- Cys - not detected unless alkylated
- Trp - may not be determined at low levels
- X - uncharacterized peak on PTH AA HPLC profile
- - no determination
- () - somewhat confident, reasonable
- [] - low confidence, possible

Instrumentation Applied biosystems Model 477A Protein Sequencer w/ on-line Model 120 PTH Amino Acid Analyzer